

Investigating the Functional Role of Asprosin, the C-terminal Propeptide of Fibrillin-1

Inaugural-Dissertation

zur

Erlangung des Doktorgrades

der Mathematisch-Naturwissenschaftlichen Fakultät

der Universität zu Köln



vorgelegt von

Yousef Ashraf Tawfik Morcos

aus Kairo, Ägypten

Köln, 2022

Berichterstatter (Gutachter): Prof. Dr. Gerhard Sengle
Prof. Dr. Ulrich Baumann

Tag der mündlichen Prüfung: 16.01.2023

To my father

Table of Contents

Abstract	5
Zusammenfassung	6
1. Introduction	8
1.1 Extracellular matrix as dynamic structural scaffold that targets and releases cytokines	8
1.1.1 ECM remodelling and metabolic health	8
1.1.2 Matrikines as proteolytic ECM fragments acting as cytokines.....	9
1.2 Fibrillins as microfibril forming entities of elastic tissues.....	10
1.2.1 Fibrillinopathies as connective tissue disorders with wide clinical spectrum.....	11
1.2.2 Adipose tissue abnormalities in patients with fibrillin-1 deficiency.....	12
1.2.3 Role of fibrillin-1 in adipose tissue homeostasis	13
1.3 Asprosin, the C-terminal propeptide of fibrillin-1	14
1.3.1 Asprosin as new hormone controlling glucose release in the liver.....	14
1.3.2 Involvement of asprosin in metabolic diseases.....	17
2. Thesis objectives	19
3. Sensitive asprosin detection in clinical samples reveals serum/saliva correlation and indicates cartilage as a source for serum Asprosin	20
4. Correlation of metabolic characteristics with maternal, fetal and placental asprosin in human pregnancy	51
5. Transglutaminase mediated asprosin oligomerization allows its tissue storage as fibers ... 65	
6. Discussion	127
6.1 Analysis and functional role of asprosin glycosylation	127
6.2 Points to be considered for sensitive asprosin detection.....	127
6.3 Correlation of asprosin levels with biological sex and feeding state	129
6.4 Sensitive detection in clinical samples suggests cartilage as a source for asprosin.....	130
6.5 Correlation between placental asprosin concentration and maternal BMI and GDM	132
6.6 Extracellular detection of asprosin as fibers in human and murine tissues.....	134
6.7 Multimerization of asprosin.....	135
6.8 Asprosin crosslinking to the ECM cellular microenvironment depends on an intact fibrillin-1 network	138
7. Outlook	140
8. References	141
9. Abbreviations	161
10. Acknowledgement	165

Abstract

Asprosin, the C-terminal pro-fibrillin-1 propeptide is described as white adipose tissue derived hormone that stimulates hepatic glucose release and activates hunger-promoting hypothalamic neurons. Currently, there is only limited knowledge about the mechanisms controlling the bioavailability of asprosin in tissues. In this thesis several aspects about the biochemical characteristics and detection of asprosin have been elucidated.

For instance, new biochemical methods for asprosin concentration and detection in several body fluids including serum, plasma, saliva, breast milk, and urine were developed. Since it was found that glycosylation impacts human asprosin detection, its glycosylation profile was analyzed. By employing a newly developed sandwich ELISA it could be revealed that serum and saliva asprosin strongly correlate depending on biological sex, and feeding status. To investigate the contribution of connective tissue-derived asprosin to serum levels two cohorts with described cartilage turnover were screened. Serum asprosin correlated with COMP, a marker for cartilage degradation upon running exercise and after total hip replacement surgery. This together with the finding that asprosin is produced by primary human chondrocytes and expressed in human cartilage suggests a contribution of cartilage to serum asprosin. In addition, by analysing a mother-child cohort established in Cologne there was a strong correlation between the maternal and fetal plasma asprosin levels and both increased with gestational diabetes mellitus (GDM) in normal-weight and obese women. Placental asprosin levels were associated with maternal but not with fetal plasma asprosin levels and with body mass index (BMI) but not with GDM. Furthermore, asprosin levels in breast milk, and urine, were determined for the first time, and propose saliva asprosin as an accessible clinical marker for future studies.

At present, little is known about the tissue distribution of asprosin. Here, by employing newly generated specific asprosin antibodies the distribution pattern of asprosin in human and murine connective tissues such as placenta, heart, kidney, liver, and muscle were determined. Thereby, asprosin was detected as extracellular fibers within connective tissue microenvironments. Further, when established cell lines were investigated for asprosin synthesis most cells derived from musculoskeletal tissues render asprosin into a crosslinked multimerized form. This multimerization is facilitated by transglutaminase activity and requires an intact fibrillin fiber network for proper linear deposition.

The gathered data contribute to a better understanding of asprosin biochemical properties and suggest a new extracellular storage mechanism of asprosin in multimerized form, which may regulate its cellular bioavailability in tissues.

Zusammenfassung

Asprosin, das C-terminale Pro-Fibrillin-1 Propeptid, wurde vor kurzem als ein aus dem weißen Fettgewebe stammendes Hormon beschrieben, das die hepatische Glukosefreisetzung anregt und die hungerfördernden Neuronen des Hypothalamus aktiviert. Derzeit gibt es nur begrenzte Kenntnisse über die Mechanismen, welche die Bioverfügbarkeit von Asprosin im Gewebe steuern. In dieser Arbeit wurden die biochemischen Eigenschaften und neue Methoden des Nachweises von Asprosin untersucht.

So wurden beispielsweise neue biochemische Methoden für die Konzentration und den Nachweis von Asprosin in verschiedenen Körperflüssigkeiten wie Serum, Plasma, Speichel, Muttermilch und Urin entwickelt. Da festgestellt wurde, dass die Glykosylierung die Detektion von Asprosin beeinflusst, wurde das Glykosylierungsprofil von humanem Asprosin analysiert. Durch den Einsatz eines neu entwickelten Sandwich-ELISAs konnte gezeigt werden, dass Serum- und Speichel-Asprosin stark mit dem biologischen Geschlecht und dem Ernährungsstatus korrelieren. Um den Anteil des aus dem Bindegewebe stammenden Asprosins an Asprosinspiegeln im Serum zu untersuchen, wurden zwei Kohorten mit beschriebenen Knorpelumsatz untersucht. Asprosin im Serum korrelierte mit COMP, einem Marker für den Knorpelabbau nach gezielten Laufübungen und nach einer Hüfttotalendoprothesenoperation. Dies und die Feststellung, dass Asprosin von primären menschlichen Chondrozyten produziert und im menschlichen Knorpel exprimiert wird, lässt auf einen Beitrag des Knorpels zum Serum Asprosin schließen. Außerdem wurde bei der Analyse einer in Köln etablierten Mutter-Kind-Kohorte eine starke Korrelation zwischen den mütterlichen und fetalen Plasma-Asprosinwerten festgestellt, und beide Werte stiegen bei normalgewichtigen und fettleibigen Frauen mit Schwangerschaftsdiabetes (GDM) an. Die Asprosinwerte in der Plazenta assoziierten mit den mütterlichen, aber nicht mit den fetalen Plasma-Asprosinwerten und mit dem Body-Mass-Index (BMI), aber nicht mit GDM. Darüber hinaus wurden zum ersten Mal Asprosinmengen in der Muttermilch und im Urin bestimmt, so dass Speichel-Asprosin als zugänglicher klinischer Marker für künftige Studien etabliert werden könnte.

Derzeit ist nur wenig über die Gewebeverteilung von Asprosin bekannt. Durch den Einsatz neuentwickelter spezifischer Asprosin-Antikörper wurde das Verteilungsmuster von Asprosin in menschlichem und murinem Bindegewebe wie Plazenta, Herz, Niere, Leber und Muskel bestimmt. Dabei wurde Asprosin in Form von extrazellulären Fasern in der zellulären Mikroumgebung von Bindegewebe nachgewiesen. Bei der Untersuchung etablierter Zelllinien auf Asprosin Synthese wurde außerdem festgestellt, dass die meisten Zellen,

welche aus dem muskuloskeletalem System stammen, Asprosin in eine vernetzte, multimerisierte Form umwandeln. Diese Multimerisierung wird durch die Gewebstransglutaminase (TG2) stabilisiert und erfordert ein intaktes Fibrillin Fasernetzwerk für eine korrekte lineare Ablagerung.

Die erzielten Ergebnisse tragen zu einem besseren Verständnis der biochemischen Eigenschaften von Asprosin bei und deuten auf einen neuen extrazellulären Speichermechanismus in multimerisierter Form hin, der seine zelluläre Bioverfügbarkeit in Geweben regulieren könnte.

1. Introduction

It is well established knowledge that the extracellular matrix (ECM) plays a fundamental role in cell growth, migration, proliferation, immunity, and apoptosis (Lu et al., 2011). Most of these activities require the metabolic reprogramming of cells. Until now, the exact mechanisms by which the ECM is involved in metabolic reprogramming remains still unclear. One idea is the concept of matrikines, which represent proteolytic fragments of ECM proteins or their receptors that serve as active hormones themselves (Parks et al., 2011; Sivaraman & Shanthi, 2018; Vallet & Ricard-Blum, 2019). Examples of such ECM derived cytokines are irisin (precursor: fibronectin domain-containing protein 5), endostatin (precursor: collagen XVIII) and endotrophin (precursor: collagen VI) which all play a critical metabolic role (M. S. O'Reilly et al., 1997; Sanchis-Gomar et al., 2012; Sun et al., 2017). A better understanding of the interplay between ECM and metabolism may provide novel therapeutic targets and guide the development of clinical approaches against various metabolic diseases.

1.1 Extracellular matrix as dynamic structural scaffold that targets and releases cytokines

The ECM of connective tissues represents a dynamic supramolecular architecture of the cellular microenvironment that is composed of multidomain glycoproteins and proteoglycans that regulate cellular processes such as polarity, migration, proliferation and differentiation (Hynes RO, 2012; Mecham, 2011). The ECM does not only fulfil structural roles by providing specific biomechanical properties to tissues, but also regulates the bioavailability of growth factors (Hynes, 2009). Thereby, the ECM targets and sequesters growth factors and guarantees their proper presentation to cells which is important for their controlled activation and release.

1.1.1 ECM remodelling and metabolic health

Various proteolytic enzymes known to be involved in the remodeling of the musculoskeletal system were shown to impact metabolic health. For instance, genetic ablation of ADAMTS-18 (A disintegrin and metalloproteinase with thrombospondin motifs-18) in mice causes visceral adiposity (Du et al., 2021), while the absence of ADAMTS-5 enhances brown adipose tissue (BAT) mass and fosters browning of white adipose tissue (WAT) (Bauters et al., 2017). The documented functions of ADAMTSs include N-terminal procollagen processing (ADAMTS-2) (Bekhouche & Colige, 2015), degradation of cartilage proteins (e.g. cartilage oligomeric matrix protein: COMP, matrilins) (Ehlen et al., 2009), cleavage of

proteoglycans such as aggrecan, the fibrillin ligand versican, and brevican (Gueye et al., 2017; Kuno et al., 2000; Stanton et al., 2011; Yang et al., 2017), as well as fibrillins (Kutz et al., 2011). Similar to MMPs (Matrix Metalloproteinases) ADAMTSs play a key role in the destruction of articular cartilage in osteoarthritis (OA) (Burrage et al., 2006; Yang et al., 2017). MMPs are a family of zinc-dependent endopeptidases that are able to degrade structural ECM proteins via cleavage at specific motifs (Parks et al., 1998). They play crucial roles in various pathological and physiological processes, such as tissue remodelling and organ development, regulation of inflammatory reactions, and cancer progression (Hidalgo & Eckhardt, 2001; Nelson et al., 2000; Stöcker et al., 2008). MMP enzymes were reported to specifically cleave sites within fibrillins (Ashworth, Murphy, et al., 1999) and collagen VI chains (Veidal et al., 2011). MMP activity was found to be upregulated during ECM remodeling processes that occur in connective tissue disorders such as Marfan Syndrome (MFS) (Xiong et al., 2008), and during muscular regeneration (Bobadilla et al., 2014; Chen & Li, 2009). Furthermore, exercise-induced remodelling leads to upregulation of MMP activity which is required for proper musculoskeletal tissue regeneration (Lo Presti et al., 2017).

1.1.2 Matrikines as proteolytic ECM fragments acting as cytokines

Matrikines as cleavage fragments from ECM protein precursors

Cleavage of ECM proteins and proteoglycans by enzymatic and non-enzymatic proteolysis results in the release of bioactive peptides that show biological activities different from their original proproteins (Maquart et al., 2004; Ricard-Blum & Salza, 2014). The size of these ECM fragments ranges from short peptides like laminin-derived peptides A13 (RQVFQVAYIIIKA) and C16 (KAFDITYVRLKF) (Malinda et al., 2008; Ponce et al., 2003) to high molecular weight proteins such as endorepellin (85 kDa), the C-terminal region of perlecan (Mongiat et al., 2003). These fragments were named “Matrikines” (Davis et al., 2000; Simeon et al., 1999) since they exert their activities by either acting as agonists or antagonists for specific cellular receptors and thereby modulate various cellular events such as cell migration, proliferation, adhesion and apoptosis (Maquart et al., 2004; Ricard-Blum & Salza, 2014). The release of these bioactive fragments from their precursor proproteins is catalysed by a variety of enzymes such as MMPs (Fukuda et al., 2011; Hamano et al., 2003; Heinz et al., 2010), cathepsins (Veillard et al., 2011; Wang et al., 2006), and propeptide convertases such as furin (Aigner et al., 2002; Lonnqvist et al., 1998; Romere et al., 2016; Yu et al., 2020). Several ECM proteins serve as precursors for matrikins such as fibrillin-1 (asprosin: C-terminal propeptide) (Jensen et al., 2014; Lonnqvist et al., 1998; Romere et al., 2016), fibrillin-2 (placensin: C-terminal propeptide) (Yu et al., 2020), collagen VI

(endotrophin: C-terminal cleavage product) (Aigner et al., 2002; Weathington et al., 2006), collagen XVIII (endostatin: 20 kDa C-terminal fragment) (Michael S O'Reilly et al., 1997), collagen IV (tumstatin: C-terminal 28 kDa fragment) (Maeshima et al., 2002), as well as perlecan (endorepellin: C-terminal peptide) (Duca et al., 2004).

Functional role of matrikines

Matrikines have been widely studied since the term was first defined in 1999 (Maquart et al., 1999). Many of them are released into the bloodstream regulating cell metabolism and are considered as hormone-like proteins such as asprosin and placensin, which were identified as glucogenic hormones and involved in hepatic glucose release (Greenhill, 2016; Romere et al., 2016; Yu et al., 2020). Also, endotrophin was reported to promote fibrosis and tumour progression (Park & Scherer, 2012a, 2012b), however, endostatin was also shown to play a significant role in the prevention of dermal and pulmonary fibrosis (Yamaguchi et al., 2012). Some of ECM-derived peptides have angiogenic activity and stimulate wound healing including the A13 and C16 peptides of laminin (Malinda et al., 2008), while others such as the F4 peptide (CNPEDCLYPVSHAHQR) derived from collagen XIX were reported to have anti-angiogenic activity (Oudart et al., 2015). Further, *in vitro* data showed that F4 inhibits melanoma cell migration and cancer progression in a mouse melanoma model (Oudart et al., 2015). Recently, the mechanism of how the F4 fragment exerts its activity was further investigated and it could be demonstrated that the F4 peptide inhibits tumor angiogenesis through $\alpha v \beta 3$ and $\alpha 5 \beta 1$ integrin interaction (Oudart et al., 2021). Additionally, matrikines were reported to be involved in the pathophysiology of various diseases such as lung diseases, atherosclerosis, (Gaggar & Weathington, 2016; Holm Nielsen et al., 2021; Staunstrup et al., 2021; Yuan et al., 2020) and cancer (Brassart-Pasco et al., 2020; Grahovac & Wells, 2014; Papadas et al., 2020).

1.2 Fibrillins as microfibril forming entities of elastic tissues

Fibrillins are large (~350 kDa) cysteine-rich, calcium-binding glycoproteins, which are encoded in humans by the *FBN1*, *FBN2*, and *FBN3* genes (fibrillin-1, -2 and -3) (Corson et al., 2004; Zhang et al., 1995) (Fig. 1). They play a fundamental role in elastic fiber formation during the development and homeostasis of connective tissues. During embryogenesis and the perinatal period, fibrillin-2 and -3 appear to have a more crucial role (Carta et al., 2006; Corson et al., 2004; Zhang et al., 1995) while throughout postnatal life the tissue presence of the continuously expressed fibrillin-1 is more crucial (Chaudhry et al., 2001; Corson et al., 2004; Handford, 2000; Jensen et al., 2014; Sabatier et al., 2011; Zeyer & Reinhardt, 2015;

Zhang et al., 1995). Fibrillins assemble into small diameter (10-12 nm) extracellular fibrillin microfibrils (FMFs) with a characteristic “beads-on-a-string”-like appearance (Keene et al., 1997; Sakai et al., 1986). FMFs are ubiquitously found throughout the connective tissue space where they provide tissue elasticity and integrity (Keene et al., 1997; Sengle et al., 2015).

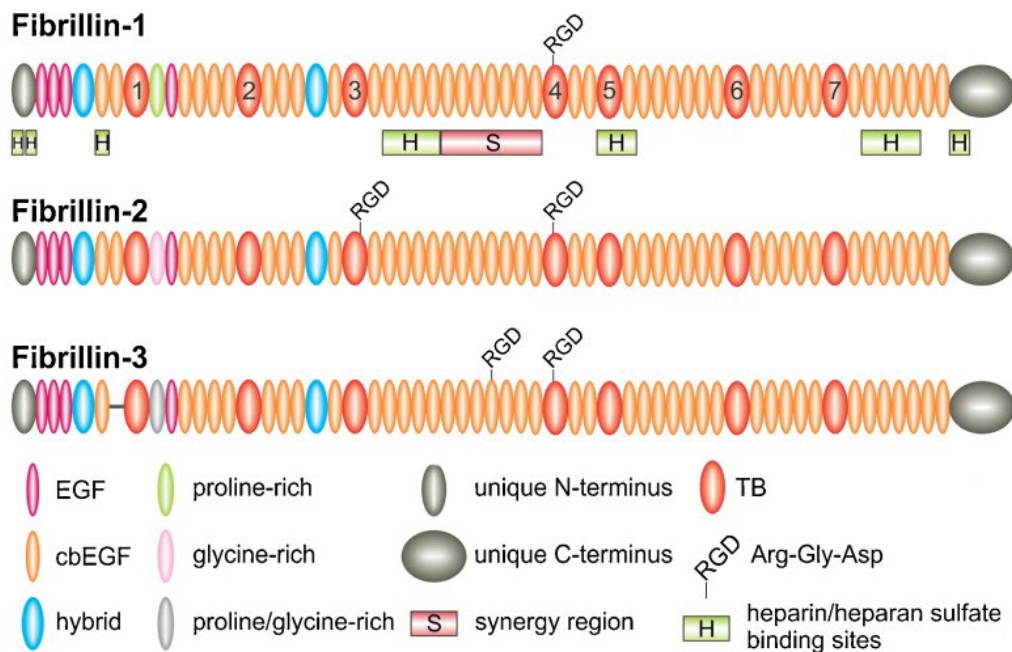


Figure 1: Multi-domain structure of members of the fibrillin family. Modified from Zeyer et. al 2015

1.2.1 Fibrillinopathies as connective tissue disorders with wide clinical spectrum

Fibrillin microfibrils not only play a crucial role in providing a scaffold for the deposition of tropoelastin in the early stages of elastic fiber formation (Wagenseil & Mecham, 2007), but also endow connective tissues with a high range of elasticity and strength. FMF integrity is crucial for the function of dynamic tissues and organs (Kielty et al., 2002) such as skeletal muscles (Smaldone et al., 2016), arteries such as the aorta (Mariko et al., 2011; Medley et al., 2002), skin (Lemaire et al., 2006; Loeys et al., 2010; Watson et al., 1999), and the lung (Robbesom et al., 2008; Tun et al., 2021). Additionally, FMF form their own elastin-independent network in tissues such as in kidney, superficial regions of the skin and ciliary zonules of the eye (Feneck et al., 2020; Hubmacher et al., 2014; Jones et al., 2019; Kriz et al., 1990; Raviola, 1971).

Fibrillins are evolutionarily conserved among mammalian species confirming their significant structural and biochemical importance (Piha-Gossack et al., 2012). In addition, FMFs also control access to cellular stimuli by targeting pluripotent growth factors, such as

TGF- β superfamily ligands, by either binding them directly (BMPs: bone morphogenetic proteins) (Zimmermann et al., 2021) or binding their carriers (LTBPs: latent TGF- β binding proteins) (Nistala et al., 2010). Overall, FMF can be viewed as dynamic architectural elements which not only define biomechanical properties of tissues but also exert extracellular control over signalling events (Sengle et al., 2015; Zimmermann et al., 2021). The importance of FMFs in organogenesis and tissue homeostasis is demonstrated by the various connective tissue disorders (“fibrillinopathies”) caused by mutations in the fibrillin genes. *FBNI* mutations lead to Marfan syndrome (MFS) which is characterized by long bone overgrowth (e.g. tall stature, scoliosis, arachnodactyly, pectus excavatum), joint laxity, reduced bone mineral density (BMD), early onset osteoarthritis and muscle weakness (Al Kaissi et al., 2013; Dietz et al., 1991; Giampietro et al., 2003). Interestingly, rare *FBNI* mutations lead to the almost opposite features such as short stature, brachydactyly, hypermuscularity, joint stiffness, and fibrotic skin (Sakai et al., 2016; Sengle et al., 2012). *FBN2* mutations lead to congenital contractural arachnodactyly (CCA), an autosomal dominant disorder that is phenotypically similar to MFS. Moreover, *Fbn2* null mice show syndactyly, reduced BMD, reduced muscle mass and forelimb contractures that resolve over time (Putnam et al., 1995; Sengle et al., 2015).

1.2.2 Adipose tissue abnormalities in patients with fibrillin-1 deficiency

The involvement of the extracellular glycoproteins fibrillin-1 and -2 in the regulation of body fat is intuitive since most mutations in the fibrillin genes (*FBNI*, *FBN2*) are associated with a slender habitus with little subcutaneous fat. In addition, between 2010 and 2014, new mutations within exon 64 at the 3' end of *FBNI* were described as causative for progeroid facial features and severe lipodystrophy and resulted in an abnormal thin phenotype (Graul-Neumann et al., 2010; Jacquinet et al., 2014; Passarge et al., 2016; Summers et al., 2005; Takenouchi et al., 2013). Recent advances in metabolic research explained the strong genotype-phenotype correlation in patients with *FBNI* 3' end mutations affected by the more appropriately called marfanoid-progeroid-lipodystrophy syndrome (MFLS) (Fig. 2A) (Passarge et al., 2016). In addition, the truncated C-terminus of fibrillin-1 in rabbits induced phenotypical symptoms like MFLS, confirming the potential role of fibrillin-1, and its C-terminal part in the pathophysiology of lipodystrophy (Chen et al., 2018). MFLS mutations were found to be clustered around the furin cleavage site (Fig. 2B), thereby causing heterozygous ablation of the 140-amino-acid long C-terminal cleavage product of fibrillin-1 which was only detectable at strongly reduced levels in the plasma of patients (Romere et al., 2016).

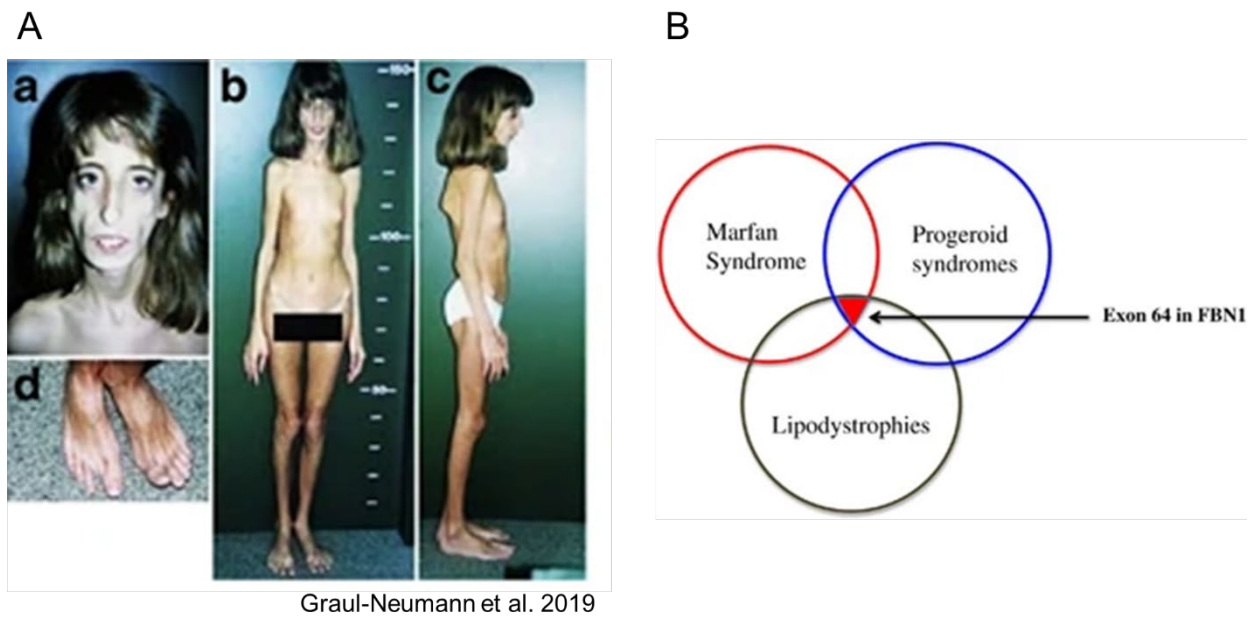


Figure 2: Lipodystrophy caused by *FBNI* mutations. **A.** Clinical manifestation of marfanoid–progeroid–lipodystrophy syndrome (MPLS). **B.** Overlapping MPLS clinical features, resulting from mutations in exon 64 of the *FBNI* gene. Modified from Passarge et al. 2016.

1.2.3 Role of fibrillin-1 in adipose tissue homeostasis

The development of adipose tissue is a series of events that starts with the differentiation of mesenchymal stem cells into preadipocytes which mature into adipocytes (Davis et al., 2016; Mariman & Wang, 2010). *In vitro* data resulting from comparative proteomic analysis and immunological techniques of differentiated mouse 3T3-L1 adipocytes revealed significant ECM remodelling events that are associated with up-and down-regulation of ECM proteins such as fibrillin-1, collagen type I, III, V, and VI, fibronectin and laminin (Fig. 3) (Choi et al., 2020; Croissandeau et al., 2002; Mariman & Wang, 2010; Muthu & Reinhardt, 2020; Ye et al., 2011). Additionally, data obtained from investigating adipogenesis of human Adipose-Derived Mesenchymal Stem cells (ADMSC) provided new insights into how fibrillin-1 is regulated during adipocyte maturation. Analysis of cells treated with adipogenic differentiation medium started to assemble a fibrillin-1 network on day 1. Interestingly, untreated cells showed a significant increase of fibrillin-1 fiber staining until day 14, although in treated cells the fibrillin-1 network started to diminish after day 3 and was hardly detected by day 14. These reported findings confirm that fibrillin-1 plays a role in the early phase of adipogenesis (Davis et al., 2016).

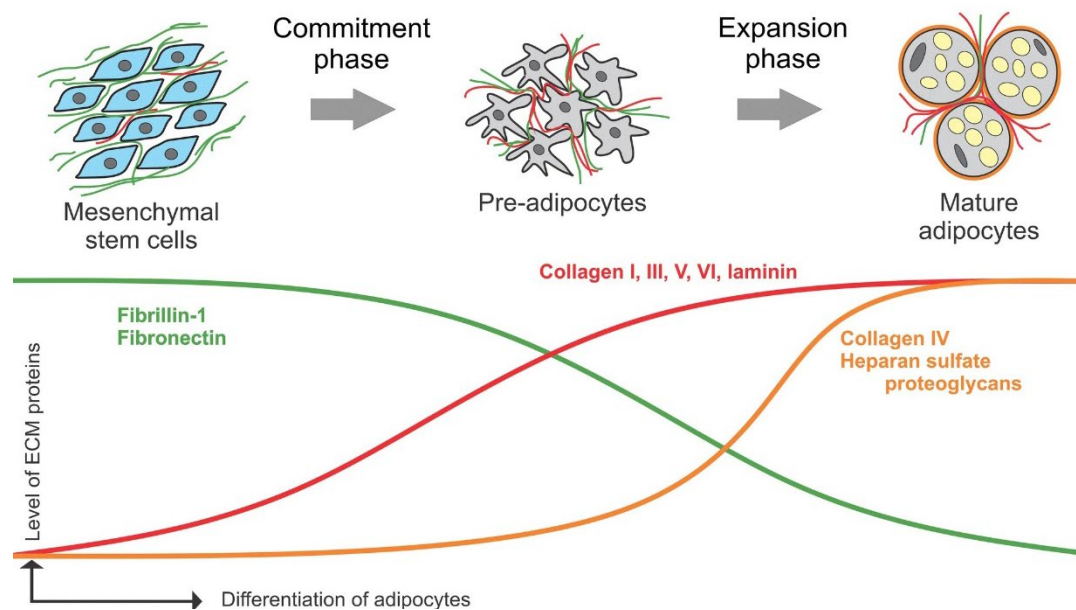


Figure 3: Schematic diagram showing relative expression changes of ECM proteins during phases of adipogenesis. Levels of ECM protein expression are depicted by colored curves. Fibrillin-1 and fibronectin (green) decrease during adipocyte differentiation. Collagen I, III, V, VI and laminin (red) expressed during differentiation and increase until final maturation. Collagen IV and heparan sulfate proteoglycans (orange) are primarily present when adipocytes are differentiated. Adapted from Muthu et al. 2020.

1.3 Asprosin, the C-terminal propeptide of fibrillin-1

During secretion, pro-fibrillins are processed to give rise to the mature forms of fibrillins by the proprotein convertase furin utilizing the consensus sequence “R-X-K/R-R”. This cleavage results in the release of C-terminal propeptides of 120-140 amino acids in length (Lonnqvist et al., 1998; Milewicz et al., 1995; Milewicz et al., 1992; Romere et al., 2016). Additionally, it has been demonstrated that only the mature fibrillin-1 can be secreted and incorporated into the ECM (Jensen et al, 2014). Secretion studies showed that mutant pro-fibrillin-1 in which the furin cleavage site was inactivated failed to leave the cell (Jensen et al., 2014). This suggests that pro-fibrillin-1 processing is essential for fibrillin-1 secretion and therefore the formation of FMF (Jensen et al., 2014).

1.3.1 Asprosin as new hormone controlling glucose release in the liver

Asprosin has been named after the Greek word for “white” because of its strong impact on white fat tissue (Romere et al., 2016). Asprosin was reported to circulate at nanomolar levels and is recruited to the liver where it induces G protein-coupled activation of the cAMP-PKA pathway and stimulates rapid glucose release into the circulation (Romere et al., 2016). Following a circadian rhythm and triggered by fasting, asprosin was shown to induce hepatic glucose release via the G-protein-coupled OLF734 receptor (Li et al., 2019; Romere et al.,

2016) and reduces insulin secretion from pancreatic β -cells (Lee et al., 2019). Asprosin has also been shown to cross the blood-brain barrier and activate hunger-stimulating AgRP (Agouti-related peptide) neurons in the hypothalamus which induces appetite in mice (Duerrschmid et al., 2017). In addition, asprosin was shown to impair insulin sensitivity in skeletal muscle cells *in vitro* (Jung et al., 2019). There are also several reports showing increased serum asprosin levels in obese patients and patients with type 2 diabetes mellitus (T2DM), as well as a positive correlation of asprosin serum concentrations with insulin resistance (Hoffmann et al., 2020). In mice, antibody-mediated neutralization of asprosin leads to reduced food intake and body weight, as well as improved insulin sensitivity (Duerrschmid et al., 2017). Therefore, asprosin currently ranges among the most promising candidates for the pharmacological therapy of obesity, T2DM and other metabolic disorders (Hoffmann et al., 2020).

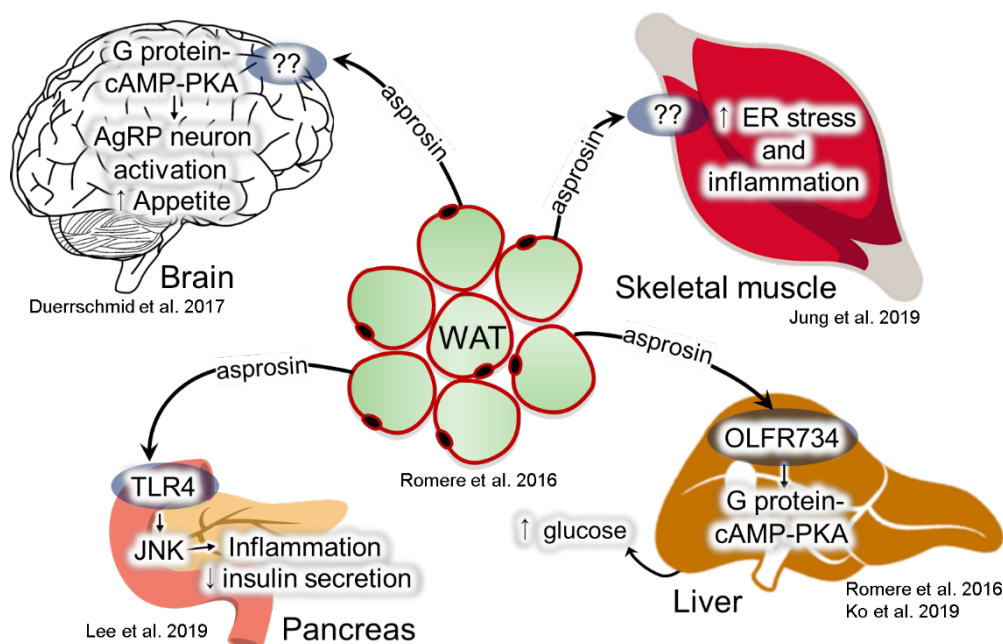


Figure 4: Overview of the function of asprosin on the metabolic system in health and disease. Asprosin stimulates hepatic glucose release, and also increases appetite via activating the AgRP neurons in the brain. *In vitro* studies showed that asprosin treatment results in apoptosis and inflammation in pancreatic B cells. Additionally, it was reported that asprosin induces inflammation and ER stress in the skeletal muscle. Modified from Janoschek et. al 2020.

Several studies have investigated the effect of asprosin *in vitro* cell culture systems. Lee et al. showed that asprosin treatment of mouse-derived pancreatic beta cells (MIN6) and human primary islets increases NF κ B phosphorylation and release of inflammatory cytokines, and therefore impaired insulin secretion. They demonstrated that the induced inflammatory response is mediated via modulation of the TLR4/JNK signalling pathway. Interestingly, an increase in TLR4 expression and JNK phosphorylation have been reported upon asprosin

treatment (Fig. 5A), and additionally, immunoprecipitation analysis demonstrated a direct interaction between asprosin and TLR4 (Lee et al., 2019). It was previously proposed that reduced insulin production and apoptosis in MIN6 cells resulted from activation of TLR4/JNK-induced inflammation (Schulthess et al., 2009). These findings suggest asprosin may be a key mediator in the pathogenesis of pancreatic beta-cells inflammation and dysfunction by altering TLR4/JNK signalling. Therefore, asprosin can be a potential therapeutic target since elevated concentrations of asprosin positively correlate with obesity (Ugur & Aydin, 2019; Wang et al., 2019), insulin resistance (Alan et al., 2019; Wang et al., 2018), diabetes mellitus type 1 (DM1) (Groener et al., 2019), and type 2 (DM2) (Naiemian et al., 2020; Zhang et al., 2019; Zhang et al., 2020).

Further, Jung et al. demonstrated that asprosin disrupts the insulin signalling pathway via PKC δ -activated ER stress and inflammation in the murine myoblast cell line (C2C12) as well as primary murine skeletal muscle (Jung et al., 2019). They reported asprosin-induced insulin resistance and impairment of glucose uptake in a dose-dependent manner. Further, they showed a reduction of insulin-stimulated IRS-1 and Akt phosphorylation after asprosin treatment. In addition, elevation of ER stress markers including PKC δ phosphorylation, and nuclear translocation as well as induction of proinflammatory cytokines were observed upon asprosin treatment (Fig. 5B). Interestingly, the increase of ER stress markers and proinflammatory cytokines were rescued after PKC δ knockdown by siRNA (Jung et al., 2019). Together, although these *in vitro* data require *in vivo* confirmation, they strongly suggest an involvement of asprosin in inflammation and insulin resistance.

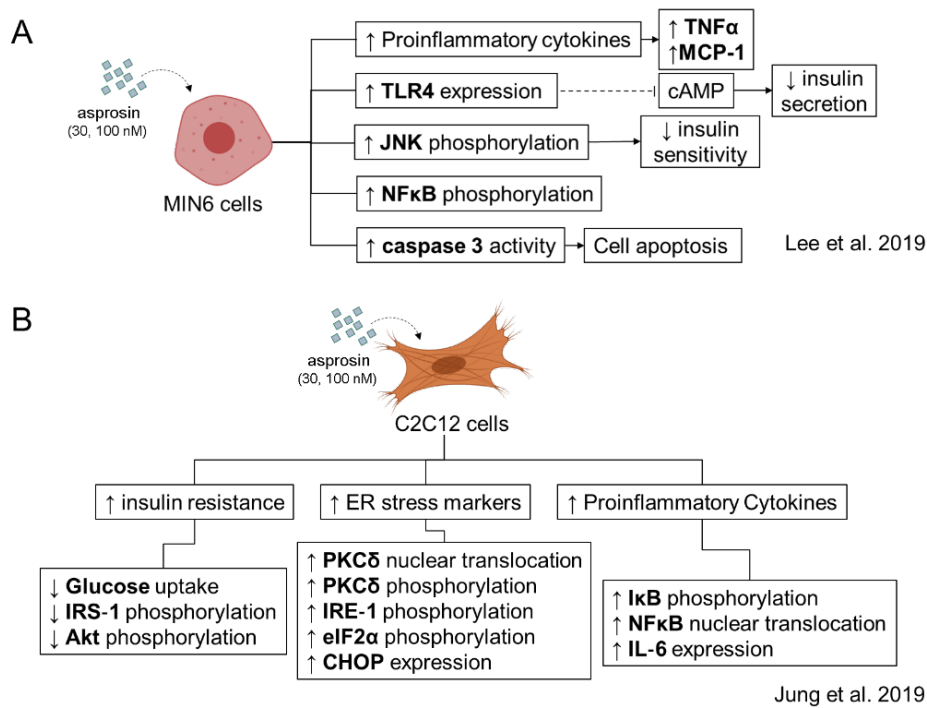


Figure 5: Summary of *in vitro* studies showing that asprosin treatment causes apoptosis and inflammation in pancreatic B cells (MIN6) (Lee et al., 2019) and inflammation and ER stress in murine myoblasts (C2C12) (Jung et al., 2019).

1.3.2 Involvement of asprosin in metabolic diseases

Extensive research has shown that asprosin engages in the pathogenesis of various diseases such as obesity, diabetes, cancer, and cardiovascular diseases (Fig. 6). Pathologically elevated asprosin levels were reported in patients with insulin resistance (Alan et al., 2019; Wang et al., 2018), diabetes mellitus type 1 (DM1) (Groener et al., 2019), diabetes mellitus type 2 (DM2) (Deng et al., 2020; Goodarzi et al., 2021; Gozel & Kilinc, 2021; Naiemian et al., 2020; Xu et al., 2022; Zhang et al., 2019; Zhang et al., 2020), as well as progressed diabetic nephropathy (Wang et al., 2021). Additionally, a significant increase in asprosin levels was observed in obese adults and children (Cheng & Yu, 2022; Corica et al., 2021; Liu et al., 2021; Ugur et al., 2022). Interestingly, treatment of obese mice with an asprosin-specific antibody resulted in a reduction in body weight and appetite, and a restoration of reduced blood glucose levels (Mishra et al., 2021). These previous findings may be important to associate the elevation in asprosin levels and the pathogenesis of cardiovascular diseases.

Moreover, data from several studies suggest an association between asprosin and cancer. Recently, asprosin has been described to be an early marker for malignant mesothelioma (Kocaman & Artas, 2020) and pancreatic cancer (Nam et al., 2022). Another research group has documented an increase in asprosin levels in invasive ductal breast cancer (Akkus et al.,

2022). Interestingly, in most patient samples an elevation of asprosin was found, a decrease in asprosin levels has been only identified in acromegaly patients (Ke et al., 2020). Further prospective clinical studies are needed to validate the findings of the aforementioned studies in other patient populations.

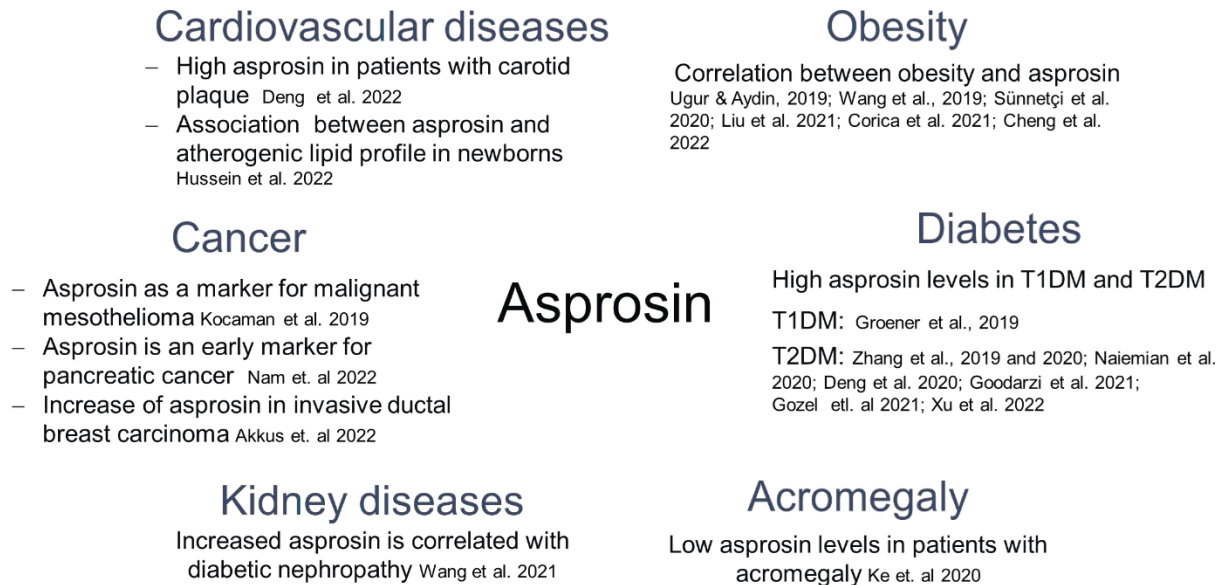


Figure 6: Summary of involvement of asprosin in various human diseases.

2. Thesis objectives

Asprosin was firstly described as fasting induced glucogenic hormone that controls hepatic glucose release and participates in the pathogenesis of various metabolic diseases. Therefore, a several studies have been conducted to establish a correlation of asprosin levels with obesity, diabetes mellitus type 1 and 2, insulin resistance, and physical exercise in defined cohorts of adults and children. In recent years, reported measurements of asprosin in clinical samples showed considerable variations across studies raising serious concerns about the reliability of the applied ELISA detection approaches (Janoschek et al., 2020).

An objective of this thesis was to establish a reliable and sensitive method for asprosin detection and measurement in biological samples across different cohorts. Additionally, the involvement of the musculoskeletal system in the production, release, and uptake of asprosin should be investigated (Fig. 7).

This thesis also aimed at providing new biochemical insight into the existence of storage mechanisms of asprosin within the extracellular microenvironment of connective tissues.

Another interesting aspect was to investigate whether asprosin storage within the ECM affects its cellular bioavailability.

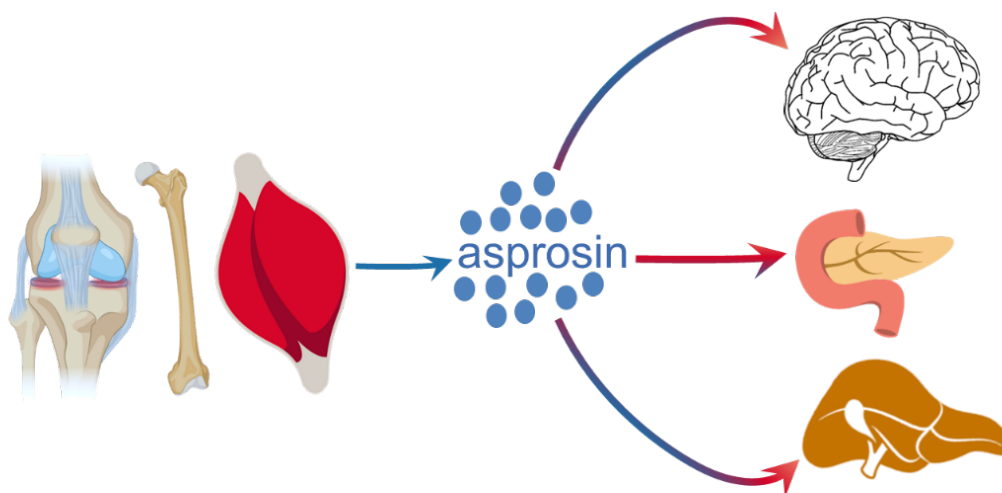


Figure 7: Schematic diagram depicting the overall hypothesis of this thesis that the musculoskeletal system is involved in metabolic reprogramming by releasing metabolically active asprosin.

3. Sensitive asprosin detection in clinical samples reveals serum/saliva correlation and indicates cartilage as a source for serum Asprosin



OPEN

Sensitive asprosin detection in clinical samples reveals serum/saliva correlation and indicates cartilage as source for serum asprosin

Yousef A. T. Morcos^{1,2}, Steffen Lütke^{1,2}, Antje Tenbrieg^{1,2}, Franz-Georg Hanisch¹, Galyna Pryymachuk³, Nadin Piekarek³, Thorben Hoffmann², Titus Keller², Ruth Janoschek², Anja Niehoff^{4,5}, Frank Zaucke⁶, Jörg Dötsch², Eva Hucklenbruch-Rother² & Gerhard Sengle^{1,2,5,7}✉

The C-terminal pro-fibrillin-1 propeptide asprosin is described as white adipose tissue derived hormone that stimulates rapid hepatic glucose release and activates hunger-promoting hypothalamic neurons. Numerous studies proposed correlations of asprosin levels with clinical parameters. However, the enormous variability of reported serum and plasma asprosin levels illustrates the need for sensitive and reliable detection methods in clinical samples. Here we report on newly developed biochemical methods for asprosin concentration and detection in several body fluids including serum, plasma, saliva, breast milk, and urine. Since we found that glycosylation impacts human asprosin detection we analyzed its glycosylation profile. Employing a new sandwich ELISA revealed that serum and saliva asprosin correlate strongly, depend on biological sex, and feeding status. To investigate the contribution of connective tissue-derived asprosin to serum levels we screened two cohorts with described cartilage turnover. Serum asprosin correlated with COMP, a marker for cartilage degradation upon running exercise and after total hip replacement surgery. This together with our finding that asprosin is produced by primary human chondrocytes and expressed in human cartilage suggests a contribution of cartilage to serum asprosin. Furthermore, we determined asprosin levels in breast milk, and urine, for the first time, and propose saliva asprosin as an accessible clinical marker for future studies.

Recently, it was discovered that the C-terminal cleavage product of profibrillin-1 serves as a fasting-induced glucogenic protein hormone that modulates hepatic glucose release¹. It is cleaved by the proprotein convertase furin in the secretory pathway and was termed “asprosin” after the Greek word for white, since it was first described to originate from white adipose tissue¹. Asprosin is released by fibrillin-1 producing connective tissues, circulates in the blood, and is recruited to the liver, where it induces G protein-coupled activation of the cAMP-PKA pathway and stimulates rapid glucose release into the circulation¹. Asprosin was also shown to directly activate appetite-promoting neurons of the hypothalamus², and neutralization of circulating asprosin with a monoclonal antibody reduced appetite and body weight in obese mice and improved their glycemic profile². Moreover, anti-asprosin

¹Center for Biochemistry, Faculty of Medicine and University Hospital of Cologne, University of Cologne, Joseph-Stelzmann-Street 52, 50931 Cologne, Germany. ²Department of Pediatrics and Adolescent Medicine, Faculty of Medicine and University Hospital Cologne, University of Cologne, Cologne, Germany. ³Department of Anatomy I, Faculty of Medicine and University Hospital Cologne, University of Cologne, Cologne, Germany. ⁴Institute of Biomechanics and Orthopaedics, German Sport University Cologne, Cologne, Germany. ⁵Cologne Center for Musculoskeletal Biomechanics (CCMB), Faculty of Medicine and University Hospital of Cologne, University of Cologne, Cologne, Germany. ⁶Dr. Rolf M. Schwiete Research Unit for Osteoarthritis, Department of Orthopaedics (Friedrichsheim), University Hospital, Goethe University, Frankfurt am Main, Germany. ⁷Center for Molecular Medicine Cologne (CMMC), University of Cologne, Cologne, Germany. ✉email: gsengle@uni-koeln.de

Figure 1. Generation of a specific polyclonal anti-asprosin antibody. (A) Domain structure of fibrillin-1 and its N- and C-terminal halves. The C-terminal propeptide sequence of fibrillin-1 after furin cleavage (furin cleavage site marked by arrow and dashed line, furin cleavage sequence underlined) yields asprosin (marked in grey). The 140 amino acids representing human asprosin S^{2732} - H^{2871} were recombinantly produced in HEK293 cells. (B) Coomassie stained quality control gel of recombinantly produced and purified (>95% purity) human asprosin. Asprosin was overexpressed with a C-terminally placed 2 × -Strep-tag II, and eluted fractions (F2-F6) after affinity chromatography were subjected to reducing SDS-PAGE using a 12% gel. (C) Mass spectrometry analysis revealed that all of the predicted three N-linked glycosylation sites (marked in red, position regarding the fibrillin-1 sequence in parentheses) are used as indicated by the +1 mass shift expected for de-N-glycosylated peptides (see also Supplementary Table S2). Underlined residues mark predicted cleavage sites of V8 and trypsin used to generate peptides of de-N-glycosylated asprosin. No unequivocal assignments of O-glycosylation sites were possible on the basis of peptide masses in MS1 spectra. Residues representing linker regions are indicated in green, thrombin cleavage (LVPRGS) site is underlined, and Strep-tag II sequences are marked in blue. (D) Removal of N-linked, as well as many common O-linked glycans, after incubation in a deglycosylation mix results in significant loss of molecular weight of human asprosin. (E) (left) Polyclonal anti-asprosin serum (pc-asp anti-asprosin antibody) raised in rabbit showed a high titer in ELISA assay detecting coated asprosin (100 ng/well). Half maximum signal was already reached at a 1:10,000 dilution. Rabbit pre-serum (before rabbit immunization) served as a control. Recombinant asprosin was coated in duplicates (100 ng/well). (right) ELISA showing high specificity of the pc-asp antibody. No cross-reactivity to the N-terminal region of fibrillin-1 (rF90), C-terminal region of fibrillin-1 (rF6), human albumin, or human IgG was detected. Data points represent mean ± SD of duplicates. (F) (left) Pc-asp antibody specifically recognizes human asprosin in western blot analysis, with no observable cross-reactivity to the N-terminal region (rF90) and C-terminal region (rF6) of fibrillin-1. (middle) Detection of N-terminal fibrillin-1 (rF90) with labmade fibrillin-1 rF90 antibody. (right) Specific detection of the C-terminal fibrillin-1 (rF6) with CPTC-FBN1-3 antibody (DSHB, Iowa, USA) which was raised against a synthetic peptide in the rF6 region. (G) Reduced signal of deglycosylated asprosin in western blot by pc-asp anti-asprosin antibody. Data were analyzed using Graphpad Prism version 8.0.2.

monoclonal antibody therapy was recently shown to be promising in the treatment of metabolic syndrome as it reduced appetite and body weight in mouse models³.

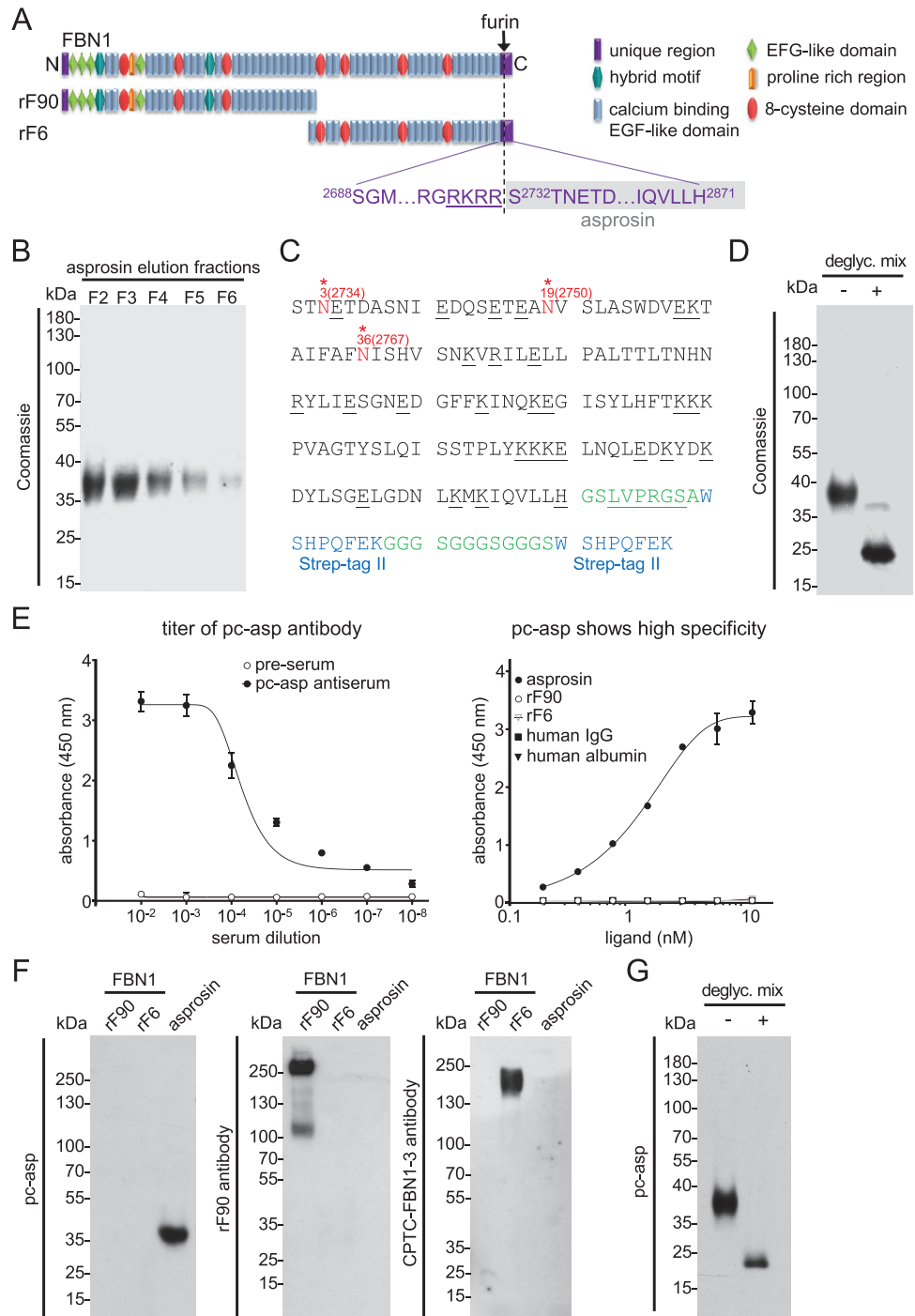
Due to its proposed crucial metabolic function, several clinical studies have been conducted to establish a correlation of asprosin levels with obesity, diabetes mellitus type 1 and 2, insulin resistance, metabolic syndrome, and physical exercise^{4–6}. However, reported measurements of asprosin in clinical samples showed considerable variations across studies raising serious concerns about the reliability of the applied ELISA detection approaches⁵. For instance, asprosin concentrations determined in blood samples from children showed huge variations of four orders of magnitude from <1 ng/ml up to >100 ng/ml^{7–10} (Supplementary Table 1). In adults reported asprosin concentrations in plasma and serum even range from <0.5 ng to >350 ng/ml (Supplementary Table 1). Additionally, the sensitivity of the employed ELISA kits appears to vary by more than one order of magnitude regarding standard detection range (0.156–10 ng/ml to 7.80–500 ng/ml), and sensitivity (0.1–2.1 ng/ml) (Supplementary Table 1).

This documented variability illustrates the need for new approaches for the sensitive and reliable measurement of asprosin in human body fluids. We therefore aimed to develop new biochemical tools and methods for asprosin detection in several body fluids. Since fibrillin-1 is known to be a structural component of the extracellular matrix architecture of connective tissue microenvironments¹¹, it is plausible that connective tissue derived asprosin contributes to blood asprosin levels. To test a potential contribution of cartilage derived asprosin to total serum asprosin levels, we measured asprosin levels in two cohorts for which release of cartilage derived components into the blood were already documented by monitoring serum levels of cartilage oligomeric matrix protein (COMP), a marker for cartilage degradation and osteoarthritis^{12,13}. We measured serum samples from athletes before and after mechanical loading by acute physical activity as well as and from osteoarthritis patients before and after hip replacement surgery. Our results not only provide new biochemical insight into the molecular requirements for sensitive asprosin detection in so far not investigated body fluids but also revealed a new correlation between asprosin levels and cartilage metabolism.

Results

Establishment of sensitive methods for human asprosin detection. *Generation of recombinant human asprosin and analysis of its glycosylation profile.* For the generation of a specific polyclonal antiserum against asprosin, we recombinantly overexpressed the human asprosin protein sequence (Fig. 1C) in HEK293 EBNA cells with a C-terminally placed double Strep-tag II for efficient affinity purification. Quality control SDS-PAGE analysis showed that asprosin was obtained with high purity after resin-coupled streptactin affinity chromatography as assessed by Coomassie staining (Fig. 1B). The molecular weight of recombinant asprosin corresponded to approximately 37 kDa, suggesting that approximately 20 kDa were added by glycosylation in HEK293 cells when compared to its calculated mass based on the amino acid sequence (Fig. 1B,C). Deglycosylation by using an enzyme mixture to remove all N-linked as well as many common O-linked glycans resulted in a band at 20 kDa which corresponds to the calculated mass of the asprosin core protein (Fig. 1D,G).

It was previously predicted that human asprosin possesses three N-glycosylation sites¹, and recently its N-glycosylation in yeast was investigated¹⁴. However, until now no data is available describing the actual sites and profiles of asprosin N-glycosylation used by human cells. To investigate these structural profiles of N-linked chains as well as to identify which N-glycosylation sites are used in human cells, we performed mass spectrometry of asprosin overexpressed in HEK293 cells after enzymatic glycan liberation and proteolytic digestion



of de-N-glycosylated peptides. Profiles of PNGaseF liberated N-glycans were characterized by one dominant high-mannose-type chain (M5) and by a prominent series of core-fucosylated complex-type chains with bi- to tetra-antennarity and sialylation with up to four residues (Supplementary Fig. S1 and Table S2). Besides these major glycans with fully processed complex-type structures, a considerable proportion of incompletely processed species of the truncated -Gal series was detected. N-Glycosylation sites were identified in the peptide mass fingerprints after de-N-glycosylation and conversion of Asn to Asp by the +1 mass shift (see Supplementary Fig. S3 and Table S3). According to these peptide mass fingerprints, all three predicted sites (N3 (N2734), N19 (N2750), and N36 (N2767)) were found to be glycosylated (Fig. 1C). Asprosin could be also O-glycosylated, as three sites in the amino-terminal region (Ser1, Thr5, Thr16) were predicted (NetOGlyc version 4.0.0.13). Chemical cleavage of O-linked chains by reductive beta-elimination revealed one signal in the MALDI survey spectrum at m/z 1706 that could be structurally assigned by PSD-MALDI-MS to a hexasaccharide alditol based on a core 2 tetrasaccharide substituted with two sialic acid residues (Supplementary Fig. S2). Based on peptide mass fingerprints of de-N-glycosylated asprosin peptides, no assignments of the O-glycosylation sites were possible.

Establishment of ELISA and SPR assays for sensitive asprosin detection. Purified asprosin was injected into a rabbit for polyclonal antibody production. The obtained serum after 60 days of immunization showed a half-maximum titer at $1:10^4$ dilution. The affinity-purified antibody showed a high specificity against human asprosin and showed no cross-reactivity to mouse asprosin or the N-terminal and C-terminal halves of fibrillin-1 (Fig. 1A) when used in western blot and direct ELISA (Fig. 1E,F and Supplementary Fig. S5D). To assess the sensitivity of the newly generated polyclonal anti-asprosin antibody (pc-asp) we employed surface plasmon resonance (SPR). Anti-asprosin antibody was immobilized onto a sensor chip and a concentration series of recombinant asprosin (0–80 nM) was flown over in solution (Fig. 2A). Obtained signals showed a linear response still in the range of 0–1.25 nM (0–50 ng/ml) (Fig. 2A, (right)). An even higher sensitivity was observed by direct ELISA when asprosin was directly coated to the microtiter well, showing a linear response in the range between 0 and 1.0 ng/ml (0–28 pM) (Fig. 2B). Next, we established a sandwich ELISA by using the newly generated pc-asp as capture and a commercially available monoclonal anti-asprosin antibody (mab-asp) (clone Birdy-1, AdipoGen Life Sciences Inc.) as detector. Titration experiments showed a linear detection signal in the range of 0–0.15 ng/ml (0–4 pM) (Fig. 2C). The linear detection range of the asprosin sandwich ELISA was 0–50 ng/ml (Supplementary Fig. S4A). Coating concentration of pc-asp as capture antibody was optimized at 3 μ g/ml, as higher coating concentrations lead to a marked decrease of the detection signal (Supplementary Fig. S4B). SPR measurements of immobilized asprosin showed that pc-asp has a molecular affinity in the < 1 nM range ($K_D = 0.29 \pm 0.30$ nM), while the K_D of mab-asp is 75-fold higher (22 ± 2 nM) (Supplementary Fig. S5A). SPR experiments also revealed that the newly generated pc-asp has a more than 100-fold higher sensitivity for immobilized asprosin compared to mab-asp (Supplementary Fig. S5B) which was also indicated by direct ELISA measurements (Supplementary Fig. S5C). The established sandwich ELISA assay can detect human asprosin with a sensitivity of < 65 pg/ml with an inter-assay coefficient of variability (CV) < 6.6% ($n = 32$), and an intra-assay CV < 5.5% ($n = 32$). We also tested any potential cross-reactivity of pc-asp against mouse asprosin and human placensin, the C-terminal propeptide of fibrillin-2 which was recently proposed to also have a metabolic function¹⁵. In direct ELISA and western blot no signals of mouse asprosin were detectable (Supplementary Fig. S5D). Also our asprosin sandwich ELISA did not detect placensin which we also overexpressed and purified with a double C-terminal Strep-tag II (Supplementary Fig. S5E–G). This finding even excluded a potential cross-reactivity of pc-asp against the Strep-tag II sequence. Deglycosylation resulted in a better detection sensitivity of asprosin by mab in ELISA (Supplementary Fig. S5H (right)) and western blot (Supplementary Fig. S5I), while direct ELISA detection by pc-asp was not altered (Supplementary Fig. S5H (left)).

Affinity column chromatography allows specific asprosin concentration and determination in serum and urine. Depending on the sensitivity of the employed assay asprosin levels in body fluids may not be detectable without pre-concentration. To selectively concentrate asprosin from body fluids we generated an affinity column by immobilizing pc-asp via CNBr to sepharose beads (Fig. 3A). After sample application, the column was washed and the captured amounts of asprosin were eluted at pH 2.5 and neutralized (see “Materials and Methods” section). Using this approach, we were able to selectively pull-down asprosin from the cell culture supernatant of RPE cells (Fig. 3B). ELISA and SPR analysis revealed an eight-fold increase of asprosin concentration by using this affinity column approach (Fig. 3B). With this approach, we were able to obtain sufficient serum asprosin amounts for western blot detection. Thereby, we could demonstrate that human asprosin circulating in serum has a molecular weight of around 40 kDa (Fig. 3C), similar to the recombinantly expressed asprosin (Fig. 1B). Utilizing the pc-asp affinity column approach allowed us also to concentrate asprosin from urine, for the first time. However, after concentration of 200 ml urine, we were able to detect about 3 ng/ml of asprosin which corresponds to 15 pg/ml present in non-concentrated urine (Fig. 3D).

Measurement of asprosin in human cell lines and clinical samples. *Secreted amounts of asprosin by human cell lines depend on tissue origin.* To test our established sandwich ELISA in complex solutions, we measured asprosin protein amounts secreted by several human cell lines into the conditioned media. Our results showed that cell lines derived from metabolically active organs such as kidney (HEK293: embryonic kidney) or liver (HepG2: liver cancer) secreted about 20-fold less asprosin into the cell culture supernatant when compared to cells derived from connective tissues such as bone (U-2 OS: bone osteosarcoma), eye (RPE: retinal pigment epithelial), lung (WI-26: fetal lung), cartilage (HCH: primary human chondrocytes derived from knee cartilage) or skin (HDF: primary human dermal fibroblasts) (Fig. 4A). However, the detected asprosin amounts correlated

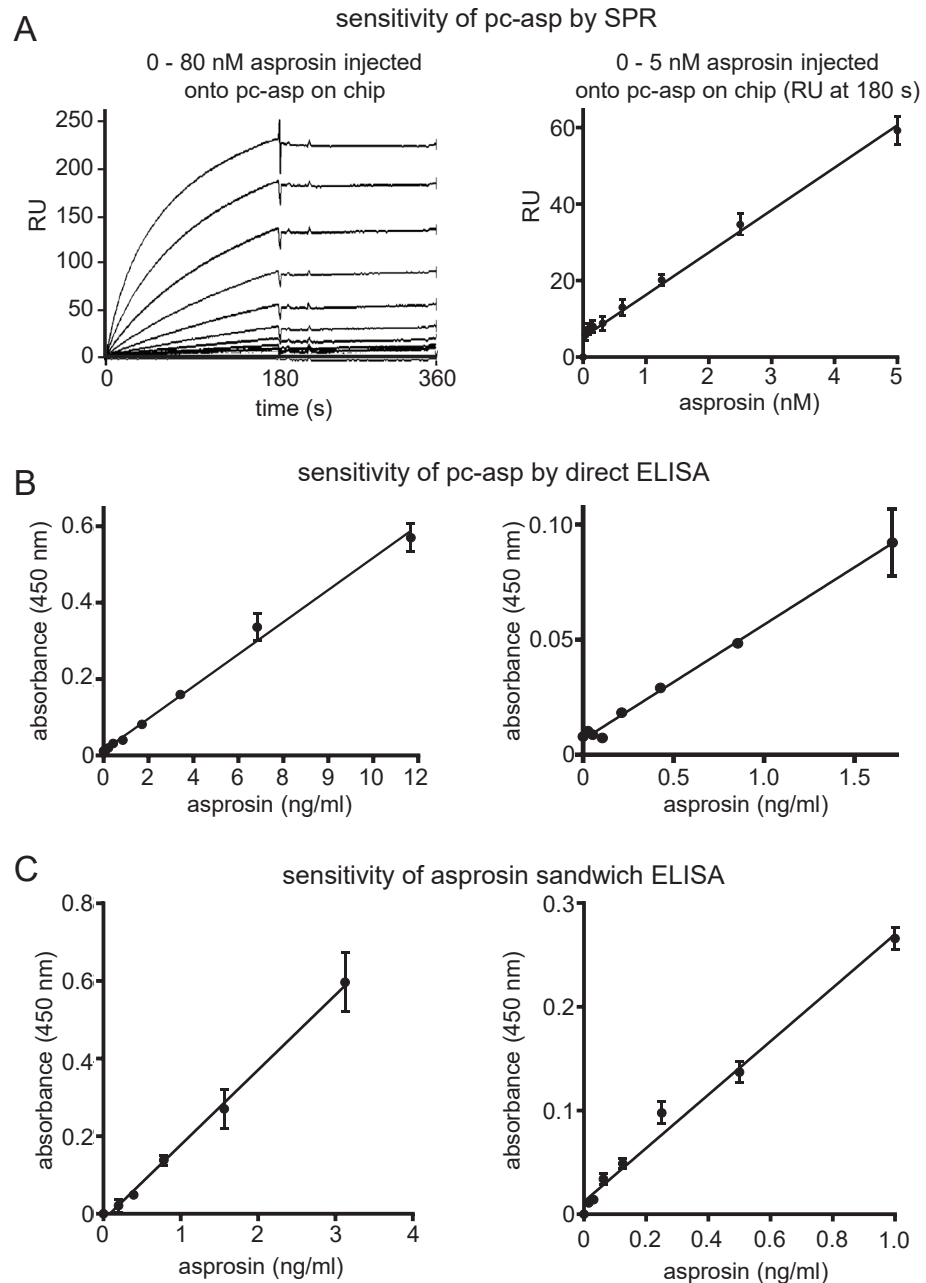


Figure 2. Establishment of assays for sensitive asprosin detection. (A) Testing of pc-asp sensitivity using surface plasmon resonance (SPR). (left) Sensorgrams showing detection of recombinant asprosin injected at 0–80 nM (0–2960 ng/ml) onto pc-asp immobilized to the sensor chip. (right) Robust and linear response of asprosin injected at 0–5 nM (0–185 ng/ml) onto pc-asp immobilized on chip. (B) Asprosin detection by direct ELISA using pc-asp as detector antibody (1:2000 dilution, 0.5 μ g/ml). Robust and linear ELISA signal response of immobilized recombinant asprosin. (C) Sensitive detection of asprosin in solution by sandwich ELISA. Pc-asp was immobilized as capture antibody (3 μ g/ml) and mab anti-asprosin (AdipoGen Life Sciences Inc., San Diego, USA) was used as detector antibody (1:2000 dilution, 0.5 μ g/ml). Data points represent mean \pm SD from duplicates. Data were analyzed using Graphpad Prism version 8.0.2.

with the secreted amounts of fibrillin-1 which were significantly higher in cells derived from extracellular matrix (ECM) protein-producing connective tissues (Fig. 4A, bottom).

Asprosin levels in serum and saliva correlate strongly and depend on biological sex and feeding status. To test the accuracy of our sandwich ELISA in clinical samples we performed spike-and-recovery and linearity-of-dilution experiments in serum and plasma (Supplementary Fig. S6). The signal recovery was not affected when our recombinant asprosin standard was serially diluted in human plasma or serum (Supplementary Fig. S6).

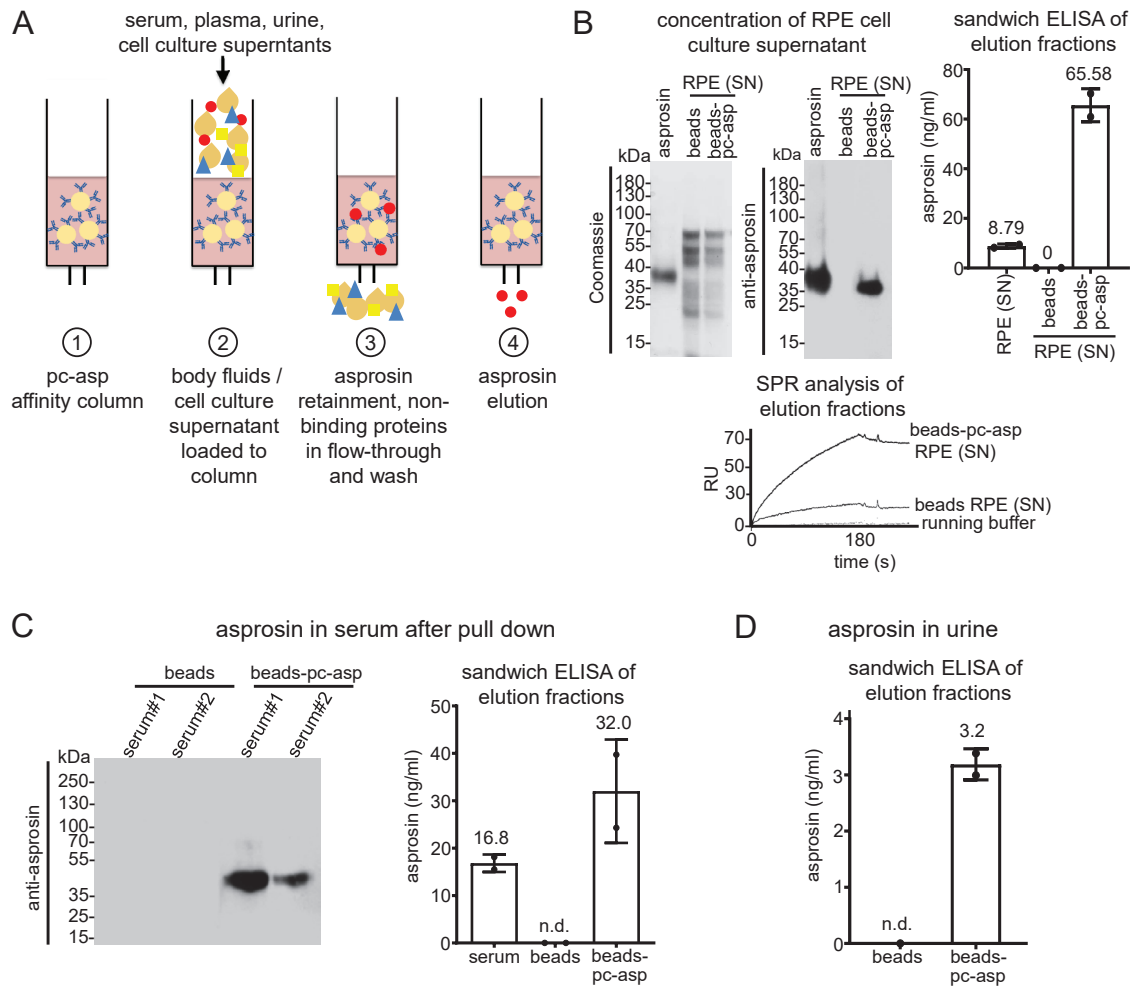


Figure 3. Affinity column chromatography allows specific asprosin concentration from serum and urine. (A) Schematic diagram showing the pull-down approach using pc-asp antibody for asprosin enrichment in cell culture supernatant and human biological samples. (B) (top left) Coomassie stain of 10% SDS-PAGE gel of recombinantly expressed and affinity-purified asprosin, pull-down from RPE media supernatant with CNBr beads (control), and pc-asp antibody coupled to CNBr beads. (top middle) Western Blot with mab anti-asprosin (1:1000, 1 µg/ml) showing specific bands of the recombinantly expressed asprosin and the endogenous asprosin of the RPE supernatant (1 L serum-free cell culture supernatant) pull-down from pc-asp antibody coupled to CNBr beads. (top right) Detection of asprosin in RPE cell culture media before and after pull-down enrichment showing an eight-fold increase of asprosin concentration by sandwich ELISA. (Bottom) Sensorgram of SPR showing detection of endogenous asprosin in RPE supernatant pull-down from CNBr beads coupled to the pc-asp antibody. Data obtained from two independent pull-down experiments. (C) (left) Western Blot analysis with mab anti-asprosin (1:1000 dilution, 1 µg/ml) of the pull-down from two human serum samples with pc-asp antibody coupled to CNBr beads showing endogenous asprosin band. (right) Quantification of the endogenous asprosin levels using sandwich ELISA in the human serum sample (1 ml serum diluted 1:10 with 10 mM Tris-HCl, pH 7.5) before and after enrichment of asprosin concentration by asprosin pull-down approach. (D) Detection of asprosin in human urine (200 ml) after enrichment using the pull-down approach. Data obtained from urine sample subjected to two independent pull-down experiments. Data were analyzed using Graphpad Prism version 8.0.2.

Measurement of serum samples from age, biological sex, and BMI matched individuals showed that asprosin levels were significantly higher in women than men (Fig. 4B). It was previously reported that asprosin serum levels increase upon fasting¹ and that asprosin can also be detected in saliva¹⁶. We were therefore interested whether a fasting-induced increase of asprosin can be also detected in saliva, and whether serum and saliva levels show a correlation. Assessment of saliva samples from the same individuals 3 h after lunch (non-fasted) or after overnight fasting (fasted) showed that fasting induced an increase of asprosin levels in saliva (Fig. 4C). We then quantified asprosin amounts in simultaneously taken serum and saliva samples from several individuals after overnight fasting and performed a Spearman correlation analysis. Our results revealed a strong correlation (Spearman correlation coefficient: $\rho = 0.9429$, $*P = 0.0167$) between asprosin levels in serum and saliva (Fig. 4D). Asprosin levels in serum and plasma from the same individuals were about ten-fold higher than in saliva. Similar

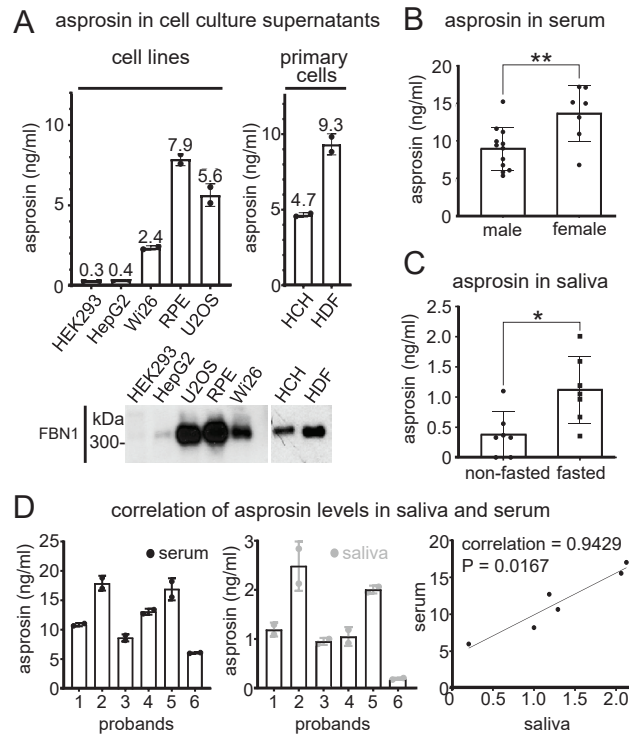


Figure 4. Asprosin levels in serum and saliva depend on biological sex, fasting, and show a strong correlation. **(A)** (top left) Endogenous asprosin levels in various human cell lines supernatants and (top right) primary human cells (human dermal fibroblasts and human chondrocytes) were measured using asprosin sandwich ELISA ($n=2$ per each group). (bottom) western blot showing the corresponding fibrillin-1 expression in cell lines supernatants. **(B)** Comparative analysis of asprosin levels in blood serum (25 μ l serum fourfold diluted in 75 μ l PBS) of male and female groups ($n=19$, $m/f=12/7$, age = 30.4 ± 6.4 years, weight (W) = 72.9 ± 11.3 kg, height (H) = 1.75 ± 0.08 m, BMI = 23.7 ± 2.9 kg/m²) using sandwich ELISA and analyzed by unpaired two-tailed t-test, $**P=0.0072$. **(C)** Assessment of asprosin levels in saliva (100 μ l saliva) in fasting (overnight fasting, 8–9 h) and non-fasting (3 h after lunch) conditions by sandwich ELISA ($n=7$, $m/f=3/4$, age = 32.3 ± 8.71 years, weight = 70.5 ± 13.8 kg, height = 1.74 ± 0.09 m, BMI = 23.3 ± 3.04 kg/m²) and analyzed by Wilcoxon matched-pairs signed-rank test, $*P=0.0156$. **(D)** (left and middle) Quantification of asprosin levels in human serum and saliva respectively in fasted condition (overnight fasting) by sandwich ELISA ($n=6$, $m/f=3/3$, age = 32.7 ± 9.09 years, weight = 64.5 ± 8.77 kg, height = 1.71 ± 0.07 m, BMI = 22.1 ± 2.44 kg/m²). (right) Correlation of asprosin levels in human serum and saliva using Spearman correlation = 0.94, $*P=0.02$, ($n=2$ per each group). Data were analyzed using Graphpad Prism version 8.0.2.

Sample	f/m	Age (years)	BMI (kg/m ²)	Asprosin (ng/ml)
Serum	7/5	31.6 ± 7.3 (27–36)	23.2 ± 3.8 (21–26)	14.7 ± 8.9 (9.1–20.4)
Plasma	7/5	31.6 ± 7.3 (27–36)	23.2 ± 3.8 (21–26)	11.5 ± 3.9 (8.9–13.9)
Saliva	8/6	30.2 ± 6.6 (26–34)	23.4 ± 3.7 (21–26)	1.07 ± 0.9 (0.5–1.6)
Breast milk	9/0	33.1 ± 4.9 (29–37)	23.4 ± 4.1 (20–27)	2.2 ± 1.4 (1.1–3.3)

Table 1. Ranges of determined asprosin concentrations (mean \pm SD) in various body fluids.

to the low asprosin concentrations detected in saliva, we detected asprosin in human breast milk in the range of (1.1–3.3 ng/ml). An overview of the ranges of detected asprosin in human body fluids is given in Table 1.

Measurement of asprosin in patient cohorts with documented cartilage turnover. *Asprosin serum levels increase after 30 min of running exercise.* Recent studies reported that asprosin serum levels are regulated by physical activity^{17,18}. For instance, it was found that plasma asprosin levels were elevated only in women upon 20 s of anaerobic exercise¹⁹. To further investigate whether physical exercise affects asprosin blood levels in men, and whether cartilage may be a potential source of serum asprosin we measured serum levels of asprosin before and after running exercise in a cohort for which release of the cartilage degradation marker cartilage oligomeric matrix protein (COMP) was already reported²⁰. 15 young male athletes (age 27.5 ± 3.1 years, Supplementary Table S7) were subjected to 30 min running exercise. Blood sampling was performed immedi-

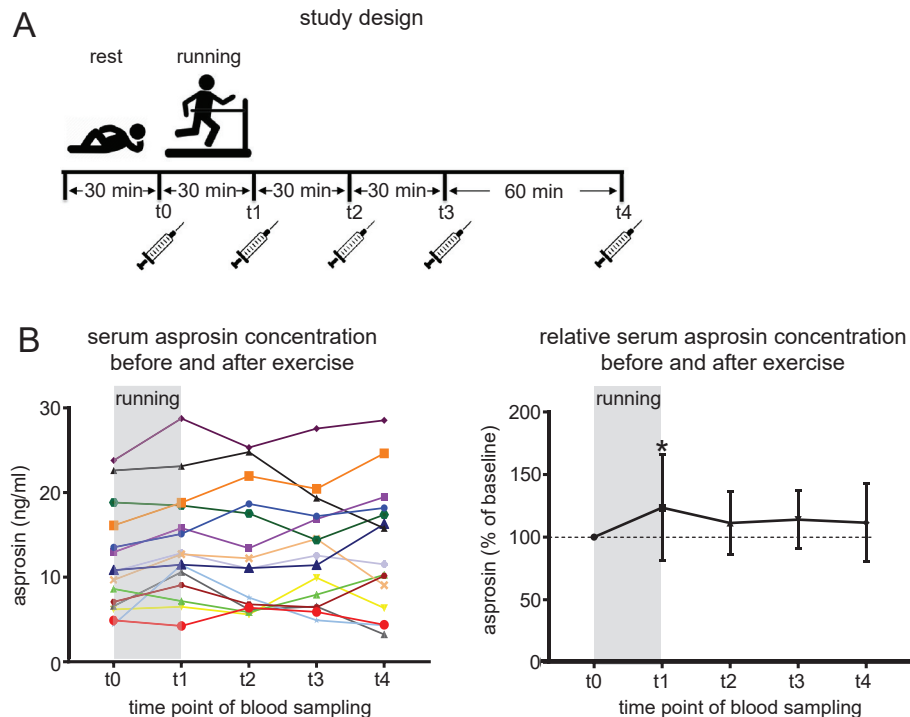


Figure 5. Asprosin serum levels increase after 30 min of running exercise. (A) Schematic diagram representing the overall study design showing exercise and rest regimens and blood sampling time points. (B) (Left) Absolute serum asprosin concentration (ng/ml) for each subject before and after running exercise ($n = 15$ subjects); t_0 : immediately before running exercise (after 30 min rest in sitting position); t_1 : immediately after exercise; t_2 , t_3 , and t_4 represent 30 min, 60 min, and 120 min after exercise, respectively. (right) Relative serum asprosin concentration after running exercise (t_1 , t_2 , t_3 , and t_4) normalized to its baseline concentration before exercise (t_0) and represented as percentage. A significant increase of asprosin concentration was observed immediately after running exercise; asprosin concentration (c) at $t_0 = 100\%$; $c(\text{asprosin } t_1)/c(\text{asprosin } t_0) = 123.7 \pm 42.3\%$; $c(\text{asprosin } t_2)/c(\text{asprosin } t_0) = 111.3 \pm 25.5\%$; $c(\text{asprosin } t_3)/c(\text{asprosin } t_0) = 114 \pm 23.40\%$; $c(\text{asprosin } t_4)/c(\text{asprosin } t_0) = 111.5 \pm 31.06\%$; $*P = 0.0385$. Serum (25 μl) fourfold diluted in PBS (75 μl) for asprosin concentration analysis. Data were analyzed using Graphpad Prism version 8.0.2.

ately before (after 30 min rest in supine position) and after the 30 min running exercise. Further blood samples were taken 30, 60, and 120 min after the end of the running exercise (Fig. 5A). Serum asprosin levels increased by about 25% on average ($123.7 \pm 42.3\%$) immediately (t_1) after 30 min running exercise and remained at an elevated but not significant level (12.5% increase) for at least 120 min after ($111.5 \pm 31.06\%$) (Fig. 5B). An overview of the determined asprosin serum levels determined in this cohort is given in Supplementary Table S4.

Asprosin levels in serum correlate with the cartilage marker COMP upon hip replacement surgery. Since we found asprosin to be secreted by primary human chondrocytes (Fig. 4A), we were interested whether serum asprosin levels correlate with cartilage related pathologies. Therefore, we measured serum asprosin levels of patients ($n = 14$) diagnosed with symptomatic hip osteoarthritis (OA) prior and after total hip replacement (THR) surgery (Fig. 6). We previously reported that COMP, a biomarker of cartilage degeneration and osteoarthritis showed a reduction, one week (t_1) after hip joint replacement surgery, and returned to pre-operative serum levels three months (t_2), and one year (t_3) post-surgery²¹. Our measurements revealed that serum asprosin levels strongly correlated with COMP levels, showing a 50% reduction at one week post-surgery before reaching 90% of pre-operative levels after three months (t_2) and up to one year (t_3) post-surgery (Fig. 6A,B, Supplementary Table S5, and S6).

Analysis of asprosin localization suggests its storage in chondrocytes and cartilage tissue. *Asprosin localization in primary human chondrocyte culture.* To further investigate the possibility of local asprosin storage in cartilage, primary human chondrocyte cultures were analyzed by immunofluorescence using pc-asp antibody (Fig. 7A). In primary human chondrocytes asprosin showed predominantly two staining patterns: a slight diffuse signal distributed in cytoplasm and in cytoplasmic processes, and intensive vesicle like structures, distributed predominantly in the cytoplasm (Fig. 7A). In most cells, both types of signals were observed simultaneously. However, an increase in signal intensity and the formation of fiber-like structures were observed in the periphery of some cytoplasmic processes (Fig. 7A), whereas less closely spaced vesicle-like structures were also detected around or in the vicinity of the cells.

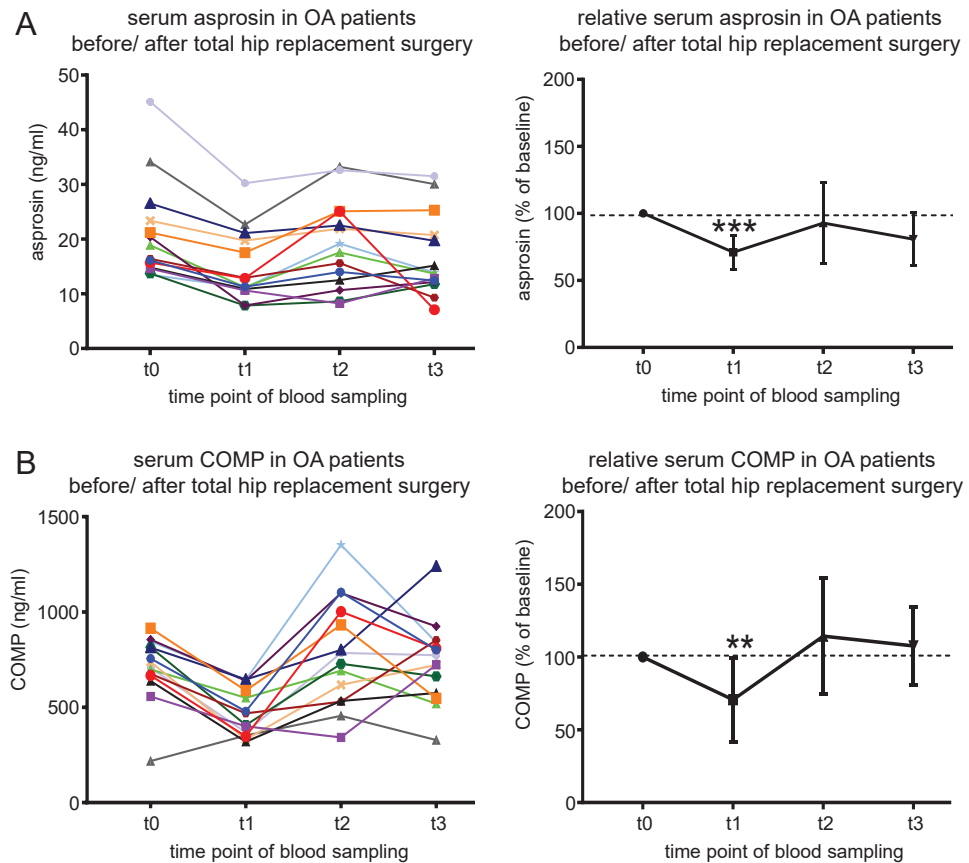


Figure 6. Asprosin levels in serum correlate with the cartilage marker COMP upon hip replacement surgery. **(A)** (left) Absolute serum asprosin (ng/ml) for each patient before and until one year after total hip replacement (THR). (right) Relative asprosin concentration after THR (t1, t2, and t3) normalized to serum asprosin at baseline (t0, before THR). **(B)** (left) Absolute serum COMP (ng/ml) for each patient before and until one year after THR. (right) Relative serum COMP (%) after THR (t1, t2, and t3) normalized to serum COMP at baseline (t0, before THR). n = 14 patients; time points: t0: within 1 week before THR, t1: 7 days postoperative, t2: 3 months postoperative, t3: about 1 year postoperative. *** $P=0.0003$, ** $P=0.0056$. Serum (25 μ l) fourfold diluted in PBS (75 μ l) for asprosin concentration analysis, and 2 μ l serum 50-fold diluted in 98 μ l PBS for COMP concentration analysis. Data were analyzed using Graphpad Prism version 8.0.2.

Asprosin localization in human cartilage. Furthermore, we investigated asprosin localization in human cartilage. The immunoreactivity of pc-asp antibody was observed, independent of the used fixatives, as an intensive signal localized to chondrocytes and their pericellular microenvironment²² (Fig. 7B, Supplementary Fig. S7). The immunoreactivity was detected in chondrocytes distributed throughout all cartilage zones. Close inspection of chondrocytes in acetone treated cryosections revealed, similar to the analysis of cultured primary chondrocytes, diffuse distributed signals surrounding the nuclei and vesicle like structures. Accumulation of vesicle like structures was observed perinuclear or in the area comparable to the lacunar space. It is noteworthy that scattered vesicles were detectable, albeit to a much lower degree and signal intensity, in the interterritorial regions. Compared to only acetone treated cryosections, the signal intensity in acetone-metanol fixed specimens appeared weaker. In 4% PFA fixed cryosections a predominantly diffuse staining pattern was seen (Supplementary Fig. S7). To increase the availability of pc-asp epitopes, we performed enzymatic antigen retrieval with empirically selected proteases. For this purpose, digestion solutions containing pepsin, hyaluronidase, proteinase K and their combination or collagenase type 1 were applied to acetone-treated sections. As expected, treatment of cartilage sections with the different enzymes separately or in combination resulted in a broader signal distribution of asprosin within chondrocyte associated areas. The strongest intensity and the largest area of chondrocyte associated asprosin signal distribution were observed when sections were treated with pepsin or enzyme mixtures (Supplementary Fig. S8). However, enzyme treatment resulted in a low preservation of morphological structures. When the sections were treated with collagenase type 1, a better preservation of cell nuclei and a significant increase of the asprosin signal were observed. Analysis of collagenase type 1 treated sections at higher magnification and in Z-stacks showed clear perinuclear signal accumulation while accumulations or clusters of vesicles-like structures distributed in the periphery of nuclei revealed a staining pattern comparable to chondrons²² (Fig. 7C).

Figure 7. Asprosin localization in primary chondrocyte cultures and cartilage tissue. (A) (left and middle) Confocal immunofluorescence microscopy of asprosin in primary human chondrocytes. Cells were incubated with pc-asp antibody (green) and DAPI (blue). Endogenous asprosin signals were predominantly observed as two staining patterns: (left, white arrows) vesicle-like structures, and (middle, white arrow heads) cytoplasmic signals with diffused distribution that significantly accumulated in cell projections forming fiber-like structures. (right) Secondary antibody only staining (negative control). These two staining patterns were simultaneously detected in the majority of chondrocytes after 11 days in culture. Shown images are representative of two independent experiments. (B) (left) Representative toluidine blue stained human articular cartilage tissue illustrating approximate thickness of the different zonal regions. (middle and right) Detection of asprosin in chondrocytes within human cartilage by confocal immunofluorescence microscopy. Overview image of cryosection from cartilage specimen fixed with acetone and incubated with pc-asp (green) and DAPI (blue) showing asprosin expression in different cartilage zones. (C) Comparative analysis of asprosin signals after acetone fixation (top panel), or acetone fixation and additional collagenase type I treatment (bottom panel). Sections were incubated with pc-asp antibody (green) and DAPI (blue). The antibody revealed both diffuse cytoplasmic signals and vesicle-like structures of asprosin as shown in overview and magnified areas (3.5-fold, marked by white boxes) under both conditions. (right) Z-projections show a prominent perinuclear and pericellular distribution of the asprosin signal. Remarkably, additional collagenase type I treatment resulted in a wider signal distribution in chondrocyte associated areas as well as in all cartilage zones. Toluidine blue staining was imaged with Zeiss AX10 light microscope and Diskus software (version number 5.0.6353 #7599). Confocal images were obtained from a Leica SP8 confocal microscope and Leica LAS AF Lite 4.0 software. Images were further processed using Fiji/ImageJ software to obtain average intensity Z-projection.

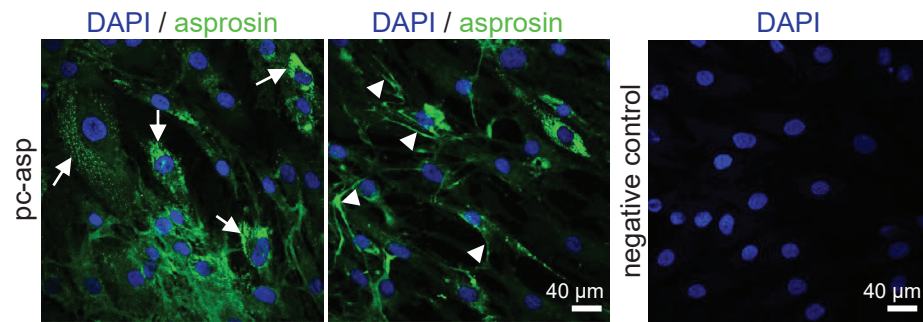
Discussion

Since its discovery as a new metabolic hormone, several clinical studies have been conducted to establish a correlation of asprosin levels with obesity, diabetes mellitus, insulin resistance, metabolic syndrome, or diabetic nephropathy^{4,6} (Supplementary Table S1). Pathologically elevated asprosin levels were reported in patients with obesity^{7,16}, insulin resistance^{23,24}, and diabetes mellitus type 1²⁵ and type 2^{26–28}. Therefore, current research attempts focus on the possibility of using anti-asprosin antibody therapy to regain metabolic health³. However, the considerable variability of reported asprosin levels in human serum, plasma, and saliva, ranging from <0.5 to >350 ng/ml raises serious concerns regarding the reliability of sensitive asprosin measurements (Supplementary Table S1). Without the availability of reliable methods for asprosin detection in clinical samples any informative correlation studies or future administration of effective anti-asprosin therapy remain futile. This prompted us to establish new biochemical approaches for the sensitive and reliable measurement of asprosin in clinical samples.

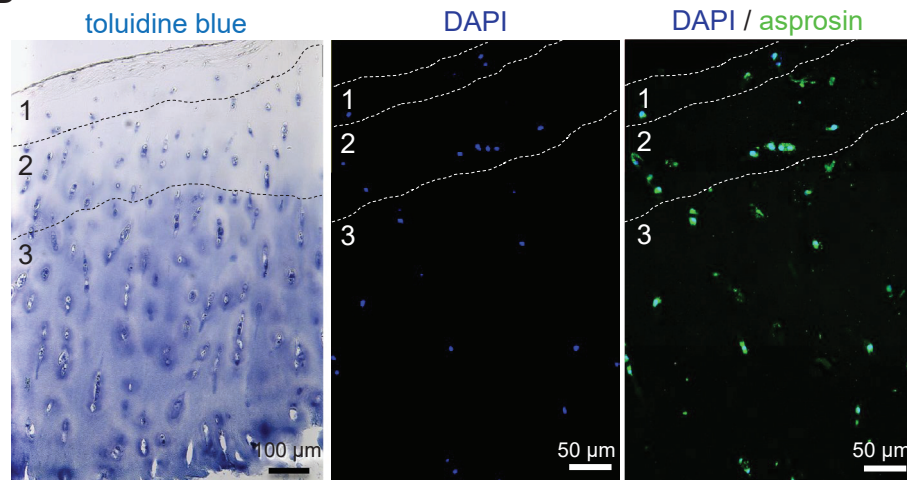
Analysis of human asprosin produced by human embryonic kidney cells revealed a significant amount of N-terminal glycosylation similar to physiological asprosin circulating in human blood (Fig. 3C) which contributes to about 50% of its molecular mass. As shown in yeast¹⁴, our analysis demonstrated that all three predicted N-glycosylation sites (N₃, N₁₉, and N₃₆) were utilized (Supplementary Fig. S3). Our analysis also showed that additional O-glycosylation of asprosin is likely (Supplementary Fig. S2). Currently, the function of asprosin glycosylation is not clear, however, similar to other proteins it is possible that it keeps asprosin more soluble and may therefore prevent its aggregation in blood²⁹. By employing our newly raised polyclonal asprosin antibody we established sensitive direct and sandwich ELISAs with a reliable detection below 0.15 ng/ml which is comparable to the stated sensitivity of commercially available ELISA kits used in previous studies⁵ (Supplementary Table S1). The high affinity of the generated pc-asp (K_D ~ 300 pM) also enabled us to selectively concentrate asprosin from complex clinical samples via antibody affinity chromatography. Using this approach we were able to determine asprosin in urine for the first time (Fig. 3D) and retrieved sufficient amounts from serum for subsequent detection by western blotting (Fig. 3C).

Our measurements suggest the following range of asprosin levels in clinical samples: serum (9–20 ng/ml), plasma (9–14 ng/ml), saliva (0.5–2 ng/ml), and breast milk (1–3 ng/ml) (Table 1). Asprosin serum and plasma levels determined by us are in agreement with ranges previously measured in large patient cohorts with over 100 individuals^{30–32} (Supplementary Table S1), suggesting that these ranges represent physiological relevant asprosin concentrations. Our investigations also provided a possible explanation for the strong deviation of reported serum and plasma asprosin levels by other studies (Supplementary Table S1). The first report about blood asprosin levels was by Romere et al.¹ who employed similar to our sandwich ELISA, a combination of polyclonal and mouse mab (capture: mouse mab against human profibrillin amino acids 2838–2865; detector: polyclonal goat against human profibrillin amino acids 2737–2750 by Abnova). However, two additional studies using the same detector but different capture antibodies reported serum asprosin levels ranging from 10–220 to 307–7454 ng/ml^{7,33}. This indicates that the choice of the capture antibody is critical for obtaining reliable asprosin measurements. Also using non-glycosylated recombinant asprosin produced in *E. Coli* for standard curve¹ generation may result in artificially skewed concentration ranges. Our biochemical investigations showed that glycosylation of asprosin may affect detection sensitivity in ELISA and western blot analysis (Fig. 1G, Supplementary Fig. S5H,I). For instance, ELISA detection sensitivity of deglycosylated asprosin by mab (clone Birdy-1) appeared to be increased (Supplementary Fig. S5H, right). Therefore, it is plausible that differences in detection sensitivity between *E. Coli* produced asprosin standards and glycosylated physiological asprosin are the underlying cause for the enormous variance of reported asprosin values. Despite 92% sequence identity between murine and human asprosin, our polyclonal antibody raised against folded and glycosylated full length human asprosin did not cross-react with murine asprosin (Supplementary Fig. S5D). Also, we so far failed to reliably detect asprosin amounts in mouse serum or plasma samples by using commercially available

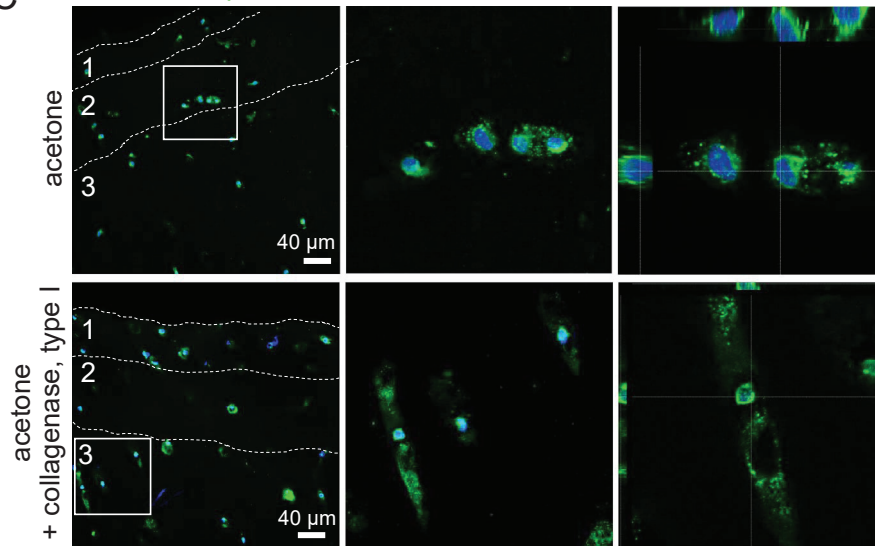
A asprosin localization in human primary chondrocyte culture



B overview of asprosin localization in human cartilage



C DAPI / asprosin magnified Z-projection



1 (superficial zone), 2 (middle zone), 3 (deep zone)

sandwich ELISA kits (unpublished results). This suggests that the availability of surface epitopes for human and murine asprosin differs. Overall, our data indicate that reported absolute asprosin levels in humans and mice should be considered with caution. For instance, it was reported that plasma asprosin levels display a circadian oscillation in mice and vary from 8 to 14 nM¹. However, similar human and murine plasma asprosin levels in the range of 5–14 nM as reported by Romere et al.¹ would correspond to 185–440 ng/ml which are at least one order of magnitude higher compared to our determined values (Table 1) and those recently measured in larger cohorts (Supplementary Table S1).

Our developed sandwich ELISA showed sufficient sensitivity to reliably detect asprosin at lower amounts in the range of 1–2 ng/ml. This allowed us to measure asprosin in breast milk, for the first time. Asprosin levels in breast milk might be an indicator of the metabolic health status of the mother, however, it may also contribute to the mother–infant communication. In the context of perinatal programming, assessing asprosin levels in breast milk might be informative, since it could be shown that other metabolic hormones like leptin, ghrelin, insulin and GLP-1 are present in breast milk and frequently correlate with the maternal BMI³⁴. Therefore, asprosin concentrations in breast milk may also depend on the maternal BMI and elicit metabolic effects in the neonate.

Our serum measurements showed that asprosin was significantly elevated in females (Fig. 4B), which is similar to previous findings³⁵. Currently, there is only limited information available regarding sex-dependent expression rates of fibrillin-1 from which asprosin is derived after furin-mediated cleavage within the C-terminal region. However, analysis of fibrillin-1 mutant mice revealed sex-dependent differences in thoracic aorta contractility, as well as aortic media injury^{36,37}. Interestingly, addition of 17 β -estradiol was found to promote fibrillin-1 production by human aortic smooth muscle cells, but not by fibroblasts³⁸, suggesting a sex- and tissue-dependent regulation of fibrillin-1 expression which may explain the observed increase of asprosin in serum samples from females.

Saliva asprosin concentration is also increased upon fasting which strongly correlated with serum asprosin levels (Fig. 4C,D). Due to the high sensitivity and low intra- and inter-assay variability compared to commercially available asprosin detection kits (Supplementary Table S1), our established sandwich ELISA may be routinely employed for the analysis of saliva as useful alternative to serum samples as its collection is simple, non-invasive and painless^{39,40}. Recently, a correlation of saliva with serum asprosin was already demonstrated and seems to be BMI-dependent¹⁶. However, the reported asprosin levels in saliva from donors with normal BMI similar to our tested cohort was reported to be around 30 ng/ml, which is 30-times higher than what we observed on average under fasting conditions (Fig. 4C, Table 1). Also recently, asprosin saliva amounts were reported to be about 25 ng/ml in a normal control group using the same commercially available ELISA kit⁴¹. Unfortunately, the kit used by both studies (Sunred Bioscience) is no longer commercially available, so that detailed information on its components and characteristics could not be retrieved.

There has been conflicting evidence reported regarding the effect of exercise on asprosin blood levels. The first report stated a sex-dependent increase of asprosin upon acute anaerobic exercise¹⁹. Serum levels of asprosin were found to be elevated only in women 15 min, 30 min, 60 min, and 24 h after a 20 s bicycle exercise. However, aerobic exercise in diabetic male rats led to a decrease of hepatic asprosin levels⁴². Recently, a significant decrease in serum asprosin was also observed in adult male individuals subjected to an aerobic exercise protocol in moderate intensity for 30 min at two different time periods of the day (morning: 08:00–10:00 h, evening: 20:00–22:00 h) at least 3 d apart. A significant decrease in asprosin serum levels was observed in normal and overweight, or obese participants of the study¹⁸. However, a comparison of absolute blood asprosin amounts determined in both studies raises concern about the informative value of the data. While Wiecek et al.¹⁹ report plasma asprosin levels in the range of 106–362 ng/ml, Ceylan et al.¹⁸ report serum asprosin levels within 0.53–1.17 ng/ml (Supplementary Table S1). Recent studies conducted with large cohorts including > 100 BMI, age, and biological sex matched controls showed that values for serum and plasma asprosin are in the same range as determined by our measurements (13–32 ng/ml) (Table 1 and Supplementary Table S1), but out of the reported ranges by both previously published exercise studies^{18,19}.

Our findings show a significant increase of asprosin after 30 min of running exercise (Fig. 5). Before the experiment, which took place in the morning, subjects were asked not to exercise for 24 h. Participants remained seated for 30 min before the first blood sample (baseline) was drawn. Our results clearly showed that upon acute running exercise asprosin release into the blood is induced and remains stable for at least 2 h afterwards. So far it is not understood by which mechanism running exercise leads to increased asprosin levels. Previously, plasma asprosin levels were reported to be increased upon a 20 s bicycle sprint in women¹⁹ which represents an exercise regime with less mechanical loading compared to treadmill running. Since these increased asprosin levels upon a low impact bicycle sprint also correlated with irisin, an exercise-induced myocyte produced cytokine⁴³, and fibrillin-1 is known to be ubiquitously expressed in connective tissues including skeletal muscle^{1,44}, muscle tissue was suggested as source of asprosin secretion¹⁹. However, since irisin and asprosin are also produced by adipocytes^{1,45} it remains difficult to assess the tissue-specific contribution to circulating asprosin levels in blood upon exercise. Measurement of asprosin in combination with tissue-specific markers may allow dissecting which musculoskeletal compartment might be challenged by a certain exercise regimen and activate asprosin synthesis or release. In this context, it is also not clear how the applied mechanical impact due to the chosen exercise regimen may be implicated in altered asprosin synthesis or release. Mechanical loading could result in cellular adaptation leading to anabolic reactions and asprosin synthesis. Alternatively, mechanical loading may lead to connective tissue degradation and thereby cause release of tissue resident asprosin into the circulation. Mechanical loading of joints due to exercise leads to degradation of cartilage and release of cartilage extracellular matrix components such as COMP into the serum^{20,46}. We previously reported that COMP levels increased upon running exercise in the same cohort²⁰. If asprosin is a component of cartilage and produced by chondrocytes (Fig. 4A), exercise induced break down of cartilage may also correlate with cartilage degradation markers such as COMP and contribute to serum levels. To test this hypothesis we analyzed asprosin and COMP levels in OA

patients before and after THR (Fig. 6). Our analysis showed a clear correlation of asprosin and COMP serum levels in both the exercise cohort and the THR cohort suggesting asprosin as component of cartilage, for the first time. Fibrillin-1 is known to be a component of cartilage and where it assembles into supramolecular microfibrils that structurally contribute to the cellular microenvironment of chondrocytes⁴⁷. It is therefore possible that also asprosin is locally stored within cartilage and released upon mechanical loading.

To further investigate the idea of local asprosin storage in cartilage, we analyzed asprosin localization in primary human chondrocyte culture and cartilage tissue (Fig. 7). Close inspection of the signal distribution in cultured primary chondrocytes and in chondrocytes embedded in cartilage tissue revealed two similar staining patterns that appeared as diffuse signals in the cytoplasm and in cytoplasmic processes, as well as vesicle-like structures (Fig. 7). Interestingly, in the periphery of some cytoplasmic processes detected signals were accumulated to fiber-like structures (Fig. 7A). Cytoplasmic processes in chondrocytes were described to be formed as active chondrocyte responses due to changes in the ECM that can result in release of cytokines or degradative enzymes⁴⁸. It appears therefore plausible that asprosin may be released into the extracellular space upon mechanical loading. Within each zone of articular cartilage the composition of the ECM is region-specific⁴⁹. This property of the matrix can significantly influence the results of immunohistochemistry, for example by inhibiting the penetration of antibodies⁵⁰. We therefore performed additional pretreatment of cartilage sections with different enzymes partially removing collagen fibers or proteoglycans. Enzyme treatment indicated that collagens, hyaluronan and other ECM components contribute to masking of asprosin detection (Fig. 7C). However, this finding still supports the hypothesis that asprosin is secreted by chondrocytes and deposited within their pericellular matrix.

Our results support the idea of local asprosin storage within tissue-specific microenvironments. Potential extracellular storage platforms could be proteoglycans or other ECM supramolecular scaffolds such as the fibronectin/elastic fiber network which have been known to act as sinks or targeting scaffolds for connective tissue derived growth factors^{11,51}. Asprosin stored in tissues may function as sensor for local energy demand. Experiments with murine myoblasts (C2C12) showed that asprosin is not only able to interfere with muscle cell insulin sensitivity⁵², but also up-regulates glucose transporter 4 (GLUT4) expression in C2C12 myotubes and thereby enhance local glucose uptake by tissue muscle cells¹⁴.

More extensive studies are required to investigate how asprosin is released into different body fluids and what exact function it serves there. Also, the mechanisms of asprosin release upon exercise require further investigation, especially considering different exercise regimen from low to high mechanical loading. Another important question is whether asprosin release is influenced by sex hormone levels which may explain the sex-specific differences we observed. Overall, our results suggest that reported absolute asprosin levels in clinical samples have to be considered with caution, since used commercially available ELISAs show a considerable variation in detection sensitivity. Our biochemical approaches and generated tools will now allow in-depth analysis of asprosin biological functions on a molecular level.

Materials and methods

Ethics statement. All research on human tissues was performed in accordance with local regulations and was approved by the Human Ethics Committee of the University Hospital of Cologne (No. 18/124, No. 15/368, No. 14-422), the local ethics committee of the Goethe University Frankfurt in Germany (No. 497/15) and the German Sport University Cologne Germany²⁰. Written Informed consent was obtained from all participating probands and patients who agreed to have materials examined for research purposes. The study was conducted in accordance with the Declaration of Helsinki.

Expression and purification of proteins. Human asprosin (S²⁷³²-H²⁸⁷¹) and human placensin (S²⁷⁸⁰-Y²⁹¹²) DNA sequences were generated by GeneArt Strings DNA Fragments service (Thermo Fisher Scientific, Massachusetts, USA) including the restriction enzymes sequences for NheI at the 5' and XhoI at the 3' ends. Double stranded synthetic cDNAs encoding for the respective protein sequences were cloned via the NheI/XhoI sites of the modified pCEP-Pu vector containing an N-terminal BM-40 signal peptide and a C-terminal double Strep-tag II downstream of the XhoI restriction site⁵³. Ligated vectors were transformed into One Shot TOP10 Chemically Competent *E. coli* (Thermo Fisher Scientific, Massachusetts, USA), and clones were verified by Sanger sequencing (Microsynth Seqlab GmbH, Göttingen, Germany). HEK-293 EBNA cells cultured in Dulbecco's modified eagle medium (DMEM) (Thermo Fisher Scientific, Massachusetts, USA) were transfected with asprosin or placensin expression vectors by using FuGENE HD Transfection Reagent (Promega GmbH, Germany) according to the manufacturer's instructions. One day after transfection, cells were selected by supplementing the medium with puromycin (1 µg/ml). The cells were expanded for large scale production in TripleFlask Cell Culture Flasks (Thermo Fisher Scientific, Massachusetts, USA). At 90% confluency, cells were incubated with serum-free DMEM containing puromycin (0.5 µg/ml) and collected after 48 h. Collected medium was filtered with a suitable membrane filter, then subjected to Strep-Tactin XT gravity flow columns (2 ml beads; IBA GmbH, Germany) at 4 °C overnight. Asprosin or placensin were eluted with elution buffer (100 mM Tris/HCl, pH 8.0, 150 mM NaCl, 1 mM EDTA, 2.5 mM desthiobiotin). The collected fractions were analyzed by Coomassie Blue Staining, concentrated and the buffer exchanged to PBS by using Amicon Ultra Centrifugal Filters (cut-off: 3 kDa) (Merck Millipore, Burlington, MA, USA). The N-terminal half of fibrillin-1 (rF90, amino acids positions: M¹-V¹⁵²⁷) with a C-terminal His₆-tag was overexpressed in HEK-293 EBNA cells followed by purification as described previously⁵⁴. C-terminal half of fibrillin-1 (rF6, amino acids position: amino acid positions V¹⁴⁸⁷-H²⁸⁷¹) was overexpressed in HEK-293 EBNA cells. The overexpression construct for rF6⁵⁵ was a kind gift from Lynn Sakai, Oregon Health and Science University, Portland, OR, USA. Recombinant human (#761902) and mouse (#762002) asprosin were purchased from Biologend (San Diego, CA, USA).

Antibodies. The pc-asp anti-asprosin antibody was generated against full-length human asprosin. Recombinantly expressed human asprosin was used to immunize a rabbit for antibody production (Pineda Antibody Service, Berlin, Germany). Preimmune serum (0.5 ml) was obtained before the immunization of the rabbit and did not show cross reactivity to asprosin tested by ELISA. The rabbit was immunized with a total amount of 500 µg asprosin in five consecutive immunizations at days 1, 14, 28, 42, and 56. The antiserum was obtained 60 days after immunization. The antiserum was affinity purified on a column of CNBr-activated Sepharose 4B (Cytiva, Uppsala, Sweden) conjugated with the recombinantly expressed asprosin (300 µg) according to the manufacturer's instructions. The antibody was eluted with 0.1 M glycine (pH 2.5) and neutralized with 3 M Tris/HCl, pH 8. The eluted antibody was concentrated by using Amicon Ultra Centrifugal Filters (cut-off: 10 kDa), (starting volume: 6 ml, end volume: 1 ml). The antibody was used as a capture antibody for sandwich ELISA at 3 µg/ml, at a 1:5000 dilution (0.2 µg/ml) for western blot, and at a 1:70 dilution (14 µg/ml) for cells and tissues immunofluorescence. Mab anti-asprosin antibody (clone Birdy-1, AG-20B-0073) (AdipoGen Life Sciences Inc., San Diego, USA) was used at a 1:1000 dilution (1 µg/ml) for western blot and at a 1:2000 dilution (0.5 µg/ml) as detection antibody in sandwich ELISA. Fibrillin-1 polyclonal antibody, raised against C-terminally His₆-tagged rF90 representing the N-terminal half of fibrillin¹⁵¹, was used at a 1:5000 dilution (0.5 µg/ml) for western blot. Fibrillin-1 rabbit monoclonal antibody (CPTC-FBN1-3) (DSHB, Iowa, USA), raised against the synthetic peptide: TCVDINECLEPR, which is contained within the C-terminal half of fibrillin-1, was used at a 1:2500 dilution (1 µg/ml).

Protein quantification. Concentrations of proteins, which were used in this study including pc-asp antibody were colorimetrically measured by BCA Protein Assay Kit (Thermo Fisher Scientific, Massachusetts, USA). In addition to the BCA assay, the concentrations of purified asprosin and placensin were spectrophotometrically measured by NanoDrop One (Thermo Fisher Scientific, Massachusetts, USA) after buffer exchange into PBS using Amicon Ultra Centrifugal Filters (cut off: 3 kDa). The protein quantification was performed using the program "Protein A280" which measures the protein absorbance at 280 nm and calculates the concentration depending on the protein extinction coefficient. The predicted extinction coefficient for human asprosin-2 × Strep-tag II: 25,440 M⁻¹ cm⁻¹, and human placensin-2 × Strep-tag II: 19,940 M⁻¹ cm⁻¹, were obtained by using the ProtParam tool provided on the ExPASy Server.

Cells. HEK293 EBNA and HEK293 (adherent epithelial cells of human embryonic kidney/ATCC CRL-1573), U2OS (adherent osteosarcoma cells from human bone/ATCC HTB-96), WI-26 (human lung fibroblast cell line/ATCC CCL95), hTERT RPE (adherent human retinal pigment epithelial cell line/ATCC CRL-4000), Hep G2 (adherent human liver cancer cell line/ATCC HB-8065), and HDF (primary human dermal fibroblasts) as well as HCH (primary human chondrocytes) were established from biopsies. Cells were cultured in DMEM with 10% fetal calf serum (FCS) and 1% penicillin/streptomycin, they were grown in incubators maintained at 37 °C and 5% CO₂. The cells were fed twice per week and split regularly.

Affinity chromatography with pc-asp column. Affinity purified pc-asp anti-asprosin antibody was coupled to CNBr-activated Sepharose 4B beads according to the manufacturer's instructions. 500 µg of purified pc-asp anti-asprosin antibody dialyzed in 0.1 M NaHCO₃, pH 8.3 containing 0.5 M NaCl (coupling buffer) was incubated with 0.5 ml CNBr agarose beads and the mixture was kept rotating at 4 °C overnight. The uncoupled sites on beads were blocked with 0.1 M Tris-HCl, pH 8.0 for 2 h at RT. Poly-Prep Chromatography Columns (Bio-Rad; Hercules, USA) were packed with uncoupled CNBr beads (negative control column) and pc-asp anti-asprosin antibody coupled CNBr beads (asprosin pull-down column). The two columns were connected in series respectively, and then samples were applied to the two columns pull-down system. Prior to application, 1 L serum-free cell culture supernatant from RPE cells or 200 ml urine were filtered through a 0.22 µm filter unit (Sterile Steritop Bottle, Merck Millipore, Darmstadt, Germany) followed by pH adjustment to 7.5 with 5 M NaOH solution. For the application of serum samples, 1 ml of serum was diluted 1:10 with 10 mM Tris-HCl, pH 7.5, and filtered through a sterile 0.22 µm syringe filter. After the samples were loaded and passed through the columns at 4 °C, the columns were washed with 100 ml of 10 mM Tris-HCl, pH 7.5. Recovery of bound proteins in the negative control and asprosin pull-down columns was done by elution in six column volumes 0.1 M Glycine (pH 2.5) and neutralization of the elution fractions with 3 M Tris-HCl, pH 8. Eluted fractions were concentrated followed by buffer exchange using Amicon Ultra Centrifugal Filters with a molecular cut-off of 3 kDa. Concentrated elution fractions were subjected to SDS-PAGE followed by Coomassie staining, western blotting, or SPR.

Enzymatic cleavage of N-glycans. The sample was placed into an Amicon Ultra centrifugation device with a 10 kDa cut-off and centrifuged at 14,000 × g (4 °C) for 10 min to exchange the buffer (0.1 M ammonium bicarbonate buffer, pH 8.0). To 20 µg asprosin in 20 µl buffer a 0.5 µl aliquot of PNGaseF (BioLabs, 250 units, containing glycerol) was added and incubated for 16 h at 37 °C. The sample was dried by vacuum rotation and taken up in 0.1% aqueous trifluoroacetic acid (100 µl) before solid-phase extraction on C18 (see below).

Solid-phase extraction of de-N-glycosylated peptides. The cartridge was activated with 80% acetonitrile/0.1% aqueous TFA and equilibrated with 0.1% aqueous TFA. The sample was applied and the run-through and wash fractions were collected in glas vials and dried by vacuum rotation.

Chemical cleavage of O-glycans. The sample was taken up in 50 μ l of 50 mM sodium hydroxide/1 M sodium borohydride and incubated for 16 h at 50 °C. The reaction was stopped by addition of a 50% aqueous solution of acetic acid. Desalting of the sample was performed in a batch procedure with a 50% Dowex 50Wx8(H+) water suspension. Borate in the dried sample was removed by distillation from acidified methanol as borate methylester in a flow of nitrogen at 40 °C. The samples (O-glycan alditols) were desalted and separated from protein/peptide contaminants by solid-phase extraction on graphitized carbon (Extract-Clean columns, Carbograph, 150 mg, 4.0 ml, Alltech, Nettetel, Germany).

Methylation of glycans and MALDI mass spectrometry. In brief, the methylation of extensively dried samples was performed according to the method by Ciucanu and Kerek based on finely powdered sodium hydroxide in dry DMSO/methyl iodide⁵⁶. Methylated glycans in methanol or peptides in 0.1% aqueous TFA were applied onto a MALDI stainless steel target (Bruker) together with an equal volume of matrix (α -cyano-4-hydroxy-cinnamic acid, saturated solution in 50% acetonitrile/0.1% aqueous TFA). MALDI-MS analysis was performed in the positive ion reflectron mode (HV acceleration 25 kV) on an UltrafleXtreme MALDI-TOF-TOF mass spectrometer (Bruker Daltonics) using the acquisition software FlexControl 3.3 and the data evaluation software FlexAnalysis 3.3 (Bruker Daltonics). Peptide and glycan sequencing was performed by laser-induced dissociation (LID) in the post-source decay (PSD) mode. Mass annotation was performed in FlexAnalysis and peak lists were generated after manual inspection of the entire mass range for correct isotope peak annotation. The molecular masses of the alditols ($M + Na$) were searched in standard mass lists, and finally identified by MS/MS using the fragmentation annotation tool provided in the GlycoWorkBench platform. Peptide identification was assisted by the Protein Prospector tool MS-digest.

Characterization of pc-asp anti-asprosin antibody. To test the specificity and sensitivity of pc-asp anti-asprosin antibody, recombinant asprosin, N-terminal fibrillin-1 (rF90), C-terminal fibrillin-1 (rF6), human albumin, and human IgG (Sigma-Aldrich, Darmstadt, Germany) were diluted in PBS and coated to the wells of a 96-well ELISA plate in 100 μ l/well followed by overnight incubation at 4 °C. After washing with PBS containing 0.05% Tween 20 (PBST), the wells were incubated with 5% milk in PBS for 2 h for blocking. Purified pc-asp anti-asprosin antibody was diluted 1:10,000 in 2.5% milk in PBS and applied to the wells for 1 h at RT. The wells were washed three times with PBST, and mouse anti-rabbit IgG-HRP conjugate (#211-032-171, Jackson ImmunoResearch, Pennsylvania, USA) was then added at dilution 1:2000 in 2.5% milk in PBS and incubated for 30 min at RT. After washing the wells with PBS, the signal was developed by adding 1-Step Ultra TMB-ELISA Substrate Solution (Thermo Fisher Scientific, Massachusetts, United States) followed by an incubation for 1–3 min. The reaction was stopped with an equal volume of 30% H₂SO₄ (stopping solution) and the optical density (OD) was measured 450 nm.

Asprosin sandwich ELISA. Pc-asp anti-asprosin antibody (capture antibody) was coated at 3 μ g/ml in antibody coating buffer (50 mM carbonate/bicarbonate buffer, pH 9.6) on 96-well ELISA plates in a volume of 100 μ l/well and incubated at 4 °C overnight. Unbound antibodies were washed off with PBST. The plate was incubated with 200 μ l of 5% milk in PBS for 2 h. Asprosin standard, human serum, and plasma samples were diluted in PBS. Cell culture media, breast milk, saliva samples, and pull-down fractions were added directly to the ELISA plate. After incubating 100 μ l of a serial dilution of asprosin standard and samples at RT for 2 h, the plate was washed for three times with PBST. 100 μ l of mab anti-asprosin antibody (detection antibody) were added to the plate at a dilution of 1:2000 (0.5 μ g/ml) in 2.5% milk in PBS for 1 h at RT. The plate was washed three times with PBST before adding 100 μ l of rabbit anti-mouse IgG-HRP conjugate (secondary antibody) at 1:2000 in 2.5% milk in PBS for 30 min at R.T. After final three washes with PBS, 100 μ l of 1-Step Ultra TMB-ELISA Substrate Solution was added and incubated for 15–20 min for color development. The reaction was stopped with an equal volume of 30% H₂SO₄ (stopping solution) and the optical density (OD) was read at 450 nm. Inter-assay CV was determined for identical sample duplicates analyzed using two different plates from the same lot number on the same ELISA plate reader. Intra-assay CV was determined for identical sample duplicates on the same plate.

Western blot. Protein samples were mixed with Laemmli Sample Buffer (Bio-Rad, Hercules, USA) containing 10% (v/v) β -mercaptoethanol and heated to 95 °C for 10 min. Samples were subjected to electrophoresis on 10%, 12%, or 7.5% SDS-PAGE. Proteins were stained using Coomassie Blue Staining. For western blotting, proteins are separated by SDS-PAGE, transferred to PVDF transfer membrane, 0.45 μ m (Thermo Fisher Scientific, Massachusetts, United States). Membranes were blocked with Pierce Protein-Free (TBS) Blocking Buffer (Thermo Fisher Scientific, Massachusetts, United States) for one hour, then incubated with the following primary antibodies: pc-asp anti-asprosin antibody, 1:5000 (0.2 μ g/ml), mab anti-asprosin antibody (clone Birdy-1), 1:1000 (1 μ g/ml), fibrillin-1 (rF90) 1:5000 (0.5 μ g/ml), fibrillin-1 rabbit monoclonal antibody (CPTC-FBN1-3) 1:2500 dilution (1 μ g/ml). and secondary antibody, mouse anti-rabbit IgG-HRP conjugate or goat anti-mouse IgG-HRP conjugate, 1:5000. All antibodies were diluted in blocking buffer. Signals were developed with Super-Signal West Pico PLUS Chemiluminescent Substrate (Thermo Fisher Scientific, Massachusetts, USA). Blotted PVDF membranes used for Fig. 1F were cut and incubated with indicated primary antibodies.

Cartilage sample preparation. Tibial plateau was obtained from one patient undergoing routine total knee joint replacement surgery. The resected tissue was incubated in isotonic sodium chloride solution 0.9% and kept for less than 3 h at 4 °C before macroscopic observation. Based on the morphological appearance (color and gloss) of the cartilage surface, a small region of healthy cartilage was selected at the lateral periphery of the

plateau and further processed. A piece of cartilage was dissected using a scalpel and embedded in OCT (Thermo Fisher Scientific, Massachusetts, USA), snap frozen and kept in -80 °C freezer until cryosectioning.

Immunofluorescence and toluidine blue staining. To identify the optimal tissue fixation and treatment for asprosin detection by the pc-asp anti-asprosin antibody, air-dried cartilage cryosections were subjected to one of the following preparations: (1) fixed with -20 °C ice cold acetone or acetone:methanol (1:1) mixture and then incubated at 4 °C for 4 min, dried for 60 min at room temperature and then rehydrated with PBS for 10 min; (2) fixed with 4% paraformaldehyde for 10 min at room temperature and washed three times with PBS for 10 min. Afterwards, sections treated with 0.1% Triton X-100 plus 0.05% Tween-20 in PBS for 15 min. For enzyme digestion, air-dried acetone treated and rehydrated cryosections were directly submitted to further incubation in the corresponding digestion solutions: pepsin digestion: 0.025% pepsin (#516,360, pepsin from porcine stomach mucosa, Sigma-Aldrich, Darmstadt, Germany) in 0.2 N HCl for 10 min at 37 °C; hyaluronidase digestion: 1 mg/ml hyaluronidase (#H3506, hyaluronidase from bovine testes, Sigma-Aldrich, Darmstadt, Germany) in digestion buffer (0.1 M sodium dihydrogen phosphate (NaH_2PO_4), 0.1 M sodium acetate (NaOAc, pH 5.0) for 10 min at 37 °C; proteinase K digestion: 10 µg/ml proteinase K (#EO0491, Thermo Fisher Scientific, Massachusetts, USA) in 50 mM Tris-HCl pH 7.5 for 1 h at 55 °C; collagenase type I digestion: 1 mg (125 Unit) of collagenase I enzyme (#LS004194, CellSystems GmbH, Troisdorf, Germany) reconstituted in 1 ml HBS buffer (#14,025,092, Thermo Fisher Scientific, Massachusetts, USA), diluted at 1:100 in HBS buffer, and incubated with the sections for 30 min at 37 °C. After digestion, sections were rinsed for 3 min with PBST (PBS with 0.05% Tween 20), then incubated with 0.2% Triton X-100 in PBST for 15 min. All specimens were then proceeded identical: incubated in blocking solution (5% normal donkey serum (Dako) containing 0.05% Tween 20 in PBS for 1 h at room temperature and then incubated with pc-asp anti-asprosin antibody at a 1:70 dilution in Antibody Dilution Buffer (AKV-Puffer) (Fa. DCS # AL120R100, Germany) containing 1 µg/mL DAPI (Thermo Fisher Scientific, Massachusetts, USA) for 1 h at room temperature, followed by two washing steps with PBST for 5 min. Slides were incubated with secondary antibody donkey anti-rabbit Alexa 568 (#A10042, Invitrogen, Thermo Fisher Scientific, Massachusetts, USA) diluted 1:300 in AKV-Puffer for 1 h in the dark at room temperature, followed by two washes with PBST for 1 min and a final PBS wash for 1 min. Slides were coverslipped with ProLong Gold Antifade Mountant (#P36934, Thermo Fisher Scientific, Massachusetts, USA).

For immunofluorescence chondrocyte cultures, chondrocytes were seeded on uncoated glass coverslips at a density of 1×10^5 cells per well in 12-well plates. Cells were kept in culture for 12 days, then washed with PBS for 5 min, fixed with ice cold acetone:methanol (1:1) for 10 min at -20 °C, blocked with 1% bovine serum albumin (#11,930.03, SERVA Electrophoresis GmbH, Heidelberg, Germany) in PBS, and then incubated with pc-asp anti-asprosin antibody (1:70) in 0.5% BSA in PBS for 1 h at room temperature. The coverslips were washed two times with PBST for 5 min and incubated with secondary antibody goat anti-rabbit Alexa 555 (# A27039, Invitrogen, Thermo Fisher Scientific, Massachusetts, USA) for 30 min in dark at room temperature, then washed two times with PBST for 1 min and one time with PBS for 1 min. Subsequently, coverslips were air-dried for 10 min and mounted to the slide using ProLong Gold Antifade Mountant with DAPI. Confocal images were obtained using a Leica SP8 confocal microscope (Leica Camera AG, Germany) and Leica LAS AF Lite 4.0 software. Images were further processed using Fiji/ImageJ software to obtain average Intensity Z-projection.

Cartilage cryosections with 10 µm thickness were stained with Toluidine Blue O (#1B481, Chroma-Gesellschaft Schmid GmbH & Co., Köngen, Germany) according to the following procedures: sections were dried for 1 h at 37 °C, washed in distilled water for three times, stained in Toluidine Blue O working solution for 2 min, washed in distilled water for 3 times, dehydrated quickly in 95% ethanol and then in 100% ethanol for two times, washed in xylol two times for 3 min, and coverslipped with EUKITT UV O. Kindler EUKITT UV mounting media (ORSAtec GmbH, Germany). Toluidine-stained cartilage sections were imaged with Zeiss AX10 light microscope equipped with Zeiss plan-Neofluar 10 ×/0.3 objective, Hitachi HV-F202 camera and Diskus software (version number 5.0.6353 #7599).

Surface plasmon resonance. SPR experiments were performed as described previously⁵⁷ using a BIAcore 2000 system (BIAcore AB, Uppsala, Sweden). Pc-asp anti-asprosin antibody was immobilized at 8000 RUs to a CM5 sensor chip using the amine coupling kit following the manufacturer's instructions (Cytiva, Uppsala, Sweden). Interaction studies were performed by injecting 0–80 nM recombinant asprosin and RPE supernatant pull-down fractions in HBS-EP buffer (0.01 M HEPES, pH 7.4, 0.15 M NaCl, 3 mM EDTA, 0.005% (v/v) surfactant P20) (Cytiva, Uppsala, Sweden). Human asprosin was immobilized at 500 RUs to a CM5 sensor chip using the amine coupling kit. Interaction studies were performed by injecting 0–40 nM pc-asp, mab and Strep-ab in HBS-EP buffer. Kinetic constants were calculated by nonlinear fitting (1:1 interaction model with mass transfer) to the association and dissociation curves according to the manufacturer's instructions (BIAevaluation version 3.0 software). Apparent equilibrium dissociation constants (K_D values) were then calculated as the ratio of k_d/k_a .

Exercise study. Fifteen male healthy participants, age = 27.5 ± 3.1 years, weight = 78 ± 7.7 kg, height = 1.81 ± 0.05 m, BMI = 23.9 ± 1.9 kg/m² were recruited by German Sport University Cologne, Cologne, Germany to study the effect of exercise on the serum asprosin level (Supplementary Table S7). Inclusion criteria were age from 20 to 35 years and physical fitness. Exclusion criteria were musculoskeletal disorder, acute and chronic injuries, trauma or surgery of lower extremities' joints. Subjects were asked not to exercise 24 h prior to the study and to come to the institute either by car or public transportation. The subjects remained seated for 30 min before the first blood sampling (t0). Further blood samples were drawn immediately afterwards (t1), and then 30 min (t2), 60 min (t3), and 120 min (t4) after running. Blood (5.0–7.5 ml) was collected by venipuncture

using serum-gel monovettes1 (Sarstedt, Nümbrecht, Germany). After blood coagulation (30 min, RT), serum was isolated by centrifugation (10 min, 3000 rpm) and stored at -80°C .

Osteoarthritis patients study. Fourteen patients diagnosed with unilateral and bilateral symptomatic hip OA, validated by conventional anterior/posterior and lateral pelvic radiographs (7 females, 7 males, age = 61.4 ± 10.5 years, height = 1.74 ± 0.07 m, weight = 79.7 ± 16.4 kg, BMI = 26.2 ± 4.7 kg/m²) at the Department of Orthopaedics at the University Hospital of the Goethe University Frankfurt in Germany voluntarily participated in the study. All patients reported pain for the ipsilateral hip although, the contralateral hip was free from any symptoms before the surgery. At the time of all follow-up measurements all patients were pain-free. The period of prospective examination began before surgery and ended nearly 1 year after initial THR. The patients were recruited and examined as previously reported²¹. Anthropometric measures of the two analyzed cohorts in this study are shown in Supplementary Table S7.

Blood and saliva samples. Fasted blood (3–5 ml) and saliva samples (1–2 ml) were collected 8–9 h after overnight fasting and for non-fasted samples, they were collected 3 h after lunch meal. Serum separator tube (SST) was used to separate serum from the whole blood specimen. Samples were allowed to clot for 30 min before centrifugation for at least 15 min at $1000 \times g$. Serum was removed, aliquoted and kept frozen at -80°C . For saliva samples, the required amount of saliva samples was collected, and subjects were asked to refrain from eating, drinking, smoking, chewing gum, brushing their teeth, or using mouthwash for at least 30 min before providing their samples. Samples were centrifuged for 5 min at $1000 \times g$ and aliquoted and kept frozen at -80°C .

Statistical analysis. Data are expressed as mean \pm SD. Statistical analyses were performed using GraphPad Prism software version 8.0.2 and the significance of differences between groups was determined by applying an unpaired two-tailed Student's test. Values of $P \leq 0.05$ were considered significant. For the exercise study, one-way analysis of variance (ANOVA) with repeated measures and Dunnett's multiple comparisons test for post hoc analysis were performed to detect significant differences in asprosin levels between time points. The significance level was set at $P \leq 0.05$.

Received: 9 June 2021; Accepted: 28 December 2021

Published online: 25 January 2022

References

- Romere, C. *et al.* Asprosin, a fasting-induced glucogenic protein hormone. *Cell* **165**, 566–579. <https://doi.org/10.1016/j.cell.2016.02.063> (2016).
- Duerrschmid, C. *et al.* Asprosin is a centrally acting orexigenic hormone. *Nat. Med.* **23**, 1444–1453. <https://doi.org/10.1038/nm.4432> (2017).
- Mishra, I. *et al.* Asprosin-neutralizing antibodies as a treatment for metabolic syndrome. *Elife* <https://doi.org/10.7554/eLife.63784> (2021).
- Mazur-Bialy, A. I. Asprosin—a fasting-induced, glucogenic, and orexigenic adipokine as a new promising player. Will it be a new factor in the treatment of obesity, diabetes, or infertility? A review of the literature. *Nutrients* **13**, 1. <https://doi.org/10.3390/nu13020620> (2021).
- Janoschek, R. *et al.* Asprosin in pregnancy and childhood. *Mol. Cell Pediatr.* **7**, 18. <https://doi.org/10.1186/s40348-020-00110-8> (2020).
- Muthu, M. L. & Reinhardt, D. P. Fibrillin-1 and fibrillin-1-derived asprosin in adipose tissue function and metabolic disorders. *J. Cell Commun. Signal* **14**, 159–173. <https://doi.org/10.1007/s12079-020-00566-3> (2020).
- Wang, M. *et al.* Serum asprosin concentrations are increased and associated with insulin resistance in children with obesity. *Ann. Nutr. Metab* **75**, 205–212. <https://doi.org/10.1159/000503808> (2019).
- Long, W. *et al.* Decreased circulating levels of asprosin in obese children. *Horm Res. Paediatr.* **91**, 271–277. <https://doi.org/10.1159/000500523> (2019).
- Sunneci Silistre, E. & Hatipoglu, H. U. Increased serum circulating asprosin levels in children with obesity. *Pediatr. Int.* **62**, 467–476. <https://doi.org/10.1111/ped.14176> (2020).
- Corica, D. *et al.* Asprosin serum levels and glucose homeostasis in children with obesity. *Cytokine* **142**, 155477. <https://doi.org/10.1016/j.cyto.2021.155477> (2021).
- Sengle, G. & Sakai, L. Y. The fibrillin microfibril scaffold: A niche for growth factors and mechanosensation?. *Matrix Biol.* **47**, 3–12. <https://doi.org/10.1016/j.matbio.2015.05.002> (2015).
- Clark, A. G. *et al.* Serum cartilage oligomeric matrix protein reflects osteoarthritis presence and severity: The Johnston County Osteoarthritis Project. *Arthritis Rheum.* **42**, 2356–2364. [https://doi.org/10.1002/1529-0131\(199911\)42:11%3c2356::AID-ANR14%3e3.0.CO;2-R](https://doi.org/10.1002/1529-0131(199911)42:11%3c2356::AID-ANR14%3e3.0.CO;2-R) (1999).
- Hunter, D. J. *et al.* Cartilage markers and their association with cartilage loss on magnetic resonance imaging in knee osteoarthritis: The Boston Osteoarthritis Knee Study. *Arthritis Res. Ther.* **9**, R108. <https://doi.org/10.1186/ar2314> (2007).
- Zhang, Y. *et al.* Expression and purification of asprosin in *Pichia pastoris* and investigation of its increase glucose uptake activity in skeletal muscle through activation of AMPK. *Enzyme Microb. Technol.* **144**, 109737. <https://doi.org/10.1016/j.enzmictec.2020.109737> (2021).
- Yu, Y. *et al.* Placensin is a glucogenic hormone secreted by human placenta. *EMBO Rep.* **21**, e49530. <https://doi.org/10.15252/embr.201949530> (2020).
- Ugur, K. & Aydin, S. Saliva and blood asprosin hormone concentration associated with obesity. *Int. J. Endocrinol.* **2019**, 2521096. <https://doi.org/10.1155/2019/2521096> (2019).
- Ceylan, H. I. & Saygin, O. An investigation of the relationship between new fasting hormone asprosin, obesity and acute-chronic exercise: Current systematic review. *Arch. Physiol. Biochem.* <https://doi.org/10.1080/13813455.2020.1767652> (2020).

18. Ceylan, H. I., Saygin, O. & Ozel Turcku, U. Assessment of acute aerobic exercise in the morning versus evening on asprosin, spexin, lipocalin-2, and insulin level in overweight/obese versus normal weight adult men. *Chronobiol. Int.* **37**, 1252–1268. <https://doi.org/10.1080/07420528.2020.1792482> (2020).
19. Wiecek, M., Szymura, J., Maciejczyk, M., Kantorowicz, M. & Szygula, Z. Acute anaerobic exercise affects the secretion of asprosin, irisin, and other cytokines: A comparison between sexes. *Front Physiol.* **9**, 1782. <https://doi.org/10.3389/fphys.2018.01782> (2018).
20. Firner, S. *et al.* Effect of increased mechanical knee joint loading during running on the serum concentration of cartilage oligomeric matrix protein (COMP). *J. Orthop. Res.* **36**, 1937–1946. <https://doi.org/10.1002/jor.23859> (2018).
21. Endres, E., van Drongelen, S., Meurer, A., Zaucke, F. & Stief, F. Effect of total joint replacement in hip osteoarthritis on serum COMP and its correlation with mechanical-functional parameters of gait analysis. *Osteoarthritis Cartilage Open* <https://doi.org/10.1016/j.ocarto.2020.100034> (2020).
22. Poole, C. A. Articular cartilage chondrons: Form, function and failure. *J. Anat.* **191**(Pt 1), 1–13. <https://doi.org/10.1046/j.1469-7580.1997.19110001.x> (1997).
23. Wang, Y. *et al.* Plasma Asprosin Concentrations Are Increased in Individuals with Glucose Dysregulation and Correlated with Insulin Resistance and First-Phase Insulin Secretion. *Mediators Inflamm.* **2018**, 9471583. <https://doi.org/10.1155/2018/9471583> (2018).
24. Alan, M. *et al.* Asprosin: A novel peptide hormone related to insulin resistance in women with polycystic ovary syndrome. *Gynecol. Endocrinol.* **35**, 220–223. <https://doi.org/10.1080/09513590.2018.1512967> (2019).
25. Groener, J. B. *et al.* Asprosin response in hypoglycemia is not related to hypoglycemia unawareness but rather to insulin resistance in type 1 diabetes. *PLoS ONE* **14**, e0222771. <https://doi.org/10.1371/journal.pone.0222771> (2019).
26. Zhang, L., Chen, C., Zhou, N., Fu, Y. & Cheng, X. Circulating asprosin concentrations are increased in type 2 diabetes mellitus and independently associated with fasting glucose and triglyceride. *Clin. Chim. Acta* **489**, 183–188. <https://doi.org/10.1016/j.cca.2017.10.034> (2019).
27. Zhang, X., Jiang, H., Ma, X. & Wu, H. Increased serum level and impaired response to glucose fluctuation of asprosin is associated with type 2 diabetes mellitus. *J. Diabetes Investig.* **11**, 349–355. <https://doi.org/10.1111/jdi.13148> (2020).
28. Naiemian, S. *et al.* Serum concentration of asprosin in new-onset type 2 diabetes. *Diabetol. Metab. Syndr.* **12**, 65. <https://doi.org/10.1186/s13098-020-00564-w> (2020).
29. Jayaprakash, N. G. & Surolia, A. Role of glycosylation in nucleating protein folding and stability. *Biochem. J.* **474**, 2333–2347. <https://doi.org/10.1042/BCJ20170111> (2017).
30. Baykus, Y. *et al.* Asprosin in umbilical cord of newborns and maternal blood of gestational diabetes, preeclampsia, severe preeclampsia, intrauterine growth retardation and macrosomic fetus. *Peptides* **120**, 170132. <https://doi.org/10.1016/j.peptides.2019.170132> (2019).
31. Hong, T. *et al.* High serum asprosin levels are associated with presence of metabolic syndrome. *Int. J. Endocrinol.* **2021**, 6622129. <https://doi.org/10.1155/2021/6622129> (2021).
32. Wang, R., Lin, P., Sun, H. & Hu, W. Increased serum asprosin is correlated with diabetic nephropathy. *Diabetol. Metab. Syndr.* **13**, 51. <https://doi.org/10.1186/s13098-021-00668-x> (2021).
33. Wen, M. S. *et al.* The role of Asprosin in patients with dilated cardiomyopathy. *BMC Cardiovasc. Disord.* **20**, 402. <https://doi.org/10.1186/s12872-020-01680-1> (2020).
34. Badillo-Suarez, P. A., Rodriguez-Cruz, M. & Nieves-Morales, X. Impact of metabolic hormones secreted in human breast milk on nutritional programming in childhood obesity. *J. Mammary Gland Biol. Neoplasia* **22**, 171–191. <https://doi.org/10.1007/s10911-017-9382-y> (2017).
35. Ke, X. *et al.* Serum levels of asprosin, a novel adipokine, are significantly lowered in patients with acromegaly. *Int. J. Endocrinol.* **2020**, 8855996. <https://doi.org/10.1155/2020/8855996> (2020).
36. Jimenez-Altayo, F. *et al.* Differences in the thoracic aorta by region and sex in a murine model of marfan syndrome. *Front Physiol.* **8**, 933. <https://doi.org/10.3389/fphys.2017.00933> (2017).
37. Altinbas, L. *et al.* Assessment of bones deficient in fibrillin-1 microfibrils reveals pronounced sex differences. *Int. J. Mol. Sci.* <https://doi.org/10.3390/ijms20236059> (2019).
38. Renard, M. *et al.* Sex, pregnancy and aortic disease in Marfan syndrome. *PLoS ONE* **12**, e0181166. <https://doi.org/10.1371/journal.pone.0181166> (2017).
39. Chojnowska, S. *et al.* Human saliva as a diagnostic material. *Adv. Med. Sci.* **63**, 185–191. <https://doi.org/10.1016/j.advms.2017.11.002> (2018).
40. Groschl, M. Saliva: A reliable sample matrix in bioanalytics. *Bioanalysis* **9**, 655–668. <https://doi.org/10.4155/bio-2017-0010> (2017).
41. Gozel, N. & Kilinc, F. Investigation of plasma asprosin and saliva levels in newly diagnosed type 2 diabetes mellitus patients treated with metformin. *Endokrynol. Pol.* <https://doi.org/10.5603/EPa2020.0059> (2020).
42. Ko, J. R. *et al.* Aerobic exercise training decreases hepatic asprosin in diabetic rats. *J. Clin. Med.* <https://doi.org/10.3390/jcm8050666> (2019).
43. Bostrom, P. *et al.* A PGC1- α -dependent myokine that drives brown-fat-like development of white fat and thermogenesis. *Nature* **481**, 463–468. <https://doi.org/10.1038/nature10777> (2012).
44. Sengle, G. *et al.* Abnormal activation of BMP signaling causes myopathy in Fbn2 null mice. *PLoS Genet.* **11**, e1005340. <https://doi.org/10.1371/journal.pgen.1005340> (2015).
45. Roca-Rivada, A. *et al.* FNDC5/irisin is not only a myokine but also an adipokine. *PLoS ONE* **8**, e60563. <https://doi.org/10.1371/journal.pone.0060563> (2013).
46. Firner, S. *et al.* Impact of knee joint loading on fragmentation of serum cartilage oligomeric matrix protein. *J. Orthop. Res.* **38**, 1710–1718. <https://doi.org/10.1002/jor.24586> (2020).
47. Keene, D. R. *et al.* Fibrillin-1 in human cartilage: Developmental expression and formation of special banded fibers. *J. Histochem. Cytochem.* **45**, 1069–1082. <https://doi.org/10.1177/002215549704500805> (1997).
48. Karim, A., Amin, A. K. & Hall, A. C. The clustering and morphology of chondrocytes in normal and mildly degenerate human femoral head cartilage studied by confocal laser scanning microscopy. *J. Anat.* **232**, 686–698. <https://doi.org/10.1111/joa.12768> (2018).
49. Sophia Fox, A. J., Bedi, A. & Rodeo, S. A. The basic science of articular cartilage: Structure, composition, and function. *Sports Health* **1**, 461–468. <https://doi.org/10.1177/1941738109350438> (2009).
50. Ahrens, M. J. & Dudley, A. T. Chemical pretreatment of growth plate cartilage increases immunofluorescence sensitivity. *J. Histochem. Cytochem.* **59**, 408–418. <https://doi.org/10.1369/0022155411400869> (2011).
51. Bishop, J. R., Schuksz, M. & Esko, J. D. Heparan sulphate proteoglycans fine-tune mammalian physiology. *Nature* **446**, 1030–1037. <https://doi.org/10.1038/nature05817> (2007).
52. Jung, T. W. *et al.* Asprosin attenuates insulin signaling pathway through PKC δ -activated ER stress and inflammation in skeletal muscle. *J. Cell Physiol.* **234**, 20888–20899. <https://doi.org/10.1002/jcp.28694> (2019).
53. Maertens, B. *et al.* Cleavage and oligomerization of gliomedin, a transmembrane collagen required for node of ranvier formation. *J. Biol. Chem.* **282**, 10647–10659. <https://doi.org/10.1074/jbc.M611339200> (2007).
54. Sengle, G. *et al.* Targeting of bone morphogenetic protein growth factor complexes to fibrillin. *J. Biol. Chem.* **283**, 13874–13888. <https://doi.org/10.1074/jbc.M707820200> (2008).

55. Reinhardt, D. P. *et al.* Fibrillin-1: Organization in microfibrils and structural properties. *J. Mol. Biol.* **258**, 104–116. <https://doi.org/10.1006/jmbi.1996.0237> (1996).
56. Ciucanu, I. K. F. A simple and rapid method for the permethylation of carbohydrates. *Carbohydr. Res.* **131**, 209–217. [https://doi.org/10.1016/0008-6215\(84\)85242-8](https://doi.org/10.1016/0008-6215(84)85242-8) (1984).
57. Wohl, A. P., Troilo, H., Collins, R. F., Baldock, C. & Sengle, G. Extracellular regulation of bone morphogenetic protein activity by the microfibril component fibrillin-1. *J. Biol. Chem.* **291**, 12732–12746. <https://doi.org/10.1074/jbc.M115.704734> (2016).

Acknowledgements

Funding for this study was provided by the Deutsche Forschungsgemeinschaft (DFG, German Research Foundation) project ID 384170921: FOR2722/D1 to A.N. (Project ID 407176282), FOR2722/D2 to F.Z., and FOR2722/M2 to E.H.R., J.D., and G.S.

Author contributions

G.S. designed research. Y.A.T.M., S.L., A.T., F.G.H., G.P., and N.P. performed research. Y.A.T.M., S.L., F.G.H., and G.P. analyzed data. A.N., T.K., T.H., R.J., J.D., E.H.-R., and F.Z. provided essential reagents. G.S. wrote the manuscript.

Funding

Open Access funding enabled and organized by Projekt DEAL.

Competing interests

The authors declare no competing interests.

Additional information

Supplementary Information The online version contains supplementary material available at <https://doi.org/10.1038/s41598-022-05060-x>.

Correspondence and requests for materials should be addressed to G.S.

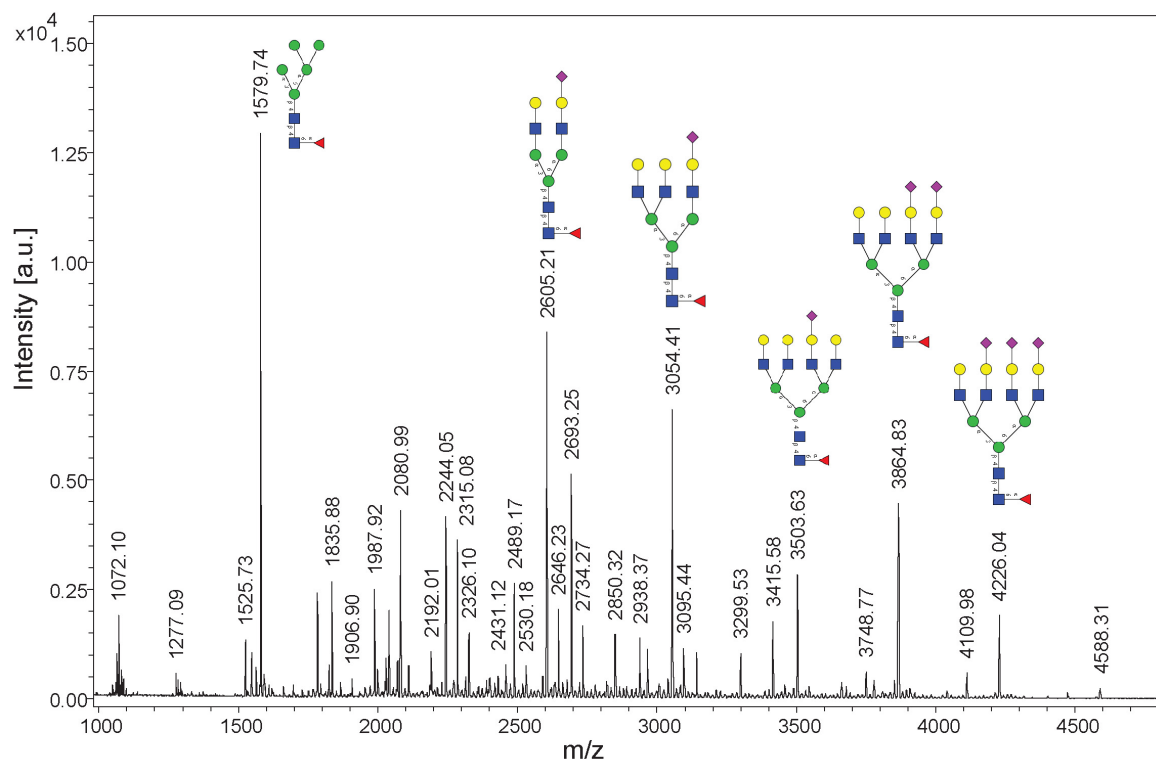
Reprints and permissions information is available at www.nature.com/reprints.

Publisher's note Springer Nature remains neutral with regard to jurisdictional claims in published maps and institutional affiliations.

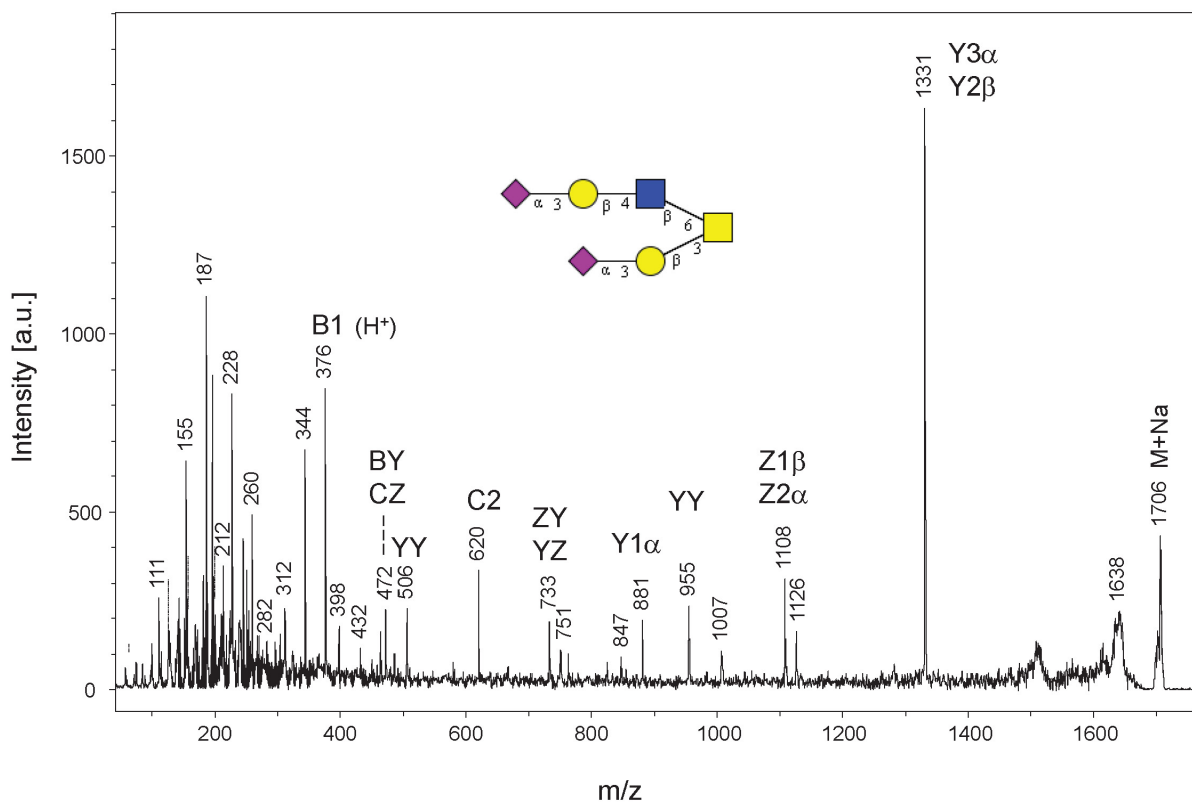


Open Access This article is licensed under a Creative Commons Attribution 4.0 International License, which permits use, sharing, adaptation, distribution and reproduction in any medium or format, as long as you give appropriate credit to the original author(s) and the source, provide a link to the Creative Commons licence, and indicate if changes were made. The images or other third party material in this article are included in the article's Creative Commons licence, unless indicated otherwise in a credit line to the material. If material is not included in the article's Creative Commons licence and your intended use is not permitted by statutory regulation or exceeds the permitted use, you will need to obtain permission directly from the copyright holder. To view a copy of this licence, visit <http://creativecommons.org/licenses/by/4.0/>.

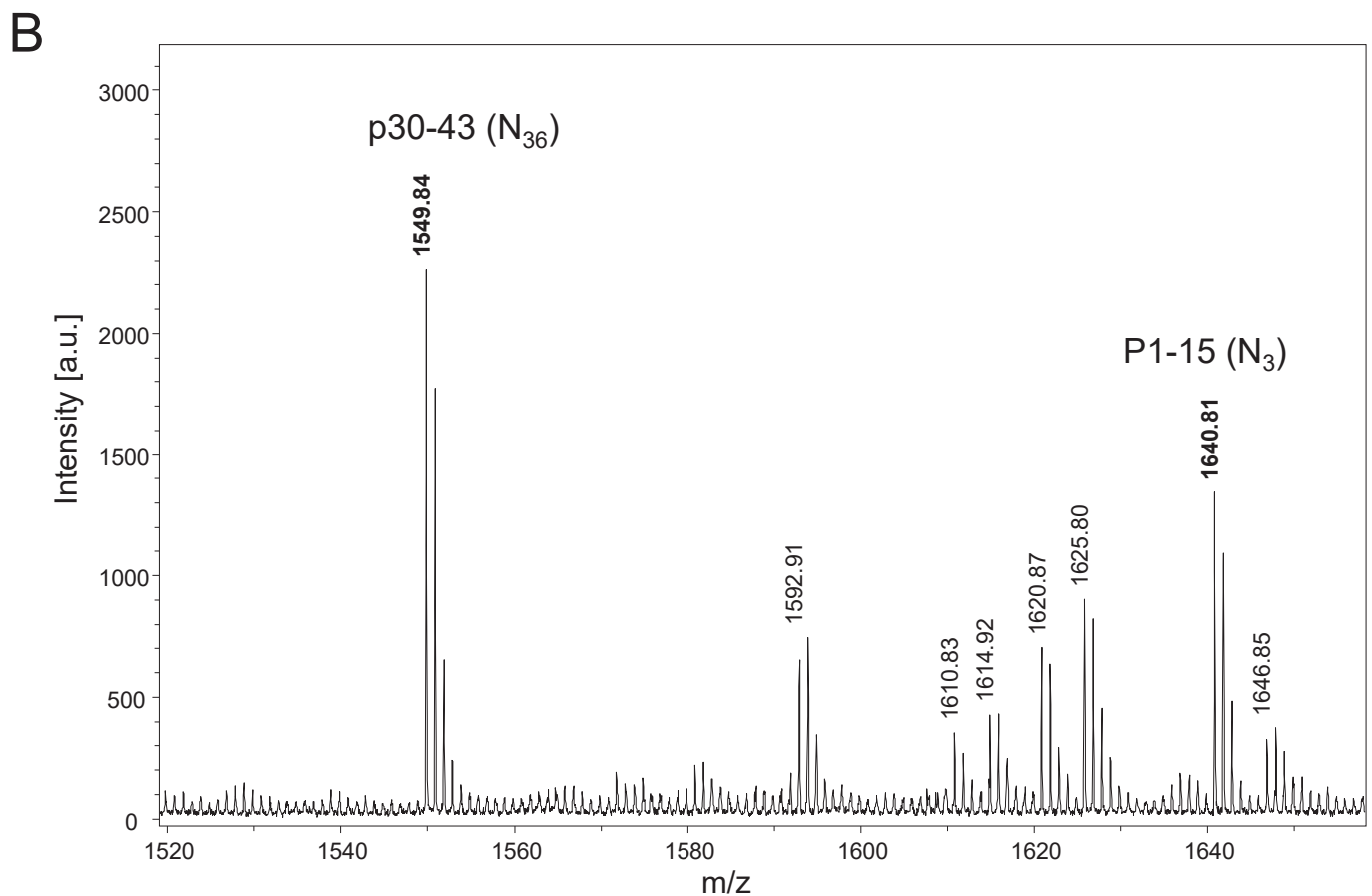
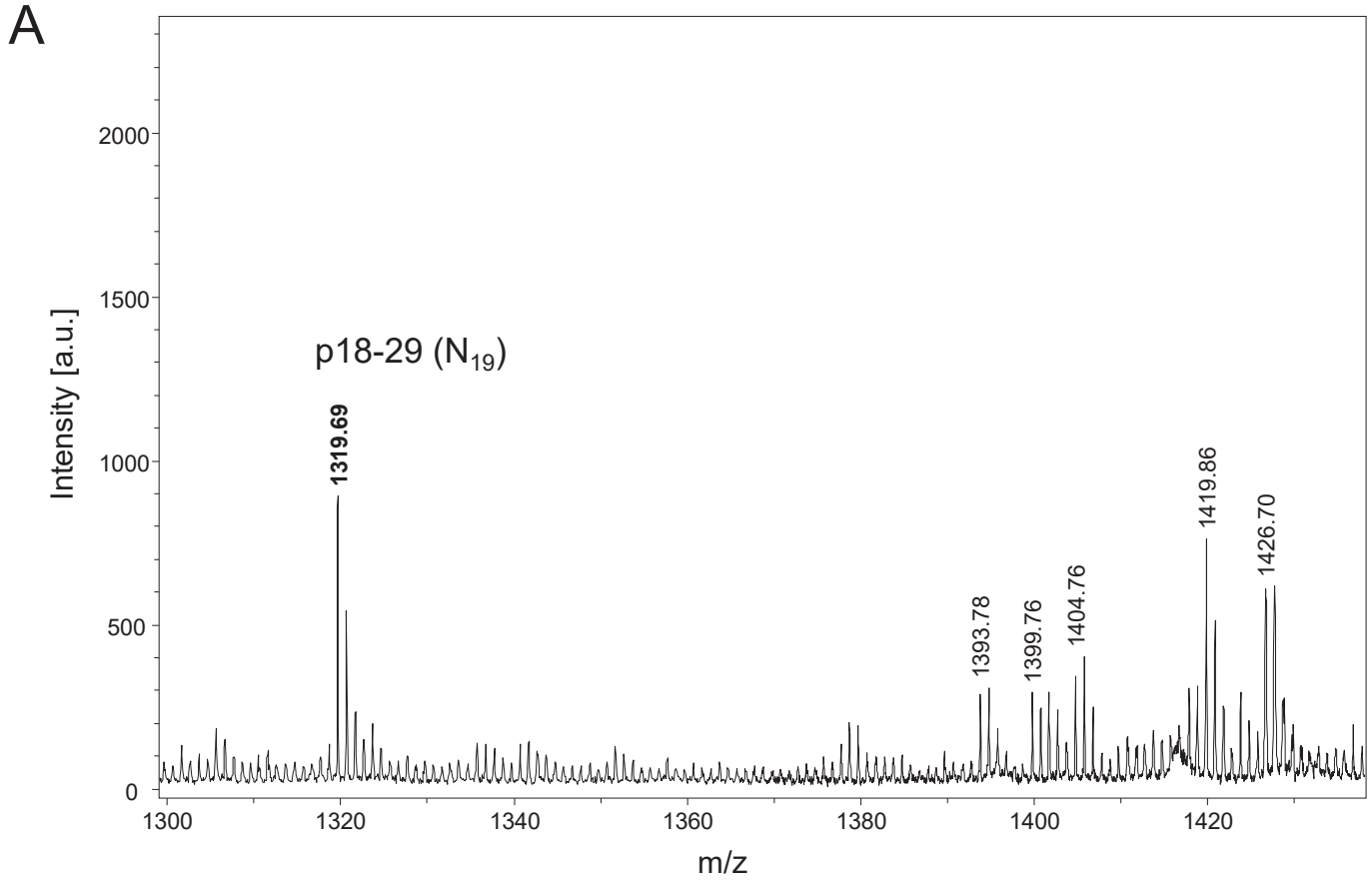
© The Author(s) 2022



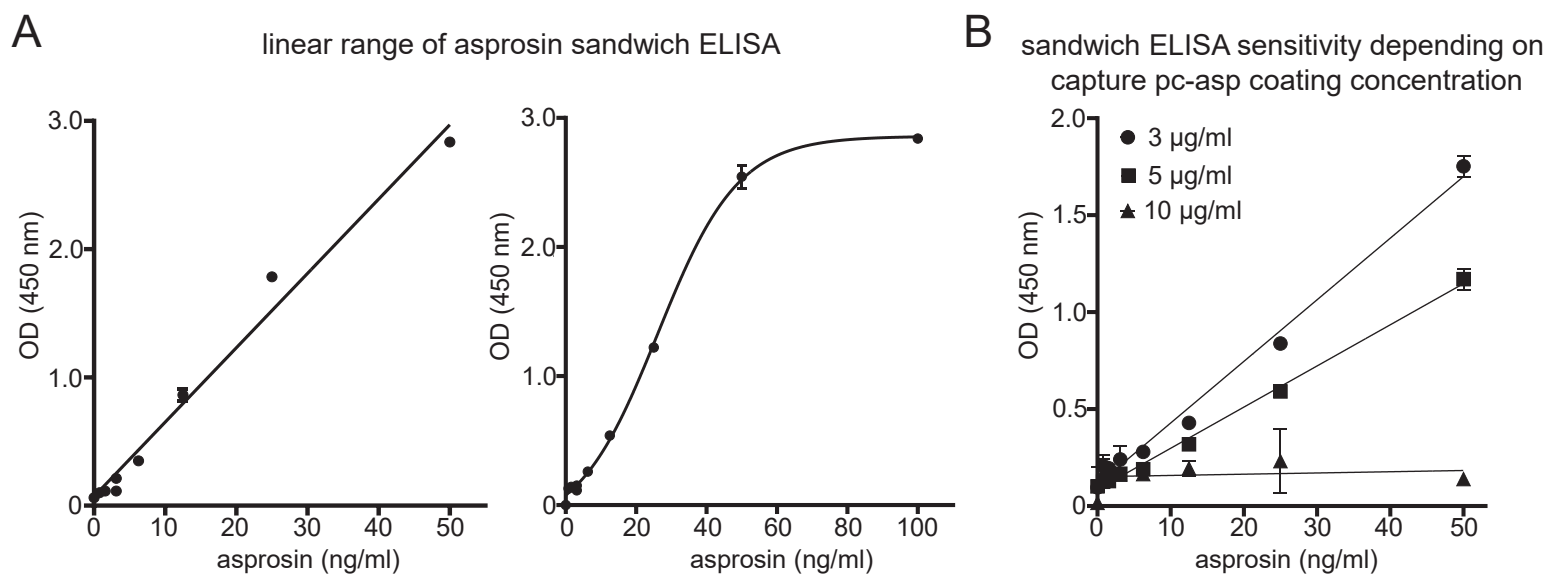
Supplementary Figure S1: Survey MALDI mass spectrum of permethylated N-glycans from recombinant asprosin. PNGaseF-liberated N-glycans were methylated and analyzed by positive ion reflectron MALDI mass spectrometry. The profile is characterized by dominant high-mannose N-glycan M5 and core-fucosylated complex-type N-glycans with two to four antennae. Besides fully processed species, the profile contains significant amounts of partially processed (truncated) –Gal species.



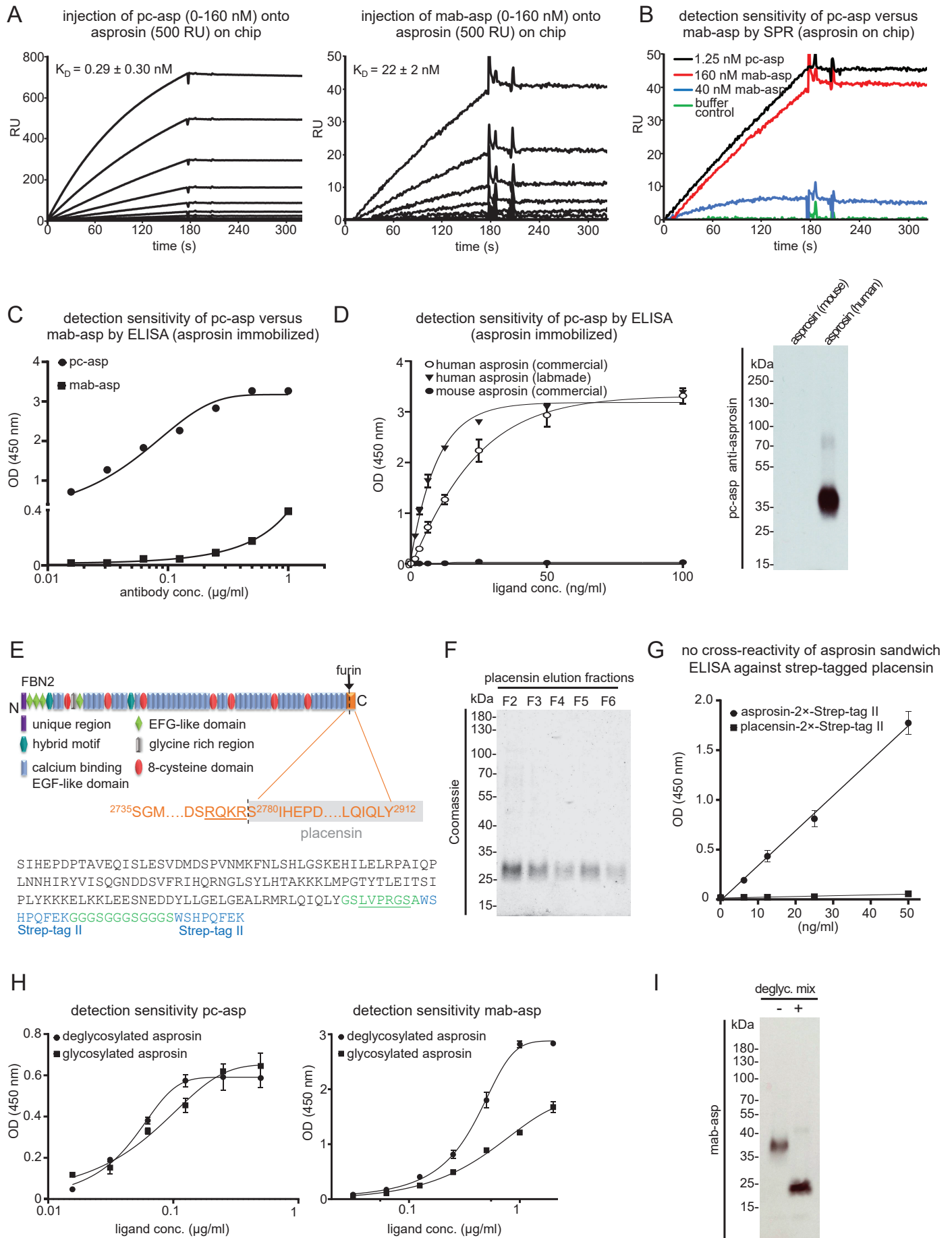
Supplementary Figure S2: Post-Source-Decay MALDI mass spectrum of permethylated O-glycan alditol detected at precursor ion mass m/z 1706. Only one major precursor ion was detectable in MALDI survey spectra of O-glycan alditols derived from recombinant asprosin. PSD analysis of the compound detected at m/z 1706 revealed a fragment pattern supporting a hexasaccharide (disialylated core 2 tetrasaccharide) of the structure shown.



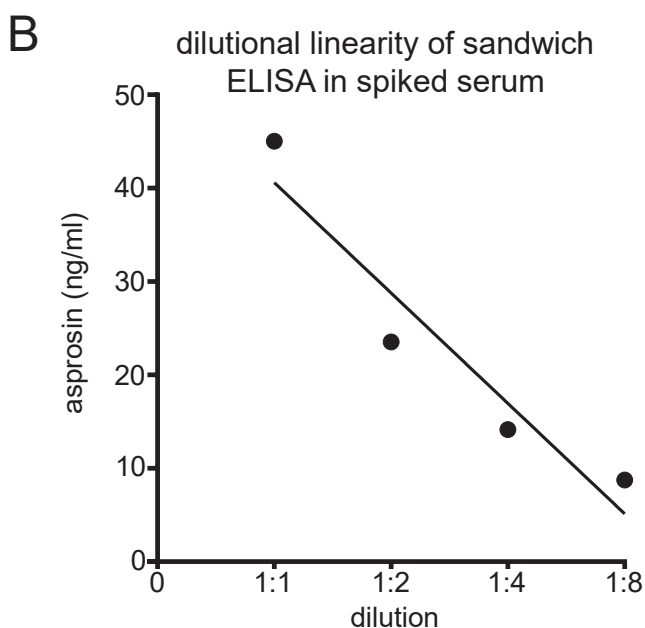
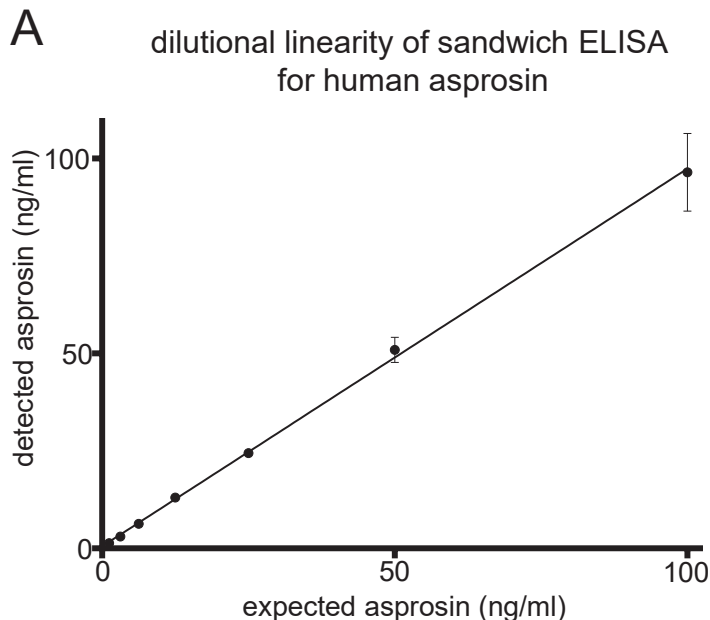
Supplementary Figure S3: MALDI mass spectra of de-N-glycosylated peptides from recombinant asprosin after double digestion with V8 and trypsin. A. The section shows a mass range of the spectrum from m/z 1300 to 1430 to highlight the signal at the monoisotopic mass m/z 1319.69, which corresponds to the native peptide mass m/z 1318.66 of p18-29 (ANVSLASWDVEK). The observed mass shift of +1 results from conversion of Asn to Asp during enzymatic liberation of N-linked glycans. **B.** The section shows a mass range of the spectrum from m/z 1520 to 1650 to highlight the signals at the monoisotopic masses m/z 1549.84 and 1640.81, which correspond to the native peptide masses m/z 1548.82 of p30-43 (TAIFAFNISHVSNK) and m/z 1639.66 of p1-15 (STNETDASNIEDQSE). The observed mass shift of +1 results from



Supplementary Figure S4: Critical parameters of established asprosin sandwich ELISA. A. Linear range of asprosin sandwich ELISA was determined to be between 0 – 50 ng/ml. **B.** Concentration of coated capture antibody (pc-asp) affects sensitivity of asprosin sandwich ELISA. Data were analyzed using Graphpad Prism version 8.0.2.



Supplementary Figure S5: Affinity of pc-asp versus mab against glycosylated and deglycosylated asprosin. **A.** Measurement of pc-asp and mab-asp affinity by SPR. Sensorgrams of injections of 2-fold serial dilutions (0-160 nM) of (left) pc-asp and (right) mab antibodies onto asprosin immobilized on chip. The calculated affinity (K_D) of pc-asp was 0.29 ± 0.3 nM and mab was 22 ± 2 nM. **B.** Sensorgrams showing higher sensitivity of pc-asp (1.25 nM) compared to mab (160 nM) to immobilized asprosin on chip. **C.** pc-asp shows a higher sensitivity against immobilized human asprosin (purchased from Biolegend, #761902) versus mab. **D.** (left) pc-asp antibody showed high specificity to human asprosin and no cross reactivity to mouse asprosin in direct ELISA assay and western blot analysis (right). **E.** (top) Domain structure of fibrillin-2 and sequence of its C-terminal propeptide, placensin (marked in grey). Placensin consists of 133 amino acids (S^{2780} - Y^{2912}) after furin cleavage from pro-fibrillin-2 (position of furin cleavage site within domain structure is marked by arrow, furin cleavage site is underlined). (bottom) Placensin sequence with a C-terminally placed double Strep-tag II which was overexpressed in HEK293 cells. Residues representing linker regions are indicated in green, thrombin cleavage (LVPRGS) site is underlined, and Strep-tag II sequences are marked in blue. **F.** Coomassie stained quality control gel of eluted fractions (F2-F6) of human placensin after affinity chromatography. **G.** Specific detection of recombinantly expressed asprosin containing a C-terminally placed double Strep-tag II by asprosin sandwich ELISA. No crossreactivity to recombinantly expressed double strep-tagged placensin was observed by asprosin sandwich ELISA. **H.** Sensitivity of pc-asp and mab to glycosylated and deglycosylated asprosin using direct ELISA. (left) Pc-asp antibody shows almost equal sensitivity to immobilized glycosylated and deglycosylated asprosin. (right) mab-asp antibody shows low sensitivity to glycosylated compared to deglycosylated asprosin. **I.** Western blot with mab anti-asprosin detecting glycosylated (≈ 37 kDa) and deglycosylated asprosin (≈ 25 kDa). (Deglycosylation was performed with Protein Deglycosylation Mix II, P6044S, NEB, Germany). ELISA data were analyzed using Graphpad Prism version 8.0.2. Association and dissociation rates were obtained using BIAevaluation version 3.0 software. Apparent equilibrium dissociation constants (K_D values) were then calculated as the ratio of k_d/k_a .

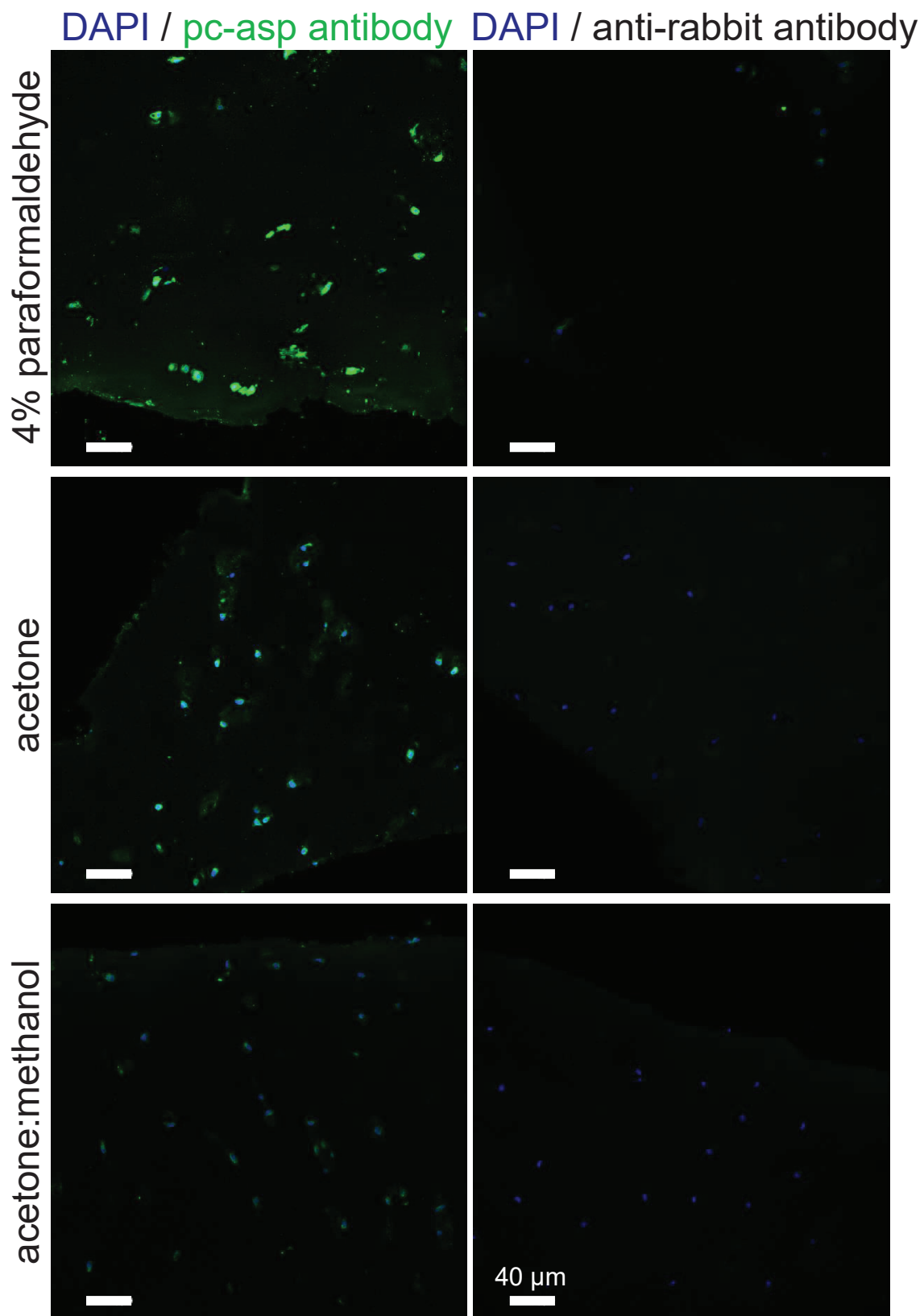


dilution factor	expected (ng/ml)	detected (ng/ml)	recovery %
1	50	45.02	90.04
2	25	23.52	94.08
4	12.5	14.14	113.12
8	6.25	7.14	114.34

C spike and recovery assessment of aspirin sandwich ELISA

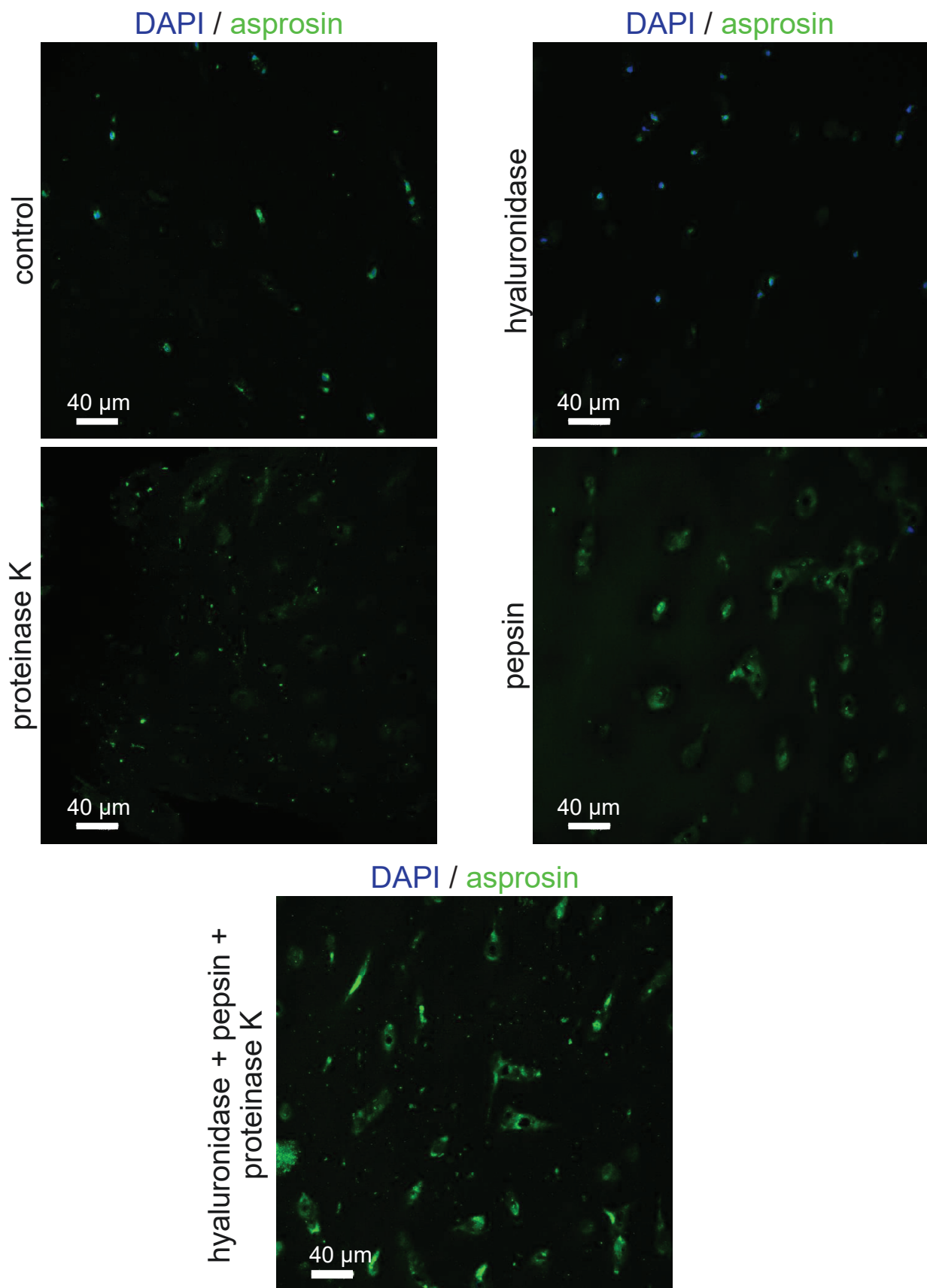
sample	expected (ng/ml)	detected (ng/ml)	recovery (%)	expected (ng/ml)	detected (ng/ml)	recovery (%)
plasma	1	30	23.18	50	59.99	119.98
	2	30	27.34		45.02	90.04
	3	30	30.63		40.30	80.61
	4	30	28.36		29.21	116.86
	5	30	26.24		25	24.08
serum	1	30	28.31		24.56	98.26
	2	30	32.37			
	3	30	25.38			
	4	30	32.22			
	5	30	36.33			

Supplementary Figure S6: Linearity of dilution and spike and recovery assessment of aspirin sandwich ELISA. **A.** Dilution of aspirin in DMEM, 10 % FCS does not affect accuracy and precision of aspirin detection, correlation of detected aspirin and expected aspirin concentrations using Spearman correlation = 0.9996. **B.** (left) Dilution of aspirin spiked serum with PBS does not affect the accuracy and precision of aspirin detection, the average recovery is 102.8 %. (right) Table showing expected and detected aspirin concentration values, in addition to estimated aspirin recovery. **C.** (left) Investigation of matrix effect on aspirin detection by using spiking aspirin in various serum and plasma samples, showing average recovery 96.8%. (right) Assessment of spiked aspirin recovery in serum samples before and after 1:2 dilution. Data were analyzed using Graphpad Prism version 8.0.2.



Supplementary Figure S7: Effect of fixation and treatments on asprosin recognition by immunostaining in human cartilage.

Immunodetection of asprosin in human chondrocytes *in situ*. Cryosections from cartilage specimen (top row) were fixed with 4% paraformaldehyde, (middle row) treated with acetone, or (bottom row) fixed with acetone:methanol mixture. The left images showed sections incubated with pc-asp asprosin antibody (green) and DAPI (blue). The right images showed sections incubated only with secondary antibody (control) and DAPI. Confocal images were obtained from a Leica SP8 confocal microscope and Leica LAS AF Lite 4.0 software. Images were further processed using Fiji/ImageJ software to obtain average intensity Z-projection.



Supplementary Figure S8: Effect of digestion by various enzymes on asprosin detection by immunostaining in human cartilage.

Cartilage cryosections were treated (top, left) with acetone only, or additionally (top, right) digested with hyaluronidase, or (middle, left) with proteinase K, or (middle, right) with pepsin, or (bottom) with a mixture of all of these enzymes together. The signal of pc-asp asprosin was detected in green, DAPI nuclei staining in blue. Confocal images were obtained from a Leica SP8 confocal microscope and Leica LAS AF Lite 4.0 software. Images were further processed using Fiji/ImageJ software to obtain average Intensity Z-projection.

Supplementary Table S2: N-linked glycans expressed on recombinant asprosin expressed in HEK293 cells. MALDI mass spectrometric analysis of methylated glycans.

M+Na (experimental)	Structural assignment	Antennarity* -
1579.74	H5N2 (M5)	
1783.84	H6N2 (M6)	
1835.88	F1H3N4	2
1987.92	H7N2 (M7)	
2039.96	F1H4N4	2
2080.99	F1H3N5	2
2192.01	H8N2 (M8)	
2244.05	F1H5N4	2
2285.08	F1H4N5	3
2489.17	F1H5N5	3
2605.21	S1F1H5N4	2
2646.23	S1F1H4N5	3
2693.25	F1H6N5	3
2734.27	F1H5N6	4
2850.32	S1F1H5N5	3
2938.37	F1H6N6	4
3054.41	S1F1H6N5	3
3299.53	S1F1H6N6	4
3415.58	S2F1H6N5	3
3503.63	S1F1H7N6	4
3864.83	S2F1H7N6	4
4226.04	S3F1H7N6	4
4588.31	S4F1H7N6	4

*Antennarity is defined only for complex-type N-glycans. Structural assignments refer to monosaccharide compositions in terms of S, N-acetylneuraminic acid; F, fucose; H, hexose; and N, N-acetylhexosamine.

Supplementary Table S3: Peptides of de-N-glycosylated asprosin after double digestion with trypsin and V8.

1 STNETDASNI EDQSETEANV SLASWDVEKT AIFAFNISHV SNKVRILELL PALTTLTNHN RYLIESGNE DGFFKINQKEG
 81 ISYLFHTKKK PVAGTYSLQI SSTPLYKKKE LNQLEDKYDK DYLSGELGDN LKMKIQVLLH

Detected	m/z (mi)	m/z (av)	Modifications	Start	End	Missed Cleavages	Sequence	N-glycosylation site
0	450.1831	450.4278		1	4	0	(-)STNE(T)	N3
1	708.2683	708.6602		12	17	1	(E)DQSETE(A)	
1	1065.5728	1066.2526		80	88	0	(E)GISYLFHTK(K)	
0	1180.4964	1181.1618		1	11	1	(-)STNETDASNIE(D)	N3
0	1190.5688	1191.2906		18	28	0	(E)ANVSLASWDVE(K)	N19
1	1193.6677	1194.4278		80	89	1	(E)GISYLFHTKK(K)	
1	1194.6154	1195.3688		79	88	1	(K)EGISYLFHTK(K)	
1	1318.6638	1319.4658	+1	18	29	1	(E)ANVSLASWDVEK(T)	N19
0	1420.6591	1421.5125		16	28	1	(E)TEANVSLASWDVE(K)	N19
1	1463.8329	1464.7182		49	61	0	(E)LLPALTTLTNHNH(Y)	
1	1548.7540	1549.6877	+1	16	29	2	(E)TEANVSLASWDVEK(T)	N19
1	1548.8169	1549.7806	+1	30	43	0	(K)TAIFAFNISHVSNK(V)	N36
1	1639.6566	1640.5774	+1	1	15	2	(-)STNETDASNIEDQSE(T)	N3
0	1676.9119	1677.9558		29	43	1	(E)KTAIFAFNISHVSNK(V)	N36
0	1803.9864	1805.1027		30	45	1	(K)TAIFAFNISHVSNKVR(I)	N36
1	1869.7468	1870.7993	+1	1	17	3	(-)STNETDASNIEDQSETE(A)	N3
0	1879.8192	1880.9281		12	28	2	(E)DQSETEANVSLASWDVE(K)	N19
0	1932.0814	1933.2779		29	45	2	(E)KTAIFAFNISHVSNKVR(I)	N36
0	2007.9142	2009.1033		12	29	3	(E)DQSETEANVSLASWDVEK(T)	N19
0	2159.1971	2160.5398		30	48	2	(K)TAIFAFNISHVSNKVRILE(L)	N36
0	2287.2921	2288.7150		29	48	3	(E)KTAIFAFNISHVSNKVRILE(L)	N36
0	2610.1326	2611.6621		5	28	3	(E)TDASNIEDQSETEANVSLASWDVE(K)	N19
0	2848.4628	2850.2236		18	43	2	(E)ANVSLASWDVEKTAIFAFNISHVSNK(V)	N19, N36

Supplementary Table S4: Serum asprosin concentrations (mean ± SD) before (t0) and after (t1 – t4) treadmill exercise (n = 15 subjects).

time points (min)	asprosin (ng/ml)	95 % confidence interval	
		lower limit	upper limit
t0 (0)	11.8 ± 6.2	8.4	15.2
t1 (30)	13.7 ± 6.5 (*)	10.1	17.4
t2 (60)	13 ± 7.1	9.1	16.9
t3 (90)	13.1 ± 6.5	9.5	16.6
t4 (120)	13.3 ± 7.6	9.1	17.5

*P = 0.0385

Supplementary Table S5: Serum asprosin concentrations (mean \pm SD before (t0) and after (t1 - t3) total hip replacement (THR) surgery (n = 14 patients).

time points (d)	asprosin (ng/ml)	95% confidence interval	
		lower limit	upper limit
t0 (0)	21.0 \pm 9.0	15.8	26.2
t1 (7)	14.8 \pm 6.5 (***)	11.1	18.6
t2 (90)	19.1 \pm 8.1	14.4	23.7
t3 (365)	16.8 \pm 7.5	12.5	21.2

***P = 0.0003

Supplementary Table S6: Serum COMP concentrations (mean \pm SD) before (t0) and after (t1 - t3) total hip replacement (THR) surgery (n = 14 patients).

time points	COMP (ng/ml)	95% confidence interval	
		lower limit	upper limit
t0	707.0 \pm 171.0	608.3	805.7
t1	467.1 \pm 124.1 (**)	395.4	538.8
t2	783.7 \pm 286.2	618.5	949.0
t3	737.1 \pm 216.0	612.4	861.7

**P = 0.0056

Supplementary Table S7: Anthropometric measures of the two analyzed cohorts in this study.

cohort	f/m	age (years)	height (m)	weight (kg)	BMI (kg/m ²)
treadmill exercise	0/15	27.5 \pm 3.1	1.8 \pm 0.05	78 \pm 7.7	23.9 \pm 1.9
total hip replacement (THR) surgery	7/7	61.4 \pm 10.5	1.74 \pm 0.07	79.7 \pm 16.4	26.2 \pm 4.7

4. Correlation of metabolic characteristics with maternal, fetal and placental asprosin in human pregnancy

RESEARCH

Correlation of metabolic characteristics with maternal, fetal and placental asprosin in human pregnancy

Thorben Hoffmann¹, Yousef Ashraf Tawfik Morcos^{1,2}, Ruth Janoschek¹, Eva-Maria Turnwald¹, Antje Gerken^{1,2}, Annette Müller³, Gerhard Sengle^{1,2,4,5}, Jörg Dötsch¹, Sarah Appel¹ and Eva Hucklenbruch-Rother¹

¹Department of Pediatrics, and Adolescent Medicine, Faculty of Medicine and University Hospital of Cologne, University of Cologne, Cologne, Germany

²Center for Biochemistry, Faculty of Medicine and University Hospital Cologne, University of Cologne, Cologne, Germany

³Center for Pediatric Pathology at the University Hospital Cologne, Cologne, Germany

⁴Center for Molecular Medicine Cologne (CMMC), University of Cologne, Cologne, Germany

⁵Cologne Center for Musculoskeletal Biomechanics (CCMB), Cologne, Germany

Correspondence should be addressed to E Hucklenbruch-Rother: eva.rother@uni-koeln.de

Abstract

Objective: Asprosin is a recently discovered hormone associated with obesity and diabetes mellitus. Little is known about asprosin's role during pregnancy, but a contribution of asprosin to pregnancy complications resulting from maternal obesity and gestational diabetes mellitus (GDM) is conceivable. We assessed the potential effects of obesity, GDM and other clinical parameters on maternal and fetal umbilical plasma asprosin concentrations and placental asprosin expression.

Design: The Cologne-Placenta Cohort Study comprises 247 female patients, from whom blood and placentas were collected at the University Hospital Cologne.

Methods: We studied the maternal and fetal umbilical plasma and placentas of pregnant women with an elective, primary section. Sandwich ELISA measurements of maternal and fetal umbilical plasma and immunohistochemical stainings of placental tissue were performed to determine the asprosin levels. Also, the relation between asprosin levels and clinical blood parameters was studied.

Results: There was a strong correlation between the maternal and fetal plasma asprosin levels and both increased with GDM in normal-weight and obese women. Asprosin immunoreactivity was measured in cultivated placental cells and placental tissue. BMI and GDM were not but pre-pregnancy exercise and smoking were correlated with maternal and/or fetal asprosin levels. Placental asprosin levels were associated with maternal but not with fetal plasma asprosin levels and with BMI but not with GDM. Placental asprosin was related to maternal insulin levels and increased upon insulin treatment in GDM patients.

Conclusions: Asprosin could potentially act as a biomarker and contribute to the clinical manifestation of pregnancy complications associated with maternal obesity.

Key Words

- ▶ obesity
- ▶ GDM
- ▶ asprosin
- ▶ insulin
- ▶ placenta
- ▶ smoking
- ▶ exercise

Endocrine Connections
(2022) 11, e220069

Introduction

Asprosin, the C-terminal cleavage product of profibrillin 1, was recently described as fasting-induced pluripotent adipokine (1). Circulating asprosin targets the liver, where it

exerts a glucogenic effect (1), and the hypothalamus, where it stimulates appetite-modulating neurons in the arcuate (2). Clinical studies showed that circulating asprosin levels

positively correlated with obesity and type 2 diabetes (3, 4). Pre-clinical studies addressing the therapeutic potential of asprosin inhibition demonstrated that anti-asprosin monoclonal antibodies can reduce blood glucose, appetite, and body weight in rodents (5).

During pregnancy, adipokines and/or their receptors are expressed in the placenta (6). Certain adipokines, such as leptin, adiponectin or resistin are increasingly found in blood and placenta as pregnancy progresses (7). High concentrations of adipokines have also been detected in the umbilical blood suggesting an important role in fetal development and metabolism (8). Additionally, adipokines are thought to promote the proliferation and invasiveness of placental trophoblast cells and affect the placental angiogenic processes (9). Thus, adipokines might affect the pregnancy outcome and fetal growth by interfering with placental development (10). In obese pregnancies, elevated maternal adipokine levels have been accused of causing adverse effects in the offspring by affecting placental function (11) and programming offspring's metabolism (12).

Even though asprosin blood levels have been shown to be increased in obese individuals, it has not yet been tested whether asprosin is elevated in obese pregnant women and their fetuses. So far, clinical data are inconsistent regarding the circulating concentrations and their correlation with BMI and GDM in pregnancy (13, 14). However, it has been recently shown that asprosin is expressed in human placenta and elevated in the plasma of pregnant women complicated with GDM and their fetal umbilical blood (14). Since there is an urgent need for a reliable and sensitive method to determine plasma asprosin levels (15), our laboratory took the initiative to develop a functional and dependable asprosin ELISA (16).

Here, we set out to test whether asprosin plasma concentrations are elevated in obese mothers and the umbilical blood of their offspring in our Cologne-Placenta Cohort (CPC) Study. Furthermore, we tested the relation between (1) maternal and (2) fetal plasma asprosin concentrations and (3) asprosin protein expression and distribution in the placenta as indicators of maternal gestational disease.

Materials and methods

Study design and recruitment

Placental tissue and blood plasma samples were taken from the CPC Study (2014–2021 at the University Hospital Cologne). The study was approved by the Ethics

Commission of Cologne University's Faculty of Medicine (ethics votum 14-244). The study aimed to analyze the intrauterine programming with regard to maternal diseases like obesity, gestational diabetes and placental dysfunction. The inclusion criteria for pregnant patients of the Department of Obstetrics and Gynecology (University Hospital of Cologne) were singleton pregnancy with delivery mode via cesarian section. Exclusion criteria were multiple pregnancies, maternal serious diseases, infections before pregnancy (e.g. HIV or hepatitis B) and pregnancy-associated diseases (e.g. gestosis and amniotic infectious disease). Consent has been obtained from each patient or subject after a full explanation of the purpose and nature of all procedures used. For immunohistochemical (IHC) analyses, patients were split regarding their BMI into normal weight (BMI <25; normal weight (NW)), overweight (BMI = 25–30; overweight (OW)) and obese (BMI >30; obese (OB)) pregnant women. The classification of gestational diabetes mellitus (GDM) was based on the oral glucose tolerance test 50 and 75 or the clinical maternity log. The total patient collective is 247 patients. Plasma samples of only a subset of 77 patients were analyzed by ELISA because of limited sample quantity, and placenta samples from a subset of 30 patients were randomly chosen for histological analyses (see Fig. 1).

Patient sample preparations

Placental tissue was obtained from the placenta directly after the cesarian section. Placental tissue was punched out centrally between the placental border and the insertion of the umbilical cord. It was incubated in 4% PFA for 24 h, followed by 70% isopropanol for 24 h and paraffinated by a tissue embedding machine (Leica ASP300). Paraffinated specimens were cut into 3- μ m slices. Maternal-fasted blood was collected on the day of delivery, and fetal umbilical blood was taken from the umbilical cord right after delivery. Reaction tubes for EDTA plasma were used to collect the blood and were centrifuged for 10 min at 3000g to gain plasma. Supernatants were kept at 80°C until usage.

Asprosin sandwich ELISA

The asprosin sandwich ELISA was produced in our laboratory, intensively tested and validated by surface plasmon resonance and interaction studies (16). The detection sensitivity ranged at <65 pg/mL. For the procedure, the capture antibody (lab-made pc-asp anti-asprosin antibody; $K_D = 0.29 \pm 0.30$ nM) was coated on 96-well ELISA plates at 3 μ g/mL in 100 μ L coating buffer (50

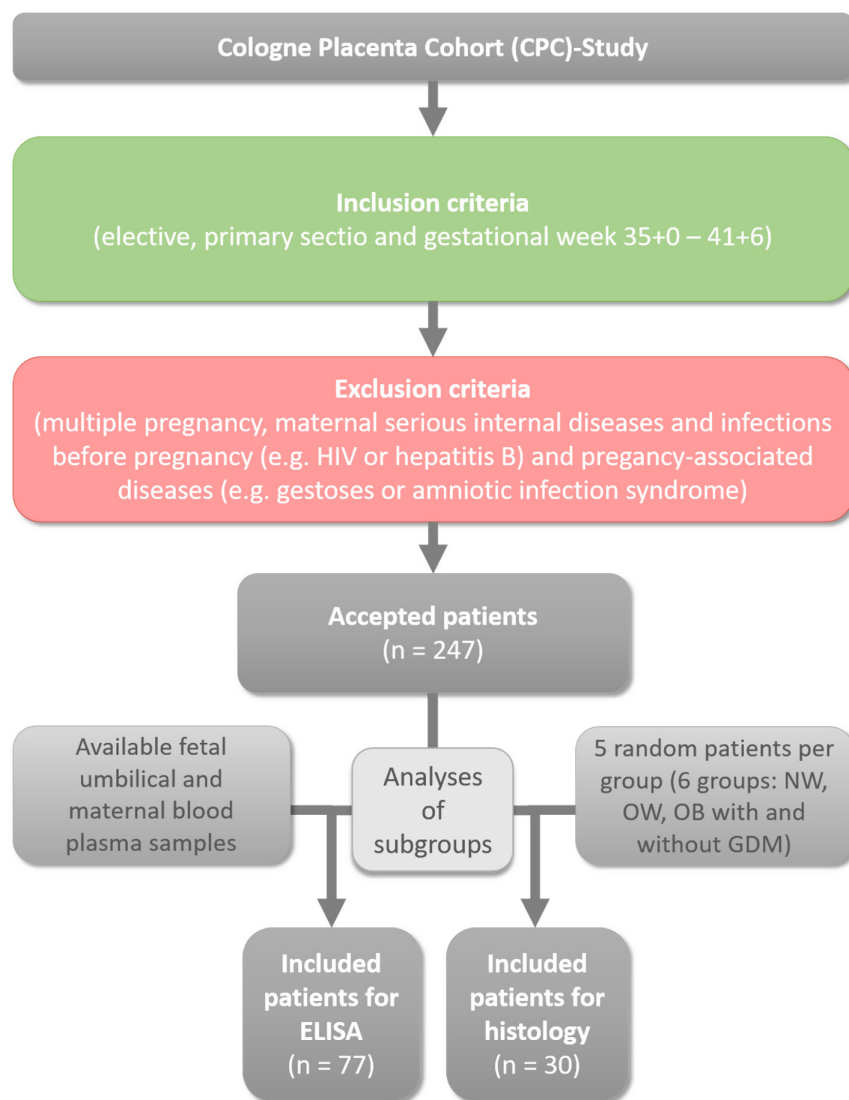


Figure 1
Overview of the study design. GDM, gestational diabetes mellitus; NW, normal weight; OB, obese; OW, overweight.

mM carbonate/bicarbonate buffer, pH 9.6) and incubated overnight at 4°C. After washing with PBST, the plate was incubated with 5% milk/PBS for 2 h for blocking. Asprosin standard and plasma samples were diluted in PBS. After 2h incubation of the samples at room temperature (RT), the plate was washed with PBST again. The detection antibody (mAB anti-asprosin antibody AG-20B-0073-C100 (AdipoGen, Liestal, Switzerland); $K_D = 22 \pm 2$ nM) was diluted 1:2000 in 2.5% milk/PBS and added to the plate for 1 h at RT. After washing the secondary antibody (polyclonal rabbit anti-mouse IgG-HRP conjugate P026002-2 (Agilent Dako) was added 1:2000 in 2.5% milk/PBS for 30 min at RT. The plate was washed again and 1-Step™ Ultra TMB-ELISA Substrate Solution (Thermo Scientific) was added and incubated for 15–20 min until the color developed. The reaction was stopped with 30% H_2SO_4 and the optical density was read at 3000 g.

Cell culture

Placental BeWo cells were seeded at 26,300 cells/cm³ on glass coverslips and kept in culture for 24 h with DMEM, high glucose, pyruvate (Gibco)/10% FBS/1% Pent/Strep. Cells were starved in DMEM, high glucose, pyruvate (Gibco)/1% FBS/1% Pent/Strep overnight. Then the cells were incubated with acetic acid buffer (0.2 M acetic acid+0.5 M NaCl) for 5 min to remove potential serum asprosin from the cell surface. Then cells were fixed with 100% methanol for 10 min and stored in PBS until usage.

Immunofluorescence staining of asprosin in BeWo cells

Fixed cells were stained with Rabbit anti-Human, Mouse Asprosin Polyclonal Antibody (MBS7607159, MyBiosource,

San Diego, CA, USA). Cells were permeabilized with PBS/0.3%Triton-X (Sigma-Aldrich) for 30 min and blocked for 1 h with SEA BLOCK blocking buffer (37527, Thermo Fisher). Primary asprosin antibody diluted 1:200 in Antibody Diluent (S0809, Agilent Dako) was added to the cells overnight at 4°C. Cells were incubated with secondary CyTM5 AffiniPure Goat Anti-Rabbit IgG (H+L) (AB_2338013, Jackson Immuno Research) for 1 h at room temperature. After that, cells were stained with 1:1000 DAPI for 10 min and embedded in InvitrogenTM Fluoromount-GTM Mounting Medium (Thermo Fisher, 00-4958-02). The negative control was performed the same way without adding a primary antibody. Pictures were taken with the fluorescence and light microscope Olympus BX53 at 100× magnification.

Immunohistochemical staining of asprosin in placental tissue

Paraffin slices were deparaffinated with 3 × 10 min Neo-Clear (109843, Sigma-Aldrich) and a descending ethanol series. Antigen-binding sites of placental tissue were retrieved in citric acid buffer for 35 min cooking in a steam cooker. Slices were permeabilized with PBS/0.3%Triton for 30 min and blocked for 1 h with SEA BLOCK blocking buffer (37527, Thermo Fisher). Primary asprosin antibody (see above), diluted 1:100 in Antibody Diluent (see above), was added to the slices overnight at 4°C. Then the tissue was incubated for 1 h at RT with HRP One-Step Polymer anti-Mouse/Rabbit (ZUC053-100, Zytomed Systems, Berlin, Germany). Subsequently, the Permanent AEC Kit (ZUC054-200s, Zytomed System, Berlin, Germany) was used for final staining. All slices were incubated for 2 min and reaction was stopped by adding aqua dest. Tissue was stained with hematoxylin for 5 min and blued for 10 min with floating tap water. Slides were brought back into organic milieu by an ascending ethanol series followed by 2 × 5 min Neo-Clear and embedded with Neo-Mount (109016, Sigma Aldrich). For the negative control, the primary antibody was changed with antibody diluent. Pictures were taken with the Olympus BX53 light and fluorescence microscope for the determination of asprosin localization and from scanned slides (Nanozoomer S360, Hamamatsu, Hamamatsu City, Japan) for semi-quantitative analysis using ImageJ software. A color threshold was applied to determine AEC stained area (hue 215-255; saturation 25-255; brightness 0-235) and total placental area (hue 0-255; saturation 10-255; brightness 0-235). AEC stained area was normalized to total placental area.

H&E stain in placenta

Placenta slices were deparaffinated as described above. Slides were stained with hematoxylin (Carl Roth, Karlsruhe, Germany) for 5 min and incubated in flowing tap water for 10 min. Thereafter, the tissue was stained with 0.5% eosin G (Carl Roth, Karlsruhe, Germany) for 2 min following an ascending ethanol series and 2 × 5 min Neo-Clear. Samples were embedded with Neo-Mount and pictures were taken at the Olympus BX53 (Olympus).

Statistics

Correlation studies were performed with Spearman correlation analyses in GraphPad Prism software including maternal, fetal and placental asprosin levels and various clinical parameters because of non-Gaussian distribution (weak correlation: Correlation Coefficient $r_s=0.2-0.39$; moderate correlation: $r_s=0.4-0.59$; strong correlation: $r_s=0.6-0.79$; * $P < 0.05$; ** $P < 0.01$; *** $P < 0.001$; **** $P < 0.0001$). Additional bar graphs show relative placental asprosin expression (normalized to the control group) as single data points, mean ± s.d. Mann-Whitney *U*-tests were used for statistical analysis (* $P < 0.05$; ** $P < 0.01$; *** $P < 0.001$; **** $P < 0.0001$).

Results

Correlation of maternal and fetal umbilical plasma asprosin levels with clinical parameters

Firstly, we determined the plasma asprosin levels in the maternal blood shortly before and fetal umbilical blood upon delivery (see Fig. 1 for study overview). Asprosin plasma concentrations ranged between 2.93 and 21.64 ng/mL (mean=8.11 ± 3.80 ng/mL) in maternal and from 1.91 to 20.13 ng/mL (mean=9.60 ± 3.87 ng/mL) in the fetal umbilical plasma (Table 1). Maternal and fetal plasma asprosin concentrations showed a strong positive correlation (Table 1).

Correlation analyses between asprosin plasma concentrations and numerous clinical characteristics and metabolic parameters, such as age, BMI, GDM diagnosis, blood insulin and glucose, HbA1c, serum triglycerides, cholesterol, LDL, HDL, cholesterol/HDL ratio, cortisol, placental weight, week of childbirth, sex of the child, birth weight, birth weight percentile and birth length, did not reveal significant results (Table 1). Still, a significant reduction of plasma asprosin levels was observed in maternal and fetal umbilical plasma if mothers reported

Table 1 Correlation analysis of human maternal and fetal umbilical plasma asprosin with maternal clinical parameters and neonatal birth information from ELISA analysis. Spearman correlation analysis: weak correlation (W): $r_s = 0.2-0.39$; moderate correlation (M): $r_s = 0.4-0.59$; strong correlation (S): $r_s = 0.60-0.79$.

Clinical parameter	Mean \pm s.d.	Maternal asprosin			Fetal umbilical asprosin		
	Min./max.	r_s	P-value	n	r_s	P-value	n
Maternal asprosin	8.11 \pm 3.80 2.93/21.64	X	X	X	0.776_S	<0.0001^b	77
Fetal umbilical asprosin	9.60 \pm 3.87 1.91/20.13	0.776_S	<0.0001^b	77	X	X	X
Age (years)	33 \pm 5 21/43	0.145	0.208	77	0.152	0.186	77
BMI (kg/m ²)	26.56 \pm 5.77 16.21/41.32	0.119	0.303	NW = 36 OW = 25 OB = 16	-0.028	0.812	NW = 36 OW = 25 OB = 16
GDM	X	0.150	0.194	Non-GDM = 56 GDM = 21	0.038	0.743	Non-GDM = 56 GDM = 21
Exercise before pregnancy	X	0.232_W	0.0421^a	Yes = 38 No = 39	0.106	0.359	Yes = 38 No = 39
Smoking before pregnancy	X	-0.293_W	0.0102^a	Yes = 35 No = 41	-0.288_W	0.0116^a	Yes = 35 No = 41
Insulin (mU/L)	13.35 \pm 9.02 0.50/61.40	0.085	0.482	71	0.089	0.459	71
Glucose (mg/dL)	72 \pm 13 35/103	0.062	0.606	72	0.090	0.452	72
HbA1c (%)	5.6 \pm 1.1 4.6/13.9	-0.067	0.592	67	-0.168	0.175	67
Triglycerides (mg/dL)	252 \pm 83 78/524	0.039	0.743	72	0.043	0.719	72
Cholesterol (mg/dL)	257 \pm 59 86/500	-0.028	0.818	72	0.116	0.331	72
LDL (mg/dL)	154 \pm 51 34/361	0.022	0.871	57	0.099	0.464	57
HDL (mg/dL)	69 \pm 17 31/119	0.149	0.270	57	0.208	0.121	57
Cholesterol/HDL	3.9 \pm 0.9 1.8/6.7	0.007	0.958	57	-0.030	0.823	57
Cortisol (μ g/L)	285 \pm 98 1/583	-0.071	0.569	67	0.020	0.872	67
Placental weight (g)	713.2 \pm 154.83 418.2/1221.2	0.015	0.899	77	-0.002	0.984	77
Gestational age at birth (week)	39.2 \pm 0.7 37.1/41.1	-0.153	0.183	77	-0.171	0.137	77
Sex of child	X	0.048	0.679	♀ = 39 ♂ = 38	0.108	0.352	♀ = 39 ♂ = 38
Birth weight (g)	3501 \pm 517 2100/4620	0.096	0.405	77	0.045	0.697	77
Birth weight percentile (%)	54 \pm 28 1/99	0.105	0.368	75	0.084	0.472	75
Birth length (cm)	52 \pm 3 45/62	-0.010	0.931	77	-0.152	0.186	77

^aP < 0.05; ^bP < 0.0001; Significant results were indicated in bold.

GDM, gestational diabetes mellitus; NW, normal weight (BMI <25); OB, obese (BMI >30); OW, overweight (BMI, 25-30).

smoking before pregnancy compared to non-smoking mothers (Table 1). Additionally, there was a weak but significant positive correlation between the level of exercise before pregnancy and maternal plasma asprosin concentration (Table 1).

However, when stratifying for BMI (NW: BMI <25; OW: BMI=25-30; OB: BMI >30) and GDM diagnosis

(yes or no), an increase in maternal and fetal plasma asprosin of normal-weight and obese mothers was observed in the GDM group (Fig. 2A and B). Solely the overweight group did not show any significance (Fig. 2A and B). There was no difference in maternal and fetal asprosin upon different GDM-treatments (Fig. 2C and D).

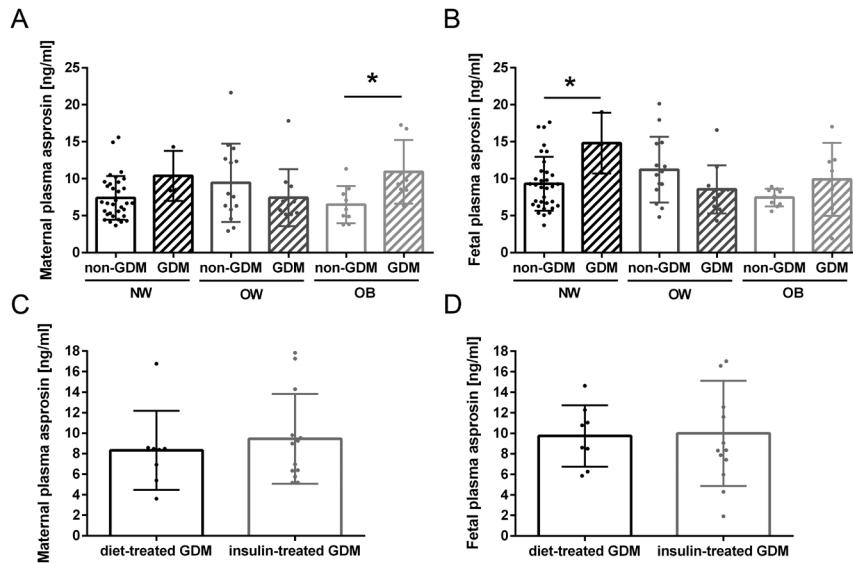


Figure 2

Maternal and fetal plasma asprosin levels upon overweight/obesity and GDM. (A and B) Maternal (A) and fetal (B) plasma asprosin levels stratified by BMI and GDM. (C and D) Maternal (C) and fetal (D) plasma asprosin levels stratified by GDM treatment (diet vs insulin). Statistics were performed with GraphPad Prism using two-way ANOVA and Mann-Whitney *U*-test (**P* < 0.05). GDM, gestational diabetes mellitus.

Asprosin expression pattern in human placental cells and tissue

To explore whether placental cells might be a source of asprosin, cultured chorionic BeWo cells were stained with the anti-asprosin antibody (Fig. 3A). In the absence of an external asprosin source, two distinct staining patterns were detectable in cultivated chorionic cells: dotted cytosolic asprosin and asprosin with a rather fibrillar appearance in the extracellular space (Fig. 3A; white arrows). To assess the pattern of immunoreactivity in human placental tissue, IHC stainings for asprosin were performed (Fig. 3B; IHC). Orientation within the tissue was achieved by the distinction of the maternal and fetal site of the placenta, identified by characteristic cell structures. Asprosin immunoreactivity was mainly detected in endothelial cells of fetal blood vessels, both in the villous parenchyma as well as in the chorion (Fig. 4B Villous parenchyma, Chorion; black arrows). Also, the epithelium of the amnion displayed immunoreactivity (Fig. 4B Amnion; black arrow). Additionally, immune cells all over the placenta displayed marked asprosin immunoreactivity (Fig. 4B Chorion, Amnion, Decidua; white arrows). In the maternal part of the placenta, individual decidual cells (Fig. 4B Decidua; gray arrow) also showed a distinct pattern of immunoreactivity.

Possible correlation between placental asprosin immunoreactivity and maternal BMI and GDM

We next performed asprosin immunohistochemistry in a subset of placentas of normal weight, overweight and obese women with and without GDM in our study

(Fig. 4A). To assess whether placental asprosin in the villi relates to its plasma levels, Spearman correlation analysis was performed. There was a positive correlation of maternal but not fetal umbilical plasma asprosin concentrations with placental asprosin immunoreactivity (Table 2). Additionally, there was a positive correlation between placental asprosin immunoreactivity and BMI (Table 2), especially significant in women with GDM (Fig. 4B). GDM alone did not affect placental asprosin content (Table 2), but interestingly, maternal circulating serum insulin correlated with placental asprosin immunoreactivity (Table 2). When comparing treatment strategies (dietary vs insulin treatment) in pregnant women with GDM, a significant increase in placental asprosin immunoreactivity occurred with insulin treatment (Fig. 4C).

Discussion

In our study, we set out to investigate the potential relation of maternal and fetal umbilical plasma asprosin concentrations to BMI, GDM and other clinical parameters in our CPC-Study. Even though we could not find a significant correlation between any single clinical parameter and plasma asprosin concentrations, the diagnosis of GDM in BMI subgroups seemed to affect asprosin concentrations in both, maternal and fetal umbilical plasma: obese pregnant women (BMI >30) and the fetal umbilical blood of normal-weight women (BMI <25) display a significant increase in plasma asprosin levels with maternal GDM; the fetal and maternal counterparts show same tendencies. While the influence of BMI in pregnancy was never addressed before, it was shown that asprosin blood levels are increased with

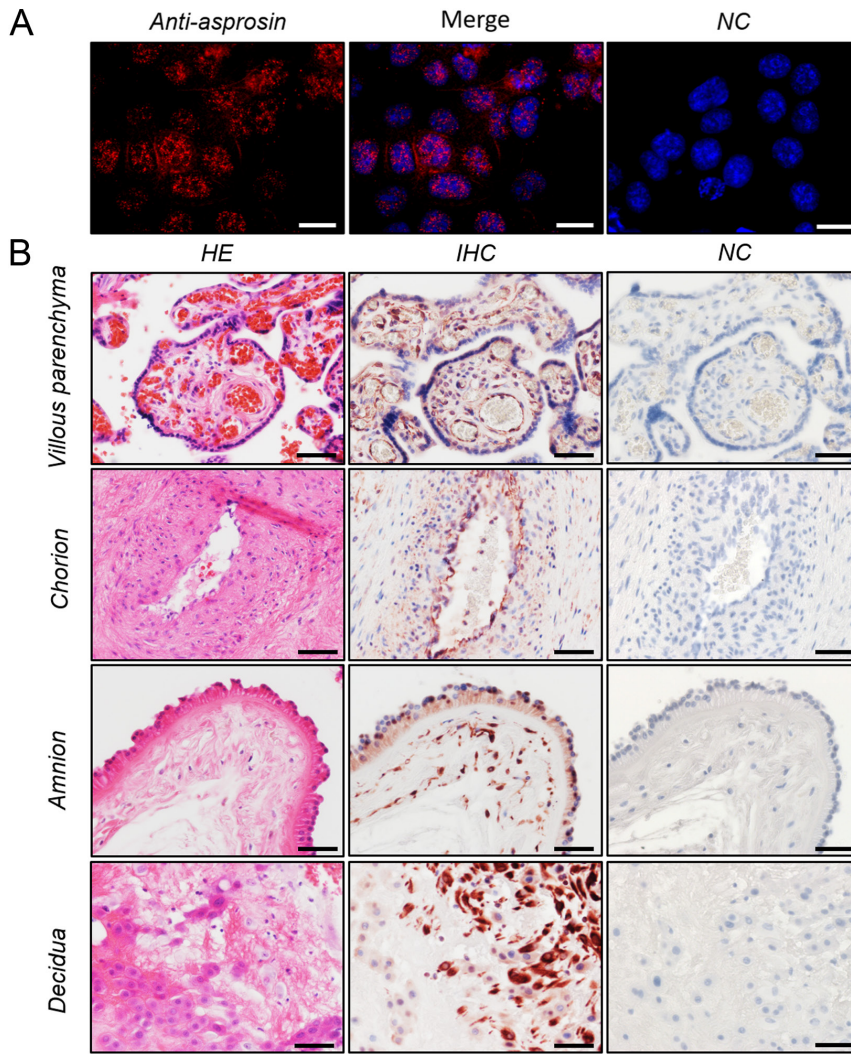


Figure 3

Immunofluorescence and -histochemistry staining of asprosin in placental cells and tissue. (A) Immunofluorescent staining of endogenous asprosin in placental BeWo cells with asprosin antibody and negative control (stained solely with Cy5 goat-anti-rabbit secondary antibody). White arrows point to fibrillar asprosin stainings. Scale bar = 20µm. (B) IHC AEC staining of asprosin in different placental areas with respective H&E-G staining and NC. Black arrows display endothelial cells, white arrows show immune cells and the gray arrow points to a decidual cell. Scale bar = 50 µm. H&E, hematoxylin and eosin; IHC, immunohistochemical; NC, negative control.

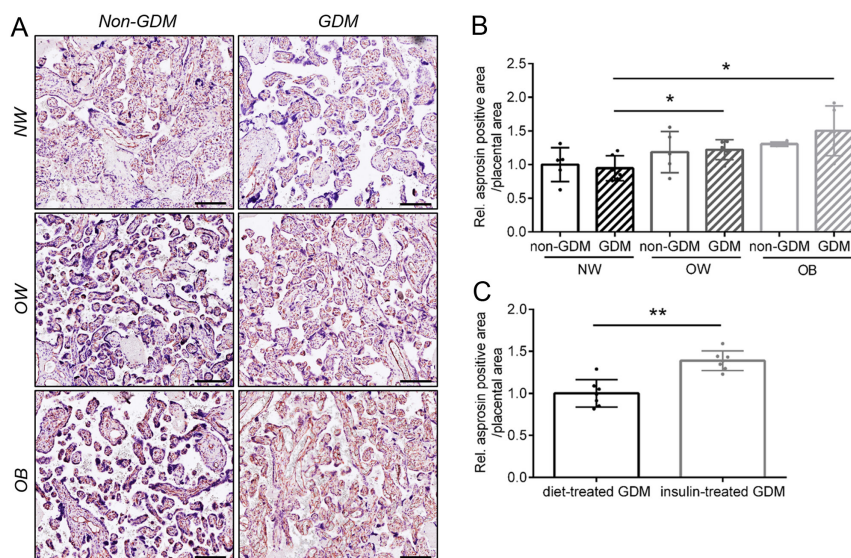


Figure 4

Analysis of asprosin levels in the placental villous parenchyma. (A) Exemplary immunohistochemical AEC+Hematoxylin staining of placental tissue for asprosin from normal weight (NW; BMI <25), overweight (OW; BMI >25 and <30) and obese (OB; BMI >30) pregnant women segregated by non-GDM and GDM patients. Scale bar = 100 µm. (B) Relative placental asprosin immunoreactivity normalized to non-GDM/normal weight level and segregated by BMI and GDM diagnosis. (C) Relative placental asprosin immunoreactivity in GDM patients. Patients were either treated by diet or with insulin and values are normalized to the diet-treated group. Statistics were performed with GraphPad Prism using Mann-Whitney *U*-test (**P* < 0.05; ***P* < 0.01). GDM, gestational diabetes mellitus; NW, normal weight; OB, obese; OW, overweight.

Table 2 Correlation analysis of human placental asprosin with maternal clinical parameters and neonatal birth information from IHC analysis. Spearman correlation analysis: weak correlation (W): $r_s = 0.2-0.39$; moderate correlation (M): $r_s = 0.4-0.59$; strong correlation (S): $r_s = 0.60-0.79$.

Clinical parameter	Mean \pm s.d.	Placental asprosin		
	Min./Max.	r_s	P-value	n
Maternal asprosin	9.23 \pm 3.55 4.48/17.82	0.459_M	0.0209^a	25
Fetal umbilical asprosin	10.93 \pm 3.92 5.39/19.00	0.249	0.230	25
Age (years)	34 \pm 4 26/43	0.187	0.322	30
BMI (kg/m ²)	27.74 \pm 6.66 16.21/41.32	0.684_S	<0.0001^b	NW = 11 OW = 10 OB = 9
GDM	X	0.000	>0.999	Non-GDM = 14 GDM = 16
Exercise before pregnancy	X	-0.143	0.450	Yes = 14 No = 16
Smoking before pregnancy	X	-0.005	0.978	Yes = 5 No = 25
Insulin (mU/L)	14.6 \pm 11.4 4.7/61.4	0.482_M	0.0126^a	26
Glucose (mg/dL)	73 \pm 11 44/93	0.204	0.307	27
HbA1c (%)	5.8 \pm 1.6 4.9/13.9	0.350	0.0580	30
Triglycerides (mg/dL)	258 \pm 91 78/452	-0.362	0.0637	27
Cholesterol (mg/dL)	249 \pm 48 180/357	-0.237	0.234	27
LDL (mg/dL)	145 \pm 43 77/243	-0.126	0.606	19
HDL (mg/dL)	67 \pm 16 36/98	0.235	0.332	19
Cholesterol/HDL	3.9 \pm 1.0 2.4/6.7	-0.206	0.399	19
Cortisol (μ g/L)	301 \pm 89 183/583	-0.247	0.225	26
Placental weight [g]	722.1 \pm 139.0 468.2/1024.2	0.025	0.895	30
Gestational age at birth (week)	39.2 \pm 0.6 37.4/40.1	0.288	0.122	30
Sex of child	X	0.004	0.983	♀ = 11 ♂ = 19
Birth weight (g)	3658 \pm 429 2990/4660	0.301	0.107	30
Birth weight percentile (%)	63 \pm 24 12/99	0.258	0.169	30
Birth length (cm)	53 \pm 3 49/62	0.114	0.550	30

^aP < 0.05; ^bP < 0.0001; Significant results were indicated in bold.

GDM, gestational diabetes mellitus; NW, normal weight (BMI <25); OB, obese (BMI >30); OW, overweight (BMI, 25–30).

GDM in both, rodents (17) and women (13, 14). Asprosin is known to trigger the glucose release from the liver (1). Thus, increased asprosin levels during pregnancy might contribute to increased blood glucose concentrations in GDM.

Although several metabolic parameters and patient characteristics of our cohort did not correlate with asprosin

plasma concentrations, two external factors seem to have an influence on asprosin levels: exercise and smoking before pregnancy. With regard to exercise and asprosin levels, so far rather contradictory data were published. On one hand, it was shown by several groups that acute aerobic exercise decreases asprosin levels in humans (18, 19, 20) and rats (21). On the other hand, acute anaerobic exercise

was shown to correlate with increased asprosin levels in women (22). Here, we see a positive correlation between the number of exercise days per week (0, 1, 2, 3 or more) during pregnancy and maternal asprosin plasma concentrations. Thus, there might be a so far undescribed dose-dependent long-term effect of chronic exercise on plasma asprosin concentrations. However, since it was not the focus of our study, we have no further information regarding the exact type and level of impact of exercise before pregnancy in our cohort. Therefore, further conclusions would be premature.

Interestingly, we found a novel correlation between asprosin plasma levels and smoking. In mothers who smoked before pregnancy, we found decreased asprosin concentrations in maternal and fetal umbilical plasma. Asprosin was shown to be an orexigenic hormone produced by white adipose tissue (1, 2) and smoking often has been demonstrated to be connected to anorexigenic effects (23, 24). Thus, decreased asprosin levels in women who started smoking before pregnancy match reports on several other adipokines that are affected by nicotine and might convey the anorexigenic effects of smoking (25). However, in our study set-up, there is a supposed 9-month phase of nicotine abstinence before the determination of plasma asprosin. Therefore, a direct effect of nicotine on circulating asprosin in our cohort seems to be rather unlikely but should be addressed in future studies.

Confirming previous reports, we see a strong positive correlation between maternal and fetal umbilical plasma asprosin levels in our cohort (13, 14). This suggests that asprosin might pass the placenta and that changes in maternal asprosin plasma levels might exert direct metabolic effects in the fetus. Additionally, asprosin might affect the placental function and therefore cause secondary consequences for the fetus. So far, very little is known about placental asprosin expression, content, or transport. By assessing asprosin immunoreactivity in placentas from our cohort and relating it to asprosin concentrations in maternal and fetal umbilical plasma, we aimed at contributing to a better understanding of asprosin's role during pregnancy. We found a positive correlation between placental asprosin immunoreactivity and maternal plasma asprosin levels, which may indicate that maternal plasma asprosin accumulates in placental tissue. In addition, the placenta might serve as a source of circulating asprosin in the mother and might thereby contribute to plasma asprosin concentrations – a concept that is supported by our finding of asprosin production in cultured chorionic cells.

We detected placental asprosin immunoreactivity in various parts of the placenta. It was stained in endothelial cells of fetal vessels in the villous parenchyma and the chorion. Former studies have shown that placental endothelial cells produce many different chemokines (26) and function as conditional innate immune cells (27). Furthermore, we detected asprosin in decidual cells in the maternal side of the placenta, which are also known to play a role in immune regulation (28). Since asprosin seems to play a role in inflammation in other tissues (29, 30), it may be possible that the production/storage of asprosin in endothelial and decidual cells contributes to inflammatory processes in the placenta, similar to leptin which is a known autocrine and paracrine regulator of placental tissue (31). Of note, also endothelial cells in the amnion and macrophages in all parts of the placenta displayed marked asprosin immunoreactivity. As macrophages are known sources for pro-inflammatory adipokines (32) and have been described to accumulate in placentas of pregnancies complicated by GDM (33), production or release of asprosin by placental macrophages might contribute to several placental pathologies. However, both, endothelial cells and macrophages are known to commonly display unspecific immunoreactivity (34), so the detected signals in these cells should be interpreted with caution. Overall, the pattern of placental asprosin immunoreactivity indicates that asprosin seems to be mainly produced in placental cells that contribute to inflammation and immune regulation, two mechanisms contributing largely to known pregnancy complications, such as the increased risk of preterm birth, fetal growth restriction, placental pathologies and hypertensive disorders leading to profound consequences in the fetus (35, 36).

It was suggested before that placental asprosin immunoreactivity might be associated with GDM (14). In our cohort, we cannot confirm this finding. However, we can report a novel association between placental asprosin immunoreactivity and maternal BMI. And interestingly, the increase of placental asprosin immunoreactivity with rising BMI is stronger in women with GDM than in women without GDM. GDM is known to modulate insulin and leptin signaling during pregnancy (37), which might suggest that asprosin, as a strong metabolic regulator, is also affected by GDM. Additionally, we found that increased individual insulin levels correlated with increased placental asprosin immunoreactivity suggesting an interdependence between asprosin and insulin in general and during pregnancy. As asprosin displays an overlap with glucagon's molecular pathways and effects, a mechanistic link between asprosin and insulin seems plausible.

In conclusion, our study contributes several novel aspects to the ongoing investigation of asprosin's role in metabolism. The correlation of placental asprosin expression with the extent of maternal obesity as well as the characterization of potential placental transport mechanisms for asprosin deserve special attention in the future. In particular, an in-depth assessment of a potential molecular interplay between insulin and asprosin might advance the development of preventive and therapeutic measures against the health consequences of obesity and diabetes – not only during pregnancy.

Declaration of interest

The authors declare that there is no conflict of interest that could be perceived as prejudicing the impartiality of the research reported.

Funding

Funding for this study was provided by the Deutsche Forschungsgemeinschaft (DFG, German Research Foundation) project ID 384170921: FOR2722/M2 to G S, J D and E H R, by the Deutsche Forschungsgemeinschaft (DFG; grant AP 229/2-1) to S A and the Marga and Walter Boll foundation (Kerpen, Germany) (grant 210-01.2-17) to S A.

Acknowledgements

The authors would like to thank my medical doctoral students Maximilian Földvary and Janina Droxler for their technical support and commitment and all patients involved for their participation.

References

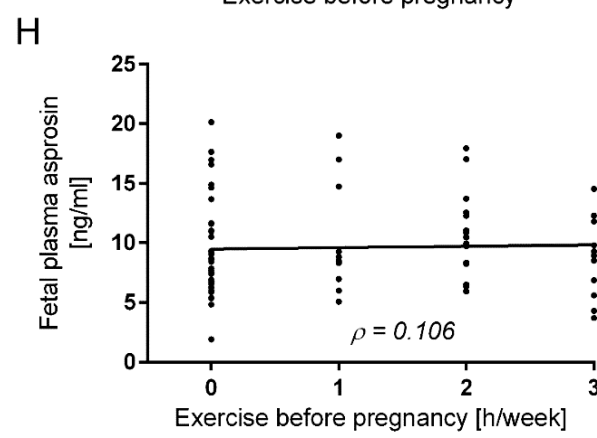
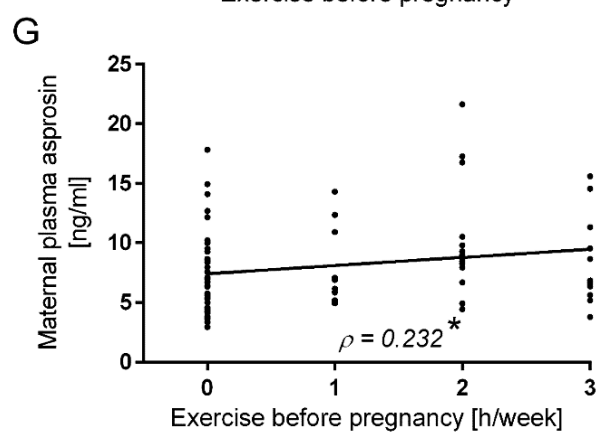
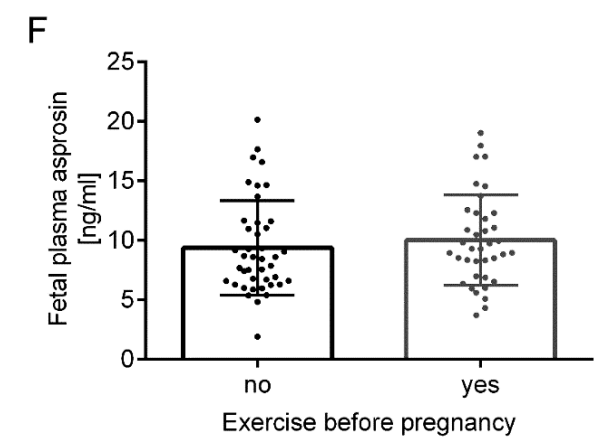
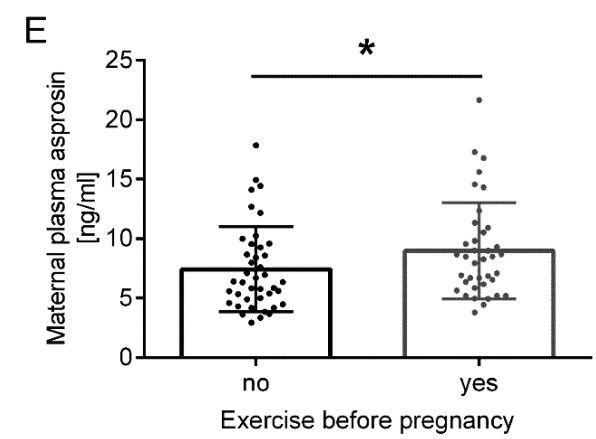
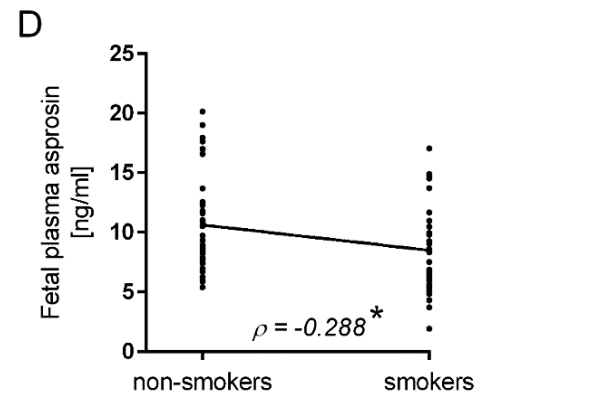
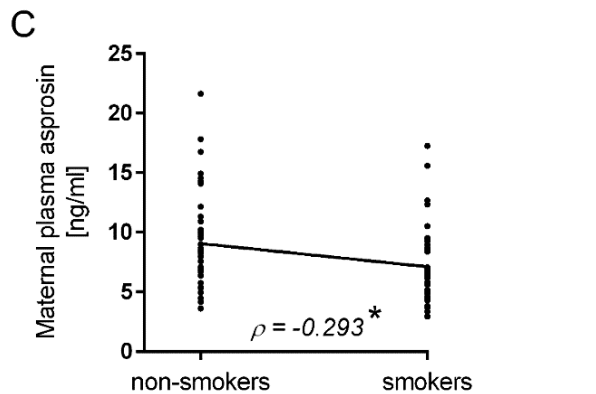
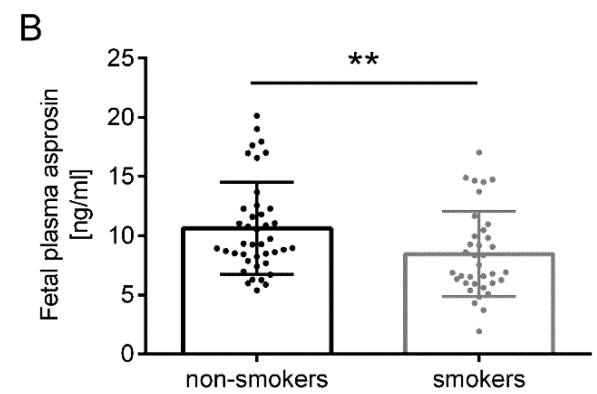
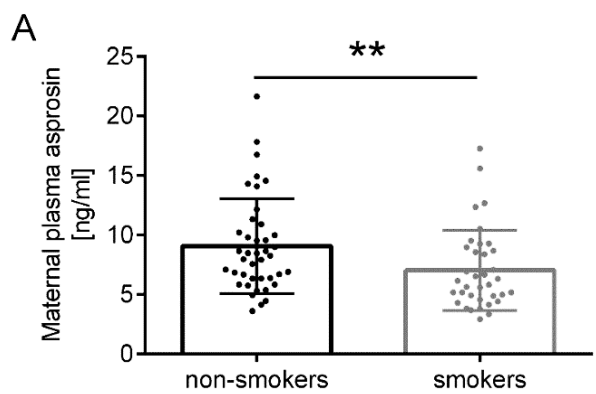
- Romere C, Duerschmid C, Bournat J, Constable P, Jain M, Xia F, Saha PK, Del Solar M, Zhu B, York B, *et al.* Asprosin, a fasting-induced glucogenic protein hormone. *Cell* 2016 **165** 566–579. (<https://doi.org/10.1016/j.cell.2016.02.063>)
- Duerschmid C, He Y, Wang C, Li C, Bournat JC, Romere C, Saha PK, Lee ME, Phillips KJ, Jain M, *et al.* Asprosin is a centrally acting orexigenic hormone. *Nature Medicine* 2017 **23** 1444–1453. (<https://doi.org/10.1038/nm.4432>)
- Ugur K & Aydin S. Saliva and blood asprosin hormone concentration associated with obesity. *International Journal of Endocrinology* 2019 **2019** 2521096. (<https://doi.org/10.1155/2019/2521096>)
- Zhang L, Chen C, Zhou N, Fu Y & Cheng X. Circulating asprosin concentrations are increased in type 2 diabetes mellitus and independently associated with fasting glucose and triglyceride. *Clinica Chimica Acta: International Journal of Clinical Chemistry* 2019 **489** 183–188. (<https://doi.org/10.1016/j.cca.2017.10.034>)
- Mishra I, Duerschmid C, Ku Z, He Y, Xie W, Silva ES, Hoffman J, Xin W, Zhang N, Xu Y, *et al.* Asprosin-neutralizing antibodies as a treatment for metabolic syndrome. *eLife* 2021 **10** e63784. (<https://doi.org/10.7554/eLife.63784>)
- Kleiblova P, Dostalova I, Bartlova M, Lacinova Z, Ticha I, Krejci V, Springer D, Kleibl Z & Haluzik M. Expression of adipokines and estrogen receptors in adipose tissue and placenta of patients with gestational diabetes mellitus. *Molecular and Cellular Endocrinology* 2010 **314** 150–156. (<https://doi.org/10.1016/j.mce.2009.08.002>)
- Hendler I, Blackwell SC, Mehta SH, Whitty JE, Russell E, Sorokin Y & Cotton DB. The levels of leptin, adiponectin, and resistin in normal weight, overweight, and obese pregnant women with and without preeclampsia. *American Journal of Obstetrics and Gynecology* 2005 **193** 979–983. (<https://doi.org/10.1016/j.ajog.2005.06.041>)
- Solis-Paredes M, Espino Y Sosa S, Estrada-Gutierrez G, Nava-Salazar S, Ortega-Castillo V, Rodriguez-Bosch M, Bravo-Flores E, Espejel-Nuñez A, Tolentino-Dolores M, Gaona-Estudillo R, *et al.* Maternal and fetal lipid and adipokine profiles and their association with obesity. *International Journal of Endocrinology* 2016 **2016** 7015626. (<https://doi.org/10.1155/2016/7015626>)
- Poleć A, Fedorcsák P, Eskild A & Tanbo TG. The interplay of human chorionic gonadotropin (hCG) with basic fibroblast growth factor and adipokines on angiogenesis in vitro. *Placenta* 2014 **35** 249–253. (<https://doi.org/10.1016/j.placenta.2014.02.002>)
- D'ippolito S, Tersigni C, Scambia G & Di Simone N. Adipokines, an adipose tissue and placental product with biological functions during pregnancy. *BioFactors* 2012 **38** 14–23. (<https://doi.org/10.1002/biof.201>)
- Stewart FM, Freeman DJ, Ramsay JE, Greer IA, Caslake M & Ferrell WR. Longitudinal assessment of maternal endothelial function and markers of inflammation and placental function throughout pregnancy in lean and obese mothers. *Journal of Clinical Endocrinology and Metabolism* 2007 **92** 969–975. (<https://doi.org/10.1210/jc.2006-2083>)
- Van Lieshout RJ, Taylor VH & Boyle MH. Pre-pregnancy and pregnancy obesity and neurodevelopmental outcomes in offspring: a systematic review. *Obesity Reviews* 2011 **12** e548–e559. (<https://doi.org/10.1111/j.1467-789X.2010.00850.x>)
- Baykus Y, Yavuzkir S, Ustebay S, Ugur K, Deniz R & Aydin S. Asprosin in umbilical cord of newborns and maternal blood of gestational diabetes, preeclampsia, severe preeclampsia, intrauterine growth retardation and macroseptic fetus. *Peptides* 2019 **120** 170132. (<https://doi.org/10.1016/j.peptides.2019.170132>)
- Zhong L, Long Y, Wang S, Lian R, Deng L, Ye Z, Wang Z & Liu B. Continuous elevation of plasma asprosin in pregnant women complicated with gestational diabetes mellitus: a nested case-control study. *Placenta* 2020 **93** 17–22. (<https://doi.org/10.1016/j.placenta.2020.02.004>)
- Janoschek R, Hoffmann T, Morcos YAT, Sengle G, Dötsch J & Hucklenbruch-Rother E. Asprosin in pregnancy and childhood. *Molecular and Cellular Pediatrics* 2020 **7** 18. (<https://doi.org/10.1186/s40348-020-00110-8>)
- Morcos YAT, Lütke S, Tenbierg A, Hanisch FG, Prymachuk G, Piekarek N, Hoffmann T, Keller T, Janoschek R, Niehoff A, *et al.* Sensitive asprosin detection in clinical samples reveals serum/saliva correlation and indicates cartilage as source for serum asprosin. *Scientific Reports* 2022 **12** 1340. (<https://doi.org/10.1038/s41598-022-05060-x>)
- Rezk MY, Elkattawy HA & Fouad RA. Plasma asprosin levels changes in pregnant and non-pregnant rats with and without gestational diabetes. *International Journal of Medical Research and Health Sciences* 2020 **9** 54–63.
- Nakhaei H, Mogharnasi M & Fanaei H. Effect of swimming training on levels of asprosin, lipid profile, glucose and insulin resistance in rats with metabolic syndrome. *Obesity Medicine* 2019 **15** 100111. (<https://doi.org/10.1016/j.obmed.2019.100111>)
- Ceylan Hİ, Saygın Ö & Özel Türkçü Ü. Assessment of acute aerobic exercise in the morning versus evening on asprosin, spexin, lipocalin-2, and insulin level in overweight/obese versus normal weight adult men. *Chronobiology International* 2020 **37** 1252–1268. (<https://doi.org/10.1080/07420528.2020.1792482>)
- Zarei M, Khodakheyr JN, Rashidlamir A & Montazeri A. The effect of combined resistance aerobic exercise training on concentrations of asprosin and complement C1q tumor necrosis factor-related protein-1

- in men with type 2 diabetes. *Sport Sciences for Health* 2021 **17** 863–871. (<https://doi.org/10.1007/s11332-021-00738-7>)
- 21 Ko JR, Seo DY, Kim TN, Park SH, Kwak HB, Ko KS, Rhee BD & Han J. Aerobic exercise training decreases hepatic asprosin in diabetic rats. *Journal of Clinical Medicine* 2019 **8** 666. (<https://doi.org/10.3390/jcm8050666>)
- 22 Wiecek M, Szymura J, Maciejczyk M, Kantorowicz M & Szygula Z. Acute anaerobic exercise affects the secretion of asprosin, irisin, and other cytokines – a comparison between sexes. *Frontiers in Physiology* 2018 **9** 1782. (<https://doi.org/10.3389/fphys.2018.01782>)
- 23 Miyata G, Meguid MM, Fetissov SO, Torelli GF & Kim HJ. Nicotine's effect on hypothalamic neurotransmitters and appetite regulation. *Surgery* 1999 **126** 255–263. ([https://doi.org/10.1016/S0039-6060\(99\)70163-7](https://doi.org/10.1016/S0039-6060(99)70163-7))
- 24 Sanigorski A, Fahey R, Cameron-Smith D & Collier GR. Nicotine treatment decreases food intake and body weight via leptin-independent pathway in *Psammomys obesus*. *Diabetes, Obesity and Metabolism* 2002 **4** 346–350. (<https://doi.org/10.1046/j.1463-1326.2002.00216.x>)
- 25 Bai XJ, Fan LH, He Y, Ren J, Xu W, Liang Q, Li HB, Huo JH, Bai L, Tian HY, *et al.* Nicotine may affect the secretion of adipokines leptin, resistin, and visfatin through activation of KATP channel. *Nutrition* 2016 **32** 645–648. (<https://doi.org/10.1016/j.nut.2015.12.001>)
- 26 Galley HF & Webster NR. Physiology of the endothelium. *British Journal of Anaesthesia* 2004 **93** 105–113. (<https://doi.org/10.1093/bja/aeh163>)
- 27 Mai J, Virtue A, Shen J, Wang H & Yang X-F. An evolving new paradigm: endothelial cells–conditional innate immune cells. *Journal of Hematology and Oncology* 2013 **6** 1–13. (<https://doi.org/10.1186/1756-8722-6-61>)
- 28 Canavan TP & Simhan HN. Innate immune function of the human decidual cell at the maternal–fetal interface. *Journal of Reproductive Immunology* 2007 **74** 46–52. (<https://doi.org/10.1016/j.jri.2006.10.004>)
- 29 Lee T, Yun S, Jeong JH & Jung TW. Asprosin impairs insulin secretion in response to glucose and viability through TLR4/JNK-mediated inflammation. *Molecular and Cellular Endocrinology* 2019 **486** 96–104. (<https://doi.org/10.1016/j.mce.2019.03.001>)
- 30 Jung TW, Kim HC, Kim HU, Park T, Park J, Kim U, Kim MK & Jeong JH. Asprosin attenuates insulin signaling pathway through PKC δ -activated ER stress and inflammation in skeletal muscle. *Journal of Cellular Physiology* 2019 **234** 20888–20899. (<https://doi.org/10.1002/jcp.28694>)
- 31 Akerman F, Lei ZM & Rao CV. Human umbilical cord and fetal membranes co-express leptin and its receptor genes. *Gynecological Endocrinology* 2002 **16** 299–306. (<https://doi.org/10.1080/gye.16.4.299.306>)
- 32 Chazaud B. A macrophage-derived adipokine supports skeletal muscle regeneration. *Nature Metabolism* 2020 **2** 213–214. (<https://doi.org/10.1038/s42255-020-0186-9>)
- 33 Yu J, Zhou Y, Gui J, Li AZ, Su XL & Feng L. Assessment of the number and function of macrophages in the placenta of gestational diabetes mellitus patients. *Journal of Huazhong University of Science and Technology* 2013 **33** 725–729. (<https://doi.org/10.1007/s11596-013-1187-7>)
- 34 Honig A, Rieger L, Kapp M, Dietl J & Kämmerer U. Immunohistochemistry in human placental tissue – pitfalls of antigen detection. *Journal of Histochemistry and Cytochemistry* 2005 **53** 1413–1420. (<https://doi.org/10.1369/jhc.5A6664.2005>)
- 35 Vannuccini S, Clifton VL, Fraser IS, Taylor HS, Critchley H, Giudice LC & Petraglia F. Infertility and reproductive disorders: impact of hormonal and inflammatory mechanisms on pregnancy outcome. *Human Reproduction Update* 2016 **22** 104–115. (<https://doi.org/10.1093/humupd/dmv044>)
- 36 Goldstein JA, Gallagher K, Beck C, Kumar R & Gernand AD. Maternal-fetal inflammation in the placenta and the developmental origins of health and disease. *Frontiers in Immunology* 2020 **11** 531543. (<https://doi.org/10.3389/fimmu.2020.531543>)
- 37 Pérez-Pérez A, Guadix P, Maymó J, Dueñas JL, Varone C, Fernández-Sánchez M & Sanchez-Margalet V. Insulin and leptin signaling in placenta from gestational diabetic subjects. *Hormone and Metabolic Research* 2016 **48** 62–69. (<https://doi.org/10.1055/s-0035-1559722>)

Received in final form 4 February 2022

Accepted 11 February 2022

Accepted Manuscript published online 11 February 2022



Supplementary figure 1: Correlation analysis of plasma asprosin with smoking and exercise before pregnancy.

A: Maternal plasma asprosin concentration separated in non-smoking and smoking patients.

B: Respective fetal plasma asprosin concentration separated in non-smoking and smoking patients.

C: Correlation analysis of maternal plasma asprosin with status of smoking.

D: Correlation analysis of respective fetal plasma asprosin with status of smoking.

E: Maternal plasma asprosin concentration separated in no exercise (no) and exercise (yes).

F: Respective plasma asprosin concentration separated in no exercise (no) and exercise (yes).

G: Correlation analysis of maternal plasma asprosin with time of weekly exercise.

H: Correlation analysis of respective fetal plasma asprosin with time of weekly exercise.

Statistics were performed with graphpad prism using Mann-Whitney U-test (*p < 0.05; **p < 0.01) and Spearman correlation analysis (ρ = Spearman's rank correlation coefficient).

5. Transglutaminase mediated asprosin oligomerization allows its tissue storage as fibers

Transglutaminase mediated asprosin oligomerization allows its tissue storage as fibers

Yousef A.T. Morcos^{1,2}, Galyna Pryymachuk^{3,10}, Steffen Lütke^{1,2}, Antje Gerken^{1,2}, Alan R. F. Godwin^{12,13}, Thomas A. Jowitt^{12,13}, Nadin Piekarek³, Thorben Hoffmann², Anja Niehoff^{6,9}, Margarete Odenthal^{4,5}, Uta Drebber⁴, Olaf Grisk¹¹, Yury Ladilov¹⁴, Wilhelm Bloch⁶, Bert Callewaert^{7,8}, Mats Paulsson^{1,5,9}, Eva Hucklenbruch-Rother², Clair Baldock^{12,13}, Gerhard Sengle^{1,2,5,9*}

¹Center for Biochemistry, Faculty of Medicine and University Hospital of Cologne, University of Cologne, Joseph-Stelzmann-Street 52, 50931 Cologne, Germany

²Department of Pediatrics and Adolescent Medicine, Faculty of Medicine and University Hospital Cologne, University of Cologne, Cologne, Germany

³Department of Anatomy I, Faculty of Medicine and University Hospital Cologne, University of Cologne, Cologne, Germany

⁴Institute of Pathology, Faculty of Medicine and University Hospital Cologne, University of Cologne, Cologne, Germany

⁵Center for Molecular Medicine Cologne (CMMC), University of Cologne, Cologne, Germany

⁶Institute of Cardiology and Sports Medicine, German Sport University Cologne, Cologne, Germany

⁷Center for Medical Genetics Ghent, Ghent University Hospital, Ghent 9000, Belgium

⁸Department of Biomolecular Medicine, Ghent University, Ghent 9000, Belgium

⁹Cologne Center for Musculoskeletal Biomechanics (CCMB), Faculty of Medicine and University Hospital of Cologne, University of Cologne, Cologne, Germany

¹⁰Institute of Anatomy, Brandenburg Medical School Theodor Fontane, Fehrbelliner Str. 38, 16816 Neuruppin, Germany

¹¹Institute of Physiology, Brandenburg Medical School Theodor Fontane, Fehrbelliner Str. 38, 16816 Neuruppin, Germany

¹²Wellcome Trust Centre for Cell-Matrix Research, School of Biological Sciences, Faculty of Biology, Medicine and Health, Manchester Academic Health Science Centre, University of Manchester, Manchester, UK

¹³Division of Cell Matrix Biology and Regenerative Medicine, School of Biological Sciences, Faculty of Biology, Medicine and Health, Manchester Academic Health Science Centre, University of Manchester, Manchester, UK

¹⁴Brandenburg Heart Center, Brandenburg Medical School Theodor, Fontane, Ladeburger Str. 17, 16321 Bernau bei Berlin, Germany

*corresponding author: Gerhard Sengle

Email: gsengle@uni-koeln.de

Running title: Asprosin oligomerization by transglutaminase activity

Keywords: Asprosin, transglutaminase 2, fibrillin, extracellular matrix, protein oligomerization, connective tissues

Abstract

Asprosin, the C-terminal furin cleavage product of profibrillin-1, was reported to act as a hormone that circulates at nanomolar levels and is recruited to the liver where it induces G protein-coupled activation of the cAMP-PKA pathway and stimulates rapid glucose release into the circulation. Although derived upon C-terminal cleavage of fibrillin-1, a multidomain extracellular matrix glycoprotein with a ubiquitous distribution in connective tissues, little is known about the mechanisms controlling the bioavailability of asprosin in tissues. In the current view, asprosin is mainly produced by white adipose tissue from where it is released into the blood in monomeric form. Here, by employing newly generated specific asprosin antibodies we monitored the distribution pattern of asprosin in human and murine connective tissues such as placenta, and muscle. Thereby we detected the presence of asprosin positive extracellular fibers. Further, by screening established cell lines for asprosin synthesis we found that most cells derived from musculoskeletal tissues render asprosin into an oligomerized form. Our analyses show that asprosin already multimerizes intracellularly, but that stable multimerization via covalent bonds is facilitated by transglutaminase activity. Further, asprosin fiber formation requires an intact fibrillin-1 fiber network for proper linear deposition. Our data suggest a new extracellular storage mechanism of asprosin in an oligomerized form which may regulate its cellular bioavailability in tissues.

Introduction

Fibrillin-1 is a large, 350 kDa extracellular matrix (ECM) glycoprotein that when mutated leads to the multi-system disorder Marfan syndrome (MFS; OMIM#154700) affecting mostly the musculoskeletal (e.g. long bone overgrowth, muscle wasting, hyperflexible joints) and cardiovascular system (e.g. aortic root aneurysm formation). The multiple clinical features of MFS reflect the ubiquitous tissue distribution pattern of fibrillin-1 (1). Since most mutations in *FBNI* result in a slender habitus with little subcutaneous fat (2), it is intuitive to speculate that fibrillin-1 plays a role in metabolism and body fat formation. In addition, specific mutations within exon 64 at the 3' end of *FBNI* were described to lead to marfanoid-progeroid-lipodystrophy syndrome (MFLS; OMIM#616914) (3), a fibrillinopathy characterized by progeroid facial features and severe lipodystrophy (3-6). A mechanistic explanation for these striking clinical features was provided by the discovery that the C-terminal cleavage product of profibrillin-1 serves as a fasting-induced glucogenic protein hormone that modulates hepatic glucose release (7). Profibrillin-1 is translated as a 2,871-amino-acid long proprotein, which is cleaved at the C-terminus by the protease furin (8). In addition to mature fibrillin-1, this cleavage generates a 140-amino-acid long C-terminal cleavage product. MFLS mutations were found to be clustered around the furin cleavage site, thereby causing heterozygous ablation of the C-terminal cleavage product which was only detectable at strongly reduced levels in plasma of patients (7). This C-terminal furin cleavage product of fibrillin-1 was termed "asprosin" after the Greek word for white because of its strong impact on white fat tissue (WAT) (7).

Asprosin was reported to circulate at nanomolar levels and is recruited to the liver where it induces G protein-coupled activation of the cAMP-PKA pathway and stimulates rapid glucose release into the circulation (7). Following a circadian rhythm and triggered by fasting, asprosin induces hepatic glucose release via the G-protein-coupled OLF734 receptor (7,9) and reduces insulin secretion from pancreatic β -cells (10). Asprosin has also

been shown to cross the blood brain barrier and activate hunger-stimulating AgRP (Agouti-related peptide) neurons in the hypothalamus which induces appetite in mice (11). In addition, asprosin was shown to impair insulin sensitivity in skeletal muscle cells *in vitro* (12). There are also several reports of increased serum asprosin levels in obese patients and patients with type 2 diabetes mellitus (T2DM) and that asprosin serum concentrations are positively correlated with insulin resistance (13). In mice, antibody-mediated neutralization of asprosin leads to reduced food intake and body weight as well as improved insulin sensitivity (11). Therefore, asprosin currently ranges among the most promising candidates for the pharmacological therapy of obesity, T2DM and other metabolic disorders (13).

Although derived from ubiquitously expressed fibrillin-1, little is known about the tissue distribution of asprosin. In the current view, asprosin is mainly produced by WAT from where it is released into the blood in monomeric form. However, our previous findings showed that asprosin is synthesized and secreted by connective tissue resident cells such as fibroblasts and chondrocytes (14) – a finding which supports the notion of local asprosin storage within tissue-specific microenvironments. Here, by employing newly generated specific asprosin antibodies we monitored the distribution pattern of asprosin in various human and murine connective tissues, including placenta, and muscle. In addition, we monitored the synthesis of asprosin in various established cell lines. Our data reveal new insight into how asprosin may be stored within the extracellular microenvironment of connective tissues and how this affects its cellular bioavailability.

Results

Extracellular storage of asprosin as fibers in tissues

Since fibrillin-1 shows a broad tissue distribution, we wanted to monitor asprosin expression and its potential intra- or extracellular storage by tissues. Recently, we were able to generate

specific anti-asprosin antibodies against human and mouse asprosin that allow the sensitive detection of asprosin in clinical samples and do not cross-react with fibrillin-1 (14).

Here, we show that also our newly generated antibody against mouse asprosin does not crossreact with human asprosin (supplementary Fig. S1). Therefore, we employed both newly generated antibodies to monitor the tissue distribution of asprosin in human and murine tissues (Fig. 1). Asprosin signals were detected as slight diffuse or vesicle like staining in hepatocytes which can be recognized by their large round nuclei (Fig. 1F, L). In skeletal and cardiac myocytes, anti-asprosin antibodies showed a crossstriated appearance with higher intensity on intercalation discs of cardiomyocytes (Fig. 1C, J). In addition, asprosin positive signals were also detected between myocytes in the form of thin fibers (Fig. 1B, I) In cryosections of cruciate ligament (Fig. 1E) and heart valve biopsies (Fig. 1D, K), asprosin positive fibers were even more pronounced. In the kidney, asprosin fibers were also observed in the glomeruli (Fig. 1G, M). Also, in human placenta asprosin positive fibers were observed (Fig.1A), which were less prominent in mouse placenta (Fig.1H), likely due to species specific differences in the placenta ECM architecture (15).

Asprosin is detected as multimers in cultures of cell lines.

To investigate asprosin synthesis and secretion by cells derived from connective tissues, we screened different cell lines for intra- and extracellular presence of asprosin by immunoblot analysis. We detected asprosin positive bands of higher molecular weight suggesting the presence of asprosin multimers (Fig. 2A). Thereby we observed a higher abundance of asprosin multimers in cell culture supernatants of cell lines derived from musculoskeletal tissues such as U2OS (bone osteosarcoma epithelial cells) or C2C12 (mouse myoblasts) when compared to WI-26 (embryonic lung fibroblasts) or RPE (retinal pigment epithelial cells) (Fig. 2A). To investigate the extracellular deposition of asprosin in cell cultures, we employed immunofluorescence analysis after 7-9 days of culture time. Interestingly, similar

to our findings in tissues we also detected asprosin positive fibers within the ECM deposited by certain cell lines such as 3T3-L1 fibroblasts (model for fibro/adipogenic progenitors present in skeletal muscle) as well as WI-26, primary human skin fibroblasts (HDF) and human chondrocytes (HCH) (Fig. 2B).

Overexpression of monomeric asprosin in musculoskeletal cells results in multimerization

To further investigate the formation of asprosin multimers in musculoskeletal cells, we transfected 3T3-L1 cells with an overexpression construct encoding for monomeric asprosin. Western blot analysis of the collected conditioned media and cell lysates after SDS-PAGE showed that most asprosin was detected in bands representing higher molecular weight multimers that persisted even under reducing conditions (Fig. 2C). However, when HEK-293 cells were transfected with the same construct, only asprosin monomers were detected in the cell culture supernatant (Fig. 2C). Interestingly, signals representing multimerized forms of asprosin were also detected in HEK-293 cell lysates and were resistant to reducing agents. Immunofluorescence analysis of cultured 3T3-L1 cells showed the presence of fibers consisting of endogenously expressed asprosin (Fig. 2B, top-left) as well as overexpressed monomeric asprosin after transfection (Fig. 2D, right).

Moreover, immunofluorescence analysis of HEK-293 cells stably transfected with human asprosin revealed a fibril like structure of the overexpressed asprosin (Fig. 2D; supplementary Fig. S2B, left-column). Also, similar asprosin positive structures were detected in stably transfected cells overexpressing murine asprosin (supplementary Fig. S2B, middle-column). However, in cells overexpressing placensin, the C-terminal propeptide of fibrillin-2 (16), we detected only intracellular signals with no evidence of fiber formation (supplementary Fig. S2B, right-column) by employing a newly generated placensin antibody (supplementary Fig. S3A-C).

Intrinsic multimerization ability of recombinant asprosin

When recombinant asprosin was subjected to size exclusion chromatography (SEC), the obtained chromatogram showed two main asprosin containing peaks eluting at fraction numbers corresponding to higher molecular weight species (Fig. 3A) than the previously determined 37 kDa of glycosylated recombinant asprosin (14). In line with this finding, analysis of asprosin fractions directly after affinity purification by native-PAGE revealed the accumulation of asprosin in the stacking gel with no detected migration into the gel (Fig. 3D, right). However, SDS-PAGE analysis of collected fractions from both peaks indicated a prominent monomeric asprosin band at 37 kDa under these denaturing conditions (Fig. 3B). Interestingly, in fractions 14-17 of the second peak an additional band migrating above 50 kDa corresponding to the size of potential asprosin dimers was also detected (Fig. 3B). To determine the size distribution and multimeric status of asprosin, SEC was performed followed by multiangle light scattering (MALS). The MALS profile indicated a polydispersity of asprosin, with a polydispersity index (PDI) of $1.140 \pm 5.561\%$ and a molecular mass ranging from ~180 kDa to ~1000 kDa (an average of 570 kDa) and average hydrodynamic radius (R_h) of 11.38 nm (Fig. 3C).

In order to identify conditions in which asprosin multimers form or dissolve, we subjected recombinant asprosin to significant changes in temperature (20°C to 90°C) (supplementary Fig. S4B), pH (3-4, 8-9) or buffers (Urea, DTT). Our findings indicated that asprosin multimers are resistant to the applied changes (supplementary Fig. S5B-G). To further determine which conditions favor or abolish asprosin multimerization, we employed the high-throughput UNcle protein stability analyzer (supplementary Fig. S4B-F). Thereby, we observed a sufficient dissociation of asprosin multimers upon SDS addition, which resulted in significant reduction of the average hydrodynamic radius from ~117 nm to ~17 nm upon addition of 2 % SDS (Fig. 4A). Asprosin dissociation upon SDS addition was monitored by electrophoresis showing separation of asprosin multimers and migration into

the gel to different positions by native-PAGE analysis (Fig. 4B, middle and right), while SDS-PAGE results remained unchanged (Fig. 4B, left). In addition, since it was reported that polyamines have a preventive effect on protein aggregation (17), we subjected asprosin to spermine and spermidine treatment. Native-PAGE analysis of asprosin after treatment with spermine or spermidine resulted in a dissociation pattern similar to SDS treatment (supplementary Fig. S5 H, I).

To examine whether asprosin oligomerization takes place intra- or extracellularly, cell-lysates and supernatants of RPE cells and stably transfected asprosin overexpressing HEK-293 cells were analyzed. Western blot analysis of cell culture supernatants of RPE cells after native-PAGE demonstrated the presence of endogenous asprosin in the stacking gel, which migrated into the gel after SDS treatment to the same positions as recombinant asprosin (Fig. 4C). Similarly, we observed the presence of asprosin multimers in the supernatant as well as cell lysates of asprosin overexpressing HEK293 cells by native SDS-PAGE (Fig. 4D), which dissociated upon SDS treatment (supplementary Fig. S5A).

Asprosin is a substrate of tissue transglutaminase

Resistance of asprosin multimer bands to reducing agents (Fig. 2A, C) indicated stable covalent linkage between monomers. Fibrillin monomers are known to be crosslinked by transglutaminase 2 (TG2) which facilitates the assembly of stable fibrillin monomers (18). In general, transglutaminases primarily catalyze the formation of an isopeptide bond between γ -carboxamide groups of glutamine residue side chains and the ϵ -amino groups of lysine residue side chains with subsequent release of ammonia. Thereby, transglutaminases are very specific for the recognition of the glutamine residue and also depend on the charge of the flanking amino acid sequence (19). Since musculoskeletal cells are known to express transglutaminases (20), we tested whether asprosin is a substrate of TG2. Addition of TG2 to monomeric asprosin resulted in a significant shift of asprosin positive immunoblot signals

towards higher molecular weight positions (Fig. 5A). A similar pattern in of bands representing asprosin oligomers was obtained when monomeric asprosin was incubated the presence of the chemical crosslinker disuccinimidylsuberat (DSS) (Fig. 5B). To confirm that asprosin is a substrate of TG2, recombinant asprosin and the co-substrate monodansylcadaverine (MDC) were incubated with TG2. Thereby, any TG2 substrate would become covalently tethered to MDC which allows sensitive detection by UV light (Fig. 5C). Subsequent to asprosin incubation with MDC and TG2, we were able to visualize monomeric and dimeric asprosin by UV light, thereby demonstrating that asprosin is a substrate of TG2 (Fig. 5D). Since covalent crosslinking of MDC adds 335.5 Da to the molecular weight of asprosin, we wanted to identify the glutamine residues via which asprosin crosslinking is mediated. Therefore, we subjected MDC tethered monomeric asprosin to a proteolytic digestion by trypsin and Lys-C and analyzed the resulting fragments by mass spectrometry analysis. Our analysis identified the glutamine residues Q99 and Q113 to be critical for TG2 mediated asprosin oligomerization (Fig. 5E).

Asprosin fiber formation requires the presence of an intact fibrillin fiber network

Since our data demonstrated an intrinsic ability of asprosin to form multimers, we wanted to investigate whether asprosin fiber formation does also occur in the absence of cells (Fig. 6). For this purpose, we incubated asprosin in presence or absence of TG2 with or without SDS pre-treatment. We observed that asprosin forms fibers that were detectable by immunofluorescence in absence of TG2. However, TG2 addition significantly promoted the formation of an elaborate asprosin fiber network of considerable density and thickness. SDS pre-treatment blocked asprosin fiber formation in absence but not in presence of TG2, although the fibers appeared to be thinner and less dense (Fig. 6).

To understand whether asprosin fiber formation is blocked or promoted by the presence of extracellular scaffolds assembled by cells, we administered recombinant asprosin

to cell cultures of several cell types showing high and low TG2 expression levels (Fig. 7A) followed by immunofluorescence analysis (Fig. 7B, C). While asprosin addition led to the formation of aggregates in cultures of U2OS cells, it resulted in robust formation of asprosin positive fibers in RPE cells or primary skin fibroblast cultures, while no fiber formation was detected in HepG2 or HEK-293 cells (Fig. 7C, supplementary Fig. S6A). Interestingly, asprosin positive fibers showed an overlapping distribution to the fibronectin and fibrillin-1 networks (Fig. 7C).

Since we previously determined that about 20 kDa of the 37 kDa monomeric asprosin is due to glycosylation (14), we wanted to investigate whether glycosylation is required for asprosin fiber formation. However, immunofluorescence analysis showed that deglycosylated asprosin is fully capable to form fibers in RPE cell cultures (supplementary Fig. S6B, C), suggesting a requirement for the core protein only. To address the question whether non-covalent multimerization is required for asprosin fiber formation, we incubated asprosin with SDS prior to the addition to cultures. However, our analysis showed that asprosin fiber formation was not affected by SDS pretreatment indicating that non-covalent association into multimers is not necessary for asprosin fiber formation (supplementary Fig. S6B, C). However, we did not observe fiber formation when placensin was added to fibroblast cultures (supplementary Fig. S3D).

Since TG2 is known to establish functional crosslinks thereby stabilizing fibronectin and fibrillin microfibril networks (21,22), we wanted to test whether TG2 may also tether asprosin to either of them. Pull down experiments revealed that asprosin interacts with the N-terminal half of fibrillin-1 and not with the C-terminal half of fibrillin-1 or full-length fibronectin (Fig. 8A, B). Also, interaction studies employing surface plasmon resonance (SPR) confirmed that asprosin binds to the N-terminal region of fibrillin-1 and not to full length fibronectin (Fig. 8C). To test whether intact fibrillin fiber assembly is required for asprosin fiber formation, we added recombinant asprosin to primary skin fibroblast cultures

of MFS patients which show a compromised fibrillin fiber formation but a normal fibronectin assembly. Immunofluorescence analysis showed that asprosin fiber formation was abolished when fibrillin fiber formation was deficient (Fig. 9). To demonstrate the role of TG2 in asprosin fiber formation, we generated a mutant form of asprosin in which the identified crucial residues for transglutaminase-mediated crosslinking Q99 and Q113 were mutated to alanine (Fig. 10A). Upon addition of mutant asprosin to RPE cells, we found a significant reduction in fiber formation compared to the control culture incubated with wild-type asprosin (Fig. 10B), suggesting that Q99 and Q113 are crucial for fiber formation. To investigate whether asprosin is also targeted to the fibrillin-1 fiber network *in vivo*, we co-labelled tissue sections for fibrillin-1 and asprosin. By employing newly generated antibodies specific for the detection of endogenous asprosin in human and murine tissues employing, we could show that asprosin co-localizes with fibrillin fibers in connective tissues such as skeletal muscle, heart, and cruciate ligament (Fig. 11).

Asprosin multimerization affects cellular uptake

To examine whether asprosin multimerization affects its internalization, we incubated several cell types including HEK-293, WI-26, and RPE with asprosin, in presence and absence of SDS for one hour followed by western blot analysis. Our analyses demonstrated that SDS mediated dissociation of non-covalently associated asprosin multimers significantly promoted asprosin uptake into RPE, WI-26, and HEK-293 cells (Fig. 12A, B). Interestingly, in the analyzed cell lysates we could not only detect monomeric asprosin at ~37 kDa but also bands corresponding to asprosin multimers (e.g. at ~70 kDa corresponding to an asprosin dimer) (Fig. 12B, C). This finding indicated a potential multimerization of asprosin during the uptake process, since asprosin multimers were only detectable in minimal amounts prior to incubation with the cell layer (Fig. 12).

Molecular modelling of asprosin suggests a cadherin like fold

By employing computational approaches we were able to generate a structural model of asprosin by employing AlphaFold2 and ColabFold (23). The predicted asprosin model showed a high local structure confidence in the last 120 C-terminal residues (S²¹-H¹⁴⁰) (Fig. 13A). In addition, we submitted the generated structure to Dali server, a protein structure comparison server (24) in order to identify structures similar to asprosin predicted structure in Protein Data Bank (PDB). The obtained data suggested that asprosin is predicted to have a cadherin-like fold (Fig. 13A).

Discussion

Currently, asprosin is mainly viewed as WAT derived hormone that is released into the blood stream to regulate glucose release in the liver (7,13). However, our findings suggest a new mechanism of asprosin storage and utilization within the ECM (Fig. 13 B). Once secreted, asprosin is targeted to assembled fibrillin fibers, whereby TG2 mediated crosslinking enables stable storage of asprosin in the form of multimers. Multimeric asprosin may be later utilized by specific activation mechanisms such as proteolytic degradation of asprosin positive fibers. Released asprosin may act locally or is transported via the circulation to other target organs.

However, since asprosin is the C-terminal propeptide of profibrillin we wondered whether it has a similar tissue distribution as fibrillin-1. By generating new asprosin specific antibodies that do not crossreact with full length fibrillin-1 (14) we were able to detect extracellular deposits of asprosin as fibers in tissues. This finding is in line with previously reported mass spectrometry data from extracted mature microfibrils isolated from the human zonular apparatus (Cain et al. 2006). In this preparation two verified fingerprint peptides of asprosin downstream of the C-terminal furin cleavage site sequence were reliably detected (Cain et al., 2006). This finding was unexpected since profibrillin-1 processing by furin is demonstrated as a prerequisite for mature fibrillin-1 deposition (25-27). Asprosin positive

fibers were more prominently observed in certain tissue microenvironments such as skeletal or cardiac muscle. However, in liver, asprosin was mainly found in intracellular vesicles (Fig. 1) indicating its rapid utilization in this metabolically active tissue.

At present, there is limited structural data on asprosin. Here, we propose a structural model by using AlphaFold suggesting a conformation similar to extracellular cadherin (EC) repeats. Cadherins are known to facilitate self-oligomerization to ensure tissue cohesion. Thereby, cadherins are known to mediate calcium-dependent cell-cell adhesion by forming trans-interactions via EC1 domains from to each other attached cells (28,29). In addition, a cis-interface involving the nonsymmetrical interaction of the EC1 domain and the EC2 domain of neighboring cadherins was proposed (30). The structural similarity of asprosin to EC repeats may endow asprosin with the capability to align into multimers in a similar fashion as cadherins (Fig. 13A). The formation of such stable multimers may then be required for further stabilization via covalent bonds by TG2 (Fig. 9A). Chelation of extracellular Ca^{2+} is known to inhibit the adhesive binding activity of cadherin ectodomains and thereby disrupts epithelial cohesion (31). However, our attempts to dissolve asprosin multimers by complexing calcium via EDTA treatment were not successful (supplementary Fig. S5F), suggesting that the presence of Ca^{2+} does not contribute to the stability of asprosin multimers.

So far, the function of asprosin fibers is unknown. We hypothesize that the oligomerization and linear deposition of asprosin as fibers represents a local asprosin storage mechanism within tissue-specific microenvironments (Fig. 9B). Asprosin stored in tissues may function as a sensor for local energy demand. From there it may be released by specific, yet unknown activation reactions into the serum. Controlled asprosin release by tissues may be a so far unexplored mechanism how tissues signal energy demand to the metabolic system. A metabolic function of asprosin in the regulation of the energy demand of tissue resident cells was already proposed in *in vitro* cell cultures. For instance, experiments with murine

myoblasts (C2C12) showed that asprosin is not only able to interfere with muscle cell insulin sensitivity (12), but also up-regulates glucose transporter 4 (GLUT4) expression in C2C12 myotubes and thereby enhance local glucose uptake by tissue muscle cells (32).

We found that asprosin is a specific substrate of TG2, a crosslinking enzyme that is known to facilitate fibronectin, fibrillin-1, and elastic fiber assembly (18,21,33,34). TG2 is very selective regarding the glutamine residues it subjects to crosslinking (19). Our experiments showed that placensin, the C-terminal propeptide of fibrillin-2, does not form higher oligomers or fibers in fibroblast cultures upon addition, despite the presence of several available glutamine residues (supplementary Fig. S3D). Recently, placensin was described as a new placenta-derived glucogenic hormone that stimulates hepatic cAMP production, protein kinase A (PKA) activity and glucose secretion (16). Also asprosin was shown to be expressed in human placenta and is elevated in the plasma of pregnant women complicated with gestational diabetes mellitus (GDM) and their offspring (umbilical blood) (35) after adjustment for maternal and neonatal clinical characteristics and lipid profiles. In placenta, asprosin fiber formation may have the function to fine tune the metabolic effects mediated by asprosin and placencin.

Our transfection experiments with HEK293 cells constructs encoding monomeric asprosin showed that asprosin multimers were also detected intracellularly, whereas in the conditioned media only monomeric asprosin was detected. In contrast, in the lysates and supernatant of 3T3-L1 cells, asprosin oligomers were found intra- and extracellularly. Intracellular TG cross-linking is a complex theme as TGs do not pass through the conventional ER/Golgi route and require Ca^{2+} for activity. Nevertheless, despite low intracellular calcium levels, multiple transamination and crosslinking substrates of intracellular TG2 have been identified (20,36). This suggests that locally increased intracellular calcium and/or as yet uncharacterized interacting proteins may facilitate formation of active TG2. Our transfection studies with an overexpression construct coding for monomeric asprosin already indicated the

formation of tetramers in cell lysates (Fig. 2B). However, native-PAGE analysis of cell lysates from asprosin overexpressing HEK293 cells indicated that non-covalently associated multimers already form intracellularly (Fig. 4D). This suggests that the intrinsic ability of asprosin monomers to form very stable multimers allows the establishment of covalent crosslinks via TG2 within the intracellular milieu despite low calcium concentrations. Also, internalization studies using monomeric asprosin that was pre-treated with SDS suggest asprosin undergoes multimerization upon uptake to the intracellular space. Uptake of monomeric asprosin was more sufficient, but multimer bands of intracellular asprosin pools were prominent subsequently (Fig. 12). These results indicate that asprosin multimerization does limit cellular uptake of asprosin likely due to reduced access of relevant epitopes recognized by cell surface receptors. It has been previously reported that protein multimerization can affect its cellular uptake and regulate pathogenesis of several diseases (37-40). For example, multimerization of Tau proteins and α -Synuclein is involved in the pathogenesis of neurodegenerative diseases such as Alzheimer's and Parkinson's diseases (41-44).

In future studies we will address not only further investigate the molecular requirements for cellular utilization of asprosin cells, but also by what specific release mechanisms asprosin may be liberated from its fibrous state.

Our data show that asprosin is specifically targeted to fibrillin-1 fibers and not to fibronectin. This finding may implicate an intact fibrillin network in the proper extracellular storage of asprosin. Fibrillin-1 is ubiquitously expressed in all tissues and is known to assemble into supramolecular microfibrils that serve as targeting scaffolds for connective tissue derived growth factors such as TGF- β and BMPs (45-49). By targeting and sequestration of asprosin in connective tissue microenvironments fibrillin-1 may be involved in the regulation of spatio-temporal energy demand of tissue resident cells.

Materials and method

Ethics statement

The use of human specimen involved in this study was approved by the institutional review boards at the Medical Faculty of the University of Cologne, the German Sports University, and Ghent University. Written informed consent was obtained from patients in accordance with institutional review board policies. Written informed consent was obtained from all participating probands and patients who agreed to have materials examined for research purposes. The study was conducted in accordance with the Declaration of Helsinki. Human samples were collected according to the Biomass code (13-091) at the University Hospital of Cologne, Cologne, Germany and Ethics Committee of the Medical School Brandenburg, Brandenburg, Germany (reference numbers: E-01-20200921, E-01-20211115). The study was approved by the ethics committee of the University Hospital of Cologne (18-052). Mice were sacrificed by cervical dislocation and immediately dissected for experiments. All animal procedures were conducted in compliance with protocols approved by the Committee on the Ethics of Animal Experiments of the Landesamt für Natur, Umwelt und Verbraucherschutz Nordrhein-Westfalen (84-02.04.2019.A326) and were in accordance with National Institutes of Health guidelines.

Antibodies

Pc-asp anti-asprosin, fibrillin-1 (rF90) polyclonal antibody, and fibrillin-1 rabbit monoclonal antibody (CPTC-FBN1-3) (DSHB, Iowa, USA) were previously described (14). Monoclonal anti-fibronectin antibody (# F7387) was purchased from Merck Millipore (Massachusetts, USA). Mab anti-asprosin antibody (clone Birdy-1, AG-20B-0073) was purchased from AdipoGen Life Sciences Inc. (San Diego, USA). StrepMAB-Classic antibody (#2-1507-001) was from IBA GmbH, Germany. Antibodies against murine asprosin (mASP(rb) Ab, (mASP(rat) Ab) were generated against full-length mouse asprosin (supplementary Fig. S3).

Recombinantly expressed mouse asprosin or human placensin were used to immunize rabbits for polyclonal antibody production (Davids Biotechnologie GmbH, Regensburg, Germany). Recombinantly expressed human asprosin (14) was used for polyclonal antibody production in a rat (Pineda, Berlin, Germany). Preimmune serum samples (0.5 ml) were obtained before the immunization and did not show cross-reactivity to asprosin tested by ELISA. Antisera were affinity purified on CNBr-activated Sepharose 4B (Cytiva, Uppsala, Sweden) columns conjugated with the respective recombinantly expressed proteins (300 µg) according to the manufacturer's instructions. Antibodies were eluted with 0.1 M glycine (pH 2.5) and neutralized with 3 M Tris/ HCl, pH 8. Eluted antibodies were concentrated by using Amicon Ultra Centrifugal Filters (cut-off: 10 kDa), (starting volume: 6 ml, end volume: 1ml). The specificity of the raised antibodies was tested by direct ELISA, pull down experiments, as well as immunofluorescence of tissues and transfected cells (supplementary Fig. S2-S5).

Expression and purification of recombinant proteins

Human asprosin, mouse asprosin, human placensin, mutant asprosin (Q99A and Q113A), and the N-terminal half of fibrillin-1 (rF90, amino acids positions: (M¹-V¹⁵²⁷) were produced and purified as previously described (14) (supplementary Fig. S2B). C-terminal half of fibrillin-1 (rF6, amino acid positions V¹⁴⁸⁷-H²⁸⁷¹) was overexpressed in HEK-293 EBNA cells. The rF6 overexpression construct (50) was a kind gift from Lynn Sakai, Oregon Health and Science University, Portland, OR, USA. cDNAs encoding for mouse asprosin, human placensin, and mutant asprosin (Q99A and Q113A) were generated by GeneArt Strings DNA Fragments service (Thermo Fisher Scientific, Massachusetts, USA). including the restriction enzymes sequences for ends. Subcloning of cDNA sequences via NheI/ XhoI restriction sites into a modified pCEP-Pu vector as well as transfection of overexpression constructs in HEK293 EBNA cells followed by establishment of stably transfected cell clones, and protein

purification from conditioned media via affinity chromatography using a C-terminally placed 2×Strep-tag II were as previously described (14).

Size exclusion chromatography with multi-angle static light scattering (SEC-MALS) and electron microscopy (EM)

Recombinant asprosin (0.5 ml, 1 µg/µl) was subjected to gel filtration using a Superose 6 Increase 10/300 GL column in PBS at 0.6 ml/min. The eluate was passed through a Wyatt DAWN Heleos II EOS 18-angle laser photometer with a Wyatt QELS detector for the measurement of hydrodynamic radius. Data were analyzed using Astra 6.1 (Wyatt, Santa Barbara, USA). Elution fractions from SEC-MALS were analyzed by EM as previously described (51).

Immunoblotting

Cells were lysed in RIPA buffer (50 mM Tris HCl, 150 mM NaCl, 1.0% (v/v) NP-40, 0.5% (w/v) sodium deoxycholate, 1.0 mM EDTA, 0.1% (w/v) SDS and 0.01% (w/v) at a pH of 7.4) supplemented with cOmplete protease inhibitor cocktail (#11697498001, Sigma-Aldrich, Darmstadt, Germany) and PhosSTOP phosphatase inhibitors (#4906837001, Sigma-Aldrich, Darmstadt, Germany). Protein concentrations were measured using Pierce BCA Protein Assay Kit (#23225, Thermo Fisher Scientific, Massachusetts, USA). To harvest cell culture supernatants, cell layers were incubated with serum free medium when cells reached 90% confluency and subsequently collected after 48 h. The collected serum free medium was filtered and concentrated with Amicon Ultra Centrifugal Filters (cut off: 3 kDa), (starting volume: 2 ml, end volume: 50 µl). Cell lysates and cell culture supernatant samples analyzed by 7.5% or 10% SDS-PAGE under reducing (with β-mercaptoethanol) or non-reducing conditions, followed by transfer to 0.45 µm PVDF transfer membranes (Thermo Fisher Scientific, Massachusetts, United States). Membranes were blocked with Pierce Protein-Free

(TBS) Blocking Buffer (#37585, Thermo Fisher Scientific, Massachusetts, United States) for one hour, then incubated with the appropriate dilutions of primary antibodies overnight at 4°C and subsequently incubated with secondary antibody, mouse anti-rabbit IgG-HRP conjugate or goat anti-mouse IgG-HRP conjugate, 1:5000 for 1 h. All antibodies were diluted into blocking buffer. Signals were developed with SuperSignal West Pico PLUS Chemiluminescent Substrate (#34579, Thermo Fisher Scientific, Massachusetts, USA).

Samples used in native-PAGE analysis were separated under non-denaturing conditions. Cells used for native-PAGE analysis were lysed using mechanical lysis (manual grinding) in non-denaturing (detergent-free) buffer (100 mM Tris/HCl pH 8.0 150 mM NaCl) supplemented with cOmplete protease inhibitor cocktail and PhosSTOP phosphatase inhibitors. Cell lysates and cell culture supernatants were mixed with native-PAGE loading buffer (62.5 mM Tris-HCl, pH 6.8, 40% glycerol, 0.01% bromophenol blue) without heating prior to native-PAGE.

Cellular uptake experiments

Cells were seeded in 6-well plates until reaching 70% confluency and were kept in DMEM (serum free medium) for 24 h. 6-well plates were placed on ice for 20 minutes prior to treatment with asprosin (50 or 100 nM) that was preincubated with or without SDS. For SDS treatment, 9 µl asprosin stock solution were mixed with 1 µl 1% SDS, which was further diluted into cell culture media to reach the indicated final asprosin concentrations. Thereby the final SDS concentration was 0.001% for which no cell toxicity was observed. After incubation with asprosin, cells were washed with ice cold PBS and incubated with acid-wash buffer (0.2 M glycine and 0.15 M NaCl, pH 3.0) for 5 min. Subsequently, cells were washed two times with PBS, and finally lysed in RIPA supplemented with cOmplete protease inhibitor cocktail and PhosSTOP phosphatase inhibitors.

Tissue preparation and immunofluorescence

Whole mouse organs and crural muscles were frozen immediately post-euthanasia. For protein isolation, the samples were snap frozen in liquid nitrogen. For cryosectioning, specimens were coated with Tissue-Tek O.C.T. compound (Sakura, The Netherlands) and frozen in ice-cold isopentane (~-150°C). Human tissue samples from the marginal border of resected specimens were treated similarly during the first five hours after resection.

For immunofluorescence analysis tissues were cut into 10 µm sections (SLEE Cryostat, Germany), thaw-mounted on glass slides (Superfrost, Thermo Fisher Scientific Massachusetts, USA) and air-dried for 1 h at 37 C. Cryosections were immersed for 4 min in ice-cold acetone and again air-dried for 1 h at RT. Specimens were transferred in humidified chamber, rehydrated with phosphate-buffered saline (PBS) for 10 min continued with permeabilization using 0.1% Triton X-100 plus 0.05% Tween-20 in PBS for either 15 min. Samples were then incubated for 60 min at RT in blocking buffer (5% normal donkey serum (Dako) plus 0.05% Tween-20 in PBS) and incubated overnight at 4°C in a humidified chamber with primary antibodies against human- or mouse-asprosin (polyclonal rabbit, dilution 1:60, lab-made). After washing 3 times for 5 min in PBS containing 0.05% Tween-20, specimens were incubated with secondary antibodies (Alexa Fluor 488-conjugated donkey anti-Rabbit IgG (H+L) # R37118, ThermoScientific, Massachusetts, USA, dilution 1:300). In the presence of DAPI (1µg/mL) (#62248, Thermo Fisher Scientific, Massachusetts, USA) for 1h at RT. Primary and secondary antibodies were diluted into Antibody Dilution Buffer (#AL120R100, DCS Diagnostics, Germany). Finally, specimens were washed once with PBS containing 0.05% Tween-20 for 5 min then twice with PBS (5 min each) and mounted with ProLong Gold Antifade Mountant (#P10144, Thermo Fisher Scientific Massachusetts, USA). Sections processed with the only secondary antibodies served as controls to exclude autofluorescence and non-specific binding. cOmplete protease inhibitor cocktail (one tablet per 50 ml PBS, cOmplete™ ULTRA Tablets, Mini, EDTA-free,

Roche) was added to all solutions and buffers used for previously described procedures, except for the permeabilization solution.

Cell culture

All cell lines used in the study were provided from American Type Culture Collection (ATCC). HDF (primary human dermal fibroblasts) from control as well as HCH (primary human chondrocytes) were established from biopsies. Cells were cultured in DMEM with 10% fetal calf serum (FCS) and 1% penicillin/ streptomycin, they were grown in incubators maintained at 37°C and 5% CO₂. Cells were fed twice per week and split regularly.

Surface plasmon resonance

SPR experiments were performed as described previously (10, 13) using a BIAcore 2000 system (BIAcore AB, Uppsala, Sweden). Recombinant human asprosin (#761902, Biolegend, San Diego, CA, USA) was immobilized at 1000 RUs to a CM5 sensor chip using the amine coupling kit following the manufacturer's instructions (Cytiva, Uppsala, Sweden). Interaction studies were performed by injecting 0-320 nM recombinant fibrillin-1 fragments (Start-EGF, or rF90), or fibronectin in HBS-EP buffer (0.01 M HEPES, pH 7.4, 0.15 M NaCl, 3 mM EDTA, 0.005% (v/v) surfactant P20) (Cytiva, Uppsala, Sweden). Kinetic constants were calculated by nonlinear fitting (1:1 interaction model with mass transfer) to the association and dissociation curves according to the manufacturer's instructions (BIAevaluation version 3.0 software). Apparent equilibrium dissociation constants (K_D values) were then calculated as the ratio of k_d/k_a.

Crosslinking by transglutaminase 2 (TG2) and fluorescent-monodansylcadaverine

20 µg of purified asprosin (5 µg/µl) was buffer exchanged by Amicon Ultra Centrifugal Filters (cut off: 3 kDa), with PBS containing 5 mM CaCl₂ and treated with 2 µg

transglutaminase 2 (#T5398, from guinea pig liver, Sigma-Aldrich, Darmstadt, Germany) (enzyme: substrate ratio, 1:10 (w/w)) in a total volume of 300 μ l. The reaction mixture was incubated at 37°C. 15 μ l of the reaction mixture was withdrawn after 5, 10, and 15 min. The reaction was directly stopped by adding 5 μ l of Laemmli Buffer and the samples were analyzed by SDS-PAGE and western blot. For the control experiment tTG was omitted or samples were treated with 0.25 M EDTA to sequester calcium ions and inhibit tTG activity. Fluorescent-monodansylcadaverine (MDC) (# D4008, Aldrich, Darmstadt, Germany) was used as amine donor and acceptor sites for tissue transglutaminase enzyme activity detection as previously suggested and described (52). MDC was dissolved in DMSO, 2 mg in 1.5 ml DMSO to obtain a stock solution of 4 mM MDC. 40 μ g of purified asprosin (5 μ g/ μ l) was buffered exchanged with PBS containing 5 mM CaCl₂ and 40 μ M MDC in a total volume of 120 μ l. the reaction mixture was then treated with 4 μ g tTG (1 μ g/ μ l) and incubated at 37°C. 15 μ l of the reaction mixture was withdrawn after 5, 10, 15, 20, 30, and 45 min, then the reaction was directly stopped by adding 5 μ l Laemmli Buffer subjected to SDS-PAGE. The gel was then fixed with 25% isopropanol, 10% acetic acid and photographed on a 300 nm UV, then subjected to Coomassie Blue Staining.

DSS (disuccinimidyl suberate) crosslinking

DSS (#21655, Thermo Fisher Scientific Massachusetts, USA) is a water-insoluble chemical crosslinker and was dissolved in dimethyl sulfoxide (DMSO), 1 mg in 55.29 μ l DMSO to obtain 800 μ M DSS, then serially diluted (1:2) into DMSO to obtain following DSS concentrations 400, 200, and 100 μ M DSS. Cross-linking reactions were conducted in a total volume of 15 μ l containing 1 μ g asprosin (0.5 μ g/ μ l), 1.5 μ l of freshly prepared DSS to obtain final DSS concentrations (80, 40, 20, and 10 μ M) and complete to the 15 μ l final volume with PBS. The reaction mixtures were incubated at RT for 30 min was directly stopped by

adding 5 μ l of Laemmli Buffer and the samples were analyzed by SDS-PAGE and western blot. For the control experiment, 1.5 μ l of DMSO was used instead of DSS.

Preparation of fluorescently labelled asprosin (Asprosin-550)

1 mg of ATTO 550 dye (#AD 550-31, ATTO-TEC GmbH, Germany) was freshly prepared by dissolving it in 100 μ l DMSO directly before coupling to asprosin. 500 μ g of purified human asprosin was buffered exchanged into a coupling buffer (PBS containing 10 mM sodium bicarbonate and 100 mM sodium hydroxide, pH 8.3) by Amicon Ultra Centrifugal Filters (cut-off: 3 kDa). The coupling reaction mixture was prepared by mixing the dissolved ATTO 550 dye and the buffer-exchanged asprosin in the coupling buffer to a final volume of 5 ml. The mixture was then incubated for 1 h, protected from light at RT. The coupling reaction mixture was concentrated by using Amicon Ultra Centrifugal Filters (cut-off: 10 kDa), (starting volume: 5 ml, end volume: 0.3 ml). The concentration of fluorescently labelled asprosin (Asprosin-550) was measured by NanoDrop One (Thermo Fisher Scientific, Massachusetts, USA). The quantification was performed by measuring the protein absorbance at 280 nm and the ATTO-550 dye absorbance at 550 nm. The integrity of the conjugated asprosin was additionally analyzed by SDS-PAGE and subjected to Coomassie Blue Staining (supplementary Fig. S1B). The fluorescence of the conjugated asprosin was visualized by ChemoStar Touch ECL & Fluorescence Imager (Intas Science Imaging Instruments GmbH, Göttingen, Germany).

UNcle analysis

Samples were diluted into 5 \times buffers resulting in a final concentration of 100 mM buffer and 150 mM NaCl. 2 μ l of protein, 2 μ l of buffer and 6 μ l of water were used for each sample. 16 buffer conditions were loaded via glass capillaries into the UNcle instrument. Dynamic light scattering measurements were performed at a constant temperature of 25°C with attenuation

set to automatic. Reported values represent the average of three readings per condition. The melting and aggregation onset measurements were performed by heating the sample to 95°C at 1°C intervals and 60 sec incubation at each temperature. The instrument acquires a full spectrum of tryptophan fluorescence using a 266 nm laser to excite and scan between 250 and 550 nm and monitors the level of scattering of both the 266 nm and 473 nm lasers. Tagg is the aggregation onset temperatures defined as the beginning of the aggregation curve, whilst the melting temperature (T_m) is defined as the mid-point in the melting curve, which represents the level of tryptophan exposure to solvent.

Asprosin structure prediction

The structure of asprosin (fibrillin-1 P3555 residues 2732-2871) was predicted in Alphafold2 using colabfold (DOI: 10.1038/s41592-022-01488-1).

Acknowledgments

We would like to thank the CECAD Cologne Proteomics Facility for conducting mass spectrometry analysis. Funding for this study was provided by the Deutsche Forschungsgemeinschaft (DFG, German Research Foundation) project ID 384170921: FOR2722/ B1 to M.P., and FOR2722/ M2 to E.H.R., and G.S. B.C. is a senior clinical investigator of the Research Foundation Flanders. This work was supported by a grants of the Special Research Fund of Ghent University (grant 01N04516C and BOF21/GOA/019 to B.C.). The Ghent University Hospital is a member of the European Reference Network for Skin Disorders (ERN-Skin).

Author contributions

Y. A. T. Morcos, C. Baldock, and G. Sengle and designed research. Y. A. T. Morcos, G. Prymachuk, A. R. F. Godwin, S. Lütke, T. A. Jowitt, T. Hoffmann, A. Tenbrieg, and N.

Piekarek performed research. Y. A. T. Morcos, G. Prymachuk, A. R. F. Godwin, T. A. Jowitt, S. Lütke, and C. Baldock analyzed data. W. Bloch, B. Callewaert, U. Drebber, O. Grisk, A. Niehoff, M. Odenthal, and Y. Ladilov provided essential reagents. M. Paulsson provided expert advice. Y. A. T. Morcos, and G. Sengle wrote the manuscript.

Conflict of interest

The authors declare no conflict of interest.

References

1. Sakai, L. Y., Keene, D. R., and Engvall, E. (1986) Fibrillin, a new 350-kD glycoprotein, is a component of extracellular microfibrils. *J Cell Biol* **103**, 2499-2509
2. Sakai, L. Y., Keene, D. R., Renard, M., and De Backer, J. (2016) FBN1: The disease-causing gene for Marfan syndrome and other genetic disorders. *Gene* **591**, 279-291
3. Passarge, E., Robinson, P. N., and Graul-Neumann, L. M. (2016) Marfanoid-progeroid-lipodystrophy syndrome: a newly recognized fibrillinopathy. *Eur J Hum Genet* **24**, 1244-1247
4. Graul-Neumann, L. M., Kienitz, T., Robinson, P. N., Baasanjav, S., Karow, B., Gillissen-Kaesbach, G., Fahsold, R., Schmidt, H., Hoffmann, K., and Passarge, E. (2010) Marfan syndrome with neonatal progeroid syndrome-like lipodystrophy associated with a novel frameshift mutation at the 3' terminus of the FBN1-gene. *Am J Med Genet A* **152A**, 2749-2755
5. Takenouchi, T., Hida, M., Sakamoto, Y., Torii, C., Kosaki, R., Takahashi, T., and Kosaki, K. (2013) Severe congenital lipodystrophy and a progeroid appearance: Mutation in the penultimate exon of FBN1 causing a recognizable phenotype. *Am J Med Genet A* **161A**, 3057-3062
6. Jacquinet, A., Verloes, A., Callewaert, B., Coremans, C., Coucke, P., de Paepe, A., Kornak, U., Lebrun, F., Lombet, J., Pierard, G. E., Robinson, P. N., Symoens, S., Van Maldergem, L., and Debray, F. G. (2014) Neonatal progeroid variant of Marfan syndrome with congenital lipodystrophy results from mutations at the 3' end of FBN1 gene. *Eur J Med Genet* **57**, 230-234
7. Romere, C., Duerrschmid, C., Bournat, J., Constable, P., Jain, M., Xia, F., Saha, P. K., Del Solar, M., Zhu, B., York, B., Sarkar, P., Rendon, D. A., Gaber, M. W., LeMaire, S. A., Coselli, J. S., Milewicz, D. M., Sutton, V. R., Butte, N. F., Moore, D. D., and Chopra, A. R. (2016) Asprosin, a Fasting-Induced Glucogenic Protein Hormone. *Cell* **165**, 566-579
8. Lonnqvist, L., Reinhardt, D., Sakai, L., and Peltonen, L. (1998) Evidence for furin-type activity-mediated C-terminal processing of profibrillin-1 and interference in the processing by certain mutations. *Hum Mol Genet* **7**, 2039-2044
9. Wiecek, M., Szymura, J., Maciejczyk, M., Kantorowicz, M., and Szygula, Z. (2018) Acute Anaerobic Exercise Affects the Secretion of Asprosin, Irisin, and Other Cytokines - A Comparison Between Sexes. *Front Physiol* **9**, 1782
10. Lee, T., Yun, S., Jeong, J. H., and Jung, T. W. (2019) Asprosin impairs insulin secretion in response to glucose and viability through TLR4/JNK-mediated inflammation. *Mol Cell Endocrinol* **486**, 96-104
11. Duerrschmid, C., He, Y., Wang, C., Li, C., Bournat, J. C., Romere, C., Saha, P. K., Lee, M. E., Phillips, K. J., Jain, M., Jia, P., Zhao, Z., Farias, M., Wu, Q., Milewicz, D. M., Sutton, V. R., Moore, D. D., Butte, N. F., Krashes, M. J., Xu, Y., and Chopra, A. R. (2017) Asprosin is a centrally acting orexigenic hormone. *Nat Med* **23**, 1444-1453
12. Jung, T. W., Kim, H. C., Kim, H. U., Park, T., Park, J., Kim, U., Kim, M. K., and Jeong, J. H. (2019) Asprosin attenuates insulin signaling pathway through PKCdelta-activated ER stress and inflammation in skeletal muscle. *J Cell Physiol* **234**, 20888-20899
13. Hoffmann, J. G., Xie, W., and Chopra, A. R. (2020) Energy Regulation Mechanism and Therapeutic Potential of Asprosin. *Diabetes* **69**, 559-566
14. Morcos, Y. A. T., Lütke, S., Tenbrieg, A., Hanisch, F.G., Pryymachuk, G., Piekarek, N., Hoffmann, T., Keller, T., Janoschek, R., Niehoff, A., Zaucke, F., Dötsch, J., Hucklenbruch-Rother, E., Sengle, G. (2021) Sensitive asprosin detection in clinical

- samples reveals serum/ saliva correlation and indicates cartilage as source for serum asprosin. *Sci Rep*
15. Schmidt, A., Morales-Prieto, D. M., Pastuschek, J., Frohlich, K., and Markert, U. R. (2015) Only humans have human placentas: molecular differences between mice and humans. *J Reprod Immunol* **108**, 65-71
 16. Yu, Y., He, J. H., Hu, L. L., Jiang, L. L., Fang, L., Yao, G. D., Wang, S. J., Yang, Q., Guo, Y., Liu, L., Shang, T., Sato, Y., Kawamura, K., Hsueh, A. J., and Sun, Y. P. (2020) Placensin is a glucogenic hormone secreted by human placenta. *EMBO Rep* **21**, e49530
 17. Shiraki, K., Kudou, M., Aso, Y., and Takagi, M. (2003) Dissolution of protein aggregation by small amine compounds. *Science and Technology of Advanced Materials* **4**, 55
 18. Qian, R. Q., and Glanville, R. W. (1997) Alignment of fibrillin molecules in elastic microfibrils is defined by transglutaminase-derived cross-links. *Biochemistry* **36**, 15841-15847
 19. Coussons, P. J., Price, N. C., Kelly, S. M., Smith, B., and Sawyer, L. (1992) Factors that govern the specificity of transglutaminase-catalysed modification of proteins and peptides. *Biochem J* **282 (Pt 3)**, 929-930
 20. Eckert, R. L., Kaartinen, M. T., Nurminskaya, M., Belkin, A. M., Colak, G., Johnson, G. V., and Mehta, K. (2014) Transglutaminase regulation of cell function. *Physiol Rev* **94**, 383-417
 21. Turner, P. M., and Lorand, L. (1989) Complexation of fibronectin with tissue transglutaminase. *Biochemistry* **28**, 628-635
 22. Akimov, S. S., and Belkin, A. M. (2001) Cell-surface transglutaminase promotes fibronectin assembly via interaction with the gelatin-binding domain of fibronectin: a role in TGFbeta-dependent matrix deposition. *J Cell Sci* **114**, 2989-3000
 23. Mirdita, M., Schutze, K., Moriwaki, Y., Heo, L., Ovchinnikov, S., and Steinegger, M. (2022) ColabFold: making protein folding accessible to all. *Nat Methods* **19**, 679-682
 24. Holm, L. (2022) Dali server: structural unification of protein families. *Nucleic Acids Res*
 25. Ashworth, J. L., Kelly, V., Rock, M. J., Shuttleworth, C. A., and Kielty, C. M. (1999) Regulation of fibrillin carboxy-terminal furin processing by N-glycosylation, and association of amino- and carboxy-terminal sequences. *J Cell Sci* **112 (Pt 22)**, 4163-4171
 26. Ritty, T. M., Broekelmann, T., Tisdale, C., Milewicz, D. M., and Mecham, R. P. (1999) Processing of the fibrillin-1 carboxyl-terminal domain. *J Biol Chem* **274**, 8933-8940
 27. Jensen, S. A., Aspinall, G., and Handford, P. A. (2014) C-terminal propeptide is required for fibrillin-1 secretion and blocks premature assembly through linkage to domains cbEGF41-43. *Proc Natl Acad Sci U S A* **111**, 10155-10160
 28. Shapiro, L., Fannon, A. M., Kwong, P. D., Thompson, A., Lehmann, M. S., Grubel, G., Legrand, J. F., Als-Nielsen, J., Colman, D. R., and Hendrickson, W. A. (1995) Structural basis of cell-cell adhesion by cadherins. *Nature* **374**, 327-337
 29. Boggon, T. J., Murray, J., Chappuis-Flament, S., Wong, E., Gumbiner, B. M., and Shapiro, L. (2002) C-cadherin ectodomain structure and implications for cell adhesion mechanisms. *Science* **296**, 1308-1313
 30. Harrison, O. J., Jin, X., Hong, S., Bahna, F., Ahlsen, G., Brasch, J., Wu, Y., Vendome, J., Felsovalyi, K., Hampton, C. M., Troyanovsky, R. B., Ben-Shaul, A., Frank, J., Troyanovsky, S. M., Shapiro, L., and Honig, B. (2011) The extracellular architecture of adherens junctions revealed by crystal structures of type I cadherins. *Structure* **19**, 244-256

31. Le, T. L., Yap, A. S., and Stow, J. L. (1999) Recycling of E-cadherin: a potential mechanism for regulating cadherin dynamics. *J Cell Biol* **146**, 219-232
32. Zhang, Y., Zhu, Z., Zhai, W., Bi, Y., Yin, Y., and Zhang, W. (2021) Expression and purification of asprosin in *Pichia pastoris* and investigation of its increase glucose uptake activity in skeletal muscle through activation of AMPK. *Enzyme Microb Technol* **144**, 109737
33. Clarke, A. W., Wise, S. G., Cain, S. A., Kielty, C. M., and Weiss, A. S. (2005) Coacervation is promoted by molecular interactions between the PF2 segment of fibrillin-1 and the domain 4 region of tropoelastin. *Biochemistry* **44**, 10271-10281
34. Rock, M. J., Cain, S. A., Freeman, L. J., Morgan, A., Mellody, K., Marson, A., Shuttleworth, C. A., Weiss, A. S., and Kielty, C. M. (2004) Molecular basis of elastic fiber formation. Critical interactions and a tropoelastin-fibrillin-1 cross-link. *J Biol Chem* **279**, 23748-23758
35. Zhong, L., Long, Y., Wang, S., Lian, R., Deng, L., Ye, Z., Wang, Z., and Liu, B. (2020) Continuous elevation of plasma asprosin in pregnant women complicated with gestational diabetes mellitus: A nested case-control study. *Placenta* **93**, 17-22
36. Rossin, F., D'Eletto, M., Falasca, L., Sepe, S., Cocco, S., Fimia, G. M., Campanella, M., Mastroberardino, P. G., Farrace, M. G., and Piacentini, M. (2015) Transglutaminase 2 ablation leads to mitophagy impairment associated with a metabolic shift towards aerobic glycolysis. *Cell Death Differ* **22**, 408-418
37. Mirbaha, H., Holmes, B. B., Sanders, D. W., Bieschke, J., and Diamond, M. I. (2015) Tau Trimers Are the Minimal Propagation Unit Spontaneously Internalized to Seed Intracellular Aggregation. *J Biol Chem* **290**, 14893-14903
38. Usenovic, M., Niroomand, S., Drolet, R. E., Yao, L., Gaspar, R. C., Hatcher, N. G., Schachter, J., Renger, J. J., and Parmentier-Batteur, S. (2015) Internalized Tau Oligomers Cause Neurodegeneration by Inducing Accumulation of Pathogenic Tau in Human Neurons Derived from Induced Pluripotent Stem Cells. *J Neurosci* **35**, 14234-14250
39. Delenclos, M., Trendafilova, T., Mahesh, D., Baine, A. M., Moussaud, S., Yan, I. K., Patel, T., and McLean, P. J. (2017) Investigation of Endocytic Pathways for the Internalization of Exosome-Associated Oligomeric Alpha-Synuclein. *Front Neurosci* **11**, 172
40. Rauch, J. N., Chen, J. J., Sorum, A. W., Miller, G. M., Sharf, T., See, S. K., Hsieh-Wilson, L. C., Kampmann, M., and Kosik, K. S. (2018) Tau Internalization is Regulated by 6-O Sulfation on Heparan Sulfate Proteoglycans (HSPGs). *Sci Rep* **8**, 6382
41. Patterson, K. R., Remmers, C., Fu, Y., Brooker, S., Kanaan, N. M., Vana, L., Ward, S., Reyes, J. F., Philibert, K., Glucksman, M. J., and Binder, L. I. (2011) Characterization of prefibrillar Tau oligomers in vitro and in Alzheimer disease. *J Biol Chem* **286**, 23063-23076
42. Domert, J., Sackmann, C., Severinsson, E., Agholme, L., Bergstrom, J., Ingelsson, M., and Hallbeck, M. (2016) Aggregated Alpha-Synuclein Transfer Efficiently between Cultured Human Neuron-Like Cells and Localize to Lysosomes. *PLoS One* **11**, e0168700
43. Chung, D. C., Carlomagno, Y., Cook, C. N., Jansen-West, K., Daughrity, L., Lewis-Tuffin, L. J., Castanedes-Casey, M., DeTure, M., Dickson, D. W., and Petrucelli, L. (2019) Tau exhibits unique seeding properties in globular glial tauopathy. *Acta Neuropathol Commun* **7**, 36
44. Kaye, R., Dettmer, U., and Lesne, S. E. (2020) Soluble endogenous oligomeric alpha-synuclein species in neurodegenerative diseases: Expression, spreading, and cross-talk. *J Parkinsons Dis* **10**, 791-818

45. Zimmermann, L. A., Correns, A., Furlan, A. G., Spanou, C. E. S., and Sengle, G. (2021) Controlling BMP growth factor bioavailability: The extracellular matrix as multi skilled platform. *Cell Signal* **85**, 110071
46. Sengle, G., Carlberg, V., Tufa, S. F., Charbonneau, N. L., Smaldone, S., Carlson, E. J., Ramirez, F., Keene, D. R., and Sakai, L. Y. (2015) Abnormal Activation of BMP Signaling Causes Myopathy in Fbn2 Null Mice. *PLoS Genet* **11**, e1005340
47. Isogai, Z., Ono, R. N., Ushiro, S., Keene, D. R., Chen, Y., Mazzieri, R., Charbonneau, N. L., Reinhardt, D. P., Rifkin, D. B., and Sakai, L. Y. (2003) Latent transforming growth factor beta-binding protein 1 interacts with fibrillin and is a microfibril-associated protein. *J Biol Chem* **278**, 2750-2757
48. Sengle, G., Charbonneau, N. L., Ono, R. N., Sasaki, T., Alvarez, J., Keene, D. R., Bachinger, H. P., and Sakai, L. Y. (2008) Targeting of bone morphogenetic protein growth factor complexes to fibrillin. *J Biol Chem* **283**, 13874-13888
49. Sengle, G., Ono, R. N., Sasaki, T., and Sakai, L. Y. (2011) Prodomains of transforming growth factor beta (TGFbeta) superfamily members specify different functions: extracellular matrix interactions and growth factor bioavailability. *J Biol Chem* **286**, 5087-5099
50. Pfaff, M., Reinhardt, D. P., Sakai, L. Y., and Timpl, R. (1996) Cell adhesion and integrin binding to recombinant human fibrillin-1. *FEBS Lett* **384**, 247-250
51. Berry, R., Jowitt, T. A., Ferrand, J., Roessle, M., Grossmann, J. G., Canty-Laird, E. G., Kammerer, R. A., Kadler, K. E., and Baldock, C. (2009) Role of dimerization and substrate exclusion in the regulation of bone morphogenetic protein-1 and mammalian tolloid. *Proc Natl Acad Sci U S A* **106**, 8561-8566
52. Aeschlimann, D., and Paulsson, M. (1991) Cross-linking of laminin-nidogen complexes by tissue transglutaminase. A novel mechanism for basement membrane stabilization. *J Biol Chem* **266**, 15308-15317

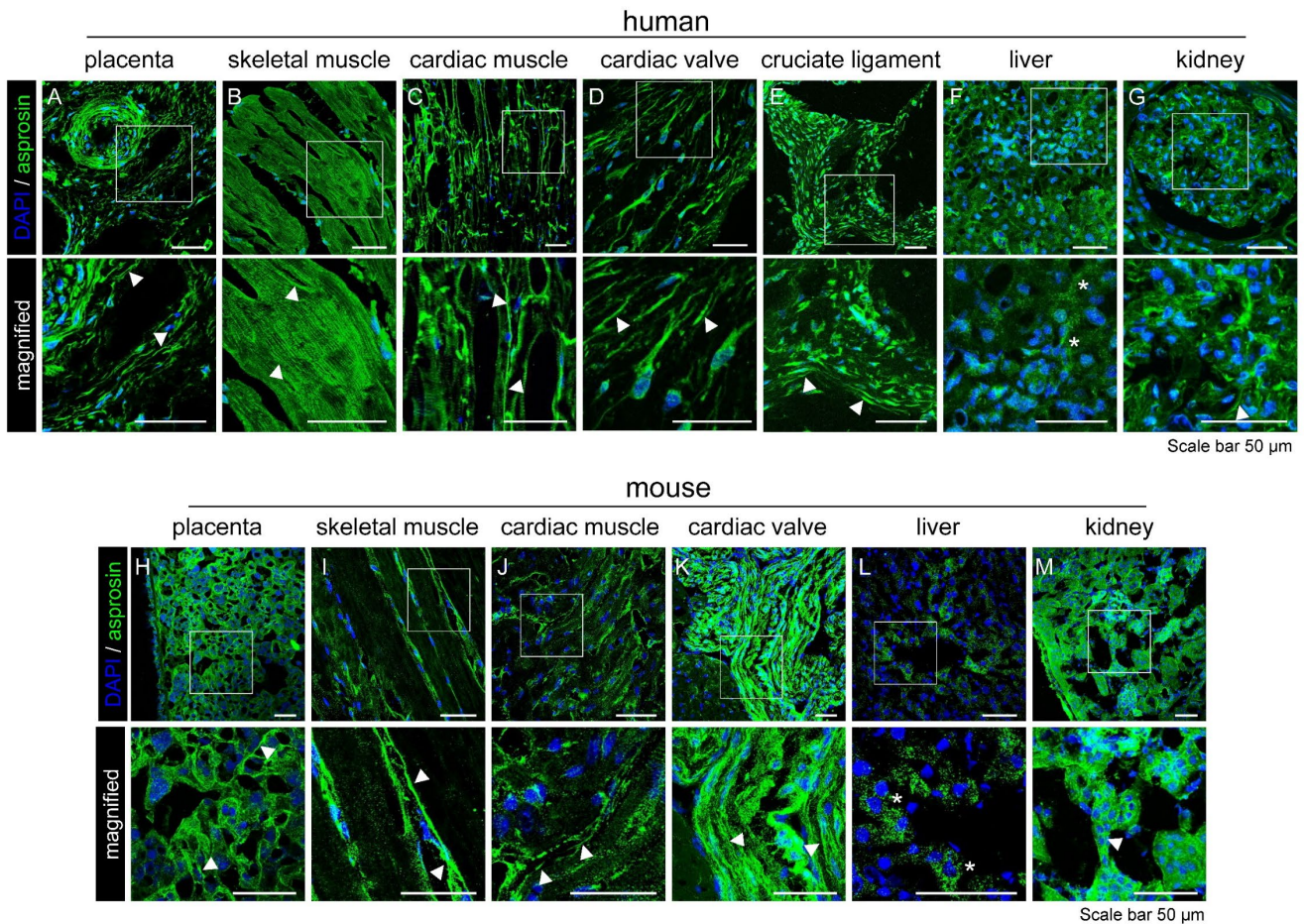


Figure 1: Detection of asprosin positive fibers in human and mouse tissues

Distribution of asprosin in human (A-G) and mouse (H-M) tissues. Cryosections were fixed with acetone and incubated with anti-human or anti- mouse asprosin antibody (green) and DAPI (blue, nuclei). Extra- and intracellular signals of endogenous asprosin were mainly detected in two staining patterns: fiber-like structures (white arrow heads) and diffused or vesicle-like structures (asterisks). 2 to 3-fold magnified areas are marked by white boxes. Images were obtained from a Leica SP8 confocal microscope and were processed using Leica Application Suite X (LAS X) software version 3.7.5.2. Fiji/ImageJ (version 1.53t) software was used to obtain average intensity Z-projection.

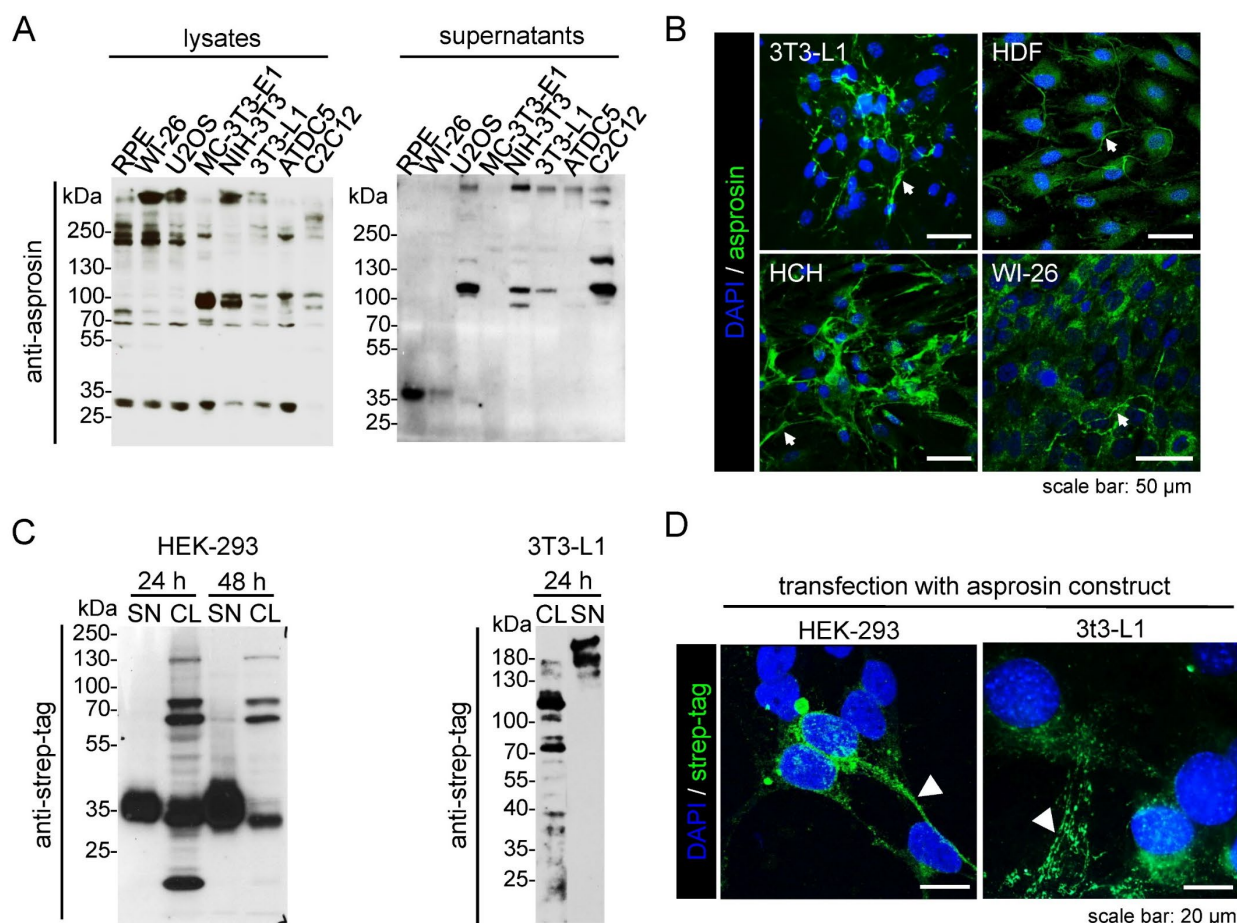


Figure 2: Asprosin multimers and fibers detected in cell culture and upon overexpression of monomeric asprosin

A. Western blot analysis of asprosin in cell lysates and cell culture from different cell lines. Asprosin was detected at the corresponding molecular weight of \sim 37 kDa and as bands of higher molecular weight in both cell lysates and supernatants. **B.** Immunofluorescence analysis of asprosin in 3T3-L1; primary human dermal fibroblasts (HDF), and primary human chondrocytes (HCH) after 7-9 days in culture and WI-26 after 3 days in culture. 3T3-L1 cells were incubated with anti-asprosin (mab-Asp Ab) (green) and DAPI (blue, nuclei). HDF, WI-26 and HCH were incubated with anti-asprosin (pc-asp Ab) (green) and DAPI (blue, nuclei). The staining reveals depositions of asprosin positive fibers as indicated by white arrow heads. **C.** Immunoblotting of cell lysates and cell culture supernatants from HEK-293 and 3T3-L1 transfected with pCEP-Pu vector overexpressing asprosin-2 \times Strep-tag II using anti-streptag (StrepMAB Ab). Immunoblots detected monomeric asprosin (\sim 37 kDa) bands in the supernatant of transfected HEK-293 cells, but high molecular weight bands in the corresponding cell lysate fraction. However, western blot analysis of supernatants and lysates of transfected 3T3-L1 cells only showed asprosin positive multimer bands. **D.**

Immunofluorescence analysis of asprosin-transfected HEK-293 and 3T3-L1 cells with anti-streptag (StrepMAB Ab) showing asprosin intra- and extracellular positive signals. The extracellular signals reveal deposition of asprosin positive fibers as indicated by white arrowheads. Images were obtained from Axiophot Microscope (Carl Zeiss, Germany) and Leica SP8 confocal microscope and were processed using Leica Application Suite X (LAS X) software version 3.7.5.2. Fiji/ImageJ (version 1.53t) software was used to obtain average intensity Z-projection.

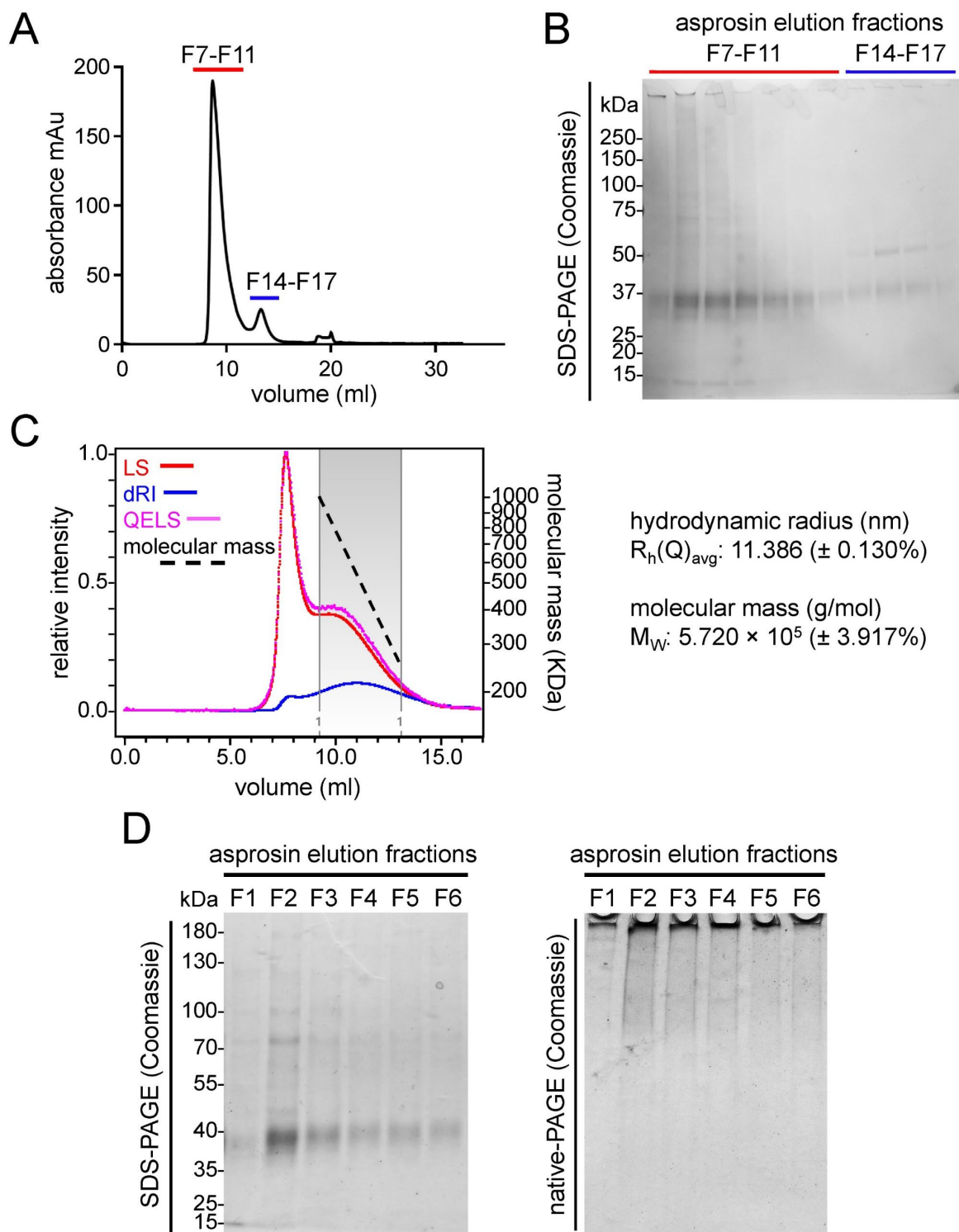


Figure 3: Asprosin forms multimers under native conditions

A. Size exclusion chromatogram of asprosin after affinity purification. Most asprosin protein elutes in one peak at 9 ml (F7-F11, marked in red), while a minor amount elutes in F14-F17 (marked in blue). **B.** SDS-PAGE analysis of asprosin containing peak elution fractions shown in A under non-reducing conditions. **C.** MALS analysis after size exclusion chromatography of affinity purified asprosin. Blue line indicates refractive index (RI), red line indicates

scattering at 90 degrees, pink line indicates dynamic light scattering (DLS). Dashed black line indicates molecular mass against elution volume, showing high polydispersity ranging from 180 to 1000 kDa (average mass of 570 kDa). **D.** Coomassie stained gels of recombinantly purified asprosin (with C-terminal 2×Strep-tag II). Eluted fractions (F2-F6) after affinity chromatography were subjected to (left) a reducing 10% SDS-PAGE gel and (right) a 10% native-PAGE gel. The Coomassie stained native-PAGE gel shows an accumulation of asprosin multimers in stacking gel and at stacking/running gel interface.

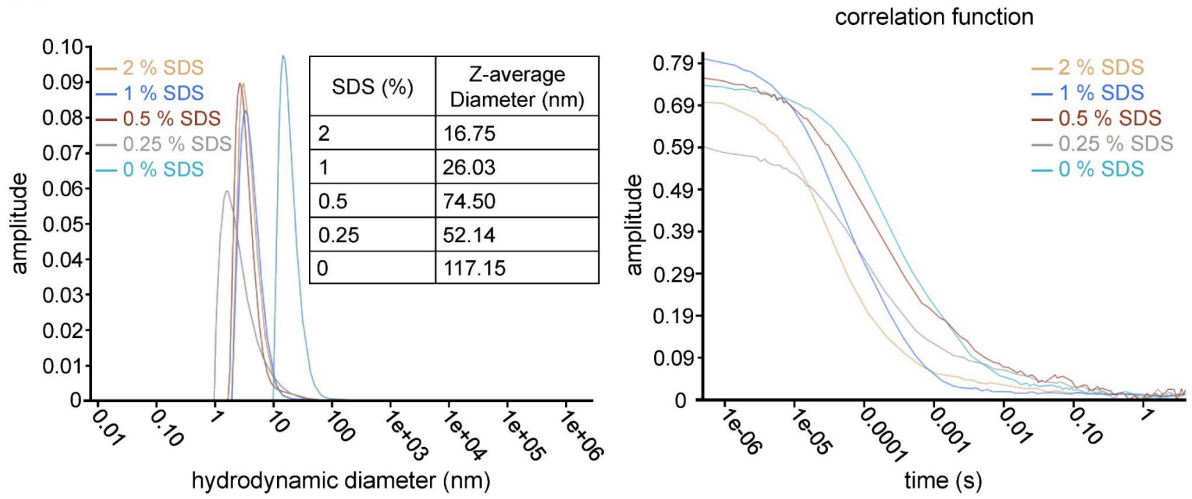
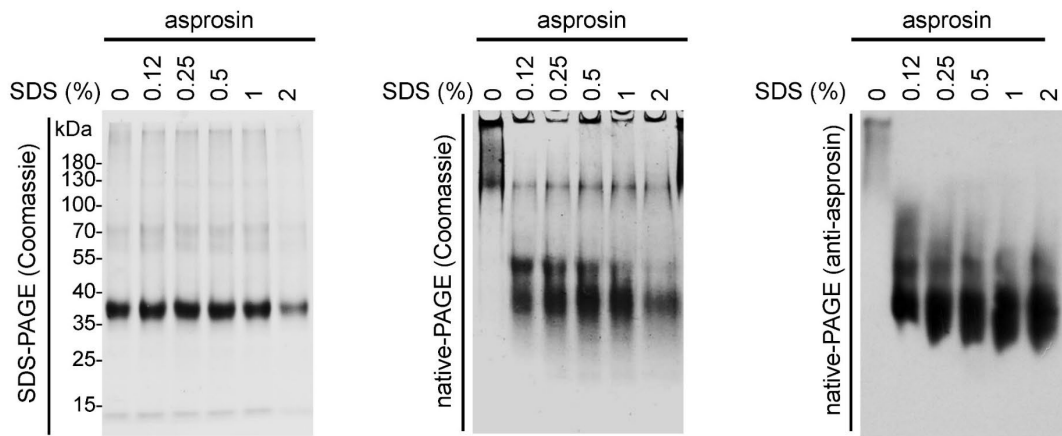
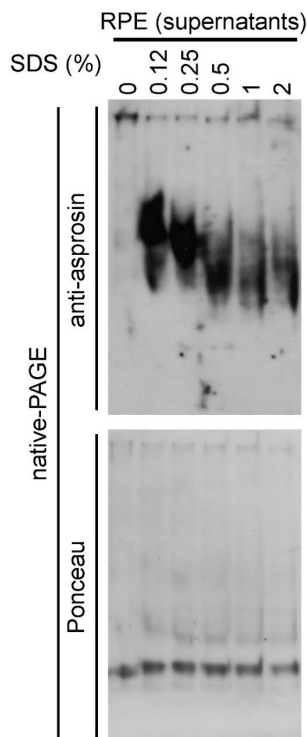
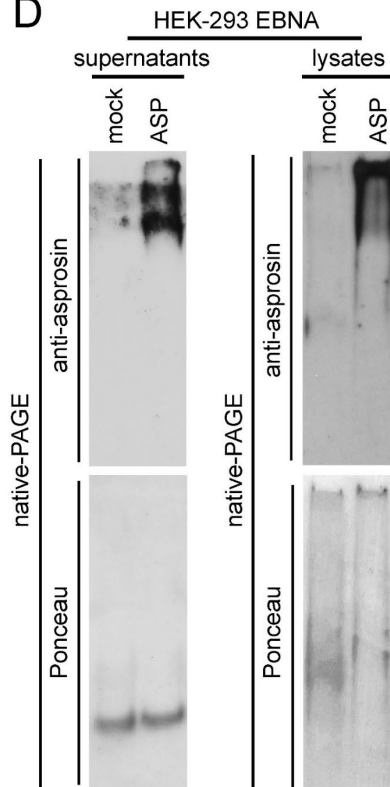
A**B****C****D**

Figure 4: Asprosin forms multimers under native conditions

A. (left) Hydrodynamic diameters of asprosin in presence of 0-2% SDS determined by UNcle analyzer. Reduction of the hydrodynamic radius from 10-100 nm to 1-10 nm with varying concentrations of SDS reflects DLS measurements (Fig. 3C). (right) Correlation functions of asprosin in presence of 0-2% SDS by UNcle indicating dissociation of asprosin multimers. **B.** Treatment of recombinantly purified asprosin with serial concentrations of SDS. (left) Coomassie staining of SDS-PAGE gel after subjecting untreated and SDS-treated asprosin shows no change in asprosin band pattern after SDS treatment. (middle, right) Coomassie staining and western blot analysis of untreated and SDS-treated asprosin subjected to native-PAGE show dissociation of asprosin multimers. **C.** Treatment of RPE cell culture supernatants with 0-2% SDS followed by 10% native-PAGE and western blot analyses. SDS-treatment resulted in dissociation of endogenous asprosin multimers similar to SDS-treated recombinant asprosin (B, right). **D.** Western blot analysis of cell culture supernatants (left) and cell lysates (right) from stably transfected HEK-293 EBNA asprosin overexpressing cells. Supernatants and cell lysates of mock and asprosin transfected cells were subjected to 10% native-PAGE followed by western blot analysis. Immunoblots show accumulation of overexpressed asprosin at stacking gel indicating that asprosin multimerization already occurs intracellularly.

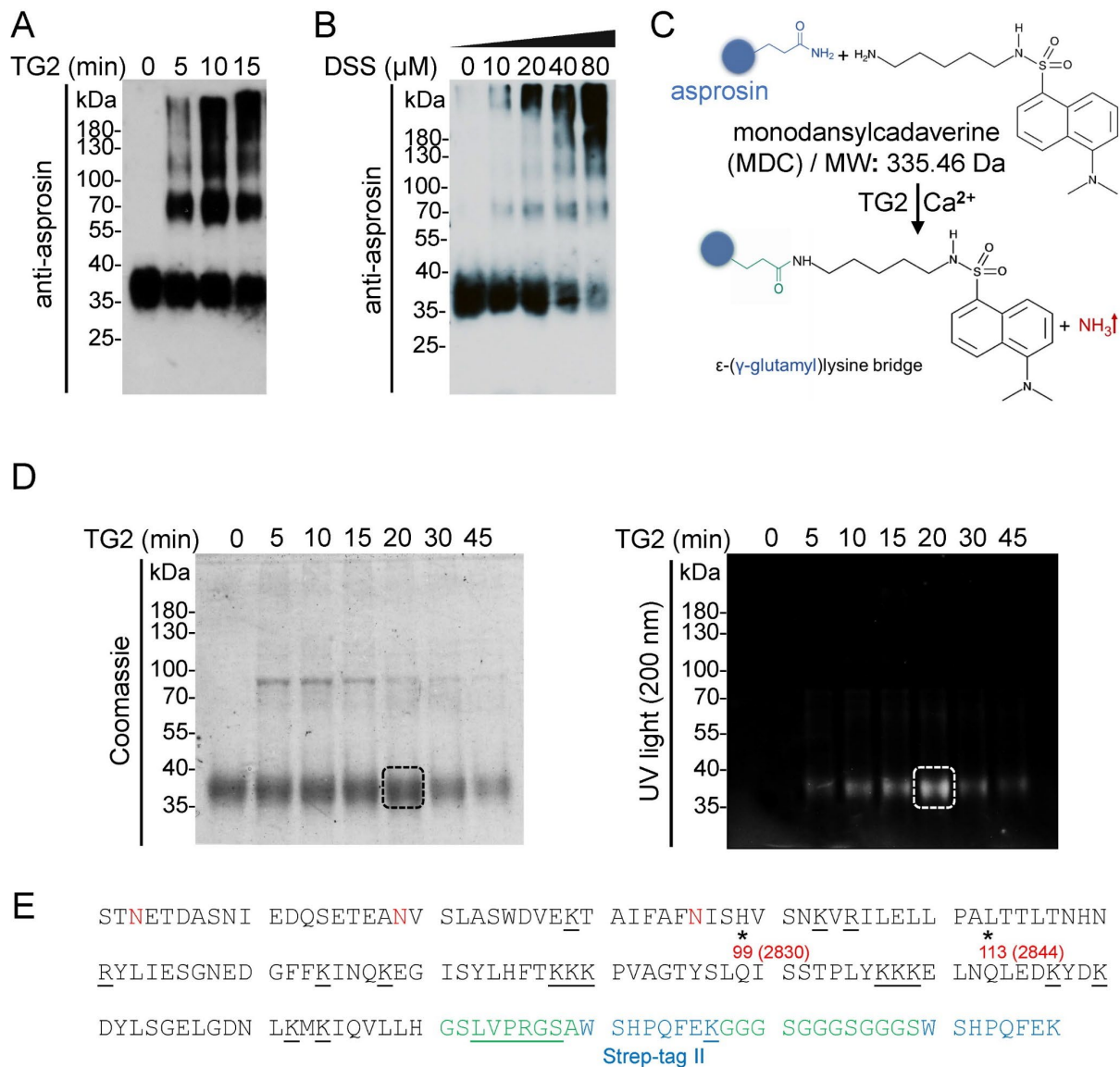


Figure 5: Asprosin is a substrate of transglutaminase 2 (TG2)

A. Incubation of monomeric recombinant asprosin with TG2 results in a significant shift of asprosin positive immunoblot signals towards higher molecular weight positions. **B.** Incubation of monomeric recombinant asprosin with a chemical crosslinker, DSS shows the same higher molecular weight bands as after incubation with TG2. **C.** The crosslinking reaction between asprosin and fluorescent monodansylcadaverine (MDC), a TG2 substrate. **D.** Incubation of monomeric recombinant asprosin with monodansylcadaverine (MDC) in the presence of TG2 results in bands corresponding to monomeric and dimeric asprosin detected by UV light. The band marked by a dashed box was analyzed by mass spectrometry to identify the potential glutamine residues subjected to TG2 modification. **E.** Mass spectrometry analysis revealed the glutamine residues (black asterisks, marked in red,

position regarding the fibrillin-1 sequence in parentheses) which could be utilized by TG2 for asprosin. Residues representing linker regions are indicated in green, thrombin cleavage (LVPRGS) site is underlined, and Strep-tag II sequences are marked in blue. The underlined residues mark predicted cleavage sites of Lys-C and trypsin used to generate peptide library of MDC-crosslinked asprosin. Anti-asprosin (pc-asp Ab) was used in the presented immunoblots in A and B.

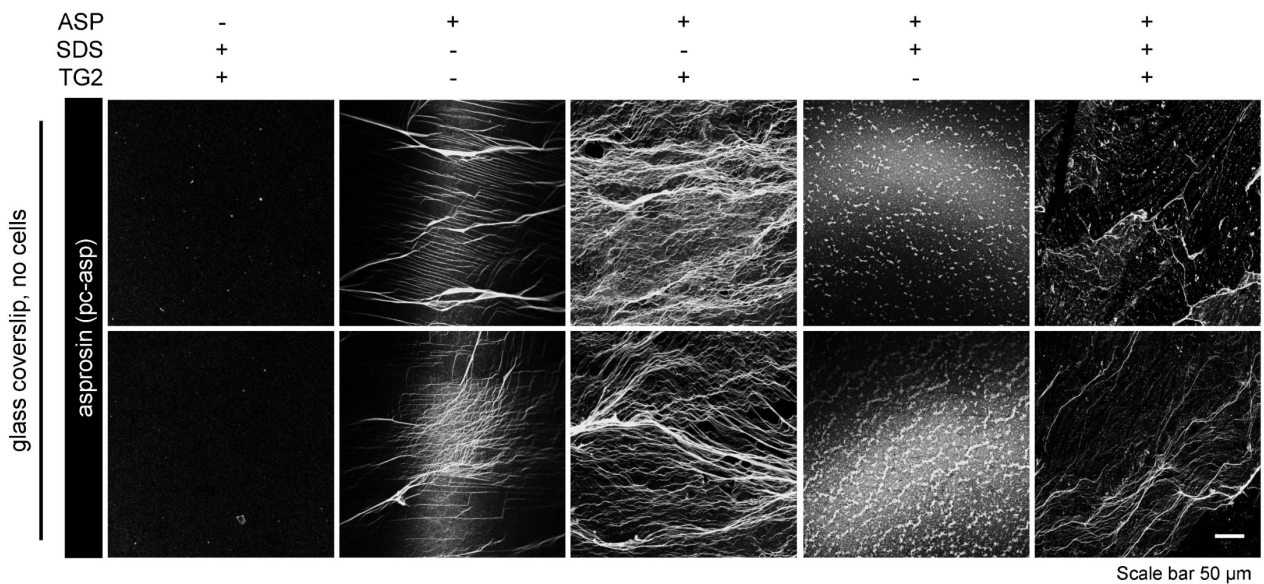


Figure 6: Asprosin fiber formation in absence of cells

Formation of asprosin fibers after incubating recombinant asprosin (8 $\mu\text{g}/\text{coverslip}$) for 48 h in presence or absence of TG2 (1 $\mu\text{g}/\text{ml}$) with or without SDS (0.001%) pre-treatment. Asprosin fibers were detected after incubating with anti-asprosin (pc-asp Ab) (white). Images were obtained from a Leica SP8 confocal microscope and were processed using Leica Application Suite X (LAS X) software (version 3.7.5.2) and Fiji/ImageJ software (version 1.53t) to obtain average intensity Z-projection. Scale bars: 50 μm .

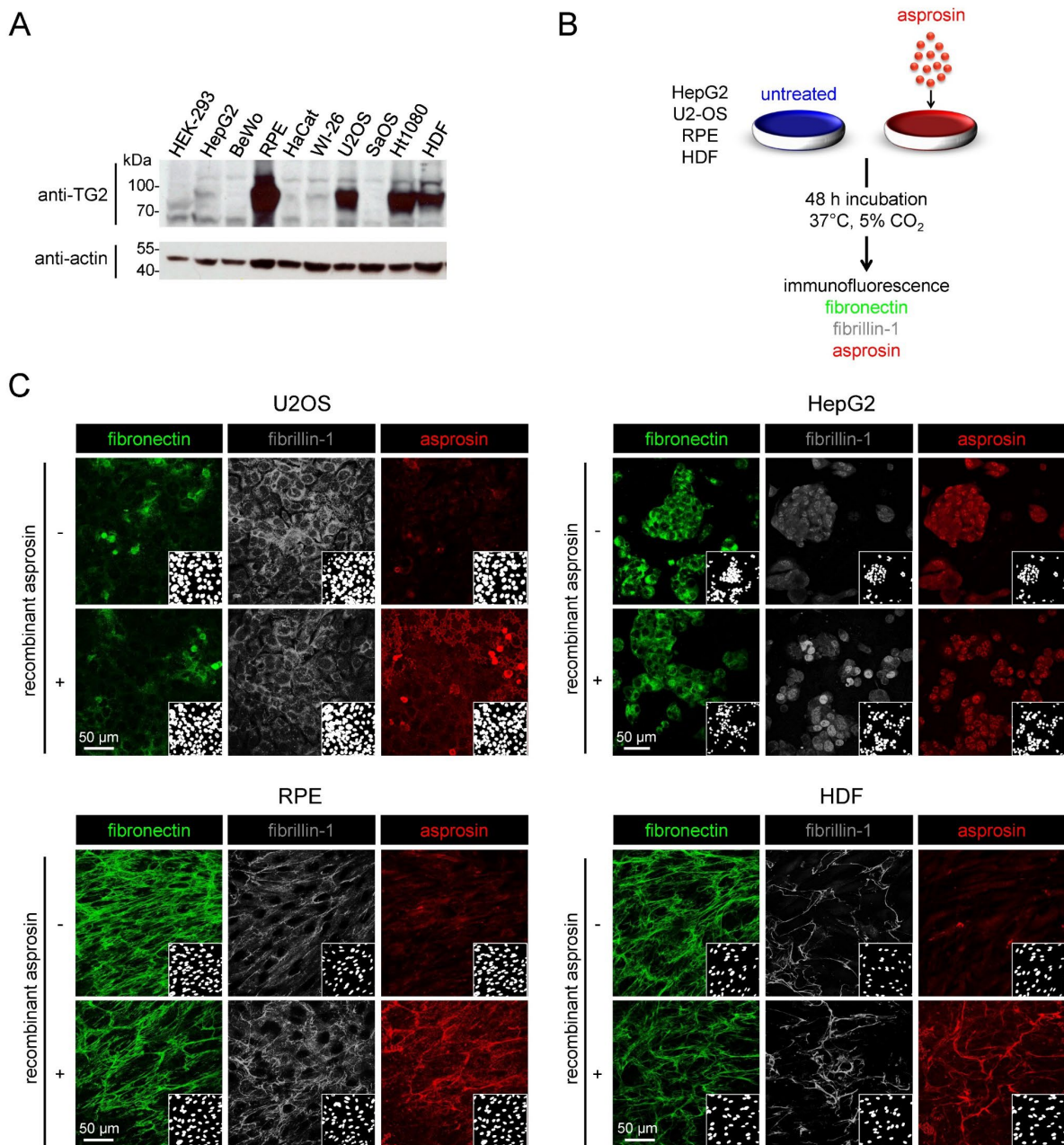


Figure 7: Assembly and ECM deposition of administered recombinant asprosin

A. (top) Western blot analysis showing the corresponding TG2 expression in cell lines lysates. (bottom) β -actin was used as a loading control. **B.** Schematic diagram illustrating the experimental design of cell lines treated with recombinant asprosin followed by immunofluorescence analysis. **C.** Recombinant asprosin ($5\mu\text{g/ml} \sim 140 \text{ nM}$) was administered to cell cultures of (top-left) U2OS, (top-right) HepG2, (bottom-left) RPE, and (bottom-right) HDF cells. 48 h after asprosin treatment, cells were immunostained with anti-fibronectin (FN1 Ab) (green), anti-fibrillin-1 (FBN1, rF90 Ab) (gray), anti-asprosin (pc-asp Ab) (red), and DAPI (white, nuclei). Immunofluorescence analysis reveals the presence of intact fibrillin-1 and fibronectin fiber network in cultures of RPE and HDF cells, but not in cultures of U2OS and HepG2 cells. Asprosin positive fibers were observed after

administration to RPE cells or HDF. However, asprosin is detected as aggregates in asprosin-treated U2OS cells, while HepG2 shows no significant differences in staining patterns before and after asprosin treatment. Images were obtained from a Leica SP8 confocal microscope and were processed using Leica Application Suite X (LAS X) software (version 3.7.5.2) and Fiji/ImageJ software (version 1.53t) to obtain average intensity Z-projection. Scale bars: 50 μm .

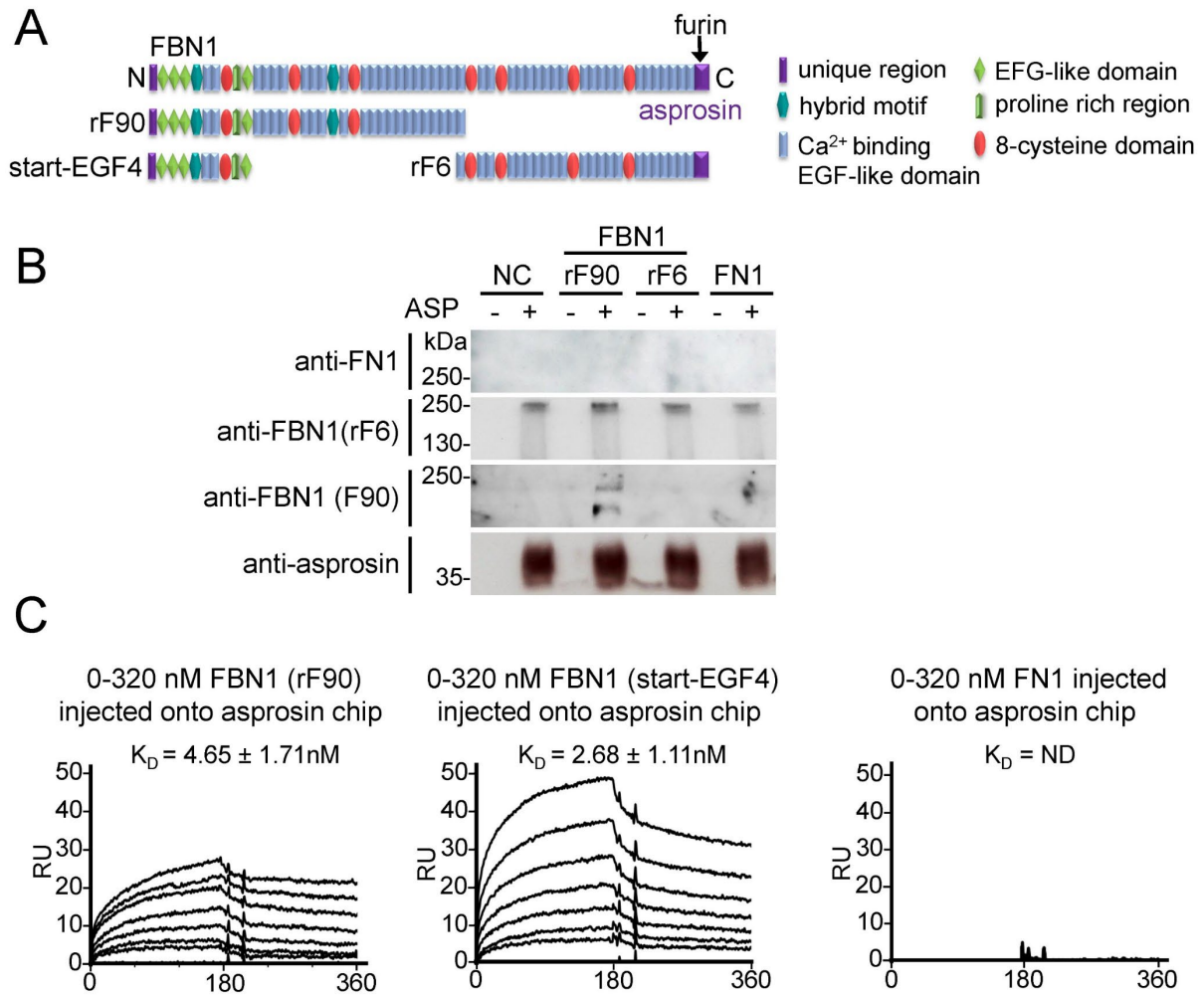


Figure 8: Asprosin interacts with the N-terminal region of fibrillin-1

Domain structure of fibrillin-1 and its N- and C-terminal halves including the start-EGF4 fragment (furin cleavage site marked by arrow). **B.** HEK-293 EBNA cells were transfected with overexpression constructs encoding for fibrillin-1 N- and C-terminal halves (rF90 and rF6). Medium obtained from non-transfected HEK-293 EBNA cells served as negative control (NC). Media obtained from the transfected with rF90 and rF6 are indicated. HEK-293 EBNA (NC) medium supplemented with fibronectin (10 μg) is indicated as FN1. The media were subjected to incubation with recombinant asprosin (double C-terminal 2 \times Strep-tag II) in presence of 0.5 $\mu\text{g}/\text{ml}$ TG2 overnight at 4 $^{\circ}\text{C}$. The mixtures were then subjected to pulldown with Strep-Tactin XT beads. After washing, the eluted fractions were subjected to immunoblot analysis with the indicated antibodies revealing the binding of asprosin to N-terminal half of fibrillin-1 (rF90). **C.** SPR binding studies suggest that asprosin interacts with the N-terminal half of fibrillin-1 (rF90) and the start-EGF4 fragment but does not bind to fibronectin.

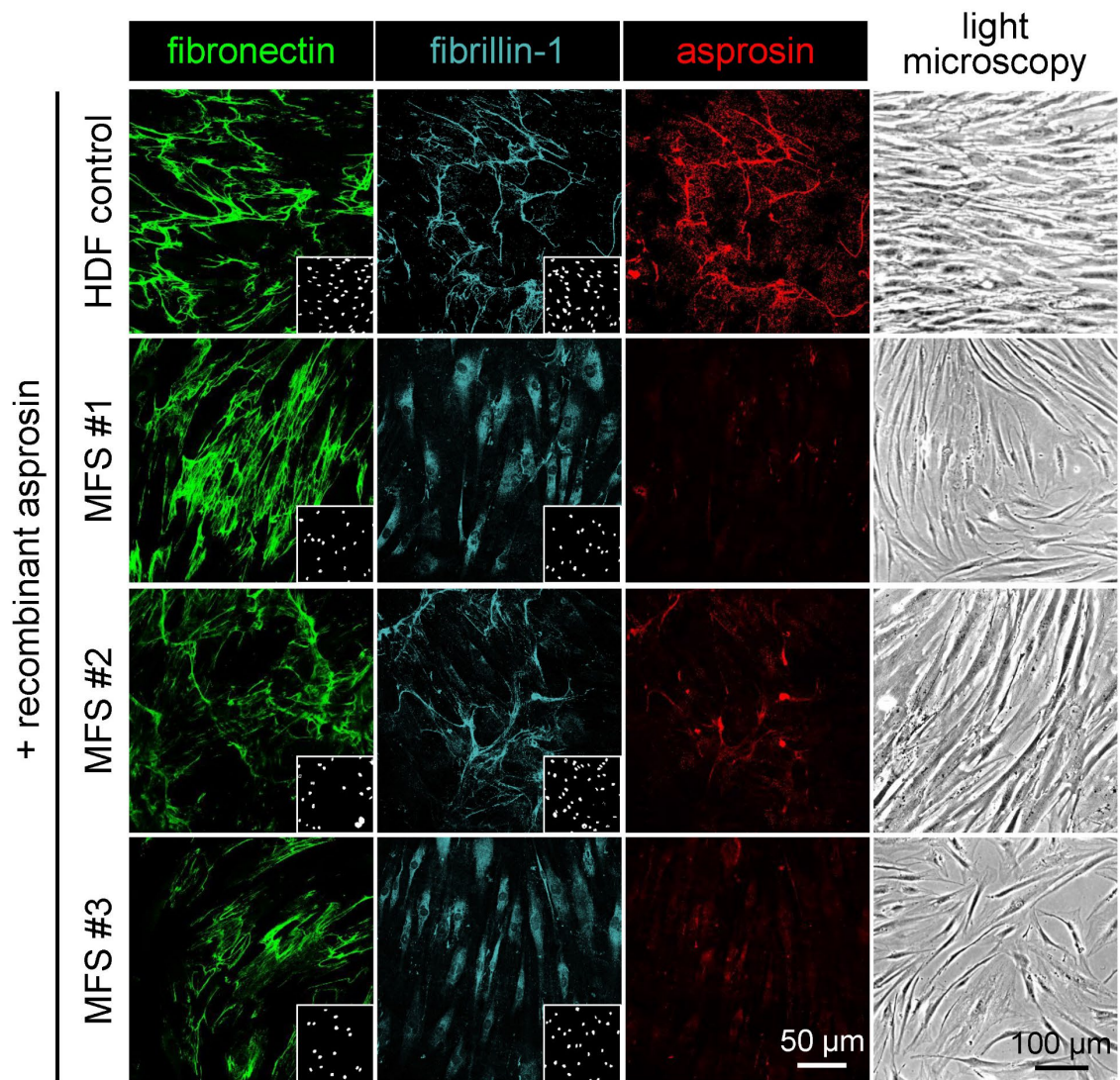


Figure 9: Linear deposition of asprosin as fibers is fibrillin-1 dependent

The formation of asprosin positive fibers after administration of recombinant asprosin ($5\mu\text{g/ml} \sim 140 \text{ nM}$) depends on the integrity of the fibrillin-1 fibril network which is deficient in primary fibroblast cultures from MFS patients. Control and MFS patient cells were incubated with anti-fibronectin (FN1 Ab) (green), anti-fibrillin-1 (FBN1, rF90 Ab) (gray), anti-asprosin (hASP(rat) Ab) (red), and DAPI (white, nuclei). Light microscopy images were obtained by Axiophot Microscope (Carl Zeiss, Germany). Fluorescence microscopy images were obtained from a Leica SP8 confocal microscope and were processed using Leica Application Suite X (LAS X) software (version 3.7.5.2) and Fiji/ImageJ software (version 1.53t) to obtain average intensity Z-projection.

A

STNETDASNI EDQSETEANV SLASWDVEKT AIFAFNISHV
 SNKVRILELL PALTTLTNHN RYLIESGNED GFFKINQKEG
 ISYLFHTKKK PVAGTYSLAI^{*} SSTPLYKKKE LNALEDKYDK
 DYLSGELGDN LKMKIQVLLH GSLVPRGSAW SHPQFEKGGG
Strep-tag II
 SGGGSGGGSW SHPQFEK
Strep-tag II

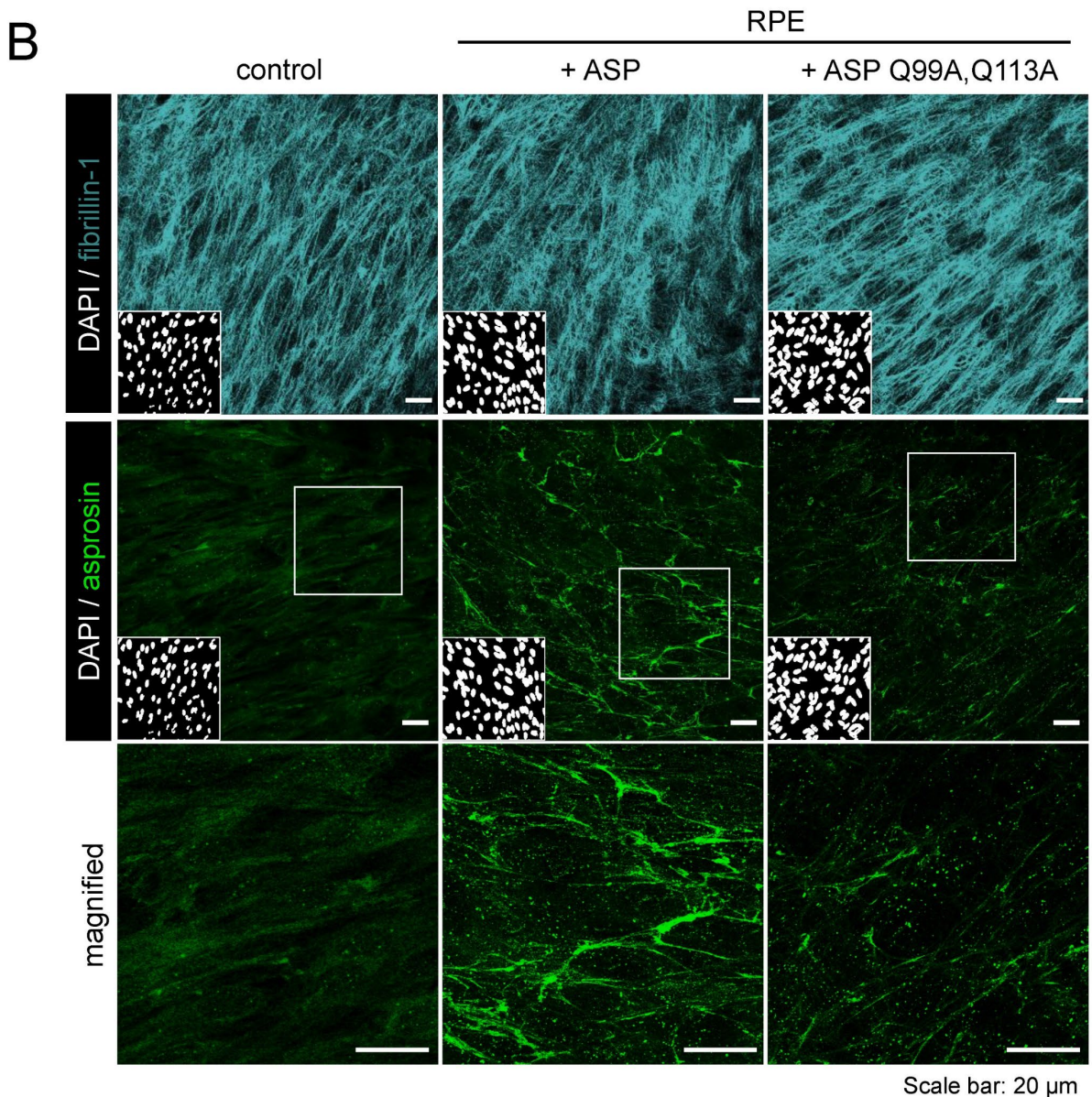


Figure 10: Mutation of critical glutamine residues abolishes asprosin fiber formation

A. Protein sequence of asprosin carrying glutamine substitutions (Q99A, Q113A, black asterisks). Residues representing linker regions are indicated in green, thrombin cleavage (LVPRGS) site is underlined, and Strep-tag II sequences are marked in blue. **B.** Comparative immunofluorescence analysis after administration of recombinant wild-type and mutated

asprosin (5 μ g/ml \sim 140 nM) to RPE cell culture. Untreated and treated RPE cells were incubated with DAPI (white, nuclei), anti-asprosin (pc-asp Ab) (green), and anti-fibrillin-1 (rF90 Ab) (gray). 3-fold magnified areas are marked by white boxes. Fibrillin-1 immunostaining (gray) reveals an intact fibrillin-1 network in untreated and treated RPE cells. (top panel) The immunofluorescence staining of asprosin in untreated cells (control) does not show asprosin positive fibers. However, (middle panel) the wild-type asprosin treated RPE cells show intact asprosin positive fibers compared to (bottom panel) mutated asprosin treated RPE cells, which show significantly disrupted fibers. Fluorescence microscopy images were obtained from a Leica SP8 confocal microscope and were processed using Leica Application Suite X (LAS X) software (version 3.7.5.2) and Fiji/ImageJ software (version 1.53t) was used to obtain average intensity Z-projection.

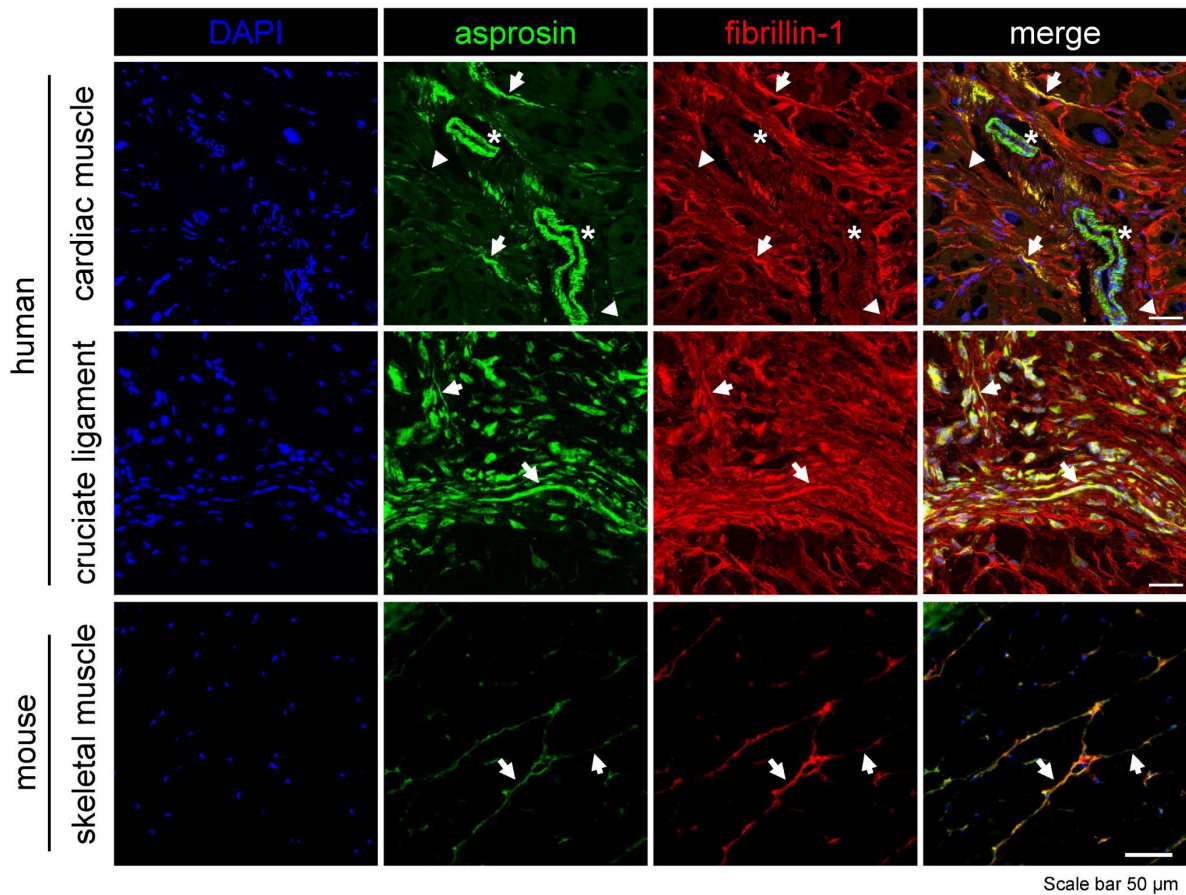


Figure 11: Asprosin colocalizes with fibrillin-1 in human and murine tissues

Confocal immunofluorescence microscopy of asprosin in indicated human and mouse tissues. Sections were fixed with acetone and incubated with asprosin antibodies (green; pc-asp Ab for human tissues, mASP(rat) Ab for murine tissues), anti-fibrillin (FBN1, rF90 Ab) (red) and DAPI (blue, nuclei). Immunostaining reveals depositions of asprosin positive fibers colocalizing with fibrillin-1 positive fibers (see merge panel). In cardiac muscle asprosin also appears as separate fine structures (arrowhead). Marked immunoreactivity for asprosin is present in the cytoplasm of vascular smooth muscle cells (VSMCs) and fibroblasts (asterisks). Images were obtained from an Olympus BX43 microscope (Olympus) equipped with a DP80 dual CCD camera and Leica SP8 confocal microscope. Images were processed using Leica Application Suite X (LAS X) software (version 3.7.5.2) and Fiji/ImageJ software (version 1.53t) was used to obtain average intensity Z-projection.

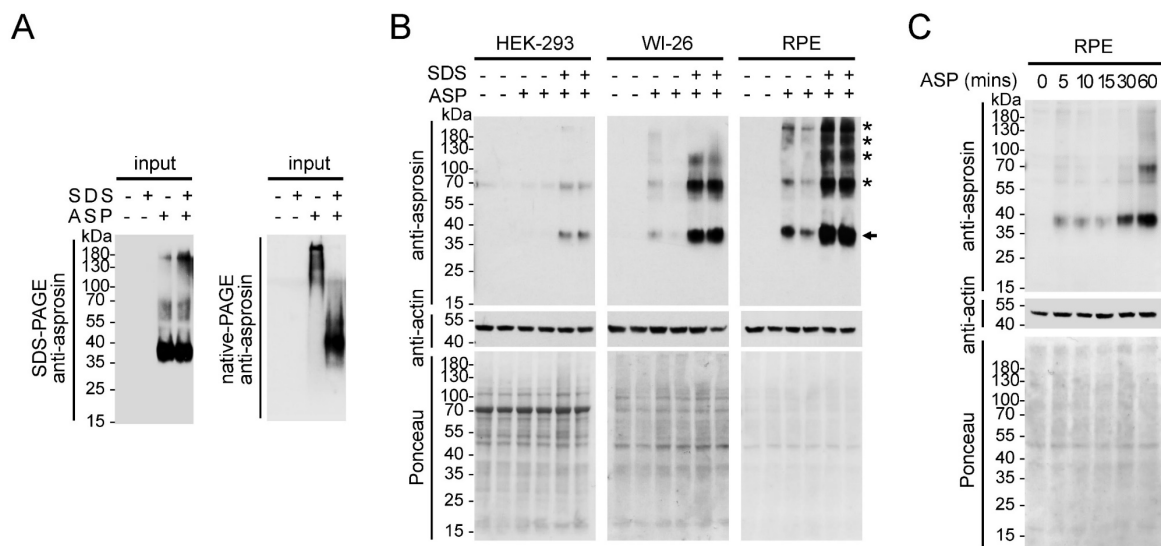


Figure 12: Asprosin oligomerization affects its cellular uptake

A. Quality control immunoblots of recombinant asprosin protein preincubated with SDS and diluted into cell culture media was subjected to (left) 10% SDS-PAGE gel and (right) 10% native-PAGE gel. Dissociation of asprosin multimers after SDS treatment can be only observed in samples subjected to native-PAGE. **B.** Comparative western blot analysis with anti-asprosin (pc-asp Ab) of cell lysates collected from (left) HEK-293, (middle) WI-26, and (right) RPE cells after administration of recombinant asprosin (3.5 $\mu\text{g/ml}$ ~100 nM) in presence and absence of SDS. Immunoblots show the enhancement of monomeric asprosin uptake in after SDS in all treated cell lines (band ~37 kDa, black arrow), additionally, in WI-26 and RPE cells asprosin positive bands of higher molecular weight (black asterisks) were also detected suggesting multimerization of administrated asprosin. **C.** Immunoblot with anti-asprosin (pc-asp Ab) of cell lysates collected from RPE cells treated with recombinant asprosin (1.75 $\mu\text{g/ml}$ ~ 50 nM) in presence of SDS after certain time points (5, 10, 15, 30, and 60 min). A significant increase of monomeric asprosin signal (band ~37 kDa) within time was observed and asprosin positive band at 70 kDa was detected corresponding to dimeric asprosin signal. β -actin and Ponceau staining were used as loading controls.

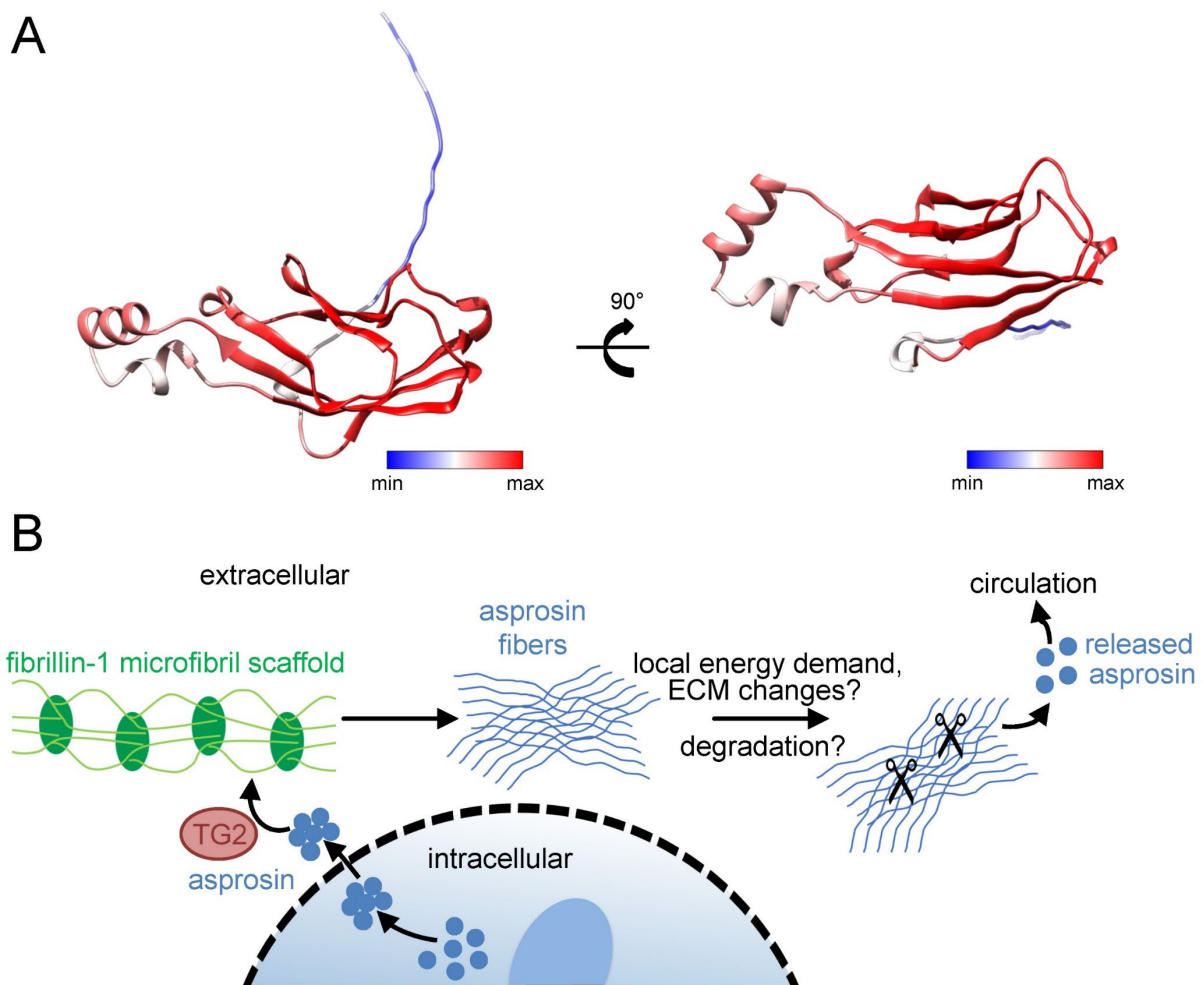
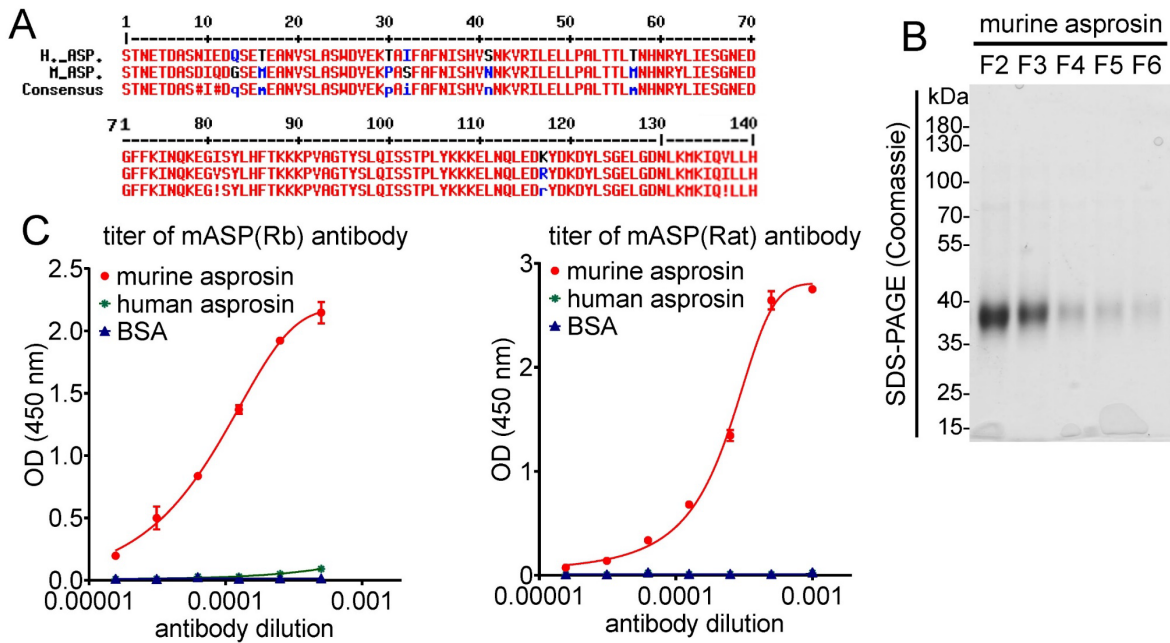


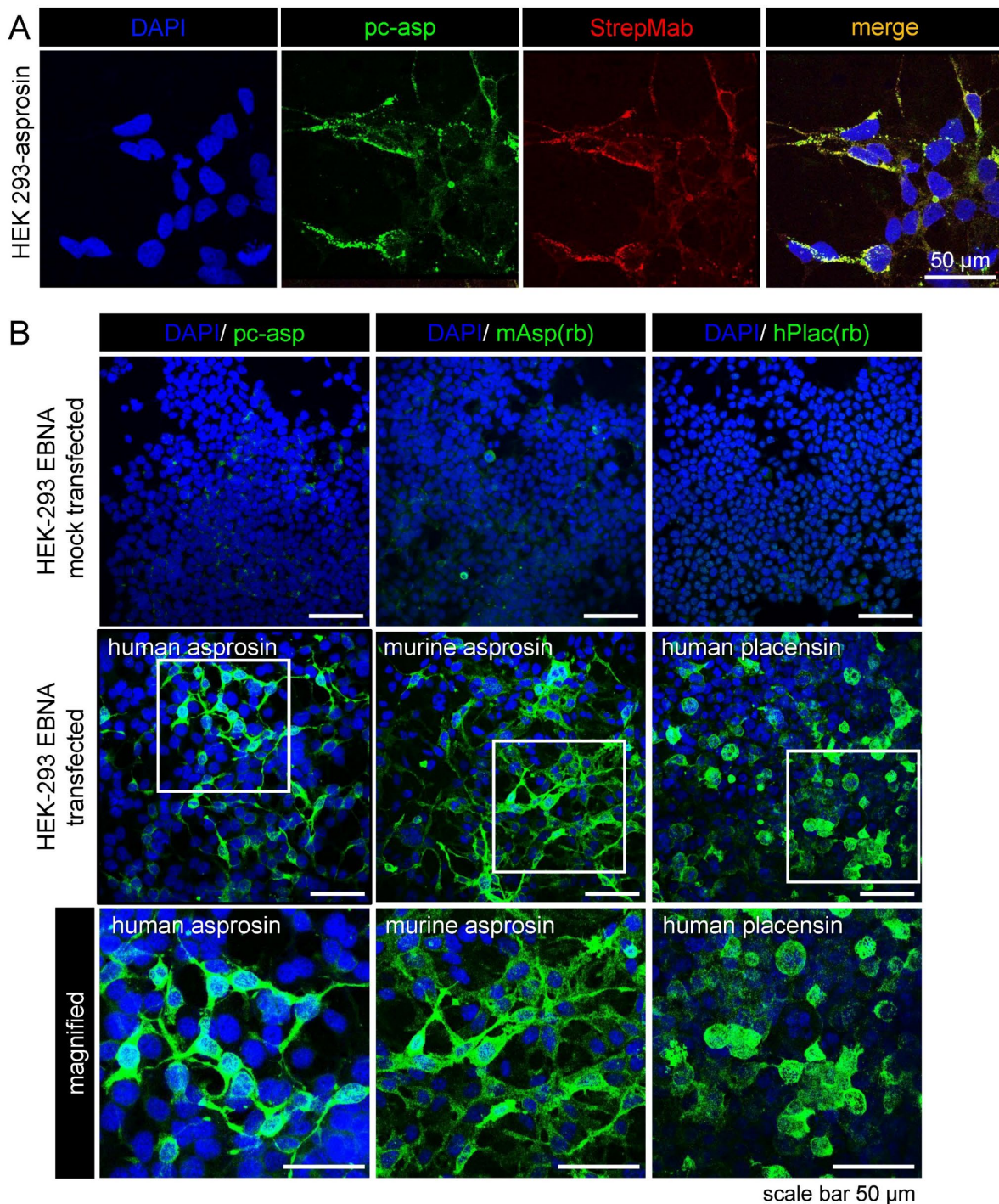
Figure 13: Mechanistic model for targeting of asprosin to the extracellular matrix

A. Model of asprosin. Asprosin assumes a cadherin-like core structure with the potential capability to multimerize via cadherin-like domains. The model is colored according to the predicted local distance difference test (pLDDT) and the per-residue confidence (red: high values, blue: low values). Image was rendered by employing ChimeraX v1.4 using the predicted model downloaded from Colab AlphaFold2. **B.** The model shows a potential mechanism of asprosin storage and utilization within the extracellular matrix. Upon secretion of asprosin may be targeted to assembled fibrillin-1 fibers. Thereby, TG2 mediated crosslinking enables stable storage of asprosin in the form of multimers. Multimeric asprosin may be later utilized by specific activation mechanisms such as proteolytic degradation of asprosin positive fibers. Released asprosin may act locally or is transported via the circulation to other target organs.



Supplementary Figure S1: Generation and evaluation of polyclonal anti murine asprosin antibodies.

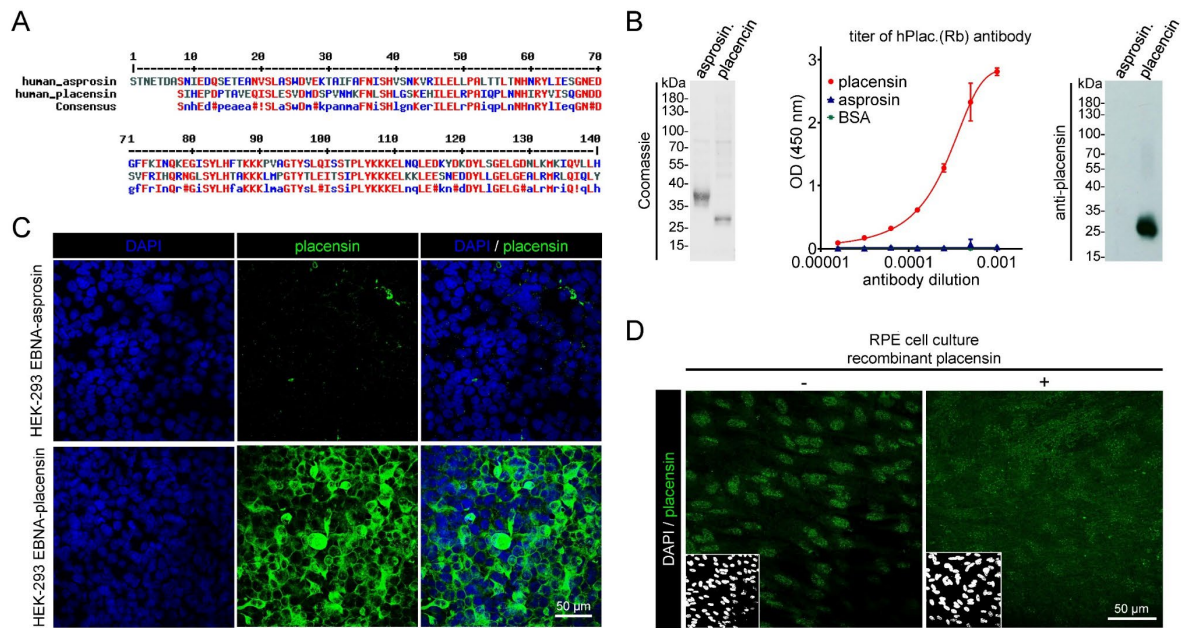
A. Sequence alignment between human and murine asprosin using Multalin software showed 92.14 % sequence identity between both proteins. Red color represents highly conserved residues; blue color represents weakly conserved residues; symbols: ! represents either I or V; # represents any one residue of NDQEBZ; i represents either I or L or T. **B.** Coomassie stained quality control gel of recombinantly produced and purified murine asprosin showing >95 % purity after affinity chromatography. **C.** Affinity purified polyclonal antibodies raised in rabbit (left) and rat (right) showed high specificity in detecting coated murine asprosin (100 ng/well) by direct ELISA with no crossreactivity to human asprosin or BSA. Data points represent mean \pm SD of duplicates.



Supplementary Figure S2: Immunofluorescence evaluation of generated labmade asprosin and placensin antibodies.

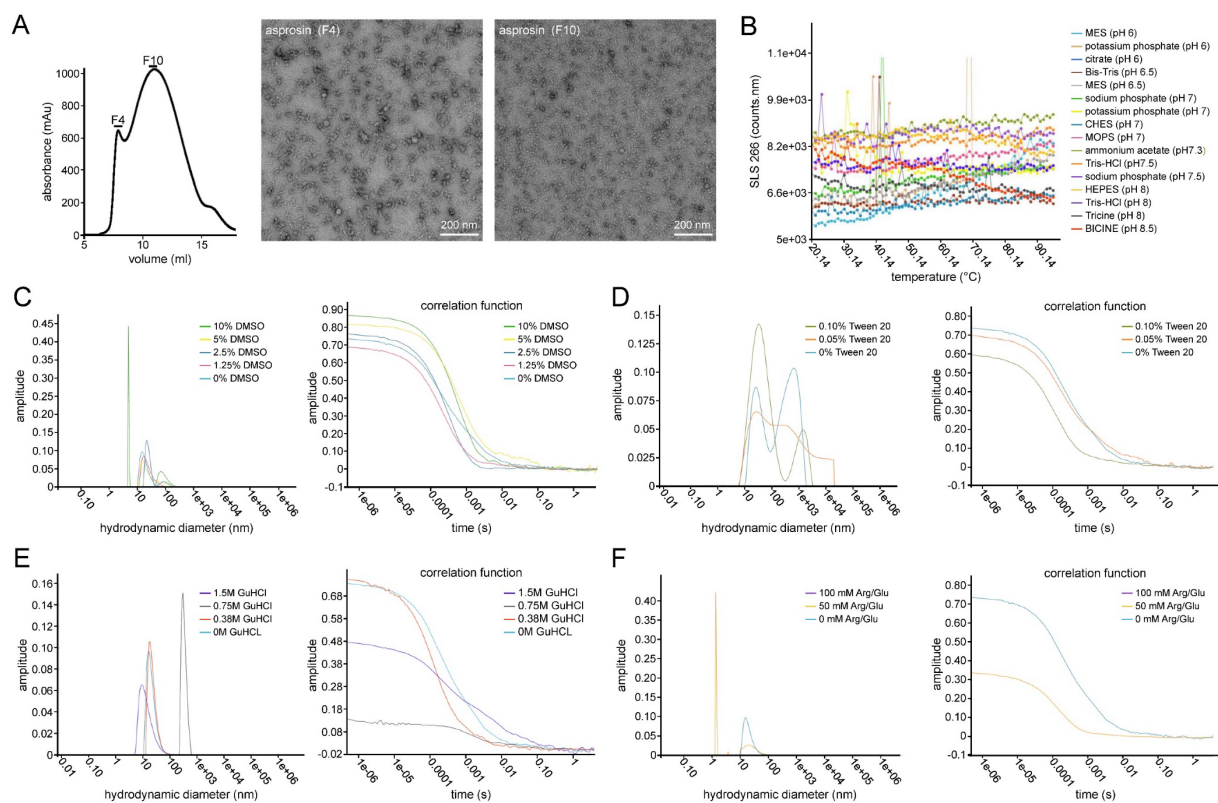
A. Immunofluorescence analysis of HEK-293 cells transfected with human asprosin-2×Strep-tag II using pc-asp (green), StrepMAB Ab (red), and DAPI (blue, nuclei) demonstrates co-localization of signals from pc-asp and StrepMab antibodies. **B.** Comparative immunostaining examination of the generated labmade human asprosin (pc-asp), mouse asprosin (mASP(rb) Ab), and human placensin (hPlac(rb) Ab) antibodies (green) in HEK-293 EBNA mock transfected cells and cells transfected with a construct expressing the indicated

protein. (top panel) No signal was detected in mock transfected cells. (middle and bottom panel) Positive staining was detected by antibodies in human asprosin, mouse asprosin, or human placensin transfected cells confirming their specificity in immunofluorescence application. Two-fold magnified areas are marked by white boxes. Images were obtained from a Leica SP8 confocal microscope and were processed using Leica Application Suite X (LAS X) software version 3.7.5.2. Fiji/ImageJ (version 1.53t) software was used to obtain average intensity Z-projection.



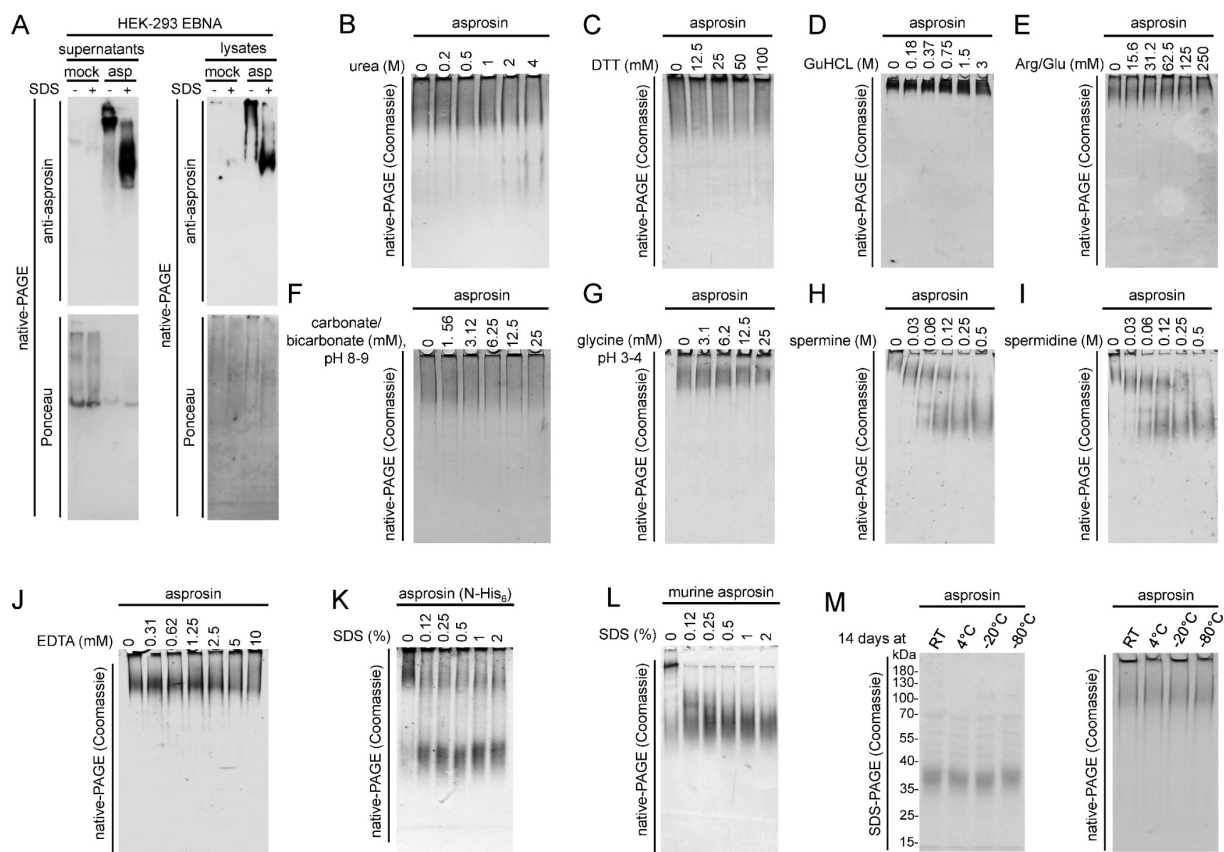
Supplementary Figure S3: Administration of placensin to RPE cells failed to form fibers.

A. Primary sequence alignment between human asprosin and human placensin performed by Multalin software program reveals 47% identity and 67% similarity between the two proteins. Red color represents highly conserved residue; Blue color represents weakly conserved residue; Symbols: ! represents either I or V; # represents any one residue of NDQEBZ; i represents either I or L or T. **B.** (left) Coomassie stained quality control gel of recombinant produced and purified (>95% purity) asprosin and placensin after affinity chromatography. (middle) Affinity purified polyclonal human-placensin antibody raised in rabbit, hPlac.(Rb) antibody showed high specificity in detecting coated placensin (100 ng / well) by ELISA. No cross reactivity to asprosin or BSA was detected indicating the specificity of the antibody. Data points represent mean \pm SD of duplicates. (right) Human placensin antibody specifically recognizes human placensin in western blot analysis, with no observable cross reactivity to asprosin. **C.** Immunofluorescence analysis of HEK-293 cells transfected with (top) human asprosin (N-His₆) and (bottom) human placensin (C-2 \times Strep-tag II) with hPlac.(Rb) antibody (green) and DAPI (blue, nuclei) shows specific intracellular placensin staining, with no cross reactivity to asprosin. **D.** Recombinant placensin (5 μ g/ml) was administered to RPE cells. 48 h after placensin treatment, cells were incubated with hPlac.(Rb) antibody (green) and DAPI (blue, nuclei). Placensin immunostaining showed only intracellular placensin signals and no presence of fibers. Images were obtained from a Leica SP8 confocal microscope and were processed using Leica Application Suite X (LAS X) software version 3.7.5.2. Fiji/ImageJ (version 1.53t) software was used to obtain average intensity Z-projection.



Supplementary Figure S4: Analysis of asprosin multimers using SEC, TEM and Uncle analyzer.

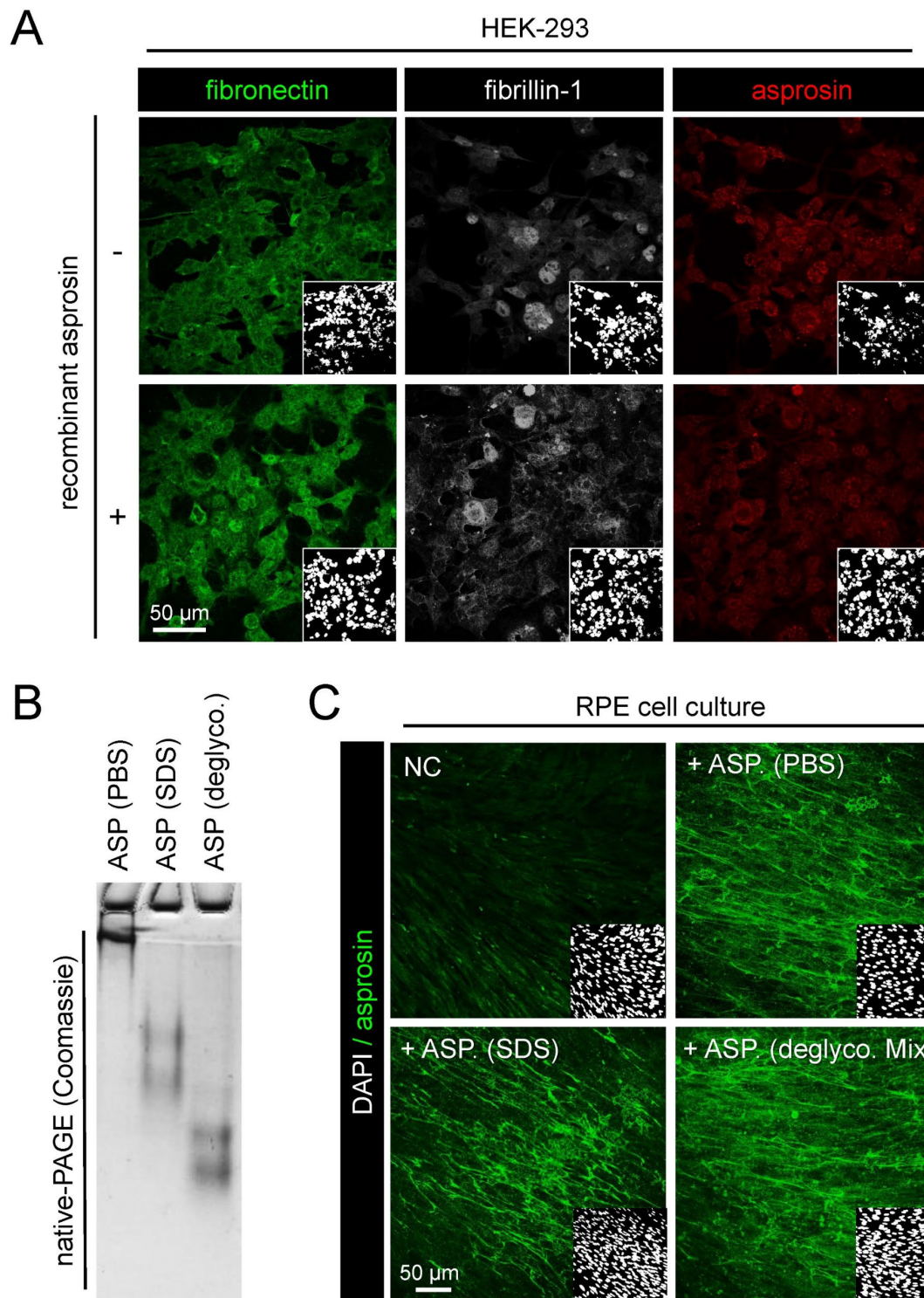
A. Recombinant asprosin subjected to SEC analysis and cryo-EM visualization of fractions 4 and 10. The overview EM images show asprosin multimers in different shapes and sizes. **B.** Examination of asprosin thermostability in several buffers at temperature ranges from 20°C to 38°C shows no significant changes in the measured static light scattering (SLS) indicating no variations in the asprosin multimeric state. **C – F.** Measurement of hydrodynamic diameters and correlation functions of asprosin in presence of different buffer showing several degrees of asprosin dissociation in the indicated buffers.



Supplementary Figure S5: Impact of pH change and denaturing agents on asproisin multimerization

A. Western blot analysis of cell culture supernatants (left) and cell lysates (right) from stably transfected HEK-293 EBNA asproisin overexpressing cells. Supernatants and cell lysates of mock and asproisin transfected cells were treated with 1% SDS and subjected to 10% native-PAGE followed by western blot analysis. Immunoblots show the dissociation of asproisin oligomers upon SDS treatment. **B.** Diluting asproisin in urea solutions ranging from 0.2M to 4M urea followed by native-PAGE analysis shows mild dissociation of asproisin oligomers in 4M Urea. **C.** Addition of dithiothreitol (DTT) up to 100 mM shows no effect on asproisin multimerization. **D.** Diluting asproisin in GuHCL solutions ranging from 0.18M to 3M then subjected to native-PAGE analysis shows no dissociation of asproisin oligomers. **E.** Treating asproisin with a serial concentration of arginine/glutamine ranging from 15.6mM to 250mM shows no dissociation of asproisin oligomers. **F.** Effect of basic pH on the multimeric state of asproisin in carbonate/bicarbonate solution (pH 8 – 9) reveals no detectable change compared to the untreated sample. **G.** Concentration-dependent increase of asproisin oligomerization in acidic conditions upon buffer exchange in glycine solution (3 – 25 mM, pH 3 – 4). Native-PAGE analysis indicates aggregation of asproisin n of asproisin multimers. **H-I.** Addition of spermine and spermidine on asproisin multimerization shows dissociation of asproisin

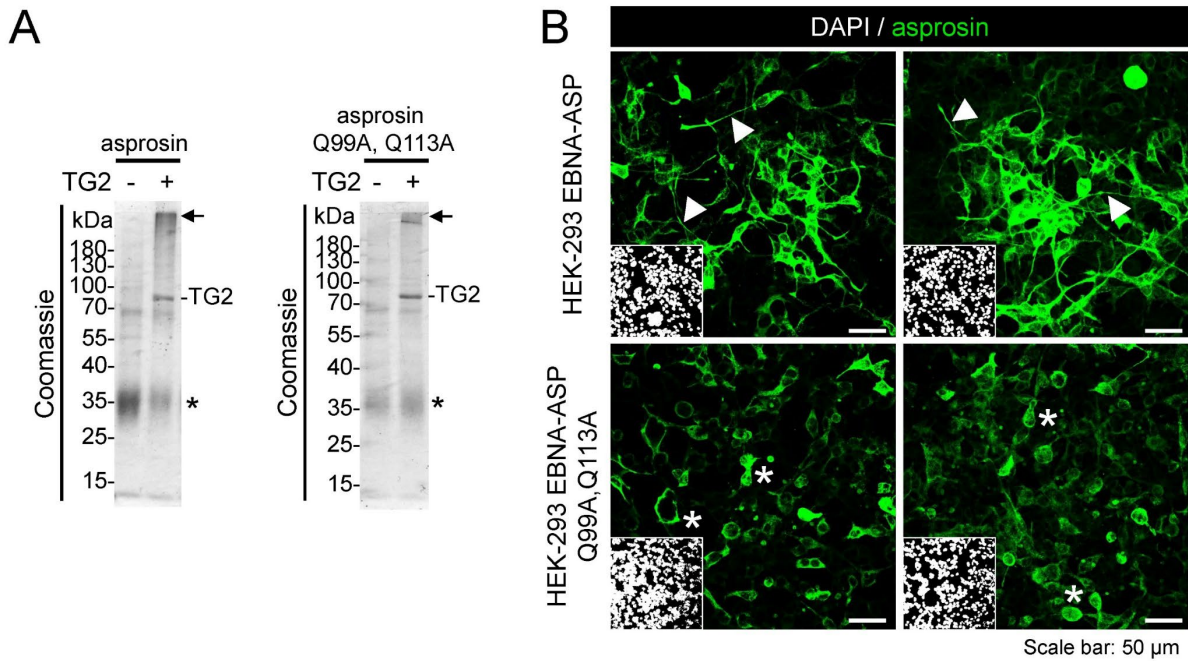
oligomers similar to SDS treatment (Fig. 4B, middle). **J.** Treatment of asprosin with EDTA shows no detectable effect on its multimeric state. **K.** Native-PAGE analysis of untreated and SDS-treated asprosin (N-His₆) shows dissociation of asprosin. **L.** Analysis of murine asprosin after and before SDS treatment shows similar pattern as human asprosin (Fig. 4B, middle). **M.** Coomassie staining of native and SDS-PAGE analyses of affinity purified asprosin after incubation at RT, 4°C, -20°C and -80°C for 14 days revealed no changes over time and temperature. For each experiment 3 µg of purified asprosin were used, samples in B and C were incubated for 10 min at 75°C before loading, and samples in D, E, F and G were incubated for 10 min at 37°C before loading.



Supplementary Figure S6: A. Impact of asprosin multimerization and glycosylation on fiber formation.

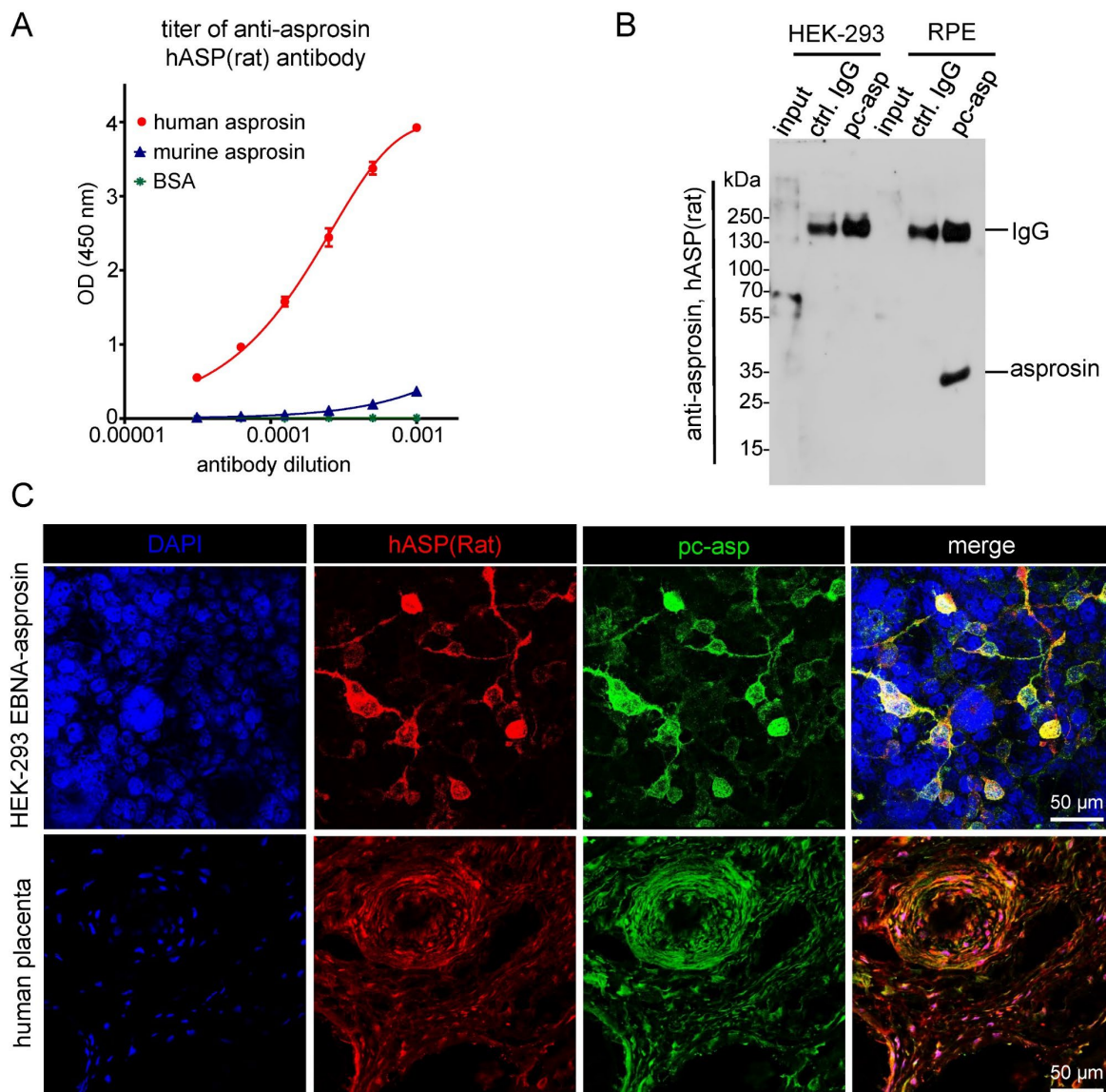
A. Immunofluorescence analysis revealed the absence of an intact fibrillin-1 and fibronectin fiber network in cultures of HEK-293 EBNA cells. Asprosin immunostaining showed no significant differences in staining patterns before and after asprosin treatment. **B.** Coomassie stained native-PAGE gel of recombinant asprosin after treatment with SDS or incubation in a

deglycosylation mix showing a change in its migration after treatment. C. Asprosin positive fibers were observed after administration of different batches of asprosin (analyzed in B) to RPE cells. Images were obtained from a Leica SP8 confocal microscope and were processed using Leica Application Suite X (LAS X) software (version 3.7.5.2) and Fiji/ImageJ software (version 1.53t) to obtain average intensity Z-projection. Scale bars: 50 μm .



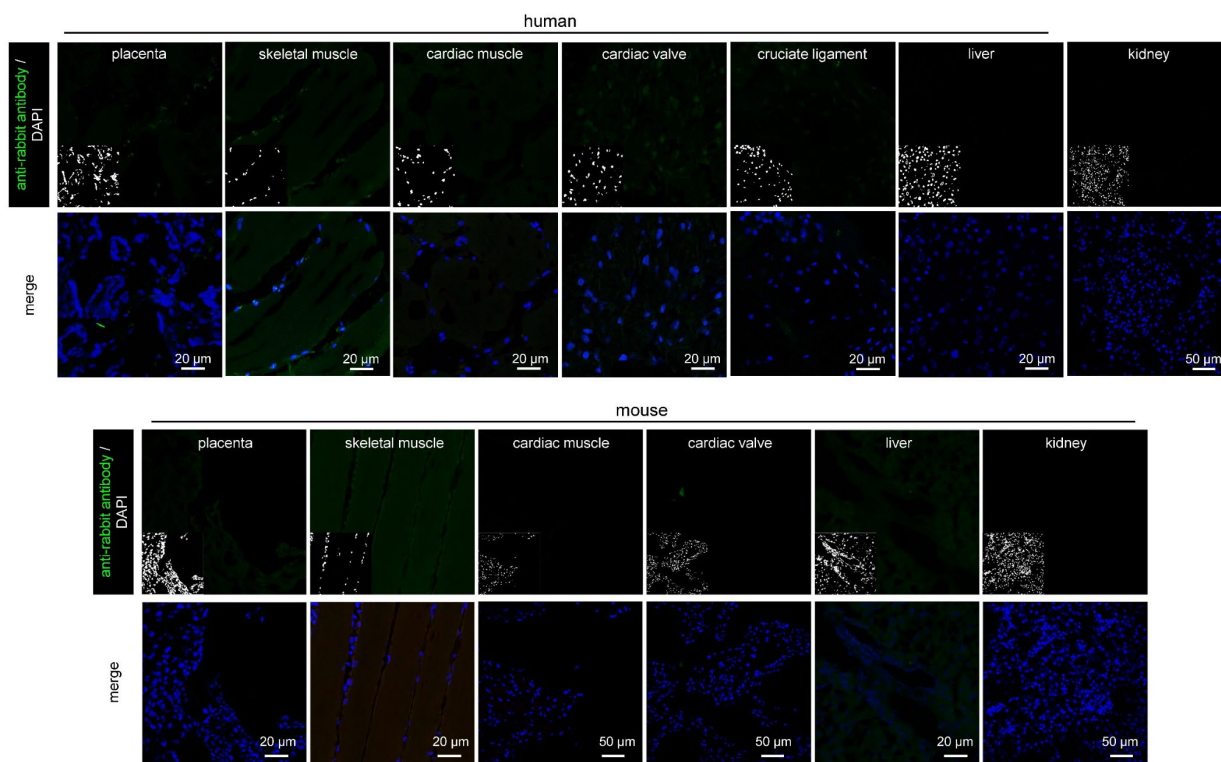
Supplementary Figure S7: Mutant asprosin does not serve as a substrate for transglutaminase-mediated fiber formation.

A. Incubation of recombinant wild-type asprosin (left) and recombinant mutant asprosin (Q99A, Q113A, sequence shown in Fig. 10A) (right) in presence of TG2 results in a significant increase of a high-molecular weight band in wild-type asprosin compared to mutant asprosin (black arrows). Also TG2 addition resulted only in a depletion of monomeric wild-type asprosin (black asterisks). **B.** Immunofluorescence analysis using pc-asp Ab (green) and DAPI (white, nuclei) in HEK-293 EBNA cells overexpressing wild-type and mutant asprosin proteins. (top panel) Representative images from two independent experiments of HEK-293 EBNA cells transfected with a wild-type asprosin construct resulting in the formation of asprosin positive fibers (white arrowheads). (bottom panel) Representative images from two independent experiments of HEK-293 EBNA cells transfected with a mutant asprosin construct show only intracellular diffused asprosin signals. Images were obtained from a Leica SP8 confocal microscope and were processed using Leica Application Suite X (LAS X) software (version 3.7.5.2) and Fiji/ImageJ software (version 1.53t) to obtain average intensity Z-projection. Scale bars: 50 μ m.



Supplementary Figure S8: Generation of anti-asprosin hASP(Rat) antibody and its application in immunoprecipitation and immunostaining.

A. Affinity purified polyclonal anti-human-asprosin antibody raised in rat hASP(Rat) shows high specificity in detecting coated human asprosin (100 ng / well) by ELISA. No cross-reactivity to murine asprosin or BSA was detected. Data points represent mean \pm SD of duplicates. **B.** Western blot analysis with hASP(Rat) ab of cell culture supernatants (input) and elution fraction after immunoprecipitation with rabbit control IgG (#26102, Thermo Fisher Scientific) (ctrl. IgG) and pc-asp antibody. **C.** Immunodetection of asprosin in cultures of asprosin overexpressing HEK-293 EBNA cells and in human placenta tissue using pc-asp (green), hASP(Rat) ab (red), and dapi (blue, nuclei) showing colocalization of the signals developed from both antibodies. Images were obtained from a Leica SP8 confocal microscope and. Images were processed using Leica LAS AF Lite 4.0 software and Fiji/ImageJ software to obtain average intensity Z-projection.



Supplementary Figure S9: Negative immunofluorescence controls of human and mouse specimens.

Images show sections incubated with secondary antibody only (negative control) and DAPI. Images were obtained from a Leica SP8 confocal microscope and were processed using Leica LAS AF Lite 4.0 software and Fiji/ImageJ software to obtain average intensity Z-projection.

6. Discussion

6.1 Analysis and functional role of asprosin glycosylation

Asprosin was predicted to harbor three N-glycosylation sites (N₃, N₁₉, and N₃₆), and three potential O-glycosylation sites within its N-terminal region (Ser1, Thr5, Thr16) (Romere et al. 2016). In this work, it could be demonstrated by mass spectrometry that all N-glycosylation sites are utilized (Morcos, Luetke, et al., 2022, Supplementary Fig. S3). Interestingly, it could be shown that human asprosin recombinantly expressed in HEK-293 shows a significant amount of N-terminal glycosylation which contributes to about 20 kDa of its molecular mass similar to physiological asprosin circulating in human serum (Morcos, Luetke, et al., 2022, Fig. 1D, 3C). Additionally, our analysis showed a likely O-glycosylation of asprosin (Morcos, Luetke, et al., 2022, Supplementary Fig. S2). Interestingly, the addition of 20 kDa due to N-glycosylation was previously noted by Ritty et al. while studying SDS-PAGE migration of several fibrillin-1 fragments, covering its C-terminus including asprosin (Ritty et al., 1999).

Also Ashworth et al. investigated the functions of the three N-glycosylation sites within a C-terminal fragment of fibrillin-1 that contained asprosin. They reported that glycosylation of the N₃ residue plays a role in the furin-mediated fibrillin-1 cleavage process (Ashworth, Kelly, et al., 1999). Removal of N₃ by site directed mutagenesis considerably improved furin-mediated processing of pro-fibrillin-1, although removal of N₁₉ or N₃₆ showed no effect. Therefore, the carbohydrate moiety linked to the N₃ site proximal to the furin cleavage sequence might be physiologically crucial in regulating the rate of mature fibrillin-1 secretion and assembly. Until now, the function of asprosin glycosylation in regulating its bioavailability has not been examined. However, similar to other proteins, it is possible that glycosylation keeps asprosin more soluble and prevents its aggregation in blood. Furthermore, glycosylation may be essential in protecting asprosin from enzymatic degradation and extending its biological half-life (Holcenberg et al., 1975; Jayaprakash & Surolia, 2017; Lis & Sharon, 1993; Vegarud & Christnsen, 1975). Further research is needed to determine how asprosin glycosylation affects its bioactivity.

6.2 Points to be considered for sensitive asprosin detection

Since the discovery of asprosin as a new hormone, extensive research and multiple clinical studies have been conducted. So far, correlations between circulating asprosin levels and various disorders, including obesity, diabetes, cancer, metabolic syndrome, and

cardiovascular diseases have been found (see the introduction, section 1.3.2); (Morcos, Luetke, et al., 2022, Supplementary Table S1). Pathologically elevated asprosin levels have been documented in patients with obesity (Ugur & Aydin, 2019; Wang et al., 2019), insulin resistance (Alan et al., 2019; Wang et al., 2018), and diabetes mellitus type 1 (DM1) (Groener et al., 2019) and type 2 (DM2) (Naiemian et al., 2020; Zhang et al., 2019; Zhang et al., 2020). Current research focuses on the prospect of pharmacological suppression of asprosin activity using anti-asprosin monoclonal antibodies (mAbs) to restore metabolic health (Mishra et al., 2021).

The enormous variability of reported serum, plasma and saliva asprosin levels ranging from <0.5 to >350 ng/ml raises serious concerns regarding the reliability of sensitive asprosin measurements (Morcos, Luetke, et al., 2022, Supplementary Table S1). Consequently, an initial objective of the project was to develop new biochemical methods for sensitive and reliable asprosin detection in clinical samples. We developed sensitive direct and sandwich ELISAs with a reliable detection below 0.15 ng/ml using our newly produced polyclonal asprosin antibody (pc-asp), which is equivalent to the reported sensitivities of commercially available ELISA kits used in earlier studies (Janoschek et al., 2020) (Morcos, Luetke, et al., 2022, Supplementary Table S1). We were also able to selectively concentrate asprosin from complex clinical samples using antibody affinity chromatography due to the strong affinity of the produced pc-asp antibody ($K_D \sim 300$ pM). With the use of this method, we were able to detect asprosin for the first time in urine (Morcos, Luetke, et al., 2022, Fig. 4D) and achieve significant serum concentrations for later identification by immunoblotting (Morcos, Luetke, et al., 2022, Fig. 4C).

According to our findings, asprosin levels in clinical samples range between 9 - 20 ng/ml in serum, 9 - 14 ng/ml in plasma, 0.5 - 2 ng/ml in saliva, and 1 - 3 ng/ml in breast milk (Morcos, Luetke, et al., 2022, Table 1). These ranges may represent physiologically relevant asprosin concentrations, since asprosin serum and plasma levels determined in this thesis are consistent with values previously observed in large patient cohorts containing more than 100 individuals (Baykus et al., 2019; Hong et al., 2021; Wang et al., 2021). In addition, a possible explanation for the large discrepancy between serum and plasma asprosin levels reported by other studies could be proposed (Morcos, Luetke, et al., 2022, Supplementary Table S1). Romere et al. published the first study on blood asprosin levels utilizing a sandwich ELISA similar to ours that utilizes pairs of polyclonal and mouse monoclonal antibodies (capture: mouse mab against human profibrillin amino acids 2838–2865; detector: polyclonal goat

against human profibrillin amino acids 2737–2750 by Abnova) (Romere et al., 2016). In two further studies employing the same detector but different capture antibodies, serum asprosin concentrations ranged from 10 - 220 to 307 - 7454 ng/ml (Wang et al., 2019; Wen et al., 2020). This clearly shows that the careful selection of a capture antibody is required for accurate and reliable asprosin measurement. Interestingly, we discovered that employing non-glycosylated recombinant asprosin generated in *E. coli* for standard curve generation may result in concentration ranges that are artificially skewed (Romere et al., 2016). Our biochemical experiments demonstrated that asprosin glycosylation may affect the detection sensitivity of asprosin in ELISA and western blot analysis (Morcos, Luetke, et al., 2022, Supplementary Fig. S4C, D). For example, the sensitivity of ELISA detection of deglycosylated asprosin using mab anti-asprosin (clone Birdy-1) appears to have increased (Morcos, Luetke, et al., 2022, Supplementary Fig. 4C). Therefore, the wide range of reported asprosin values may be due to differences in detection sensitivity between asprosin standards generated in *E. coli* and glycosylated asprosin present in clinical samples.

6.3 Correlation of asprosin levels with biological sex and feeding state

The newly developed sandwich ELISA demonstrated sufficient sensitivity to consistently identify asprosin at lower concentrations in the 1-2 ng/ml range. Therefore, it was possible to measure asprosin amounts in breast milk for the first time. Asprosin levels in breast milk may be an indicator of the mother's metabolic health and may be informative in the context of perinatal programming since it is known that other metabolic hormones, including leptin, ghrelin, insulin, and GLP-1, are also secreted into human milk and frequently correlate with maternal BMI (Badillo-Suarez et al., 2017). Therefore, the release of asprosin into breast milk may be regulated by the BMI of the mother, resulting in metabolic alterations in the infant.

Our serum measurements revealed that asprosin levels are considerably higher in females (Morcos, Luetke, et al., 2022, Fig. 3B) and comparable to previous findings in newborns, children, and adults (Baykus et al., 2019; Corica et al., 2021; Long et al., 2019; Sunnetci Silistre & Hatipoglu, 2020). There is currently limited information regarding the sex-dependent expression rates of the asprosin precursor fibrillin-1. Analysis of fibrillin-1 mutant mice, however, revealed sex-dependent changes in thoracic aortic contractility and aortic media injury (Altinbas et al., 2019; Jimenez-Altayo et al., 2017). Interestingly, 17 β -estradiol was reported to stimulate fibrillin-1 production in human aortic smooth muscle cells, but not in fibroblasts (Renard et al., 2017), indicating a sex and tissue dependent regulation of

fibrillin-1 expression that may explain the observed increase of asprosin levels in female blood samples.

Interestingly, we found elevated asprosin serum levels during fasting that strongly correlated with saliva asprosin levels (Morcos, Luetke, et al., 2022, Fig. 3B, C). Due to the high sensitivity and low intra- and inter-assay variability of our developed sandwich ELISA in comparison to commercially available asprosin detection kits (Morcos, Luetke, et al., 2022, Supplementary Table S1), it may be routinely used for the analysis of saliva as a non-invasive alternative to blood samples (Chojnowska et al., 2018; Groschl, 2017). Recently, a correlation between saliva and serum asprosin was established that appears to be BMI dependent (Ugur & Aydin, 2019). However, reported saliva asprosin levels from individuals with normal BMI were around 30 ng/ml, which is 30 times higher than what we observed on average under fasting conditions in our control cohort with normal BMI (Morcos et al., 2022), Fig. 3C). However, saliva asprosin concentrations of another control cohort were measured to be 25 ng/ml using the same commercially available ELISA kit (Gozel & Kilinc, 2020). Unfortunately, the kit used in both studies (Sunred Bioscience) is no longer available, making it impossible to retrieve details regarding its components and characteristics.

6.4 Sensitive detection in clinical samples suggests cartilage as a source for asprosin

Regarding the impact of exercise on asprosin blood levels, conflicting information has been reported. In the first study, asprosin levels increased after acute anaerobic exercise in a sex-dependent manner (Wiecek et al., 2018). Serum asprosin levels were elevated only in women 15 minutes, 30 minutes, 60 minutes, and 24 hours after a 20-second bicycle activity. Interestingly, in diabetic male rats aerobic exercise reduced hepatic asprosin levels (Ko et al., 2019). Recently, adult male subjects who performed an aerobic exercise program at a moderate intensity for 30 minutes at two different time intervals of the day (morning: 08:00–10:00 h, evening: 20.00–22.00 h), at least 3 days apart, also showed a significant reduction in serum asprosin. Serum levels of asprosin dropped significantly in both normal and overweight or obese individuals participating in the study (Ceylan et al., 2020). However, a comparison of absolute blood asprosin levels determined in the two studies raises questions about the reliability of the data. While Wiecek et al. report plasma asprosin concentrations ranging from 106 to 362 ng/ml (Wiecek et al., 2018), Ceylan et al. reported serum asprosin concentrations between 0.53 and 1.17 ng/ml (Ceylan et al., 2020) (Supplementary Table S1). Recent studies with larger cohorts, including >100 BMI, age and gender matched controls, demonstrated that concentrations of serum and plasma asprosin are in the same range as

determined by our measurements (13 - 32 ng/ml) (Table 1 and Supplemental Table S1). However, the reported serum asprosin levels by both previous exercise studies lie significantly outside of this range (Ceylan et al., 2020; Wiecek et al., 2018).

Our results demonstrate a considerable increase in asprosin following 30 minutes of running exercise (Fig. 5). Subjects weren't allowed to exercise for 24 hours prior to the morning trial. Prior to taking the first blood sample (baseline sample), participants sat still for 30 minutes. Our findings clearly demonstrated that acute running activity induces asprosin release into the blood, which is subsequently stable for at least two hours. The mechanism by which running exercise induces an increase in asprosin levels is still unknown. Previously, it was reported that plasma asprosin levels in women increased after a 20-second cycling sprint (Wiecek et al., 2018), an exercise routine with less mechanical impact than treadmill running. Since fibrillin-1 is widely expressed in connective tissues, including skeletal muscle (Romere et al., 2016; Sengle et al., 2015), and since these elevated asprosin levels after a low-impact bicycle sprint were linked with irisin, an exercise-induced myocyte-produced cytokine (Bostrom et al., 2012), muscle tissue was proposed as potential source of asprosin secretion (Wiecek et al., 2018). However, the tissue-specific contribution to exercise-induced increases in circulating asprosin levels is unclear, since irisin and asprosin are also generated by adipocytes (Roca-Rivada et al., 2013; Romere et al., 2016). Measurements of asprosin in conjunction with tissue-specific biomarkers may reveal which musculoskeletal compartment may be challenged by a particular exercise program and activate asprosin synthesis or its tissue release. Thereby it is also not clear how different mechanical impacts caused by specific exercise programs could potentially change the way asprosin is produced or released. Mechanical stimuli may induce cellular adaptation resulting in anabolic processes and asprosin production. Instead, mechanical loading could cause connective tissues to degrade, releasing asprosin into the bloodstream that is normally sequestered within tissue microenvironments. Exercise-induced mechanical loading of the joints causes cartilage to degrade and releases cartilage-derived proteins such as COMP into the serum (Firner et al., 2018; Firner et al., 2020). In the analyzed exercise cohort, it was previously observed that COMP levels rose after running exercise (Firner et al., 2018). We therefore hypothesized that if asprosin was a component of cartilage, exercise-induced cartilage breakdown would correlate with degradation markers like COMP in the serum. To test this hypothesis, we examined the levels of asprosin and COMP in osteoarthritis (OA) patients both before and after total hip replacement (THR) (Fig. 6). Our data revealed a significant correlation between asprosin and COMP serum levels in both the exercise group and the THR cohort,

indicating for the first time that asprosin may be a component of cartilage. This is not surprising since fibrillin-1 is a well known component of cartilage, where it forms supramolecular microfibrils that structurally support the cellular microenvironment of chondrocytes (Keene et al., 1997). It seems therefore plausible that asprosin may be also locally stored within cartilage.

Asprosin is produced and secreted by connective tissue resident cells including chondrocytes and fibroblasts, which supports the theory that asprosin is locally stored inside tissue-specific microenvironments (Fig. 3A). Proteoglycans or other supramolecular scaffolds found in the extracellular matrix (ECM), such as the fibronectin/elastic fiber network, which has been shown to act as sinks or targeting scaffolds for growth factors derived from connective tissue (Bishop et al., 2007; Sengle & Sakai, 2015), could serve as potential extracellular storage platforms. A sensor for the local energy demand may be asprosin stored in tissues. Asprosin has been shown in experiments with murine myoblasts (C2C12) to be able to increase local glucose uptake by tissue muscle cells (Zhang et al., 2021) by upregulating the expression of the glucose transporter GLUT4. This increases the local sensitivity of muscle cells to insulin (Jung et al., 2019).

6.5 Correlation between placental asprosin concentration and maternal BMI and GDM

In our Cologne-Placenta Cohort (CPC) study, we examined the relationship between maternal and fetal umbilical plasma asprosin concentrations and BMI, gestational diabetes mellitus (GDM), and other clinical parameters. Even though we could not find a significant correlation between any clinical parameter and plasma asprosin concentrations, the diagnosis of GDM in BMI subgroups appeared to affect asprosin concentrations in both maternal and fetal umbilical plasma: obese pregnant women (BMI >30) and the fetal umbilical blood of normal-weight women (BMI <25) showed a significant increase in plasma asprosin levels with maternal GDM. Previously, it was reported that asprosin blood levels increased in women (Baykus et al., 2019; Hu et al., 2021) as well as in rodents (Alan et al., 2019; Rezk et al., 2020) with GDM. The influence of BMI on pregnancy has never been studied. Since, liver glucose release is triggered by asprosin (Luis et al., 2020), GDM may be caused by elevated asprosin levels during pregnancy. Interestingly, we found a novel association between smoking and asprosin plasma levels. Asprosin concentrations in maternal and fetal umbilical plasma were lower in mothers who smoked before pregnancy. This represents an interesting finding, since asprosin was described as an orexigenic hormone (Duerschmid et al., 2017; Luis et al., 2020), and smoking has been linked to anorexigenic effects (Miyata et

al., 1999; Sanigorski et al., 2002). Therefore, decreased asprosin levels in women who started smoking before pregnancy match reports on several other nicotine-sensitive adipokines and may indicate the anorexigenic effects of smoking (Bai et al., 2016). However, our study required a 9-month nicotine abstinence period before plasma asprosin testing. Therefore, a direct effect of nicotine on circulating asprosin in our cohort seems unlikely but should be investigated in future studies.

Our cohort showed a strong positive correlation between maternal and fetal umbilical plasma asprosin levels (Baykus et al., 2019; Hu et al., 2021). This suggests that asprosin may cross the placenta and affect the metabolism of the fetus. Little is known about placental asprosin expression, content, or transport. Our investigations contributed to a better understanding of the role of asprosin in pregnancy by measuring asprosin immunoreactivity in placentas from our cohort and correlate it to maternal and fetal umbilical plasma concentrations. We found a positive correlation between placental asprosin immunoreactivity and maternal plasma asprosin levels, suggesting that placental tissues accumulate maternal plasma asprosin. Our finding of asprosin production in cultured chorionic cells suggests that the maternal placenta may contribute to plasma asprosin concentrations (Hoffmann et al., 2022, Fig. 3).

Placental asprosin immunoreactivity was found throughout the placenta, but asprosin positive signals were also detected in endothelial cells of fetal vessels in the villous parenchyma and chorion. Former studies have shown that placental endothelial cells produce many chemokines (Galley & Webster, 2004) and function as conditional innate immune cells (Takenouchi et al., 2013). We also found asprosin in decidual cells on the maternal side of the placenta, which regulate immune function (Canavan & Simhan, 2007). Asprosin seems to play a role in inflammation in other tissues (Lee et al., 2019), so it may be possible that the production/storage of asprosin by endothelial and decidual cells contributes to placental inflammation, similar to leptin, which is an autocrine and paracrine regulator of placental tissue (Akerman et al., 2002). Asprosin immunoreactivity was also found in amnion endothelial cells and placental macrophages. As macrophages produce pro-inflammatory adipokines (Chazaud, 2020) and accumulate in the placentas of GDM-complicated pregnancies (Jiang et al., 2021), they may contribute to several placental pathologies by producing or releasing asprosin. However, since endothelial cells and macrophages often exhibit unspecific immunoreactivity (Honig et al., 2005), their signals should be interpreted with caution. The pattern of placental asprosin immunoreactivity suggests that asprosin is mostly produced in placental cells that regulate inflammation and immune regulation, two mechanisms that contribute to pregnancy complications like preterm birth, fetal growth

restriction, placental pathologies, and hypertensive disorders that have serious consequences for the fetus (Goldstein et al., 2020; Vannuccini et al., 2016).

GDM was previously linked to placental asprosin immunoreactivity (Hu et al., 2021) which could be verified in our cohort. However, we found a so far not observed association between placental asprosin immunoreactivity and maternal BMI. As maternal BMI rises, placental asprosin immunoreactivity increases more in women with GDM than in those without. Asprosin, a metabolic regulator, may be affected by GDM because it modulates insulin and leptin signaling during pregnancy (Pérez-Pérez et al., 2016). We also found that increased individual insulin levels correlated with increased placental asprosin immunoreactivity, suggesting a general interdependence between asprosin and insulin during pregnancy.

In conclusion, our study adds new information to the metabolic effects of asprosin. In the future, placental asprosin expression and maternal obesity should be correlated. In particular, an in-depth assessment of a potential molecular interaction between insulin and asprosin may help to develop preventive and therapeutic measures against obesity and diabetes, not just during pregnancy.

6.6 Extracellular detection of asprosin as fibers in human and murine tissues

Asprosin is primarily characterized as a WAT-derived hormone that is secreted into the bloodstream to regulate hepatic glucose release (Hoffmann et al., 2020; Romere et al., 2016). Since asprosin is the C-terminal propeptide of pro-fibrillin, we questioned whether it had a comparable ubiquitous tissue distribution as fibrillin-1. By generating new asprosin-specific antibodies that do not crossreact with full-length fibrillin-1 (Morcos, 2021), we were able to detect extracellular deposits of asprosin in the form of fibers in tissues for the first time. Furthermore, the existence of fibers was discovered to be more prominent in specific tissue microenvironments, such as skeletal and cardiac muscle. However, in the liver, asprosin was detected predominantly in intracellular vesicles (Morcos, Prymachuk, et al., 2022, Fig. 1), indicating its rapid utilization in this metabolically active tissue.

This aforementioned finding is in line with what Cain et al. had previously reported in 2006. By using mass spectrometry, they were able to reliably identify two verified fingerprint peptides downstream of the C-terminal furin cleavage site sequence (asprosin sequence) in extracted mature microfibrils isolated from the human zonular apparatus (Cain et al. 2006). This finding was unexpected since pro-fibrillin-1 processing by furin is demonstrated as a

prerequisite for mature fibrillin-1 deposition (Ashworth, Kelly, et al., 1999; Jensen et al., 2014; Ritty et al., 1999). However, our finding that asprosin is targeted to the fibrillin microfibril network provides now an explanation for the detection of asprosin signature peptides in microfibril preparations.

```
STNETDASNI EDQSETEANV SLASWDVEKT AIFAFNISHV
SNKVRILELL PALTTLTNHN RYLIESGNED GFFKINQKEG
ISYLFHTKKK PVAGTYSLQI SSTPLYKKKE LNQLEDKYDK
DYLSGELGDN LKMKIQVLLH
```

Figure 8: Primary sequence of human asprosin showing the identified two peptides (highlighted in dark gray) from 13 separately prepared human zonular microfibril preparations by mass spectrometry analysis. Modified from Cain et al. 2006.

Currently, the role of asprosin fibers is unknown. We hypothesize that asprosin is stored locally in tissue-specific microenvironments by oligomerization and linear deposition as fibers (Morcos, Prymachuk, et al., 2022, Fig. 1). Asprosin deposition in tissues may serve as an energy demand sensor. From there, it may be released into the serum via certain, yet unidentified activation events. Regulating asprosin release by tissues may be an undiscovered mechanism, by which tissues communicate their energy demand to the metabolic system in order to maintain body homeostasis and adapt to external conditions. *In vitro* studies have suggested that asprosin has a metabolic role in controlling the energy needs of tissue-resident cells. Experiments with murine myoblasts (C2C12) demonstrated that asprosin not only inhibits muscle cell insulin sensitivity (Jung et al., 2019), but also up-regulates glucose transporter 4 (GLUT4) expression in C2C12 myotubes and enhances local glucose uptake by tissue muscle cells (Zhang et al., 2021).

6.7 Multimerization of asprosin

Analyzing recombinant asprosin purified from conditioned HEK-293 EBNA medium via size exclusion chromatography (SEC) resulted in a chromatograph with two peaks corresponding to two main asprosin species with distinct molecular weights. Interestingly, non-reducing SDS-PAGE analysis followed by Coomassie staining of the eluted SEC peak fractions mainly showed the presence of a monomeric asprosin band at 37 kDa (Morcos, Prymachuk, et al., 2022, Fig. 4A, B). This finding indicated the presence of soluble asprosin multimers in the analyzed peak fractions, which dissociate into monomers upon exposure to SDS. Only native-PAGE analysis allowed to us show the oligomerization of freshly purified recombinant

asprosin as accumulated asprosin in the stacking gel, while SDS-PAGE analysis of the same fractions showed monomeric asprosin bands (Morcos, Pryymachuk, et al., 2022, Fig. 4D).

To gain more insights about the oligomeric state and size of asprosin, purified asprosin was analyzed by SEC coupled to multi-angle static light scattering (MALS). Interestingly, MALS measurements revealed a polydispersity of asprosin, with an average molecular mass of approximately 570 kDa (molecular mass ranges from ~1000 kDa to 180 kDa) and an average hydrodynamic radius (R_h) of 11.3 nm (Morcos, Pryymachuk, et al., 2022, Fig.4C). Additionally, the electron microscopy (EM) analysis of selected fractions (which were subjected to MALS) visualized asprosin multimers with various molecular shapes indicating different degrees of oligomerization (Morcos, Pryymachuk, et al., 2022, Supplementary Fig. S5A). These findings raise a number of questions, including: What is the functional role of asprosin oligomerization? Do tissues and cell lines also produce endogenous asprosin in the form of multimers? Does asprosin multimerization takes place intra- or extracellularly?

It is known that larger proteins are more resistant to degradation, and that increasing the oligomerization state of proteins represents a protein stabilization mechanism that was reported in several organisms (Ali & Imperiali, 2005; Arnold et al., 2001; Tanaka et al., 2004; Tarafdar et al., 2014; Wintrose & Arnold, 2000). Our findings showed that multimerization of asprosin confers significant thermostability as indicated by the absence of any degradation products after exposure to RT, 4°C, -20°C and -80°C for 14 days (Morcos, Pryymachuk, et al., 2022, Supplementary Fig. S4H). Interestingly, by employing the UNcle multifunctional protein stability analysis system we revealed no dramatic changes in asprosin thermal stability at a concentration of 1 µg/µl in several buffers (pH 6-8.5) and temperatures ranging from 20.2°C to 38.2°C (Morcos, Pryymachuk, et al., 2022, Supplementary Fig. S5B). This finding further emphasizes that oligomerization makes asprosin more resistant to changes in temperature.

Investigating how asprosin multimers dissociate was another crucial question we explored. Initially, we investigated the effect of pH change on asprosin oligomerization. Both acidic glycine solution (0-25 mM, pH 3-4) and the basic carbonate/bicarbonate solution (0-25 mM, pH 8-9) failed to dissociate asprosin multimers (Morcos, Pryymachuk, et al., 2022, Supplementary Fig. S4D, E). However, we found that asprosin oligomerization is enhanced at higher glycine concentrations, which is not unexpected given that asprosin has an acidic isoelectric point (pI) of 5.8. Furthermore, asprosin multimers were also resistant to dissociation upon applying reducing agents such as DTT (0-100 mM) which is expected since

it does not contain cysteine residues and therefore served as a control reagent (Morcos, Pryymachuk, et al., 2022, Supplementary Fig. S4C). Treatment with urea (0–4 M) led to a minimal dissociation of asprosin multimers (Morcos, Pryymachuk, et al., 2022, Supplementary Fig. S4B). To gain further insight into the buffer conditions disrupting asprosin oligomerization, we employed the novel and high-throughput UNcle protein stability analyzer. It could detect changes in the average hydrodynamic radius (R_h) of asprosin in several solutions simultaneously (Morcos, Pryymachuk, et al., 2022, Supplementary Fig. S5C – F). As a result, we could identify SDS as a promising candidate to dissociate asprosin multimers, since the average hydrodynamic radius was substantially reduced from ~117 nm to ~17 nm with the highest SDS concentration, 2% (Morcos, Pryymachuk, et al., 2022, Fig. 5A), while Tween20, DMSO, and GuHCL did not seem to show a pronounced effect. Native-PAGE analysis of asprosin treated with SDS indicated a dissociation of asprosin multimers by induced down-shifting of asprosin bands. We still detected several asprosin bands corresponding to the presence of multiple homooligomeric species and thereby confirming our EM observation that asprosin forms multimers of various sizes and shapes (Morcos, Pryymachuk, et al., 2022, Fig. 5B, middle and right).

Native-PAGE analysis of cell culture supernatants of RPE cells revealed an endogenous asprosin band in the stacking gel. Interestingly, this band also resolved upon SDS treatment similar to the recombinant asprosin (Morcos, Pryymachuk, et al., 2022, Fig. 5C). This finding strongly demonstrates the secretion of endogenous asprosin as multimers. Moreover, our transfection experiments with HEK-293 cells producing monomeric asprosin revealed presence of asprosin multimers under native conditions in analyzed cell lysates and supernatants suggesting intracellular multimerization of asprosin (Morcos, Pryymachuk, et al., 2022, Fig. 5D).

Multiple studies have documented that proteins are in equilibrium between different multimeric forms. The regulation of this equilibrium plays a central role in controlling their activity and function. For example, carbamoyl phosphate synthase (CPS) which exists in a balance between inactive dimers and active tetramers (Cabo-Bilbao et al., 2006; Kim & Raushel, 2001; Mora et al., 2002; Ono, 2007). Cell culture data demonstrated that exogenous asprosin uptake is significantly improved upon asprosin treatment with SDS (Morcos, Pryymachuk, et al., 2022, Fig. 12A, B). This data implies that the state of multimerization can modulate its cellular uptake, and consequently its bioactivity. Taken together, these findings provide new biochemical insights into mechanisms controlling asprosin bioavailability.

Therefore, we propose asprosin oligomerization as an extracellular target mechanism, which allows it to be stored in latent form until future usage. We also suggest that association/dissociation of asprosin multimers plays a key role in the communication to metabolic organs to maintain energy balance and homeostasis. Further investigations are needed to identify biological factors regulating asprosin oligomerization. Moreover, our results might explain asprosin fiber deposition in tissues, since asprosin multimerization could play an important role in the initial steps of asprosin fibers assembly.

6.8 Asprosin crosslinking to the ECM cellular microenvironment depends on an intact fibrillin-1 network

Interestingly, we discovered that asprosin is a substrate of the crosslinking enzyme tissue transglutaminase (TG2), which is known to assist the assembly of fibronectin, fibrillin-1, and elastic fibers (Clarke et al., 2005; Qian & Glanville, 1997; Rock et al., 2004; Turner & Lorand, 1989). TG2 is highly selective in regards to the glutamine residues that it subjects to crosslinking (Coussons et al., 1992). Placensin, the C-terminal propeptide of fibrillin-2, did not form higher multimers or fibers in fibroblast cultures upon addition, despite a sequence homology of >40% and the presence of multiple accessible glutamine residues (Morcos, Prymachuk, et al., 2022, Supplementary Fig. S3D). Recent research has identified placensin as a new placenta-derived glucogenic hormone that promotes hepatic cAMP synthesis, protein kinase A (PKA) activity, and glucose release. Asprosin has also been reported to be expressed in human placenta and to be higher in the plasma of pregnant women with gestational diabetes mellitus (GDM) and their offspring (umbilical blood) (Zhong et al., 2020) after adjusting for maternal and neonatal clinical features and lipid profiles. Asprosin fiber synthesis in the placenta may serve the purpose of fine-tuning the metabolic effects mediated by asprosin and placencin.

Our transfection experiments with HEK-293 cells producing monomeric asprosin demonstrated that asprosin denaturation-resistant multimers were also found intracellularly, although in the conditioned media only monomeric asprosin was detected (Morcos, Prymachuk, et al., 2022, Fig. 3A). In contrast, asprosin multimers were identified intracellularly and extracellularly in the 3T3-L1 cell lysates and supernatants (Morcos, Prymachuk, et al., 2022, Fig. 3A). Intracellular TG crosslinking is a complicated topic, as TGs do not pass the usual ER/Golgi pathway and require Ca^{2+} for activation. Despite low intracellular calcium levels, several transamination and crosslinking substrates of intracellular TG2 have been discovered (Eckert et al., 2014; Rossin et al., 2015). This indicates that

locally elevated intracellular calcium and/or unidentified interacting proteins may enhance production of active TG2. The formation of tetramers in cell lysates was already indicated by our transfection investigations utilizing a monomeric asprosin-encoding overexpression construct (Morcos, Prymachuk, et al., 2022, Fig. 3). In HEK-293 cells, multimers may not be released due to extracellularly absorption of asprosin. In future investigations, we will investigate not only how oligomerized asprosin is utilized by cells, but also by what precise release mechanisms asprosin can be liberated from its fibrous state.

Our studies demonstrate that asprosin is specifically deposited on fibrillin fibers and not fibronectin fibers (Morcos, Prymachuk, et al., 2022, Fig. 7C). This finding may suggest that an intact fibrillin network is necessary for the correct extracellular storage of asprosin. Fibrillin is found in all tissues and is known to assemble into supramolecular microfibrils that serve as targeting scaffolds for connective tissue-derived growth factors such as TGF- and BMPs (Isogai et al., 2003; Sengle et al., 2008; Sengle et al., 2011; Sengle & Sakai, 2015; Zimmermann et al., 2021). By targeting and sequestering asprosin in connective tissue microenvironments, fibrillin may participate in regulating the spatiotemporal energy requirement of tissue-resident cells.

7. Outlook

Asprosin, the C-terminal propeptide of fibrillin-1, was identified as a metabolic hormone. Our central hypothesis is that the musculoskeletal system influences metabolic health by releasing bioactive fragments from muscle, cartilage, and bone in response to connective tissue disorders or exercise-induced ECM degradation. In light of this research endeavor, fibrillinopathies are considered as appropriate model disorders. For instance, the involvement of fibrillin-1 and -2 in the regulation of body fat is intuitive since most mutations in the fibrillin genes are causative for syndromes characterized by a slender habitus with little subcutaneous fat. Therefore, studying the basic mechanisms underlying asprosin and placensin bioavailability, signaling and tissue targeting has the potential to open up new therapeutic avenues not only for connective tissue disorders, but also for more common metabolic disorders.

Currently, it is not clear (1) by which mechanisms asprosin and placensin are released into different body fluids, and (2) which exact functions they may serve there. Moreover, the mechanisms of asprosin release upon exercise require further investigation. More experimental investigations are needed to uncover the underlying molecular mechanisms regulating asprosin oligomerization and cellular utilization. The mechanisms by which asprosin participates in organ crosstalk should be further investigated. It will be interesting to investigate how asprosin released from musculoskeletal tissues activates hunger-stimulating AgRP neurons in the hypothalamus or modulates metabolic functions in the liver. Thus, in the future, the gathered biochemical knowledge can be used to address new questions for clinical metabolic research.

8. References

- Aigner, T., Hambach, L., Soder, S., Schlotzer-Schrehardt, U., & Poschl, E. (2002). The C5 domain of Col6A3 is cleaved off from the Col6 fibrils immediately after secretion. *Biochem Biophys Res Commun*, 290(2), 743-748. <https://doi.org/10.1006/bbrc.2001.6227>
- Akerman, F., Lei, Z., & Rao, C. (2002). Human umbilical cord and fetal membranes co-express leptin and its receptor genes. *Gynecological endocrinology*, 16(4), 299-306.
- Akkus, G., Koyuturk, L. C., Yilmaz, M., Hancer, S., Ozercan, I. H., & Kuloglu, T. (2022). Asprosin and meteorin-like protein immunoreactivity in invasive ductal breast carcinoma stages. *Tissue Cell*, 77, 101855. <https://doi.org/10.1016/j.tice.2022.101855>
- Al Kaissi, A., Zwettler, E., Ganger, R., Schreiner, S., Klaushofer, K., & Grill, F. (2013). Musculo-skeletal abnormalities in patients with Marfan syndrome. *Clin Med Insights Arthritis Musculoskelet Disord*, 6, 1-9. <https://doi.org/10.4137/CMAMD.S10279>
- Alan, M., Gurlek, B., Yilmaz, A., Aksit, M., Aslanipour, B., Gulhan, I., Mehmet, C., & Taner, C. E. (2019). Asprosin: a novel peptide hormone related to insulin resistance in women with polycystic ovary syndrome. *Gynecol Endocrinol*, 35(3), 220-223. <https://doi.org/10.1080/09513590.2018.1512967>
- Ali, M. H., & Imperiali, B. (2005). Protein oligomerization: how and why. *Bioorg Med Chem*, 13(17), 5013-5020. <https://doi.org/10.1016/j.bmc.2005.05.037>
- Altinbas, L., Bormann, N., Lehmann, D., Jeuthe, S., Wulsten, D., Kornak, U., Robinson, P. N., Wildemann, B., & Kararigas, G. (2019). Assessment of Bones Deficient in Fibrillin-1 Microfibrils Reveals Pronounced Sex Differences. *Int J Mol Sci*, 20(23). <https://doi.org/10.3390/ijms20236059>
- Arnold, F. H., Wintrobe, P. L., Miyazaki, K., & Gershenson, A. (2001). How enzymes adapt: lessons from directed evolution. *Trends Biochem Sci*, 26(2), 100-106. [https://doi.org/10.1016/s0968-0004\(00\)01755-2](https://doi.org/10.1016/s0968-0004(00)01755-2)
- Ashworth, J. L., Kelly, V., Rock, M. J., Shuttleworth, C. A., & Kielty, C. M. (1999). Regulation of fibrillin carboxy-terminal furin processing by N-glycosylation, and association of amino- and carboxy-terminal sequences. *J Cell Sci*, 112 (Pt 22), 4163-4171. <https://doi.org/10.1242/jcs.112.22.4163>
- Ashworth, J. L., Murphy, G., Rock, M. J., Sherratt, M. J., Shapiro, S. D., Shuttleworth, C. A., & Kielty, C. M. (1999). Fibrillin degradation by matrix metalloproteinases: implications for connective tissue remodelling. *Biochem J*, 340 (Pt 1), 171-181. <https://www.ncbi.nlm.nih.gov/pubmed/10229672>
- Badillo-Suarez, P. A., Rodriguez-Cruz, M., & Nieves-Morales, X. (2017). Impact of Metabolic Hormones Secreted in Human Breast Milk on Nutritional Programming in

- Childhood Obesity. *J Mammary Gland Biol Neoplasia*, 22(3), 171-191.
<https://doi.org/10.1007/s10911-017-9382-y>
- Bai, X.-J., Fan, L.-H., He, Y., Ren, J., Xu, W., Liang, Q., Li, H.-B., Huo, J.-H., Bai, L., & Tian, H.-Y. (2016). Nicotine may affect the secretion of adipokines leptin, resistin, and visfatin through activation of KATP channel. *Nutrition*, 32(6), 645-648.
- Bauters, D., Cobbaut, M., Geys, L., Van Lint, J., Hemmeryckx, B., & Lijnen, H. R. (2017). Loss of ADAMTS5 enhances brown adipose tissue mass and promotes browning of white adipose tissue via CREB signaling. *Mol Metab*, 6(7), 715-724.
<https://doi.org/10.1016/j.molmet.2017.05.004>
- Baykus, Y., Yavuzkir, S., Ustebay, S., Ugur, K., Deniz, R., & Aydin, S. (2019). Asprosin in umbilical cord of newborns and maternal blood of gestational diabetes, preeclampsia, severe preeclampsia, intrauterine growth retardation and macrosemic fetus. *Peptides*, 120, 170132. <https://doi.org/10.1016/j.peptides.2019.170132>
- Bekhouche, M., & Colige, A. (2015). The procollagen N-proteinases ADAMTS2, 3 and 14 in pathophysiology. *Matrix Biol*, 44-46, 46-53.
<https://doi.org/10.1016/j.matbio.2015.04.001>
- Bishop, J. R., Schuksz, M., & Esko, J. D. (2007). Heparan sulphate proteoglycans fine-tune mammalian physiology. *Nature*, 446(7139), 1030-1037.
<https://doi.org/10.1038/nature05817>
- Bobadilla, M., Sainz, N., Rodriguez, J. A., Abizanda, G., Orbe, J., de Martino, A., Garcia Verdugo, J. M., Paramo, J. A., Prosper, F., & Perez-Ruiz, A. (2014). MMP-10 is required for efficient muscle regeneration in mouse models of injury and muscular dystrophy. *Stem Cells*, 32(2), 447-461. <https://doi.org/10.1002/stem.1553>
- Bostrom, P., Wu, J., Jedrychowski, M. P., Korde, A., Ye, L., Lo, J. C., Rasbach, K. A., Bostrom, E. A., Choi, J. H., Long, J. Z., Kajimura, S., Zingaretti, M. C., Vind, B. F., Tu, H., Cinti, S., Hojlund, K., Gygi, S. P., & Spiegelman, B. M. (2012). A PGC1-alpha-dependent myokine that drives brown-fat-like development of white fat and thermogenesis. *Nature*, 481(7382), 463-468. <https://doi.org/10.1038/nature10777>
- Brassart-Pasco, S., Brezillon, S., Brassart, B., Ramont, L., Oudart, J. B., & Monboisse, J. C. (2020). Tumor Microenvironment: Extracellular Matrix Alterations Influence Tumor Progression. *Front Oncol*, 10, 397. <https://doi.org/10.3389/fonc.2020.00397>
- Burrage, P. S., Mix, K. S., & Brinckerhoff, C. E. (2006). Matrix metalloproteinases: role in arthritis. *Front Biosci*, 11, 529-543. <https://www.ncbi.nlm.nih.gov/pubmed/16146751>
- Cabo-Bilbao, A., Spinelli, S., Sot, B., Agirre, J., Mechaly, A. E., Muga, A., & Guerin, D. M. (2006). Crystal structure of the temperature-sensitive and allosteric-defective chaperonin GroELE461K. *J Struct Biol*, 155(3), 482-492.
<https://doi.org/10.1016/j.jsb.2006.06.008>

- Canavan, T. P., & Simhan, H. N. (2007). Innate immune function of the human decidual cell at the maternal–fetal interface. *Journal of reproductive immunology*, 74(1-2), 46-52.
- Carta, L., Pereira, L., Arteaga-Solis, E., Lee-Arteaga, S. Y., Lenart, B., Starcher, B., Merkel, C. A., Sukoyan, M., Kerkis, A., Hazeki, N., Keene, D. R., Sakai, L. Y., & Ramirez, F. (2006). Fibrillins 1 and 2 perform partially overlapping functions during aortic development. *J Biol Chem*, 281(12), 8016-8023.
<https://doi.org/10.1074/jbc.M511599200>
- Ceylan, H. I., Saygin, O., & Ozel Turkcu, U. (2020). Assessment of acute aerobic exercise in the morning versus evening on asprosin, spexin, lipocalin-2, and insulin level in overweight/obese versus normal weight adult men. *Chronobiol Int*, 37(8), 1252-1268.
<https://doi.org/10.1080/07420528.2020.1792482>
- Chaudhry, S. S., Gazzard, J., Baldock, C., Dixon, J., Rock, M. J., Skinner, G. C., Steel, K. P., Kielty, C. M., & Dixon, M. J. (2001). Mutation of the gene encoding fibrillin-2 results in syndactyly in mice. *Hum Mol Genet*, 10(8), 835-843.
<https://doi.org/10.1093/hmg/10.8.835>
- Chazaud, B. (2020). A macrophage-derived adipokine supports skeletal muscle regeneration. *Nature Metabolism*, 2(3), 213-214.
- Chen, M., Yao, B., Yang, Q., Deng, J., Song, Y., Sui, T., Zhou, L., Yao, H., Xu, Y., Ouyang, H., Pang, D., Li, Z., & Lai, L. (2018). Truncated C-terminus of fibrillin-1 induces Marfanoid-progeroid-lipodystrophy (MPL) syndrome in rabbit. *Dis Model Mech*, 11(4). <https://doi.org/10.1242/dmm.031542>
- Chen, X., & Li, Y. (2009). Role of matrix metalloproteinases in skeletal muscle: migration, differentiation, regeneration and fibrosis. *Cell Adh Migr*, 3(4), 337-341.
<https://www.ncbi.nlm.nih.gov/pubmed/19667757>
- Cheng, J. X., & Yu, K. (2022). New Discovered Adipokines Associated with the Pathogenesis of Obesity and Type 2 Diabetes. *Diabetes Metab Syndr Obes*, 15, 2381-2389. <https://doi.org/10.2147/DMSO.S376163>
- Choi, S., Goswami, N., & Schmidt, F. (2020). Comparative Proteomic Profiling of 3T3-L1 Adipocyte Differentiation Using SILAC Quantification. *J Proteome Res*, 19(12), 4884-4900. <https://doi.org/10.1021/acs.jproteome.0c00475>
- Chojnowska, S., Baran, T., Wilińska, I., Sienicka, P., Cabaj-Wiater, I., & Knaś, M. (2018). Human saliva as a diagnostic material. *Adv Med Sci*, 63(1), 185-191.
<https://doi.org/10.1016/j.advms.2017.11.002>
- Clarke, A. W., Wise, S. G., Cain, S. A., Kielty, C. M., & Weiss, A. S. (2005). Coacervation is promoted by molecular interactions between the PF2 segment of fibrillin-1 and the domain 4 region of tropoelastin. *Biochemistry*, 44(30), 10271-10281.
<https://doi.org/10.1021/bi050530d>

- Corica, D., Aversa, T., Curro, M., Tropeano, A., Pepe, G., Alibrandi, A., Ientile, R., & Wasniewska, M. (2021). Asprosin serum levels and glucose homeostasis in children with obesity. *Cytokine*, *142*, 155477. <https://doi.org/10.1016/j.cyto.2021.155477>
- Corson, G. M., Charbonneau, N. L., Keene, D. R., & Sakai, L. Y. (2004). Differential expression of fibrillin-3 adds to microfibril variety in human and avian, but not rodent, connective tissues. *Genomics*, *83*(3), 461-472. <https://doi.org/10.1016/j.ygeno.2003.08.023>
- Coussons, P. J., Price, N. C., Kelly, S. M., Smith, B., & Sawyer, L. (1992). Factors that govern the specificity of transglutaminase-catalysed modification of proteins and peptides. *Biochem J*, *282* (Pt 3), 929-930. <https://doi.org/10.1042/bj2820929>
- Croissandeau, G., Basak, A., Seidah, N. G., Chretien, M., & Mbikay, M. (2002). Proprotein convertases are important mediators of the adipocyte differentiation of mouse 3T3-L1 cells. *J Cell Sci*, *115*(Pt 6), 1203-1211. <https://doi.org/10.1242/jcs.115.6.1203>
- Davis, G. E., Bayless, K. J., Davis, M. J., & Meininger, G. A. (2000). Regulation of tissue injury responses by the exposure of matricryptic sites within extracellular matrix molecules. *Am J Pathol*, *156*(5), 1489-1498. [https://doi.org/10.1016/S0002-9440\(10\)65020-1](https://doi.org/10.1016/S0002-9440(10)65020-1)
- Davis, M. R., Arner, E., Duffy, C. R., De Sousa, P. A., Dahlman, I., Arner, P., & Summers, K. M. (2016). Expression of FBN1 during adipogenesis: Relevance to the lipodystrophy phenotype in Marfan syndrome and related conditions. *Mol Genet Metab*, *119*(1-2), 174-185. <https://doi.org/10.1016/j.ymgme.2016.06.009>
- Deng, X., Zhao, L., Guo, C., Yang, L., Wang, D., Li, Y., Xia, H., Wang, C., Cai, Z., Li, L., Zhao, Z., & Yuan, G. (2020). Higher Serum Asprosin Level is Associated with Urinary Albumin Excretion and Renal Function in Type 2 Diabetes. *Diabetes Metab Syndr Obes*, *13*, 4341-4351. <https://doi.org/10.2147/DMSO.S283413>
- Dietz, H. C., Cutting, G. R., Pyeritz, R. E., Maslen, C. L., Sakai, L. Y., Corson, G. M., Puffenberger, E. G., Hamosh, A., Nanthakumar, E. J., Curristin, S. M., & et al. (1991). Marfan syndrome caused by a recurrent de novo missense mutation in the fibrillin gene. *Nature*, *352*(6333), 337-339. <https://doi.org/10.1038/352337a0>
- Du, C., Wang, C., Guan, X., Li, J., Du, X., Xu, Z., Li, B., Liu, Y., Fu, F., Huo, H., & Zheng, Z. (2021). Asprosin is associated with anorexia and body fat mass in cancer patients. *Support Care Cancer*, *29*(3), 1369-1375. <https://doi.org/10.1007/s00520-020-05621-8>
- Duca, L., Floquet, N., Alix, A. J., Haye, B., & Debelle, L. (2004). Elastin as a matrikine. *Crit Rev Oncol Hematol*, *49*(3), 235-244. <https://doi.org/10.1016/j.critrevonc.2003.09.007>
- Duerrschnid, C., He, Y., Wang, C., Li, C., Bournat, J. C., Romere, C., Saha, P. K., Lee, M. E., Phillips, K. J., Jain, M., Jia, P., Zhao, Z., Farias, M., Wu, Q., Milewicz, D. M., Sutton, V. R., Moore, D. D., Butte, N. F., Krashes, M. J., . . . Chopra, A. R. (2017).

- Asprosin is a centrally acting orexigenic hormone. *Nat Med*, 23(12), 1444-1453.
<https://doi.org/10.1038/nm.4432>
- Eckert, R. L., Kaartinen, M. T., Nurminskaya, M., Belkin, A. M., Colak, G., Johnson, G. V., & Mehta, K. (2014). Transglutaminase regulation of cell function. *Physiol Rev*, 94(2), 383-417. <https://doi.org/10.1152/physrev.00019.2013>
- Ehlen, H. W., Sengle, G., Klatt, A. R., Talke, A., Muller, S., Paulsson, M., & Wagener, R. (2009). Proteolytic processing causes extensive heterogeneity of tissue matrilin forms. *J Biol Chem*, 284(32), 21545-21556. <https://doi.org/10.1074/jbc.M109.016568>
- Feneck, E. M., Souza, R. B., Lewis, P. N., Hayes, S., Pereira, L. V., & Meek, K. M. (2020). Developmental abnormalities in the cornea of a mouse model for Marfan syndrome. *Exp Eye Res*, 194, 108001. <https://doi.org/10.1016/j.exer.2020.108001>
- Firner, S., Willwacher, S., de Mares, M., Bleuel, J., Zaucke, F., Bruggemann, G. P., & Niehoff, A. (2018). Effect of increased mechanical knee joint loading during running on the serum concentration of cartilage oligomeric matrix protein (COMP). *J Orthop Res*, 36(7), 1937-1946. <https://doi.org/10.1002/jor.23859>
- Firner, S., Zaucke, F., Heilig, J., de Mares, M., Willwacher, S., Bruggemann, G. P., & Niehoff, A. (2020). Impact of knee joint loading on fragmentation of serum cartilage oligomeric matrix protein. *J Orthop Res*, 38(8), 1710-1718.
<https://doi.org/10.1002/jor.24586>
- Fukuda, H., Mochizuki, S., Abe, H., Okano, H. J., Hara-Miyauchi, C., Okano, H., Yamaguchi, N., Nakayama, M., D'Armiento, J., & Okada, Y. (2011). Host-derived MMP-13 exhibits a protective role in lung metastasis of melanoma cells by local endostatin production. *Br J Cancer*, 105(10), 1615-1624.
<https://doi.org/10.1038/bjc.2011.431>
- Gaggar, A., & Weathington, N. (2016). Bioactive extracellular matrix fragments in lung health and disease. *J Clin Invest*, 126(9), 3176-3184.
<https://doi.org/10.1172/JCI83147>
- Galley, H. F., & Webster, N. R. (2004). Physiology of the endothelium. *British journal of anaesthesia*, 93(1), 105-113.
- Giampietro, P. F., Peterson, M., Schneider, R., Davis, J. G., Raggio, C., Myers, E., Burke, S. W., Boachie-Adjei, O., & Mueller, C. M. (2003). Assessment of bone mineral density in adults and children with Marfan syndrome. *Osteoporos Int*, 14(7), 559-563.
<https://doi.org/10.1007/s00198-003-1433-0>
- Goldstein, J. A., Gallagher, K., Beck, C., Kumar, R., & Gernand, A. D. (2020). Maternal-Fetal Inflammation in the Placenta and the Developmental Origins of Health and Disease. *Frontiers in immunology*, 11, 2786.

- Goodarzi, G., Setayesh, L., Fadaei, R., Khamseh, M. E., Aliakbari, F., Hosseini, J., & Moradi, N. (2021). Circulating levels of asprosin and its association with insulin resistance and renal function in patients with type 2 diabetes mellitus and diabetic nephropathy. *Mol Biol Rep*, 48(7), 5443-5450. <https://doi.org/10.1007/s11033-021-06551-2>
- Gozel, N., & Kilinc, F. (2020). Investigation of plasma asprosin and saliva levels in newly diagnosed type 2 diabetes mellitus patients treated with metformin. *Endokrynol Pol*. <https://doi.org/10.5603/EP.a2020.0059>
- Gozel, N., & Kilinc, F. (2021). Investigation of plasma asprosin and saliva levels in newly diagnosed type 2 diabetes mellitus patients treated with metformin. *Endokrynol Pol*, 72(1), 37-43. <https://doi.org/10.5603/EP.a2020.0059>
- Grahovac, J., & Wells, A. (2014). Matrikine and matricellular regulators of EGF receptor signaling on cancer cell migration and invasion. *Lab Invest*, 94(1), 31-40. <https://doi.org/10.1038/labinvest.2013.132>
- Graul-Neumann, L. M., Kienitz, T., Robinson, P. N., Baasanjav, S., Karow, B., Gillessen-Kaesbach, G., Fahsold, R., Schmidt, H., Hoffmann, K., & Passarge, E. (2010). Marfan syndrome with neonatal progeroid syndrome-like lipodystrophy associated with a novel frameshift mutation at the 3' terminus of the FBN1-gene. *Am J Med Genet A*, 152A(11), 2749-2755. <https://doi.org/10.1002/ajmg.a.33690>
- Greenhill, C. (2016). Asprosin — new hormone involved in hepatic glucose release. *Nature Reviews Endocrinology*, 12(6), 312-312. <https://doi.org/10.1038/nrendo.2016.66>
- Groener, J. B., Valkanou, A., Kender, Z., Pfeiffenberger, J., Kihm, L., Fleming, T., Nawroth, P. P., & Kopf, S. (2019). Asprosin response in hypoglycemia is not related to hypoglycemia unawareness but rather to insulin resistance in type 1 diabetes. *PLoS One*, 14(9), e0222771. <https://doi.org/10.1371/journal.pone.0222771>
- Groschl, M. (2017). Saliva: a reliable sample matrix in bioanalytics. *Bioanalysis*, 9(8), 655-668. <https://doi.org/10.4155/bio-2017-0010>
- Gueye, N. A., Mead, T. J., Koch, C. D., Biscotti, C. V., Falcone, T., & Apte, S. S. (2017). Versican Proteolysis by ADAMTS Proteases and Its Influence on Sex Steroid Receptor Expression in Uterine Leiomyoma. *J Clin Endocrinol Metab*, 102(5), 1631-1641. <https://doi.org/10.1210/jc.2016-3527>
- Hamano, Y., Zeisberg, M., Sugimoto, H., Lively, J. C., Maeshima, Y., Yang, C., Hynes, R. O., Werb, Z., Sudhakar, A., & Kalluri, R. (2003). Physiological levels of tumstatin, a fragment of collagen IV alpha3 chain, are generated by MMP-9 proteolysis and suppress angiogenesis via alphaV beta3 integrin. *Cancer Cell*, 3(6), 589-601. [https://doi.org/10.1016/s1535-6108\(03\)00133-8](https://doi.org/10.1016/s1535-6108(03)00133-8)

- Handford, P. A. (2000). Fibrillin-1, a calcium binding protein of extracellular matrix. *Biochim Biophys Acta*, 1498(2-3), 84-90. [https://doi.org/10.1016/s0167-4889\(00\)00085-9](https://doi.org/10.1016/s0167-4889(00)00085-9)
- Heinz, A., Jung, M. C., Duca, L., Sippl, W., Taddese, S., Ihling, C., Rusciani, A., Jahreis, G., Weiss, A. S., Neubert, R. H., & Schmelzer, C. E. (2010). Degradation of tropoelastin by matrix metalloproteinases--cleavage site specificities and release of matrikines. *FEBS J*, 277(8), 1939-1956. <https://doi.org/10.1111/j.1742-4658.2010.07616.x>
- Hidalgo, M., & Eckhardt, S. G. (2001). Development of Matrix Metalloproteinase Inhibitors in Cancer Therapy. *JNCI Journal of the National Cancer Institute*, 93(3), 178-193. <https://doi.org/10.1093/jnci/93.3.178>
- Hoffmann, J. G., Xie, W., & Chopra, A. R. (2020). Energy Regulation Mechanism and Therapeutic Potential of Asprosin. *Diabetes*, 69(4), 559-566. <https://doi.org/10.2337/dbi19-0009>
- Holcenberg, J. S., Schmer, G., & Teller, D. C. (1975). Biologic and physical properties of succinylated and glycosylated *Acinetobacter* glutaminase-asparaginase. *J Biol Chem*, 250(11), 4165-4170. <https://www.ncbi.nlm.nih.gov/pubmed/1126947>
- Holm Nielsen, S., Edsfeldt, A., Tengryd, C., Gustafsson, H., Shore, A. C., Natali, A., Khan, F., Genovese, F., Bengtsson, E., Karsdal, M., Leeming, D. J., Nilsson, J., & Goncalves, I. (2021). The novel collagen matrikine, endotrophin, is associated with mortality and cardiovascular events in patients with atherosclerosis. *J Intern Med*, 290(1), 179-189. <https://doi.org/10.1111/joim.13253>
- Hong, T., Li, J. Y., Wang, Y. D., Qi, X. Y., Liao, Z. Z., Bhadel, P., Ran, L., Yang, J., Yan, B., Liu, J. H., & Xiao, X. H. (2021). High Serum Asprosin Levels Are Associated with Presence of Metabolic Syndrome. *Int J Endocrinol*, 2021, 6622129. <https://doi.org/10.1155/2021/6622129>
- Honig, A., Rieger, L., Kapp, M., Dietl, J., & Kämmerer, U. (2005). Immunohistochemistry in human placental tissue—pitfalls of antigen detection. *Journal of Histochemistry & Cytochemistry*, 53(11), 1413-1420.
- Hu, Y., Xu, Y., Zheng, Y., Kang, Q., Lou, Z., Liu, Q., Chen, H., Ji, Y., Guo, L., Chen, C., Ruan, L., & Chen, J. (2021). Increased plasma asprosin levels in patients with drug-naive anorexia nervosa. *Eat Weight Disord*, 26(1), 313-321. <https://doi.org/10.1007/s40519-020-00845-3>
- Hubmacher, D., Reinhardt, D. P., Plesec, T., Schenke-Layland, K., & Apte, S. S. (2014). Human eye development is characterized by coordinated expression of fibrillin isoforms. *Invest Ophthalmol Vis Sci*, 55(12), 7934-7944. <https://doi.org/10.1167/iovs.14-15453>
- Hynes, R. O. (2009). The extracellular matrix: not just pretty fibrils. *Science*, 326(5957), 1216-1219. <https://doi.org/10.1126/science.1176009>

- Hynes RO, Y. K. (2012). *Extracellular matrix biology*. Cold Spring Harbor perspectives in biology. Cold Spring Harbor Laboratory Press, Cold Spring Harbor, NY.
- Isogai, Z., Ono, R. N., Ushiro, S., Keene, D. R., Chen, Y., Mazzieri, R., Charbonneau, N. L., Reinhardt, D. P., Rifkin, D. B., & Sakai, L. Y. (2003). Latent transforming growth factor beta-binding protein 1 interacts with fibrillin and is a microfibril-associated protein. *J Biol Chem*, 278(4), 2750-2757. <https://doi.org/10.1074/jbc.M209256200>
- Jacquinet, A., Verloes, A., Callewaert, B., Coremans, C., Coucke, P., de Paepe, A., Kornak, U., Lebrun, F., Lomet, J., Pierard, G. E., Robinson, P. N., Symoens, S., Van Maldergem, L., & Debray, F. G. (2014). Neonatal progeroid variant of Marfan syndrome with congenital lipodystrophy results from mutations at the 3' end of FBN1 gene. *Eur J Med Genet*, 57(5), 230-234. <https://doi.org/10.1016/j.ejmg.2014.02.012>
- Janoschek, R., Hoffmann, T., Morcos, Y. A. T., Sengle, G., Dotsch, J., & Hucklenbruch-Rother, E. (2020). Asprosin in pregnancy and childhood. *Mol Cell Pediatr*, 7(1), 18. <https://doi.org/10.1186/s40348-020-00110-8>
- Jayaprakash, N. G., & Surolia, A. (2017). Role of glycosylation in nucleating protein folding and stability. *Biochem J*, 474(14), 2333-2347. <https://doi.org/10.1042/BCJ20170111>
- Jensen, S. A., Aspinall, G., & Handford, P. A. (2014). C-terminal propeptide is required for fibrillin-1 secretion and blocks premature assembly through linkage to domains cbEGF41-43. *Proc Natl Acad Sci U S A*, 111(28), 10155-10160. <https://doi.org/10.1073/pnas.1401697111>
- Jiang, A., Feng, Z., Yuan, L., Zhang, Y., Li, Q., & She, Y. (2021). Effect of sodium-glucose co-transporter-2 inhibitors on the levels of serum asprosin in patients with newly diagnosed type 2 diabetes mellitus. *Diabetol Metab Syndr*, 13(1), 34. <https://doi.org/10.1186/s13098-021-00652-5>
- Jimenez-Altayo, F., Siegert, A. M., Bonorino, F., Meirelles, T., Barbera, L., Dantas, A. P., Vila, E., & Egea, G. (2017). Differences in the Thoracic Aorta by Region and Sex in a Murine Model of Marfan Syndrome. *Front Physiol*, 8, 933. <https://doi.org/10.3389/fphys.2017.00933>
- Jones, W., Rodriguez, J., & Bassnett, S. (2019). Targeted deletion of fibrillin-1 in the mouse eye results in ectopia lentis and other ocular phenotypes associated with Marfan syndrome. *Dis Model Mech*, 12(1). <https://doi.org/10.1242/dmm.037283>
- Jung, T. W., Kim, H. C., Kim, H. U., Park, T., Park, J., Kim, U., Kim, M. K., & Jeong, J. H. (2019). Asprosin attenuates insulin signaling pathway through PKCdelta-activated ER stress and inflammation in skeletal muscle. *J Cell Physiol*, 234(11), 20888-20899. <https://doi.org/10.1002/jcp.28694>
- Ke, X., Duan, L., Gong, F., Zhang, Y., Deng, K., Yao, Y., Wang, L., Pan, H., & Zhu, H. (2020). Serum Levels of Asprosin, a Novel Adipokine, Are Significantly Lowered in

Patients with Acromegaly. *Int J Endocrinol*, 2020, 8855996.

<https://doi.org/10.1155/2020/8855996>

Keene, D. R., Jordan, C. D., Reinhardt, D. P., Ridgway, C. C., Ono, R. N., Corson, G. M., Fairhurst, M., Sussman, M. D., Memoli, V. A., & Sakai, L. Y. (1997). Fibrillin-1 in human cartilage: developmental expression and formation of special banded fibers. *J Histochem Cytochem*, 45(8), 1069-1082.

<https://doi.org/10.1177/002215549704500805>

Kielty, C. M., Wess, T. J., Haston, L., Ashworth, J. L., Sherratt, M. J., & Shuttleworth, C. A. (2002). Fibrillin-rich microfibrils: elastic biopolymers of the extracellular matrix. *J Muscle Res Cell Motil*, 23(5-6), 581-596.

<https://www.ncbi.nlm.nih.gov/pubmed/12785107>

Kim, J., & Raushel, F. M. (2001). Allosteric control of the oligomerization of carbamoyl phosphate synthetase from *Escherichia coli*. *Biochemistry*, 40(37), 11030-11036.

<https://doi.org/10.1021/bi011121u>

Ko, J. R., Seo, D. Y., Kim, T. N., Park, S. H., Kwak, H. B., Ko, K. S., Rhee, B. D., & Han, J. (2019). Aerobic Exercise Training Decreases Hepatic Asprosin in Diabetic Rats. *J Clin Med*, 8(5).

<https://doi.org/10.3390/jcm8050666>

Kocaman, N., & Artas, G. (2020). Can novel adipokines, asprosin and meteorin-like, be biomarkers for malignant mesothelioma? *Biotech Histochem*, 95(3), 171-175.

<https://doi.org/10.1080/10520295.2019.1656344>

Kriz, W., Elger, M., Lemley, K., & Sakai, T. (1990). Structure of the glomerular mesangium: a biomechanical interpretation. *Kidney Int Suppl*, 30, S2-9.

<https://www.ncbi.nlm.nih.gov/pubmed/2259073>

Kuno, K., Okada, Y., Kawashima, H., Nakamura, H., Miyasaka, M., Ohno, H., & Matsushima, K. (2000). ADAMTS-1 cleaves a cartilage proteoglycan, aggrecan.

FEBS Lett, 478(3), 241-245. <https://www.ncbi.nlm.nih.gov/pubmed/10930576>

Kutz, W. E., Wang, L. W., Bader, H. L., Majors, A. K., Iwata, K., Traboulsi, E. I., Sakai, L. Y., Keene, D. R., & Apte, S. S. (2011). ADAMTS10 protein interacts with fibrillin-1 and promotes its deposition in extracellular matrix of cultured fibroblasts. *J Biol Chem*, 286(19), 17156-17167.

<https://doi.org/10.1074/jbc.M111.231571>

Lee, T., Yun, S., Jeong, J. H., & Jung, T. W. (2019). Asprosin impairs insulin secretion in response to glucose and viability through TLR4/JNK-mediated inflammation. *Mol Cell Endocrinol*, 486, 96-104.

<https://doi.org/10.1016/j.mce.2019.03.001>

Lemaire, R., Bayle, J., & Lafyatis, R. (2006). Fibrillin in Marfan syndrome and tight skin mice provides new insights into transforming growth factor-beta regulation and systemic sclerosis. *Curr Opin Rheumatol*, 18(6), 582-587.

<https://doi.org/10.1097/01.bor.0000245719.64393.57>

- Li, E., Shan, H., Chen, L., Long, A., Zhang, Y., Liu, Y., Jia, L., Wei, F., Han, J., Li, T., Liu, X., Deng, H., & Wang, Y. (2019). OLF734 Mediates Glucose Metabolism as a Receptor of Asprosin. *Cell Metab*, 30(2), 319-328 e318. <https://doi.org/10.1016/j.cmet.2019.05.022>
- Lis, H., & Sharon, N. (1993). Protein glycosylation. Structural and functional aspects. *Eur J Biochem*, 218(1), 1-27. <https://doi.org/10.1111/j.1432-1033.1993.tb18347.x>
- Liu, L. J., Kang, Y. R., & Xiao, Y. F. (2021). Increased asprosin is associated with non-alcoholic fatty liver disease in children with obesity. *World J Pediatr*, 17(4), 394-399. <https://doi.org/10.1007/s12519-021-00444-x>
- Lo Presti, R., Hopps, E., & Caimi, G. (2017). Gelatinases and physical exercise: A systematic review of evidence from human studies. *Medicine (Baltimore)*, 96(37), e8072. <https://doi.org/10.1097/MD.00000000000008072>
- Loeys, B. L., Gerber, E. E., Riegert-Johnson, D., Iqbal, S., Whiteman, P., McConnell, V., Chillakuri, C. R., Macaya, D., Coucke, P. J., De Paepe, A., Judge, D. P., Wigley, F., Davis, E. C., Mardon, H. J., Handford, P., Keene, D. R., Sakai, L. Y., & Dietz, H. C. (2010). Mutations in fibrillin-1 cause congenital scleroderma: stiff skin syndrome. *Sci Transl Med*, 2(23), 23ra20. <https://doi.org/10.1126/scitranslmed.3000488>
- Long, W., Xie, X., Du, C., Zhao, Y., Zhang, C., Zhan, D., Li, Z., Ning, Q., & Luo, X. (2019). Decreased Circulating Levels of Asprosin in Obese Children. *Horm Res Paediatr*, 91(4), 271-277. <https://doi.org/10.1159/000500523>
- Lonnqvist, L., Reinhardt, D., Sakai, L., & Peltonen, L. (1998). Evidence for furin-type activity-mediated C-terminal processing of profibrillin-1 and interference in the processing by certain mutations. *Hum Mol Genet*, 7(13), 2039-2044. <https://doi.org/10.1093/hmg/7.13.2039>
- Lu, P., Takai, K., Weaver, V. M., & Werb, Z. (2011). Extracellular matrix degradation and remodeling in development and disease. *Cold Spring Harb Perspect Biol*, 3(12). <https://doi.org/10.1101/cshperspect.a005058>
- Luis, C., Fernandes, R., Soares, R., & von Hafe, P. (2020). A state of the art review on the novel mediator asprosin in the metabolic syndrome. *Porto Biomed J*, 5(6), e108. <https://doi.org/10.1097/j.pbj.0000000000000108>
- Maeshima, Y., Sudhakar, A., Lively, J. C., Ueki, K., Kharbanda, S., Kahn, C. R., Sonenberg, N., Hynes, R. O., & Kalluri, R. (2002). Tumstatin, an endothelial cell-specific inhibitor of protein synthesis. *Science*, 295(5552), 140-143. <https://doi.org/10.1126/science.1065298>
- Malinda, K. M., Wysocki, A. B., Koblinski, J. E., Kleinman, H. K., & Ponce, M. L. (2008). Angiogenic laminin-derived peptides stimulate wound healing. *The International Journal of Biochemistry & Cell Biology*, 40(12), 2771-2780. <https://doi.org/10.1016/j.biocel.2008.05.025>

- Maquart, F. X., Pasco, S., Ramont, L., Hornebeck, W., & Monboisse, J. C. (2004). An introduction to matrikines: extracellular matrix-derived peptides which regulate cell activity. Implication in tumor invasion. *Crit Rev Oncol Hematol*, 49(3), 199-202. <https://doi.org/10.1016/j.critrevonc.2003.06.007>
- Maquart, F. X., Simeon, A., Pasco, S., & Monboisse, J. C. (1999). [Regulation of cell activity by the extracellular matrix: the concept of matrikines]. *J Soc Biol*, 193(4-5), 423-428. <https://www.ncbi.nlm.nih.gov/pubmed/10689625> (Regulation de l'activite cellulaire par la matrice extracelulaire: le concept de matrikines.)
- Mariko, B., Pezet, M., Escoubet, B., Bouillot, S., Andrieu, J. P., Starcher, B., Quaglino, D., Jacob, M. P., Huber, P., Ramirez, F., & Faury, G. (2011). Fibrillin-1 genetic deficiency leads to pathological ageing of arteries in mice. *J Pathol*, 224(1), 33-44. <https://doi.org/10.1002/path.2840>
- Mariman, E. C., & Wang, P. (2010). Adipocyte extracellular matrix composition, dynamics and role in obesity. *Cell Mol Life Sci*, 67(8), 1277-1292. <https://doi.org/10.1007/s00018-010-0263-4>
- Mecham, R. (2011). *The extracellular matrix: an overview*.
- Medley, T. L., Cole, T. J., Gatzka, C. D., Wang, W. Y., Dart, A. M., & Kingwell, B. A. (2002). Fibrillin-1 genotype is associated with aortic stiffness and disease severity in patients with coronary artery disease. *Circulation*, 105(7), 810-815. <https://doi.org/10.1161/hc0702.104129>
- Milewicz, D. M., Grossfield, J., Cao, S. N., Kielty, C., Covitz, W., & Jewett, T. (1995). A mutation in FBN1 disrupts profibrillin processing and results in isolated skeletal features of the Marfan syndrome. *J Clin Invest*, 95(5), 2373-2378. <https://doi.org/10.1172/JCI117930>
- Milewicz, D. M., Pyeritz, R. E., Crawford, E. S., & Byers, P. H. (1992). Marfan syndrome: defective synthesis, secretion, and extracellular matrix formation of fibrillin by cultured dermal fibroblasts. *J Clin Invest*, 89(1), 79-86. <https://doi.org/10.1172/JCI115589>
- Mishra, I., Duerschmid, C., Ku, Z., He, Y., Xie, W., Silva, E. S., Hoffman, J., Xin, W., Zhang, N., Xu, Y., An, Z., & Chopra, A. R. (2021). Asprosin-neutralizing antibodies as a treatment for metabolic syndrome. *Elife*, 10. <https://doi.org/10.7554/eLife.63784>
- Miyata, G., Meguid, M. M., Fetissoff, S. O., Torelli, G. F., & Kim, H.-J. (1999). Nicotine's effect on hypothalamic neurotransmitters and appetite regulation. *Surgery*, 126(2), 255-263.
- Mongiati, M., Sweeney, S. M., San Antonio, J. D., Fu, J., & Iozzo, R. V. (2003). Endorepellin, a Novel Inhibitor of Angiogenesis Derived from the C Terminus of Perlecan. *Journal of Biological Chemistry*, 278(6), 4238-4249. <https://doi.org/10.1074/jbc.m210445200>

- Mora, P., Rubio, V., & Cervera, J. (2002). Mechanism of oligomerization of Escherichia coli carbamoyl phosphate synthetase and modulation by the allosteric effectors. A site-directed mutagenesis study. *FEBS Lett*, *511*(1-3), 6-10. [https://doi.org/10.1016/s0014-5793\(01\)03246-x](https://doi.org/10.1016/s0014-5793(01)03246-x)
- Morcos, Y., Luetke, S., Tenbieg, A., Hanisch, F. G., Prymachuk, G., Piekarek, N., Hoffmann, T., Keller, T., Janoschek, R., Niehoff, A., Zaucke, F., Dotsch, J., Hucklenbruch-Rother, E., & Sengle, G. (2022). Sensitive asprosin detection in clinical samples reveals serum/saliva correlation and indicates cartilage as source for serum asprosin. *Sci Rep*, *12*(1), 1340. <https://doi.org/10.1038/s41598-022-05060-x>
- Morcos, Y. A. T., Lütke, S., Tenbieg, A., Hanisch, F.G., Prymachuk, G., Piekarek, N., Hoffmann, T., Keller, T., Janoschek, R., Niehoff, A., Zaucke, F., Dötsch, J., Hucklenbruch-Rother, E., Sengle, G. (2021). Sensitive asprosin detection in clinical samples reveals serum/ saliva correlation and indicates cartilage as source for serum asprosin. *Sci Rep*.
- Muthu, M. L., & Reinhardt, D. P. (2020). Fibrillin-1 and fibrillin-1-derived asprosin in adipose tissue function and metabolic disorders. *J Cell Commun Signal*, *14*(2), 159-173. <https://doi.org/10.1007/s12079-020-00566-3>
- Naiemian, S., Naeemipour, M., Zarei, M., Lari Najafi, M., Gohari, A., Behroozikhah, M. R., Heydari, H., & Miri, M. (2020). Serum concentration of asprosin in new-onset type 2 diabetes. *Diabetol Metab Syndr*, *12*, 65. <https://doi.org/10.1186/s13098-020-00564-w>
- Nam, H., Hong, S. S., Jung, K. H., Kang, S., Park, M. S., Kang, S., Kim, H. S., Mai, V. H., Kim, J., Lee, H., Lee, W., Suh, Y. J., Lim, J. H., Kim, S. Y., Kim, S. C., Kim, S. H., & Park, S. (2022). A Serum Marker for Early Pancreatic Cancer With a Possible Link to Diabetes. *J Natl Cancer Inst*, *114*(2), 228-234. <https://doi.org/10.1093/jnci/djab191>
- Nelson, A. R., Fingleton, B., Rothenberg, M. L., & Matrisian, L. M. (2000). Matrix Metalloproteinases: Biologic Activity and Clinical Implications. *Journal of Clinical Oncology*, *18*(5), 1135-1135. <https://doi.org/10.1200/jco.2000.18.5.1135>
- Nistala, H., Lee-Arteaga, S., Smaldone, S., Siciliano, G., Carta, L., Ono, R. N., Sengle, G., Arteaga-Solis, E., Levasseur, R., Ducy, P., Sakai, L. Y., Karsenty, G., & Ramirez, F. (2010). Fibrillin-1 and -2 differentially modulate endogenous TGF-beta and BMP bioavailability during bone formation. *J Cell Biol*, *190*(6), 1107-1121. <https://doi.org/10.1083/jcb.201003089>
- O'Reilly, M. S., Boehm, T., Shing, Y., Fukai, N., Vasios, G., Lane, W. S., Flynn, E., Birkhead, J. R., Olsen, B. R., & Folkman, J. (1997). Endostatin: An Endogenous Inhibitor of Angiogenesis and Tumor Growth. *Cell*, *88*(2), 277-285. [https://doi.org/10.1016/s0092-8674\(00\)81848-6](https://doi.org/10.1016/s0092-8674(00)81848-6)
- O'Reilly, M. S., Boehm, T., Shing, Y., Fukai, N., Vasios, G., Lane, W. S., Flynn, E., Birkhead, J. R., Olsen, B. R., & Folkman, J. (1997). Endostatin: an endogenous

- inhibitor of angiogenesis and tumor growth. *Cell*, 88(2), 277-285.
[https://doi.org/10.1016/s0092-8674\(00\)81848-6](https://doi.org/10.1016/s0092-8674(00)81848-6)
- Ono, S. (2007). Mechanism of depolymerization and severing of actin filaments and its significance in cytoskeletal dynamics. *Int Rev Cytol*, 258, 1-82.
[https://doi.org/10.1016/S0074-7696\(07\)58001-0](https://doi.org/10.1016/S0074-7696(07)58001-0)
- Oudart, J. B., Brassart-Pasco, S., Vautrin, A., Sellier, C., Machado, C., Dupont-Deshorgue, A., Brassart, B., Baud, S., Dauchez, M., Monboisse, J. C., Harakat, D., Maquart, F. X., & Ramont, L. (2015). Plasmin releases the anti-tumor peptide from the NC1 domain of collagen XIX. *Oncotarget*, 6(6), 3656-3668.
<https://doi.org/10.18632/oncotarget.2849>
- Oudart, J. B., Villemin, M., Brassart, B., Sellier, C., Terryn, C., Dupont-Deshorgue, A., Monboisse, J. C., Maquart, F. X., Ramont, L., & Brassart-Pasco, S. (2021). F4, a collagen XIX-derived peptide, inhibits tumor angiogenesis through alphavbeta3 and alpha5beta1 integrin interaction. *Cell Adh Migr*, 15(1), 215-223.
<https://doi.org/10.1080/19336918.2021.1951425>
- Papadas, A., Arauz, G., Cicala, A., Wiesner, J., & Asimakopoulos, F. (2020). Versican and Versican-matrikines in Cancer Progression, Inflammation, and Immunity. *J Histochem Cytochem*, 68(12), 871-885. <https://doi.org/10.1369/0022155420937098>
- Park, J., & Scherer, P. E. (2012a). Adipocyte-derived endotrophin promotes malignant tumor progression. *J Clin Invest*, 122(11), 4243-4256. <https://doi.org/10.1172/JCI63930>
- Park, J., & Scherer, P. E. (2012b). Endotrophin - a novel factor linking obesity with aggressive tumor growth. *Oncotarget*, 3(12), 1487-1488.
<https://doi.org/10.18632/oncotarget.796>
- Parks, W. C., Mecham, R. P., & ScienceDirect. (1998). *Matrix metalloproteinases*. Academic Press.
- Parks, W. C., Parks, W. C., Mecham, R., & SpringerLink. (2011). *Extracellular Matrix Degradation* (1st 2011. ed.). Springer Berlin Heidelberg : Imprint: Springer.
- Passarge, E., Robinson, P. N., & Graul-Neumann, L. M. (2016). Marfanoid-progeroid-lipodystrophy syndrome: a newly recognized fibrillinopathy. *Eur J Hum Genet*, 24(9), 1244-1247. <https://doi.org/10.1038/ejhg.2016.6>
- Pérez-Pérez, A., Guadix, P., Maymó, J., Dueñas, J. L., Varone, C., Fernández-Sánchez, M., & Sanchez-Margalet, V. (2016). Insulin and leptin signaling in placenta from gestational diabetic subjects. *Hormone and Metabolic Research*, 48(01), 62-69.
- Piha-Gossack, A., Sossin, W., & Reinhardt, D. P. (2012). The evolution of extracellular fibrillins and their functional domains. *PLoS One*, 7(3), e33560.
<https://doi.org/10.1371/journal.pone.0033560>

- Ponce, M. L., Hibino, S., Lebioda, A. M., Mochizuki, M., Nomizu, M., & Kleinman, H. K. (2003). Identification of a potent peptide antagonist to an active laminin-1 sequence that blocks angiogenesis and tumor growth. *Cancer Res*, 63(16), 5060-5064. <https://www.ncbi.nlm.nih.gov/pubmed/12941835>
- Putnam, E. A., Zhang, H., Ramirez, F., & Milewicz, D. M. (1995). Fibrillin-2 (FBN2) mutations result in the Marfan-like disorder, congenital contractural arachnodactyly. *Nat Genet*, 11(4), 456-458. <https://doi.org/10.1038/ng1295-456>
- Qian, R. Q., & Glanville, R. W. (1997). Alignment of fibrillin molecules in elastic microfibrils is defined by transglutaminase-derived cross-links. *Biochemistry*, 36(50), 15841-15847. <https://doi.org/10.1021/bi971036f>
- Raviola, G. (1971). The fine structure of the ciliary zonule and ciliary epithelium. With special regard to the organization and insertion of the zonular fibrils. *Invest Ophthalmol*, 10(11), 851-869. <https://www.ncbi.nlm.nih.gov/pubmed/4107306>
- Renard, M., Muino-Mosquera, L., Manalo, E. C., Tufa, S., Carlson, E. J., Keene, D. R., De Backer, J., & Sakai, L. Y. (2017). Sex, pregnancy and aortic disease in Marfan syndrome. *PLoS One*, 12(7), e0181166. <https://doi.org/10.1371/journal.pone.0181166>
- Rezk, M. Y., Elkattawy, H. A., & Fouad, R. A. (2020). Plasma asprosin levels changes in pregnant and non-pregnant rats with and without gestational diabetes. *International Journal of Medical Research & Health Sciences*, 9(3), 54-63.
- Ricard-Blum, S., & Salza, R. (2014). Matricryptins and matrikines: biologically active fragments of the extracellular matrix. *Experimental Dermatology*, 23(7), 457-463. <https://doi.org/10.1111/exd.12435>
- Ritty, T. M., Broekelmann, T., Tisdale, C., Milewicz, D. M., & Mecham, R. P. (1999). Processing of the fibrillin-1 carboxyl-terminal domain. *J Biol Chem*, 274(13), 8933-8940. <https://doi.org/10.1074/jbc.274.13.8933>
- Robbesom, A. A., Koenders, M. M., Smits, N. C., Hafmans, T., Versteeg, E. M., Bulten, J., Veerkamp, J. H., Dekhuijzen, P. N., & van Kuppevelt, T. H. (2008). Aberrant fibrillin-1 expression in early emphysematous human lung: a proposed predisposition for emphysema. *Mod Pathol*, 21(3), 297-307. <https://doi.org/10.1038/modpathol.3801004>
- Roca-Rivada, A., Castela, C., Senin, L. L., Landrove, M. O., Baltar, J., Belen Crujeiras, A., Seoane, L. M., Casanueva, F. F., & Pardo, M. (2013). FNDC5/irisin is not only a myokine but also an adipokine. *PLoS One*, 8(4), e60563. <https://doi.org/10.1371/journal.pone.0060563>
- Rock, M. J., Cain, S. A., Freeman, L. J., Morgan, A., Mellody, K., Marson, A., Shuttleworth, C. A., Weiss, A. S., & Kielty, C. M. (2004). Molecular basis of elastic fiber formation. Critical interactions and a tropoelastin-fibrillin-1 cross-link. *J Biol Chem*, 279(22), 23748-23758. <https://doi.org/10.1074/jbc.M400212200>

- Romere, C., Duerrschmid, C., Bournat, J., Constable, P., Jain, M., Xia, F., Saha, P. K., Del Solar, M., Zhu, B., York, B., Sarkar, P., Rendon, D. A., Gaber, M. W., LeMaire, S. A., Coselli, J. S., Milewicz, D. M., Sutton, V. R., Butte, N. F., Moore, D. D., & Chopra, A. R. (2016). Asprosin, a Fasting-Induced Glucogenic Protein Hormone. *Cell*, *165*(3), 566-579. <https://doi.org/10.1016/j.cell.2016.02.063>
- Rossin, F., D'Eletto, M., Falasca, L., Sepe, S., Cocco, S., Fimia, G. M., Campanella, M., Mastroberardino, P. G., Farrace, M. G., & Piacentini, M. (2015). Transglutaminase 2 ablation leads to mitophagy impairment associated with a metabolic shift towards aerobic glycolysis. *Cell Death Differ*, *22*(3), 408-418. <https://doi.org/10.1038/cdd.2014.106>
- Sabatier, L., Miosge, N., Hubmacher, D., Lin, G., Davis, E. C., & Reinhardt, D. P. (2011). Fibrillin-3 expression in human development. *Matrix Biology*, *30*(1), 43-52. <https://doi.org/10.1016/j.matbio.2010.10.003>
- Sakai, L. Y., Keene, D. R., & Engvall, E. (1986). Fibrillin, a new 350-kD glycoprotein, is a component of extracellular microfibrils. *J Cell Biol*, *103*(6 Pt 1), 2499-2509. <https://www.ncbi.nlm.nih.gov/pubmed/3536967>
- Sakai, L. Y., Keene, D. R., Renard, M., & De Backer, J. (2016). FBN1: The disease-causing gene for Marfan syndrome and other genetic disorders. *Gene*, *591*(1), 279-291. <https://doi.org/10.1016/j.gene.2016.07.033>
- Sanchis-Gomar, F., Lippi, G., Mayero, S., Perez-Quilis, C., & Garcia-Gimenez, J. L. (2012). Irisin: a new potential hormonal target for the treatment of obesity and type 2 diabetes. *J Diabetes*, *4*(3), 196. <https://doi.org/10.1111/j.1753-0407.2012.00194.x>
- Sanigorski, A., Fahey, R., Cameron-Smith, D., & Collier, G. (2002). Nicotine treatment decreases food intake and body weight via a leptin-independent pathway in *Psammomys obesus*. *Diabetes, obesity and metabolism*, *4*(5), 346-350.
- Schulthess, F. T., Paroni, F., Sauter, N. S., Shu, L., Ribaux, P., Haataja, L., Strieter, R. M., Oberholzer, J., King, C. C., & Maedler, K. (2009). CXCL10 impairs beta cell function and viability in diabetes through TLR4 signaling. *Cell Metab*, *9*(2), 125-139. <https://doi.org/10.1016/j.cmet.2009.01.003>
- Sengle, G., Carlberg, V., Tufa, S. F., Charbonneau, N. L., Smaldone, S., Carlson, E. J., Ramirez, F., Keene, D. R., & Sakai, L. Y. (2015). Abnormal Activation of BMP Signaling Causes Myopathy in Fbn2 Null Mice. *PLoS Genet*, *11*(6), e1005340. <https://doi.org/10.1371/journal.pgen.1005340>
- Sengle, G., Charbonneau, N. L., Ono, R. N., Sasaki, T., Alvarez, J., Keene, D. R., Bachinger, H. P., & Sakai, L. Y. (2008). Targeting of bone morphogenetic protein growth factor complexes to fibrillin. *J Biol Chem*, *283*(20), 13874-13888. <https://doi.org/10.1074/jbc.M707820200>

- Sengle, G., Ono, R. N., Sasaki, T., & Sakai, L. Y. (2011). Prodomains of transforming growth factor beta (TGFbeta) superfamily members specify different functions: extracellular matrix interactions and growth factor bioavailability. *J Biol Chem*, 286(7), 5087-5099. <https://doi.org/10.1074/jbc.M110.188615>
- Sengle, G., & Sakai, L. Y. (2015). The fibrillin microfibril scaffold: A niche for growth factors and mechanosensation? *Matrix Biol*, 47, 3-12. <https://doi.org/10.1016/j.matbio.2015.05.002>
- Sengle, G., Tsutsui, K., Keene, D. R., Tufa, S. F., Carlson, E. J., Charbonneau, N. L., Ono, R. N., Sasaki, T., Wirtz, M. K., Samples, J. R., Fessler, L. I., Fessler, J. H., Sekiguchi, K., Hayflick, S. J., & Sakai, L. Y. (2012). Microenvironmental regulation by fibrillin-1. *PLoS Genet*, 8(1), e1002425. <https://doi.org/10.1371/journal.pgen.1002425>
- Simeon, A., Monier, F., Emonard, H., Wegrowski, Y., Bellon, G., Monboisse, J. C., Gillery, P., Hornebeck, W., & Maquart, F. X. (1999). Fibroblast-cytokine-extracellular matrix interactions in wound repair. *Curr Top Pathol*, 93, 95-101. https://doi.org/10.1007/978-3-642-58456-5_10
- Sivaraman, K., & Shanthi, C. (2018). Matrikines for therapeutic and biomedical applications. *Life Sci*, 214, 22-33. <https://doi.org/10.1016/j.lfs.2018.10.056>
- Smaldone, S., Clayton, N. P., del Solar, M., Pascual, G., Cheng, S. H., Wentworth, B. M., Schaffler, M. B., & Ramirez, F. (2016). Fibrillin-1 Regulates Skeletal Stem Cell Differentiation by Modulating TGFbeta Activity Within the Marrow Niche. *J Bone Miner Res*, 31(1), 86-97. <https://doi.org/10.1002/jbmr.2598>
- Stanton, H., Melrose, J., Little, C. B., & Fosang, A. J. (2011). Proteoglycan degradation by the ADAMTS family of proteinases. *Biochim Biophys Acta*, 1812(12), 1616-1629. <https://doi.org/10.1016/j.bbadis.2011.08.009>
- Staunstrup, L. M., Bager, C. L., Frederiksen, P., Helge, J. W., Brunak, S., Christiansen, C., & Karsdal, M. (2021). Endotrophin is associated with chronic multimorbidity and all-cause mortality in a cohort of elderly women. *EBioMedicine*, 68, 103391. <https://doi.org/10.1016/j.ebiom.2021.103391>
- Stöcker, W., Grams, F., Reinemer, P., Bode, W., Baumann, U., Gomis-Rüth, F.-X., & McKay, D. B. (2008). The metzincins - Topological and sequential relations between the astacins, adamalysins, serralysins, and matrixins (collagenases) define a super family of zinc-peptidases. *Protein Science*, 4(5), 823-840. <https://doi.org/10.1002/pro.5560040502>
- Summers, K. M., Nataatmadja, M., Xu, D., West, M. J., McGill, J. J., Whight, C., Colley, A., & Ades, L. C. (2005). Histopathology and fibrillin-1 distribution in severe early onset Marfan syndrome. *Am J Med Genet A*, 139(1), 2-8. <https://doi.org/10.1002/ajmg.a.30981>

- Sun, K., Park, J., Kim, M., & Scherer, P. E. (2017). Endotrophin, a multifaceted player in metabolic dysregulation and cancer progression, is a predictive biomarker for the response to PPARgamma agonist treatment. *Diabetologia*, *60*(1), 24-29. <https://doi.org/10.1007/s00125-016-4130-1>
- Sunnetci Silistre, E., & Hatipogl, H. U. (2020). Increased serum circulating asprosin levels in children with obesity. *Pediatr Int*, *62*(4), 467-476. <https://doi.org/10.1111/ped.14176>
- Takenouchi, T., Hida, M., Sakamoto, Y., Torii, C., Kosaki, R., Takahashi, T., & Kosaki, K. (2013). Severe congenital lipodystrophy and a progeroid appearance: Mutation in the penultimate exon of FBN1 causing a recognizable phenotype. *Am J Med Genet A*, *161A*(12), 3057-3062. <https://doi.org/10.1002/ajmg.a.36157>
- Tanaka, Y., Tsumoto, K., Yasutake, Y., Umetsu, M., Yao, M., Fukada, H., Tanaka, I., & Kumagai, I. (2004). How oligomerization contributes to the thermostability of an archaeon protein. Protein L-isoaspartyl-O-methyltransferase from *Sulfolobus tokodaii*. *J Biol Chem*, *279*(31), 32957-32967. <https://doi.org/10.1074/jbc.M404405200>
- Tarafdar, P. K., Vedantam, L. V., Sankhala, R. S., Purushotham, P., Podile, A. R., & Swamy, M. J. (2014). Oligomerization, conformational stability and thermal unfolding of Harpin, HrpZPss and its hypersensitive response-inducing c-terminal fragment, C-214-HrpZPss. *PLoS One*, *9*(12), e109871. <https://doi.org/10.1371/journal.pone.0109871>
- Tun, M. H., Borg, B., Godfrey, M., Hadley-Miller, N., & Chan, E. D. (2021). Respiratory manifestations of Marfan syndrome: a narrative review. *J Thorac Dis*, *13*(10), 6012-6025. <https://doi.org/10.21037/jtd-21-1064>
- Turner, P. M., & Lorand, L. (1989). Complexation of fibronectin with tissue transglutaminase. *Biochemistry*, *28*(2), 628-635. <https://doi.org/10.1021/bi00428a032>
- Ugur, K., & Aydin, S. (2019). Saliva and Blood Asprosin Hormone Concentration Associated with Obesity. *Int J Endocrinol*, *2019*, 2521096. <https://doi.org/10.1155/2019/2521096>
- Ugur, K., Erman, F., Turkoglu, S., Aydin, Y., Aksoy, A., Lale, A., Karagoz, Z. K., Ugur, I., Akkoc, R. F., & Yalniz, M. (2022). Asprosin, visfatin and subfatin as new biomarkers of obesity and metabolic syndrome. *Eur Rev Med Pharmacol Sci*, *26*(6), 2124-2133. https://doi.org/10.26355/eurev_202203_28360
- Vallet, S. D., & Ricard-Blum, S. (2019). Lysyl oxidases: from enzyme activity to extracellular matrix cross-links. *Essays Biochem*, *63*(3), 349-364. <https://doi.org/10.1042/EBC20180050>
- Vannuccini, S., Clifton, V. L., Fraser, I. S., Taylor, H. S., Critchley, H., Giudice, L. C., & Petraglia, F. (2016). Infertility and reproductive disorders: impact of hormonal and inflammatory mechanisms on pregnancy outcome. *Hum Reprod Update*, *22*(1), 104-115. <https://doi.org/10.1093/humupd/dmv044>

- Vegarud, G., & Christnsen, T. B. (1975). Glycosylation of Proteins: a new method of enzyme stabilization. *Biotechnol Bioeng*, *17*(9), 1391-1397. <https://doi.org/10.1002/bit.260170918>
- Veidal, S. S., Karsdal, M. A., Vassiliadis, E., Nawrocki, A., Larsen, M. R., Nguyen, Q. H., Hagglund, P., Luo, Y., Zheng, Q., Vainer, B., & Leeming, D. J. (2011). MMP mediated degradation of type VI collagen is highly associated with liver fibrosis--identification and validation of a novel biochemical marker assay. *PLoS One*, *6*(9), e24753. <https://doi.org/10.1371/journal.pone.0024753>
- Veillard, F., Saidi, A., Burden, R. E., Scott, C. J., Gillet, L., Lecaille, F., & Lalmanach, G. (2011). Cysteine cathepsins S and L modulate anti-angiogenic activities of human endostatin. *J Biol Chem*, *286*(43), 37158-37167. <https://doi.org/10.1074/jbc.M111.284869>
- Wagenseil, J. E., & Mecham, R. P. (2007). New insights into elastic fiber assembly. *Birth Defects Res C Embryo Today*, *81*(4), 229-240. <https://doi.org/10.1002/bdrc.20111>
- Wang, B., Sun, J., Kitamoto, S., Yang, M., Grubb, A., Chapman, H. A., Kalluri, R., & Shi, G. P. (2006). Cathepsin S controls angiogenesis and tumor growth via matrix-derived angiogenic factors. *J Biol Chem*, *281*(9), 6020-6029. <https://doi.org/10.1074/jbc.M509134200>
- Wang, M., Yin, C., Wang, L., Liu, Y., Li, H., Li, M., Yi, X., & Xiao, Y. (2019). Serum Asprosin Concentrations Are Increased and Associated with Insulin Resistance in Children with Obesity. *Ann Nutr Metab*, *75*(4), 205-212. <https://doi.org/10.1159/000503808>
- Wang, R., Lin, P., Sun, H., & Hu, W. (2021). Increased serum asprosin is correlated with diabetic nephropathy. *Diabetol Metab Syndr*, *13*(1), 51. <https://doi.org/10.1186/s13098-021-00668-x>
- Wang, Y., Qu, H., Xiong, X., Qiu, Y., Liao, Y., Chen, Y., Zheng, Y., & Zheng, H. (2018). Plasma Asprosin Concentrations Are Increased in Individuals with Glucose Dysregulation and Correlated with Insulin Resistance and First-Phase Insulin Secretion. *Mediators Inflamm*, *2018*, 9471583. <https://doi.org/10.1155/2018/9471583>
- Watson, R. E. B., Griffiths, C. E. M., Craven, N. M., Shuttleworth, C. A., & Kielty, C. M. (1999). Fibrillin-Rich Microfibrils are Reduced in Photoaged Skin. Distribution at the Dermal-Epidermal Junction. *Journal of Investigative Dermatology*, *112*(5), 782-787. <https://doi.org/10.1046/j.1523-1747.1999.00562.x>
- Weathington, N. M., van Houwelingen, A. H., Noerager, B. D., Jackson, P. L., Kraneveld, A. D., Galin, F. S., Folkerts, G., Nijkamp, F. P., & Blalock, J. E. (2006). A novel peptide CXCR ligand derived from extracellular matrix degradation during airway inflammation. *Nat Med*, *12*(3), 317-323. <https://doi.org/10.1038/nm1361>

- Wen, M. S., Wang, C. Y., Yeh, J. K., Chen, C. C., Tsai, M. L., Ho, M. Y., Hung, K. C., & Hsieh, I. C. (2020). The role of Asprosin in patients with dilated cardiomyopathy. *BMC Cardiovasc Disord*, 20(1), 402. <https://doi.org/10.1186/s12872-020-01680-1>
- Wiecek, M., Szymura, J., Maciejczyk, M., Kantorowicz, M., & Szygula, Z. (2018). Acute Anaerobic Exercise Affects the Secretion of Asprosin, Irisin, and Other Cytokines - A Comparison Between Sexes. *Front Physiol*, 9, 1782. <https://doi.org/10.3389/fphys.2018.01782>
- Wintrade, P. L., & Arnold, F. H. (2000). Temperature adaptation of enzymes: lessons from laboratory evolution. *Adv Protein Chem*, 55, 161-225. [https://doi.org/10.1016/s0065-3233\(01\)55004-4](https://doi.org/10.1016/s0065-3233(01)55004-4)
- Xiong, W., Knispel, R. A., Dietz, H. C., Ramirez, F., & Baxter, B. T. (2008). Doxycycline delays aneurysm rupture in a mouse model of Marfan syndrome. *J Vasc Surg*, 47(1), 166-172; discussion 172. <https://doi.org/10.1016/j.jvs.2007.09.016>
- Xu, L., Cui, J., Li, M., Wu, Q., Liu, M., Xu, M., Shi, G., Yin, J., & Yang, J. (2022). Association Between Serum Asprosin and Diabetic Nephropathy in Patients with Type 2 Diabetes Mellitus in the Community: A Cross-Sectional Study. *Diabetes Metab Syndr Obes*, 15, 1877-1884. <https://doi.org/10.2147/DMSO.S361808>
- Yamaguchi, Y., Takihara, T., Chambers, R. A., Veraldi, K. L., Larregina, A. T., & Feghali-Bostwick, C. A. (2012). A peptide derived from endostatin ameliorates organ fibrosis. *Sci Transl Med*, 4(136), 136ra171. <https://doi.org/10.1126/scitranslmed.3003421>
- Yang, C. Y., Chanalaris, A., & Troeberg, L. (2017). ADAMTS and ADAM metalloproteinases in osteoarthritis - looking beyond the 'usual suspects'. *Osteoarthritis Cartilage*, 25(7), 1000-1009. <https://doi.org/10.1016/j.joca.2017.02.791>
- Ye, F., Zhang, H., Yang, Y. X., Hu, H. D., Sze, S. K., Meng, W., Qian, J., Ren, H., Yang, B. L., Luo, M. Y., Wu, X., Zhu, W., Cai, W. J., & Tong, J. B. (2011). Comparative proteome analysis of 3T3-L1 adipocyte differentiation using iTRAQ-coupled 2D LC-MS/MS. *J Cell Biochem*, 112(10), 3002-3014. <https://doi.org/10.1002/jcb.23223>
- Yu, Y., He, J. H., Hu, L. L., Jiang, L. L., Fang, L., Yao, G. D., Wang, S. J., Yang, Q., Guo, Y., Liu, L., Shang, T., Sato, Y., Kawamura, K., Hsueh, A. J., & Sun, Y. P. (2020). Placensin is a glucogenic hormone secreted by human placenta. *EMBO Rep*, 21(6), e49530. <https://doi.org/10.15252/embr.201949530>
- Yuan, M., Li, W., Zhu, Y., Yu, B., & Wu, J. (2020). Asprosin: A Novel Player in Metabolic Diseases. *Front Endocrinol (Lausanne)*, 11, 64. <https://doi.org/10.3389/fendo.2020.00064>
- Zeyer, K. A., & Reinhardt, D. P. (2015). Fibrillin-containing microfibrils are key signal relay stations for cell function. *Journal of Cell Communication and Signaling*, 9(4), 309-325. <https://doi.org/10.1007/s12079-015-0307-5>

- Zhang, H., Hu, W., & Ramirez, F. (1995). Developmental expression of fibrillin genes suggests heterogeneity of extracellular microfibrils. *Journal of Cell Biology*, 129(4), 1165-1176. <https://doi.org/10.1083/jcb.129.4.1165>
- Zhang, L., Chen, C., Zhou, N., Fu, Y., & Cheng, X. (2019). Circulating asprosin concentrations are increased in type 2 diabetes mellitus and independently associated with fasting glucose and triglyceride. *Clin Chim Acta*, 489, 183-188. <https://doi.org/10.1016/j.cca.2017.10.034>
- Zhang, X., Jiang, H., Ma, X., & Wu, H. (2020). Increased serum level and impaired response to glucose fluctuation of asprosin is associated with type 2 diabetes mellitus. *J Diabetes Investig*, 11(2), 349-355. <https://doi.org/10.1111/jdi.13148>
- Zhang, Y., Zhu, Z., Zhai, W., Bi, Y., Yin, Y., & Zhang, W. (2021). Expression and purification of asprosin in *Pichia pastoris* and investigation of its increase glucose uptake activity in skeletal muscle through activation of AMPK. *Enzyme Microb Technol*, 144, 109737. <https://doi.org/10.1016/j.enzmictec.2020.109737>
- Zhong, L., Long, Y., Wang, S., Lian, R., Deng, L., Ye, Z., Wang, Z., & Liu, B. (2020). Continuous elevation of plasma asprosin in pregnant women complicated with gestational diabetes mellitus: A nested case-control study. *Placenta*, 93, 17-22. <https://doi.org/10.1016/j.placenta.2020.02.004>
- Zimmermann, L. A., Correns, A., Furlan, A. G., Spanou, C. E. S., & Sengle, G. (2021). Controlling BMP growth factor bioavailability: The extracellular matrix as multi skilled platform. *Cell Signal*, 85, 110071. <https://doi.org/10.1016/j.cellsig.2021.110071>

9. Abbreviations

A	alanine
aa	amino acid
ADAMTS	a disintegrin and metalloproteinase with thrombospondin motifs
ADMSC	adipose-Derived Mesenchymal Stem cells
AgRP	Agouti-related peptide
AU	absorbance unit
BMD	bone mineral density
BMI	Body-Mass-Index
BMP	bone morphogenetic protein
BSA	bovine serum albumin
cAMP	cyclic adenosine monophosphate
cbEGF	calcium binding epidermal growth factor-like domain
CCA	congenital contractural arachnodactyly
cDNA	complementary DNA
COMP	cartilage oligomeric matrix protein
CPS	carbamoyl phosphate synthase
C-terminus	carboxy terminus
Da	Dalton
DAPI	4',6-Diamidino-2-phenylindole dihydrochloride
DLS	dynamic light scattering
DMEM	Dulbecco's Modified Eagle Medium
DMSO	dimethyl sulfoxide
DNA	deoxyribonucleic acid
DSS	disuccinimidyl suberate
DTT	dithiothreitol
ECM	extracellular matrix
EDTA	ethylenediaminetetraacetic acid
EGF	epidermal growth factor

ELISA	enzyme-linked immunosorbent assay
EM	electron microscopy
ER	endoplasmic reticulum
FBN	fibrillin
FBS	fetal bovine serum
FGF	fibroblast growth factor
FMF	fibrillin microfibrils
GDM	gestational diabetes mellitus
GLP-1	Glucagon-like Peptide-1
h	hour
HDF	human dermal fibroblasts:
his6-tag	six-histidine-tag
HRP	horseradish peroxidase
IF	immunofluorescence
LTBP	latent transforming growth factor-beta binding protein
m	minutes
mAB	monoclonal antibody
MALS	multi-angle static light scattering
MDC	monodansylcadaverine
MFLS	marfanoid-progeroid-lipodystrophy syndrome
MFS	Marfan syndrome
min	minute
MMP	matrix metalloproteinase
mRNA	messenger RNA
MS	mass spectrometry
N	asparagine
NF- κ B	nuclear factor kappa-light-chain-enhancer of activated B cells
nm	nanometer
N-terminus	amino terminus
O/N	overnight

OA	osteoarthritis
OD	optical density
OLFR	olfactory receptor
PBS	phosphate-buffered saline
PBST	phosphate-buffered saline with tween 20
PDB	Protein Data Bank
Pen/strep	penicillin-streptomycin
PFA	paraformaldehyde
PKA	protein kinase A
PKC δ	protein kinase C-delta
pLDDT	predicted local distance difference test
pSMAD	phospho-Smad
PTM	post-translational modification
Q	glutamine
Rh	hydrodynamic radius
RU	response units
s	seconds
SD	standard deviation
SDS	sodium dodecyl sulfate
SDS-PAGE	sodium dodecyl sulfate-polyacrylamide-gel electrophoresis
SEC	size exclusion chromatography
siRNA	small interfering RNA
SPR	surface plasmon resonance
strep-tag	streptavidin tag
T1DM	type 1 diabetes mellitus
T2DM	type 2 diabetes mellitus
TB	TGF β -binding protein-like domain
TBS	tris-buffered saline
TBST	tris-buffered saline with tween 20
TG2	transglutaminase 2

TGF- β	transforming growth factor beta
TLR4	Toll-like receptor 4
UV	ultraviolet
VSMCs	vascular smooth muscle cells
WAT	white adipose tissue

10. Acknowledgement

I would like to extend my deepest gratitude to Gerhard for his guidance and feedback throughout this work. It has been a pleasure to have the opportunity to work with such a supportive supervisor.

I would also like to thank Raimund Wagener and Ulrich Baumann for taking the time to be there for me as a member of my thesis advisory committee, for their insightful comments and suggestions, and fruitful discussions. I would also like to thank Matthias Hammerschmidt for being a chair in the defense.

I am also very grateful to have had the chance to work with Galyna Pryymachuk for a part of this work. She was very supportive. I would like also to thank Alan Godwin and Clair Baldock for their contributions and suggestions in this work.

Many special thanks go to Antje for her excellent technical assistance, help and dedication, especially for the longer days she had to stay. We made a great team that supports the project and fosters a positive work environment. I would like to specially thank Steffen for his pleasant company and our nice talks in- and outside the lab, and about the various aspects of our projects. I particularly valued his technical expertise in Biacore, which supports this work.

I also want to thank the entire lab for creating a pleasant work atmosphere. Many thanks to Laura and Annkatrin who have always been helpful in many aspects in the lab., Antje and Dagmar for their help in ordering and solve any problems within the lab. I would like to thank Chara for our fruitful scientific discussion which was very helpful. I would also like to express my thanks to all technicians in the institute for biochemistry for ordering reagents, providing protocols and technical help.

I would like to express my gratitude to the members of research group FOR2722 for organizing summer schools, seminars, and conferences as well as giving us a chance to present our work and get fruitful feedback and input.

Lastly, I would like to thank my family, my mother and brother; and especially my wife Bella for the years of love and support which she has given me and without whom I wouldn't be where I am today.

The work described here was funded by the Deutsche Forschungsgemeinschaft (DFG, German Research Foundation) project ID 384170921: FOR2722/M2

Erklärung zur Dissertation
gemäß der Promotionsordnung vom 12. März 2020

Diese Erklärung muss in der Dissertation enthalten sein.
(This version must be included in the doctoral thesis)

„Hiermit versichere ich an Eides statt, dass ich die vorliegende Dissertation selbstständig und ohne die Benutzung anderer als der angegebenen Hilfsmittel und Literatur angefertigt habe. Alle Stellen, die wörtlich oder sinngemäß aus veröffentlichten und nicht veröffentlichten Werken dem Wortlaut oder dem Sinn nach entnommen wurden, sind als solche kenntlich gemacht. Ich versichere an Eides statt, dass diese Dissertation noch keiner anderen Fakultät oder Universität zur Prüfung vorgelegen hat; dass sie - abgesehen von unten angegebenen Teilpublikationen und eingebundenen Artikeln und Manuskripten - noch nicht veröffentlicht worden ist sowie, dass ich eine Veröffentlichung der Dissertation vor Abschluss der Promotion nicht ohne Genehmigung des Promotionsausschusses vornehmen werde. Die Bestimmungen dieser Ordnung sind mir bekannt. Darüber hinaus erkläre ich hiermit, dass ich die Ordnung zur Sicherung guter wissenschaftlicher Praxis und zum Umgang mit wissenschaftlichem Fehlverhalten der Universität zu Köln gelesen und sie bei der Durchführung der Dissertation zugrundeliegenden Arbeiten und der schriftlich verfassten Dissertation beachtet habe und verpflichte mich hiermit, die dort genannten Vorgaben bei allen wissenschaftlichen Tätigkeiten zu beachten und umzusetzen. Ich versichere, dass die eingereichte elektronische Fassung der eingereichten Druckfassung vollständig entspricht.“

Teilpublikationen:

Morcos, Y. A., Lütke, S., Tenbieg, A., Hanisch, F. G., Prymachuk, G., Piekarek, N., ... & Sengle, G. (2022). Sensitive asprosin detection in clinical samples reveals serum/saliva correlation and indicates cartilage as source for serum asprosin. *Scientific reports*, 12(1), 1-19.

Hoffmann, T., **Morcos, Y. A. T.**, Janoschek, R., Turnwald, E. M., Gerken, A., Müller, A., ... & Hucklenbruch-Röther, E. (2022). Correlation of metabolic characteristics with maternal, fetal and placental asprosin in human pregnancy. *Endocrine Connections*, 11(3).

Datum, Name und Unterschrift

17.10.2022, Yousef Ashraf Tawfik Morcos



Morcos, Yousef Ashraf Tawfik, M.Sc.

* 27.02.1993, male

Citizenship Egyptian
Occupational Address Department of Pediatrics and Adolescent
Medicine, University of Cologne
c/o Center for Biochemistry
Joseph-Stelzmann Str. 52
50931 Cologne
Telephone (private) +49 176 592 85786
E-mail ymorcos@uni-koeln.de



Current position

Doctoral candidate, Centre for Biochemistry, Faculty of Medicine, University of Cologne

Academic education

- 2016 – 2018 Molecular Medicine, Ulm University, Master, grade: 1.5 (very good)
Thesis: Analysis of Novel TERF1 isoform
- 2009 – 2014 Pharmaceutical Sciences, Cairo University, Bachelor, grade: 85.4% (Excellent with honors)

Professional career

- since 2019 Doctoral candidate, Centre for Biochemistry, Faculty of Medicine, University of Cologne
- 2017 - 2018 Research Assistant, Urology Research Laboratory, University Hospital Ulm, Ulm University
- 2016 Research Assistant, Biotechnology Department, National Organization for Research and Control of Biological Products (NORCB), Giza, Egypt
- 2015 Pharmacist (Military service), Infantry Training Center, Cairo, Egypt

Professional Skills

Immunohistochemistry, Immunofluorescence, Western Blot, ELISA, Protein Purification, Proteomic analysis, FACS, Cloning, Cell Culture, qPCR

Internships and Training

- 2022 MaxQuant Summer School for Computational Mass Spectrometry-Based Proteomics, Barcelona, Spain
- 2021 Academic Writing in the Natural and Life Sciences, Cologne, Germany
- 2020 Good Scientific Practice for the Experimental Disciplines, Cologne, Germany
- 2019 Laboratory Animal Science Training (FELASA B), Cologne, Germany
- 2015 Training Program on Common Technical Document (CTD) for Biological Products Registration at Central Administration of Pharmaceutical Affairs (CAPA), Cairo, Egypt
- 2013 Pharmaceutical Production Internship at Eva Pharma factory, Giza, Egypt
- 2012 Pharmaceuticals Quality control internship at Amoun Pharmaceutical Company, Cairo, Egypt

Honors/ Awards/ Memberships

2019 Member, German Society for Matrix Biology (DGMB)
2018 DAAD scholarship
2016 - 2017 Support Establishment Foundation scholarship, Vaduz

Languages

Arabic: Native
English: *Fluent*
German: *Fluent*
Spanish: *Elementary*

Publications

Morcós, Y. A., Lütke, S., Tenbrieg, A., Hanisch, F. G., Pryymachuk, G., Piekarek, N., ... & Sengle, G. (2022). *Sensitive asprosin detection in clinical samples reveals serum/saliva correlation and indicates cartilage as source for serum asprosin. Scientific reports, 12(1), 1-19.*

Hoffmann, T., Morcos, Y. A. T., Janoschek, R., Turnwald, E. M., Gerken, A., Müller, A., ... & Hucklenbruch-Rother, E. (2022). *Correlation of metabolic characteristics with maternal, fetal and placental asprosin in human pregnancy. Endocrine Connections, 11(3).*

Morcós, Y. A. T., Najjar, G., Meessen, S., Witt, B., Azoitei, A., Kumar, M., ... & Günes, C. (2019). *A novel tissue and stem cell specific TERF1 splice variant is downregulated in tumour cells. International journal of molecular sciences, 21(1), 85.*

References

Prof. Dr. Gerhard Sengle

Department of Pediatrics and Adolescent Medicine, University Hospital Cologne
Joseph-Stelzmann Str. 52, 50931, Cologne, Germany
(+49) 0221-478-97260
gsengle@uni-koeln.de

Prof. Dr. Cagatay Günes

Clinic of Urology, University Hospital Ulm
Eythstraße 20, D-89075, Ulm, Germany
(+49) 0731-500-58019
Cagatay.Guenes@uniklinik-ulm.de

Prof. Dr. Uwe Knippschild

General and Visceral Surgery, Research Laboratory, University Hospital Ulm
Albert-Einstein-Allee 23, 89081, Ulm, Germany
(+49) 0731-500-53580
uwe.knippschild@uniklinik-ulm.de